



Universidade de Brasília
Instituto de Ciências Exatas
Departamento de Matemática

INSTABILITIES IN FLOWS OF MAGNETIC FLUIDS

INSTABILIDADES EM ESCOAMENTOS DE FLUIDOS MAGNÉTICOS

por

Pavel Zenon Sejas Paz

Orientador: Prof. Dr. Yuri Dumaresq Sobral

Co-orientador: Prof. Dr. Francisco Ricardo Da Cunha

Brasília, 29 de outubro de 2020

Universidade de Brasília
Instituto de Ciências Exatas
Departamento de Matemática

Instabilidades em escoamentos de fluidos magnéticos

por

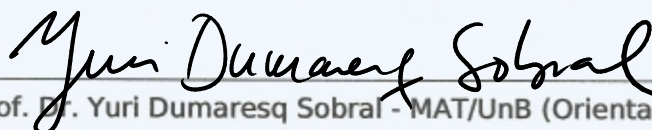
Pavel Zenon Sejas Paz*

Tese apresentada ao Departamento de Matemática da
Universidade de Brasília, como parte dos requisitos para
obtenção do grau de

DOUTOR EM MATEMÁTICA

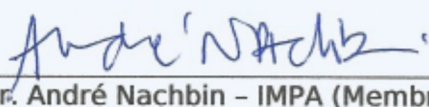
Brasília, 29 de outubro de 2020.

Comissão Examinadora:


Prof. Dr. Yuri Dumaresq Sobral - MAT/UnB (Orientador)


Prof. Dr. Lucas Conque Seco Ferreira - MAT/UnB (Membro)


Prof. Dr. André Von Borries Lopes - UnB (Membro)


Prof. Dr. André Nachbin - IMPA (Membro)

*O autor foi bolsista do CNPq e CAPES durante a elaboração desta tese.

Ficha catalográfica elaborada automaticamente,
com os dados fornecidos pelo(a) autor(a)

Sejas Paz, Pavel Zenon
Si INSTABILITIES IN FLOWS OF MAGNETIC FLUIDS / Pavel Zenon
Sejas Paz; orientador Yuri Dumaresq Sobral; co-orientador
Francisco Ricardo Da Cunha. -- Brasília, 2020.
165 p.

Tese (Doutorado - Doutorado em Matemática) --
Universidade de Brasília, 2020.

1. Estabilidade Hidrodinâmica. 2. Fluidos Magneticos. 3.
Equação de Evolução da Magnetização. 4. Equação de Orr
Sommerfeld. 5. Instabilidade de Plateau-Rayleigh. I.
Dumaresq Sobral, Yuri, orient. II. Da Cunha, Francisco
Ricardo , co-orient. III. Título.

Agradecimentos

Agradeço a Deus, por me permitir chegar até aqui.

À minha esposa Vivian por ter me apoiado desde o primeiro momento em que eu decidi continuar os meus estudos no doutorado. Meu amor, você trabalhou tanto ou mais do que eu no cuidado da casa e também das nossas lindas filhas, por isso devo destacar meu eterno amor e gratidão pelo seu amor e dedicação para conosco. Agradeço às minhas filhas Valentina e Catalina que com a sua simples presença foram e são uma motivação para continuar.

Agradeço à minha mãe, Ana Maria Paz Lara, por sempre me apoiar, por me ajudar na documentação para a revalidação do meu diploma. Pelas palavras de incentivo, que foram muito úteis, e por tudo o que ela faz por mim.

Gostaria de agradecer aos meus irmãos Maria Jose, Ariel e Karina, porque nos momentos difíceis estiveram comigo apoiando-me nesta caminhada de continuar os meus estudos fora do nosso país. Obrigado irmãozinhos, eu adoro vocês! Agradeço a todos os meus sobrinhos e cunhados pelo seu amor por mim e pela minha família, obrigado Vanesita, Natalia, Franz, Ingrid, obrigada aos pequeninos, Sammy, Niko, Wayra, Lucy, Liam.

Eu gostaria de agradecer a todos que me deram palavras de incentivo e sempre se preocuparam conosco, em particular gostaria de agradecer aos meus queridos sogros Elizabeth e Reynaldo, pelo apoio emocional e financeiro. Agradeço também por nos visitar aqui em Brasília e pelo belo momento que passamos juntos. Agradeço às minhas cunhadas pelas demonstração de carinho, Erika, Sofia, Cielo, Belen e Maria José.

Gostaria de agradecer à minha madrinha Bertha, ao meu padrinho Hugo, à Karem e à Alina por todo o amor e carinho não só comigo mas também com a minha família.

Meus eternos agradecimentos ao meu orientador de doutorado, Prof. Yuri Dumaresq Sobral. Muito obrigado por me aceitar como orientando, obrigado por todos os ensinamentos e a paciência em todos esses anos, não só aprendi a parte acadêmica, mas também como trabalhar com dedicação. Agradeço por ter-me fornecido o equipamento para fazer esta tese e também por todo o apoio e empenho que o senhor me deu quando se abriu a porta do doutorado Sanduíche. Eu e minha família sempre seremos gratos. Espero e desejo continuar no futuro uma colaboração juntos.

Agradeço ao meu co-orientador Prof. Francisco Ricardo da Cunha, pelas disciplinas que ministra de forma tão magistral, por ter me proporcionado um espaço confortável e bem cuidado no ambiente do Vortex. Agradeço também ao pessoal do Vortex, principalmente ao Alvaro, Andrey, Igor, Felipe, Yuri e Victor, que mesmo sendo da matemática me fizeram sentir como alguém da mecânica.

Aos meus amigos do MAT, gostaria de agradecer à minha irmã acadêmica Camila, porque quando minha filha nasceu, gentilmente abriu as portas de sua casa para nos ajudar. Aos meus amigos da minha sala Nathalia e Michell pelas conversas agradáveis que tivemos. Gostaria de agradecer ao meu amigo Felipe, porque quando tive um problema de saúde ele estava aí para ajudar não só a mim mas também a minha família, valeu Felipe!

O caminho de seguir uma pós-graduação no Brasil tem me trazido a imensa alegria de me dar um grande amigo para a vida, um irmão, como se costuma dizer no meio acadêmico, um amigo de olho vermelho, deixo aqui o meu agradecimento ao meu grande amigo Santiago Miler Quispe Mamani. Em Juiz de Fora, já tínhamos uma grande amizade, mas uma vez em Brasília nossa amizade foi crescendo. Grande amigo Santiago, muito obrigado por sua amizade sincera, eu espero que no futuro possamos colaborar fazendo pesquisa juntos.

Agradeço aos meus professores pelos excelentes cursos que ministraram, em particular ao Prof. Ricardo Parreira e ao Prof. Marcelo Furtado. Agradeço ao meu professor e amigo do mestrado Grigori Chapiro, muito obrigado por tudo que você me ensinou no mestrado, no doutorado foi muito útil e espero que possamos pesquisar juntos num futuro.

Agradeço aos professores André Nachbin, André Lopes e Lucas Seco, por terem aceitado participar de minha banca e pelas observações que fizeram para enriquecer o meu trabalho.

Agradeço a Universidade de Brasília por ter me recebido de portas abertas. Sou grato à Diretoria de Desenvolvimento Social (DDS) pelo apoio financeiro.

Agradeço às agências de fomento que me permitiram fazer meu doutorado, à Capes e ao CNPq, pela bolsa de estudos durante o meu doutorado. Agradeço à FAP-DF pelo apoio financeiro para apresentar o meu trabalho no exterior. À Capes pela bolsa para fazer o doutorado Sanduíche. Agradeço ao sistema público de ensino do Brasil por me dar a oportunidade, como estrangeiro, de continuar minha formação no Brasil.

Acknowledgments

I would like to thank Prof. Neil J. Balmforth for the kindness in accepting me to do a doctoral visit to UBC and for the financial support on my second trip to Vancouver. Thank you very much for teaching me the beautiful problem of Plateau-Rayleigh's instability and for allowing me to participate in your course on asymptotic methods. At the same time, I would like to thank Prof. Ian Frigaard, for allowing me to participate in the course on visco-plastic fluids. I thank the Department of Mathematics at the University of British Columbia for giving me a comfortable space to develop my work. I am grateful to the good friends I made in the beautiful city of Vancouver, especially Natham, Brian and Ivonne, thank you very much for making my stay pleasant during my visit there.

RESUMO

Neste trabalho, apresentamos dois estudos de problemas de estabilidades em escoamentos de fluidos magnéticos. O primeiro é um estudo sobre a estabilidade de um escoamento de Poiseuille no plano bidimensional de um fluido magnético na presença de um campo magnético aplicado. O fluido é incompressível e sua magnetização é acoplada ao escoamento por meio de uma equação fenomenológica simples. Os autovalores do sistema linearizado são calculados usando um esquema de diferenças finitas e estudados com relação aos parâmetros adimensionais do problema. Estudamos os casos de campos magnéticos aplicados horizontal e vertical. Nossos resultados indicam que o escoamento é desestabilizado pela presença de um campo magnético aplicado horizontalmente, enquanto que é estabilizado quando um campo é aplicado verticalmente. Caracterizamos a estabilidade do fluxo calculando os diagramas de estabilidade em termos dos parâmetros adimensionais e, o mais importante, determinamos a mudança do número de Reynolds crítico em termos dos parâmetros magnéticos. Além disso, mostramos que o limite superparamagnético, no qual a magnetização do fluido é desacoplada da hidrodinâmica, recupera o mesmo número de Reynolds crítico puramente hidrodinâmico, independentemente da direção do campo aplicado e dos valores dos outros parâmetros magnéticos adimensionais. O segundo estudo é sobre a instabilidade de Plateau-Rayleigh para jatos de fluidos magnéticos. Apresentamos uma teoria superparamagnética simplificada que leva em consideração a permeabilidade magnética da região externa. Nossos resultados indicam que a estabilidade do jato é apenas marginalmente afetada quando se considera uma região externa magneticamente permeável. Em seguida, construímos uma teoria completa para um fluido magnético na qual a equação de evolução da magnetização, idêntica à usada no primeiro problema, é levada em consideração. No regime de ondas longas, construímos um sistema de leis de conservação que é usado como base para uma análise de estabilidade linear. A construção desta teoria provou ser complicada porque as condições de contorno para as grandezas magnéticas tiveram que ser consideradas cuidadosamente ao longo da superfície livre de jato. Os resultados indicam que a estabilidade do sistema é marginalmente melhorada quando a magnetização relaxa com o fluxo em escalas de tempo moderadas. Por outro lado, o termo precessional na equação de evolução da magnetização tende a aproximar o sistema de um regime superparamagnético.

Palavras-chave: Estabilidade hidrodinâmica, Fluidos magnéticos, Equação de Orr-Sommerfeld, Equação de Shliomis, Instabilidade de Plateau-Rayleigh.

ABSTRACT

In this work, we present two studies of problems of instabilities in flows of magnetic fluids. The first one is a study on the stability of a two-dimensional plane Poiseuille flow of a magnetic fluids in the presence of an applied magnetic field. The fluid is incompressible and its magnetization is coupled to the flow through a simple phenomenological equation. The eigenvalues of the linearized system are computed using a finite difference scheme and studied with respect to the dimensionless parameters of the problem. We study the cases of horizontal and vertical applied magnetic fields. Our results indicate that the flow is further destabilized by the presence of a horizontal applied magnetic field, whereas it is stabilized when a vertical applied field is present. We characterize the stability of the flow by computing the stability diagrams in terms of the dimensionless parameters and, most importantly, we determine the change of the critical Reynolds number in terms of the magnetic parameters. Furthermore, we show that the superparamagnetic limit, in which the magnetization of the fluid is decoupled from the hydrodynamics, recovers the same purely hydrodynamic critical Reynolds number, regardless of the applied field direction and of the values of the other dimensionless magnetic parameters. The second study is the Plateau-Rayleigh instability for jets of magnetic fluids. We present a simplified superparamagnetic theory that takes into consideration the magnetic permeability of the outer region. Our results indicate that the stability of the jet is only marginally affected when considering a magnetically permeable outer region. We then built a complete theory for a magnetic fluid in which the magnetization evolution equation, identical to the one used in the first problem, is taken into account. In the long waves regime, we constructed a system of conservation laws that are used as the basis for a linear stability analysis. The construction of this theory proved to be complicated because the boundary conditions for the magnetic quantities had to be considered carefully across the jet free surface. The results indicate that the stability of the system is marginally improved when the magnetization relaxes with the flow over moderate time scales. On the other hand, the precessional term in the magnetization evolution equation tends to approach the system to a superparamagnetic regime.

Keywords: Hydrodynamic stability, Magnetic fluids, Orr-Sommerfeld equation, Shliomis's equation, Plateau-Rayleigh's instability.

SUMMARY

I	GENERAL INTRODUCTION	1
1	INTRODUCTION	2
1.1	STABILITY IN FLUID MECHANICS	4
1.1.1	INTUITIVE IDEAS OF STABILITY OR INSTABILITY	4
1.2	THE PRESENT INVESTIGATION	6
2	THE EQUATIONS OF HYDRODYNAMICS	8
2.1	PRELIMINARIES	8
2.2	CONSERVATION EQUATIONS	10
2.3	STRESS TENSORS	13
3	MAGNETISM AND MAGNETIC FLUIDS	15
3.1	FERROFLUIDS	15
3.2	THE MAGNETO-STATIC LIMIT OF MAXWELL'S EQUATIONS	16
3.2.1	THE MAXWELL'S EQUATIONS	16
3.2.2	THE MAGNETOSTATIC LIMIT	16
3.3	THE BOUNDARY CONDITIONS	17
3.4	THE MAGNETIZATION	20
3.5	THE MAGNETIZATION OF A FERROFLUID	22
3.5.1	THE EQUILIBRIUM MAGNETIZATION	22
3.6	THE MAGNETIC RELAXATION TIME	24
3.6.1	OUT OF THE EQUILIBRIUM	26
3.7	THE MAGNETIC STRESS TENSOR	26
3.8	THE EQUATIONS OF MOTION OF A FERROFLUID	28

II	STABILITY OF PLANE PARALLEL FLOWS OF MAGNETIC FLUIDS	33
4	INTRODUCTION	34
5	OVERVIEW OF THE BASIC RESULTS OF HYDRODYNAMIC STABILITY	36
5.1	THE BASE STATE	36
5.2	THE LINEAR STABILITY PROBLEM	39
5.2.1	THE THEOREM OF SQUIRE	42
5.3	THE INVISCID LIMIT	43
5.4	NUMERICAL SOLUTION OF THE ORR-SOMMERFELD STABILITY PROBLEM	46
6	STABILITY OF SYMMETRIC MAGNETIC FLUIDS	53
6.1	SUPER-PARAMAGNETIC CASE	54
6.2	BASE STATE: KELVIN FORCE	56
6.2.1	THE VELOCITY BASE STATE	58
6.2.2	THE MAGNETIC BASE STATE	59
6.3	THE STABILITY EQUATIONS	60
6.3.1	LINEAR STABILITY ANALYSIS	60
6.3.2	NUMERICAL SOLUTION	63
6.4	RESULTS	64
6.4.1	HORIZONTAL APPLIED MAGNETIC FIELD	65
6.4.2	VERTICAL APPLIED MAGNETIC FIELD	68
6.5	DISCUSSION AND FINAL REMARKS	69
6.6	FUTURE DIRECTIONS	71
7	CONCLUSION AND FUTURE DIRECTIONS	74
III	LONG-WAVE APPROXIMATION OF PLATEAU-RAYLEIGH INSTABILITY OF MAGNETIC FLUIDS	76
8	INTRODUCTION	77
8.1	GENERAL FRAMEWORK FOR THE RAYLEIGH-PLATEAU INSTABILITY	80
8.2	THE PLATEAU-RAYLEIGH INSTABILITY	82
8.2.1	THE INVISCID CASE	82
8.2.2	THE STABILITY ANALYSIS	83
8.2.3	THE VISCOUS CASE	87
9	LONG WAVES APPROXIMATION OF THE PLATEAU-RAYLEIGH INSTABILITY	89
9.1	THE LONG-WAVE APPROXIMATION	89
9.2	THE INVISCID CASE	90

9.2.1	THE STABILITY ANALYSIS	92
9.3	THE VISCOUS CASE.....	94
9.3.1	NUMERICAL APPROACH TO THE NONLINEAR REGIMES	98
10	THE PLATEAU-RAYLEIGH INSTABILITY FOR SUPER-PARAMAGNETIC FLUIDS.....	109
10.1	THE INVISCID SUPER-PARAMAGNETIC CASE	109
10.1.1	THE CASE OF A MAGNETICALLY IMPERMEABLE OUTER REGION.....	112
10.1.2	THE CASE OF A MAGNETICALLY PERMEABLE OUTER REGION	116
10.2	THE VISCOUS MAGNETIC CASE.....	118
10.2.1	NUMERICAL APPROACH TO THE NONLINEAR REGIMES	121
11	THE PLATEAU-RAYLEIGH INSTABILITY COUPLED WITH MAGNETIZATION	126
11.1	THE FULL MAGNETIC MODEL.....	126
11.1.1	SCALING ARGUMENTS.....	126
11.1.2	LIMITING CASES	135
11.1.3	LINEAR STABILITY ANALYSIS.	136
12	CONCLUSION AND FUTURE DIRECTIONS	140
	REFERENCES.....	142
	APPENDIX.....	148
I.1	PERTURBATION OF MODIFIED THE NAVIER-STOKES EQUATION.....	149
I.2	PERTURBATION OF THE MAGNETIZATION EVOLUTION EQUATION	151
II.3	YOUNG LAPLACE MEAN CURVATURE.....	153
II.4	NORMAL STRESS BALANCE.....	154
II.5	TANGENTIAL STRESS BALANCE	154

Part I

General Introduction

CHAPTER 1

INTRODUCTION

Magnetic fluids are colloidal suspensions of very small magnetizable particles that, become magnetized and react under the presence of an applied magnetic field [33]. This gives these magnetic fluids the property of being remotely controlled by magnetic fields, making them suitable for a vast number of applications [33, 30]. Applications include magnetic targeting of a drug: in which the chemotherapeutic drug is coated with a magnetic fluid and injected into the cancerous tumor and using a suitable magnetic field, the drug is located and maintained at a specific area of the tumor, maximizing its effectiveness [17, 19]. Magnetic hyperthermia is a cancer therapy in which magnetic particles are strategically placed into the tumor, under the action of alternating magnetic fields, the magnetic nanoparticles absorb a large amount of energy and transform it into heat, thus acting significantly against the tumor [20, 22]. In the area of magnetic resonance imaging (MRI), magnetic nanoparticles are useful as contrast agents. Paramagnetic contrast agents have been used for a long time, but more recently superparamagnetic iron oxide nanoparticles have also been found to influence the contrast of magnetic resonance imaging. Different of the paramagnetic contrast agents, superparamagnetic nanoparticles can be functionalized and adapted to various kind of soft tissue [23, 24]. In fact, the invention of ferrofluids is attributed to the development of liquid rocket fuels that could be pumped in the absence of gravity via magnetic fields [32]. The response of magnetic fluids to the presence of a magnet allows us to control the flow of the fluid and this particular feature has opened a wide range of applications in different areas of knowledge.

Since the late nineteenth century, the areas of hydrodynamic stability and magneto-hydrodynamic (MHD) have been widely studied by the scientific community. Later, in the mid-twentieth century, the artificial creation of magnetic fluids gave rise to what is known

today as ferrohydrodynamics (FHD). Similar to MHD, FHD results from a combination of the equations of fluid dynamics and electromagnetism. We emphasize that MHD is related to electrically conducting fluids, thus involving electrical and magnetic quantities, whereas FHD only deals with fluids that are not electrically conductive, and therefore only magnetic quantities are considered in the magnetostatic limit.

In the first part of this work, the linear analysis of hydrodynamic stability predicts the response of a fluid flow in laminar regime to small perturbations. Briefly, a disturbance of small amplitude is imposed in the base state flow in the governing equations. If the amplitude of this small perturbation grows with time, the flow is unstable to small disturbances. If the amplitude of the disturbances decays with time, the flow is stable. In case the perturbation does not grow or decay, the flow is neutrally stable and our forces are concentrated to find the critical value of the parameter for which transition happens, that is, to identify the Reynolds critical number.

If the external applied magnetic field is absent, the fluid behaves like an ordinary suspension, this is because the Brownian motion randomly orients the magnetic dipoles of the particles, resulting in a non-magnetized medium. On the other hand, in the presence of an applied external magnetic field, the magnetic dipoles begin to sense, due to the magnetic field gradients, the magnetic force and at the same time, the magnetic torques resulting from the misalignment between the dipole and the magnetic field.

There have been studies of hydrodynamic stability and transition of flows of magnetic fluids in the presence of magnetic fields, but most of them were related to conducting magnetizable magnetic fluids in the context of magnetohydrodynamics, such as [11], and only a few were related to non-conducting magnetic fluids, in the context of ferrohydrodynamics. A classical example of the latter studies is the theoretical investigation of a plane Couette flow of a magnetic fluid in the presence of an applied magnetic field [60]. An unstable regime was found for some values of the relevant parameters. The Taylor-Couette instability of magnetic fluids was also broadly studied in different contexts, such as its destabilization driven by temperature gradients [54] or its stabilization obtained by an array of magnets [35]. More recently, a thorough numerical bifurcation analysis was carried out in [13] focusing in understanding the early appearance of turbulence in Couette flows of magnetic fluids under the presence of magnetic fields. Finally, there have also been studies of interfacial instabilities, either in free surface problems [10] or in two-fluid interfaces [46]. However, in these two last references, the flows are either rheometric or inertia plays no role on the early dynamics of the instabilities.

The second part of this investigation started during an academic visit to the University of British Columbia in Canada. The aim was to study a new problem that combines magnetic fluids and a promising application of them. We have chosen to study the nonlinear stability problem of a slender cylindrical jet, known as the Plateau-Rayleigh stability problem.

The phenomenon of break-up of a liquid jet into droplets has attracted the attention of researchers and engineers in the last centuries. The problem was first investigated by Lord Rayleigh, initially for flows in the inviscid limit in [47], and then for the viscous case in [48]. Since then, the problem has taken several directions and also the different technological applications have been increasing, among them are the process of atomization, ink-jet printing, drug delivery and manufacturing systems.

The break-up is caused by the presence of small external disturbances which grow spatially due to capillary instability, as described by Rayleigh [47]. In the case of capillary instability, the growth rate of disturbances is caused by the opposite effect of the axial and radial curvature of the interface that was initially observed by Savart (1833) and investigated by Plateau (1873).

1.1 Stability in Fluid Mechanics

In this work, we present two studies that combine the classical theory of hydrodynamic stability and the non-Newtonian fluid known as magnetic fluids, also called as ferrofluids. The first study is about the problem of linear stability analysis of a magnetic fluid flow between parallel plates. The second one is about the Plateau-Rayleigh stability problem and the formation of droplets from a cylindrical jet of magnetic fluid.

1.1.1 Intuitive ideas of stability or instability

Consider the following system governed by an ordinary differential equation with initial value problem (IVP):

$$\begin{cases} \frac{du}{dt} = f(u), \\ u(0) = u_0. \end{cases} \quad (1.1)$$

In this problem, the points u^* at which $f(u^*) = 0$ are called equilibrium points:

$$\frac{du^*}{dt} = f(u^*) = 0, \quad (1.2)$$

and if $u_0 = u^*$, the system remain valid at

$$u(t) = u^*, \quad \forall t. \quad (1.3)$$

At this stage, we can ask what happens to the system when a small disturbance u_p is introduced, that is:

$$u(t) = u^* + u_p(t). \quad (1.4)$$

Substituting this expression in (1.1), we have in the left-hand side

$$\frac{du}{dt} = \frac{d(u^* + u_p)}{dt} = \frac{du^*}{dt} + \frac{du_p}{dt} = \frac{du_p}{dt}, \quad (1.5)$$

and using a Taylor series around u^* , the right hand side is given by,

$$f(u) = f(u^* + u_p) = f(u^*) + f'(u^*)u_p + \mathcal{O}(u_p^2). \quad (1.6)$$

From (1.5) and (1.6) we can formulate a new IVP:

$$\begin{cases} \frac{du_p}{dt} = f'(u^*)u_p, \\ u_p(0) = u_{p0}. \end{cases} \quad (1.7)$$

The ordinary differential equation with initial condition in (1.7) is a initial value problem and its solution is given by,

$$u_p(t) = u_p(0) \exp(f'(u^*)t). \quad (1.8)$$

The behavior of the solution $u_p(t)$ depends on the amplitude $u_p(0)$, the sign of $f'(u^*)$ and the evolution is given by the dependency of the temporal variable t in the exponential function. The possible outcomes are given in Table (1.1). If we obtain $f'(u^*)$ with positive sign, this indicates that $u_p(t)$ grows and that the equilibrium state will not be maintained, for this reason u^* is unstable. If $f'(u^*)$ is equal to zero, this means that $u_p(t)$ will be constant and equal to $u_p(0) = u_0 - u^*$ and that u does not depend on u^* being that u^* has a neutral behavior for either growth or decrease of $u(t)$ and if $f'(u^*)$ is negative, the value of u_p negligible for large enough times, in this case u^* is said stable.

Table 1.1: Stability analysis depending on the sign of $f'(u^*)$.

	$f'(u^*) > 0$	$f'(u^*) = 0$	$f'(u^*) < 0$
u_p	Increase	Constant	Decrease
u^*	Unstable	Stable (neutral)	Stable

Let's consider $\mathbf{u} \in \mathbb{R}^3$ a vector valued function that satisfies the following ODE with an initial value problem,

$$\begin{cases} \frac{d\mathbf{u}}{dt} = \mathbf{f}(\mathbf{u}), \\ \mathbf{u}(0) = \mathbf{u}_0. \end{cases} \quad (1.9)$$

with $\mathbf{f} : \mathbb{R}^3 \rightarrow \mathbb{R}^3$. The linearized system for the perturbation \mathbf{u}_p is given by:

$$\begin{cases} \frac{d\mathbf{u}_p}{dt} = \nabla\mathbf{f}(\mathbf{u}^*)\mathbf{u}_p, \\ \mathbf{u}_p(0) = \mathbf{u}_{p0}. \end{cases} \quad (1.10)$$

In this expression $\nabla\mathbf{f}(\mathbf{u}^*)$ indicates the Jacobian matrix of \mathbf{f} . As in the previous case, the solution can be found by setting $\mathbf{u}_p = \mathbf{v}e^{\lambda t}$,

$$\lambda(\mathbf{v}e^{\lambda t}) = \frac{d(\mathbf{v}e^{\lambda t})}{dt} = \nabla\mathbf{f}(\mathbf{u}^*)\mathbf{v}e^{\lambda t}.$$

Thus,

$$\lambda \mathbf{v} = \nabla \mathbf{f}(\mathbf{u}^*) \mathbf{v}. \quad (1.11)$$

The stability depends on the eigenvalues λ of $\nabla \mathbf{f}(\mathbf{u}^*)$ and its respective associated eigenvectors \mathbf{v} on (1.11). The concepts presented here give us an idea of what stability means in the sense of ODEs, where the amplification of a small disturbance causes the system to leave the equilibrium state. In what follows we will use these concepts for the flow of a fluid.

1.2 The Present Investigation

Considering the first problem, the purpose of this work is to examine the coupled problem of the stability of a ferro-hydrodynamics flow between a two rigid parallel plates, in which the new feature is the use of a phenomenological magnetization equation coupling the magnetism of the fluid to the flow. In the present investigation, linear stability of a ferrofluid flow between two parallel plate walls under an applied magnetic field is analyzed. For this, a base state is determined by assuming the hydrodynamic unidirectional fully developed flow. To continue the analysis, two dimensional perturbation is imposed to the base state. The linearized perturbations equations are expressed in terms of the amplitude function by introducing plane waves disturbances. These equations are then reduced into a Orr-Sommerfeld type system involving the magnetization disturbances. The generalized eigenvalue problem is solved by a finite difference scheme as reported in the references [7, 25]. The results are compared with purely hydrodynamic case. A dimensionless magnetic parameter is identified and the marginal stability curves and the critical Reynolds numbers for a different magnetic parameter values are obtained.

The effect of applied magnetic field on the flow stability is studied, and a particular attention is made in the following question: Does the applied magnetic field stabilize or destabilize the flow? For a given magnetic parameter, can a Reynolds number that stabilizes the flow be found?

Next, considering the second problem, the purpose of this work is to examine the coupled capillar-magnetic problem of the Plateau-Rayleigh stability when a magnetic fluid is considered. In the present investigation, a stability analysis of a magnetic fluid cylinder jet flow under an applied magnetic field in the axial direction is carried out. To this end, the hypothesis of disturbances of with long wavelengths is assumed to derive an asymptotic approximation of the Navier-Stokes equations. To continue the analysis an equation for the evolution of the magnetization is considered. The linearized perturbations equations are expressed in terms of the amplitude function by introducing a time and spatial depending exponential function. These equations are then reduced into a dispersion equation type

involving the magnetization disturbances. The results are compared with purely hydrodynamic case and the previous works. Dimensionless magnetic parameters are obtained.

The effect of applied magnetic field on the flow stability is studied, and a particular attention is made in the following question: Does the applied magnetic field stabilize or destabilize the flow? Is there a physical parameter that prevents the formation of drops? What is the relation which new magnetic mode? not mentioned before. What can we conclude about the pinch-off when a magnetic fluid is considered?

The rest of this work is structured as follows: in part I, a general introduction and a review of the main concepts used in this research are presented. In Chapter 2, the classical hydrodynamic stability model problem, as well as the governing equations and physical parameters of the problem, are presented. In Chapter 3, the fundamental results about magnetic fluids and magnetization evolution equations are derived. In Part II, the stability of plane parallel flows of magnetic fluids is presented. In Chapter 5, the classical problem of hydrodynamic stability of parallel plate flows and the Orr-Sommerfeld equation are presented. In Chapter 6, the linear stability analysis and the base state flow is carried out and the numerical method used to solve the plane parallel flow for symmetric magnetic fluids is presented. The results are presented for two different configurations of applied fields, following [44, 62]. In Part III, the Plateau-Rayleigh instability problem is presented. In chapter 9, the inviscid and viscous Plateau-Rayleigh instability for the hypotheses of long wavelengths are derived. A numerical solution for the non-linear problem is obtained and compared with [69]. In Chapter 10, the long wave approximation of the Plateau-Rayleigh instability for super-paramagnetic fluids is presented. The linear stability is compared with [33] and the non-linear numerical approach is compared with [66]. In chapter 11, the non-linear governing equations for the long wavelengths approximation of the Plateau-Rayleigh instability for magnetic fluids are derived. The numerical solution of this approach is use to study the pinch-off and perform the stability analysis. Finally, a discussion and some directions for future work are presented in Chapters 7 and 12.

CHAPTER 2

THE EQUATIONS OF HYDRODYNAMICS

In this chapter, we present the set of equations that govern the flow of a fluid. We follow the classical references which give us tools to carry out the proposed research.

2.1 Preliminaries

We start with the work done by Osborne Reynolds in his famous paper [49], and with Fig. (2.1) where a sketch of the experiment done by him is shown.

Reynolds' experiment (1883) has shown the existence of two types of flow, laminar flow and turbulent flow. The objective of the experiment was to visualize the water flow pattern through a glass tube with the help of a tracer (dye). As illustrated in Fig. (2.1), a glass tube, at the end of which a convergent tube is fitted, is kept within a reservoir and linked to an external system containing a valve, which has the function of regulating the flow. A coloring liquid is injected into the tube that makes it possible to visualize the flow patterns.

For small flow rates the coloring liquid forms a continuous thread parallel to the axis of the tube, see Fig. (2.2) (a). Higher flow rates induce oscillations that are amplified as the flow rate increases until it ends with the disappearance of the thread, that is, a complete mixing inside the glass tube of the coloring liquid, indicating that the thread was diluted by the flow. It is possible to conclude that two different types of flow occur and that the two types are separated by a transition. In the first case, in which colored threads are observed, it is concluded that the particles travel without transverse agitation, maintaining the cylindrical shape with which it was generated. In the second case, the particles have important transversal speeds, since the thread disappears due to the dissolution of the

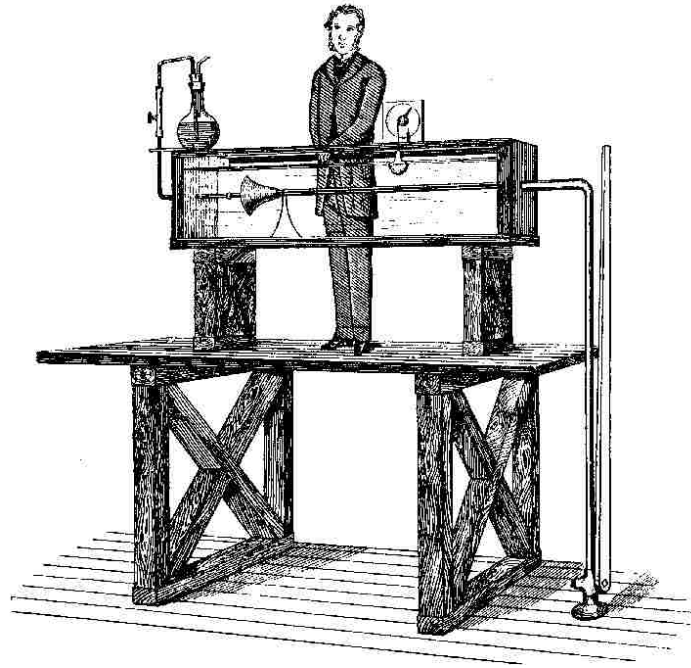


Figure 2.1: Sketch of the experiment done by Osborne Reynolds, taken from his 1883 paper [49].

particles in the water volume, see Fig. (2.2) (c).

For a laminar flow, the fluid moves in parallel layers, that slide relative to one another. In this regime, any tendency for instability is dampened by viscous shear forces. For turbulent flow, the particles present a chaotic movement at the macroscopic level, that is, the velocity has components that are transversal to the dominant direction of the fluid flow.

The transition between these two regimes happens when inertial effect are large enough to prevent the viscous dissipation of local instabilities of the flow. Non linear inertial mechanisms amplify these disturbances and destroy the ordered laminar flow structure and then unsteady disordered motion dominates the dynamics of the flow. The parameter identifying the transition is the Reynolds number, which is given by,

$$Re = \frac{\text{Inertial Forces}}{\text{Viscous Forces}} = \frac{\rho U D}{\eta},$$

where ρ is the density of the fluid, U is the average velocity of the tube, D is the diameter of the tube and η is the dynamic viscosity of the fluid, in Reynolds experiment. In other flows, the parameters change accordingly, but it is always inertial effects and viscous effects that determine the transition. For example, for the flow between parallel plates the Reynolds number is defined in Section 5.1.

We can now intuitively understand that if a fluid maintains its velocity profile as time

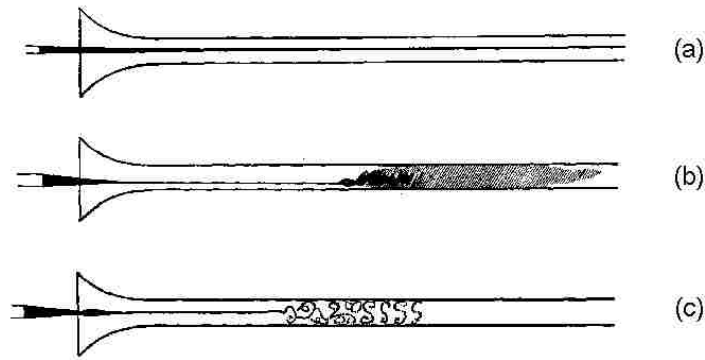


Figure 2.2: Sketch of the three different types of flow classified by Reynolds's work [49]. a) Laminar b) transitional and c) Turbulent.

evolves will be called stable, and if it changes to another type of flow we will call this type of flow unstable.

The natural question we can ask ourselves at this moment is whether we can explain these phenomena from the dynamic point of view.

2.2 Conservation Equations

In this section, we are going to define the equations that govern the flow of fluids, for this, we are going to start with the continuum hypotheses. In general, a fluid is a material that deforms continuously when subjected to a shear stress [4].

The continuum hypotheses gives us a clear idea of what is the concept of continuous deformation [4]. In a context of continuum mechanics, we deal with the macroscopic properties of the medium, for example: temperature, velocity, pressure, specific mass and others. These properties are taken as average values found in elements of volume with a large dimension compared to the free mean path of the molecules, so that these dimensions are large enough to allow that the discontinuity effects of matter do not appear, but in such a way that these dimensions are small compared to the dimension of the medium. By accepting the continuum hypotheses, we admit that the elements of volume, of infinitesimal dimensions, contain a large number of molecules. Consequently, the medium is considered as a continuum, so that the differential and integral calculus machinery can be applied and their properties defined point by point.

The Knudsen number K_n is the dimensionless physical parameter to verify the validity of the continuum hypotheses and is defined as:

$$K_n = \frac{\lambda}{L}, \quad (2.1)$$

where λ is the molecular free mean path and L is a representative macroscopic scale of the flow. If the Knudsen number is close to one, this means that the molecular mean free path is comparable to the length scale, $K_n \sim 1$, so that the hypotheses is not a good approach, problems of this type belong to the area of statistical mechanics. If the Knudsen number is much less than one, $K_n \ll 1$, the continuum hypotheses is strictly valid and its study is focused on classical fluid mechanics.

The fluid flow is governed by a set of balance equations: the continuity equation, the linear momentum equation, the angular momentum equation and the energy equation. In this work, we do not consider effects of temperature changes, so that in the isothermal case, the later is not needed. In the following, we present a brief deduction of the other equations. The reader interested in a more detail derivation of these equations is invited to check reference [4].

In what follows, we are going to determine how an intensive¹ property of the fluid varies when it is limited to a control volume of the analyzed system. In order to do this, we are going to use the *Leibniz's Rule* [27], for a real function $f(x, t)$ defined in a rectangle $R = [a, b] \times [c, d] \in \mathbb{R} \times \mathbb{R}$, integrable in x for $t \in \mathbb{R}$, then the temporal derivative of the integral quantities can be written as

$$\frac{d}{dt} \int_a^b f(x, t) dx = \int_a^b \frac{\partial f(x, t)}{\partial t} dx, \quad (2.2)$$

for constant integration limits. For integration limits depending on time, the result is obtained in the following form,

$$\frac{d}{dt} \int_{a(t)}^{b(t)} f(x, t) dx = \int_{a(t)}^{b(t)} \frac{\partial f(x, t)}{\partial t} dx + f(b(t), t)b'(t) - f(a(t), t)a'(t). \quad (2.3)$$

Considering a function described in terms of a control volume $V \in \mathcal{R}$, where \mathcal{R} is a continuous euclidean space, so that this volume is time dependent, since its boundaries S are deformable. Therefore, we obtain *Leibniz's theorem* as being

$$\frac{d}{dt} \int_{V(t)} f(x, t) dV = \int_{V(t)} \frac{\partial f(x, t)}{\partial t} dV + \int_{S(t)} f(x, t) u_k n_k dS \quad (2.4)$$

where $u_k n_k$ is the inner product between the velocity field \mathbf{u} , with components u_k , $k = 1, 2, 3$, and the unitary vector \mathbf{n} , with components n_k , $k = 1, 2, 3$, that is normal to the surface S . By Eq. (2.4), the *Leibniz's rule* reduces to the *Reynolds's transport theorem* where (\cdot) denotes any intensive fluid property

$$\frac{d}{dt} \int_V (\cdot) dV = \int_V \frac{\partial (\cdot)}{\partial t} dV + \int_S (\cdot) \mathbf{u} \cdot \mathbf{n} dS. \quad (2.5)$$

¹An intensive property is independent of the amount of mass. The value of an extensive property varies directly with the mass.

Therefore, we can find the mass conservation equation by taking $(\cdot) = \rho$, where ρ is the fluid density:

$$\frac{d}{dt} \int_V \rho dV = \int_V \frac{\partial \rho}{\partial t} dV + \int_S \rho \mathbf{u} \cdot \mathbf{n} dS. \quad (2.6)$$

Using the divergence theorem [3] on the second term of right side,

$$\frac{Dm}{Dt} = \int_V \frac{\partial \rho}{\partial t} dV + \int_V \nabla \cdot (\rho \mathbf{u}) dV. \quad (2.7)$$

Expression above with m constant give us,

$$\int_V \left(\frac{\partial \rho}{\partial t} + \nabla \cdot (\rho \mathbf{u}) \right) dV = 0. \quad (2.8)$$

This expression is valid for an arbitrary volume V , then by applying the Du Bois-Raymond lemma [3],

$$\frac{\partial \rho}{\partial t} + \nabla \cdot (\rho \mathbf{u}) = 0, \quad (2.9)$$

If a flow is incompressible, then ρ is constant and we get the continuity equation:

$$\nabla \cdot \mathbf{u} = 0. \quad (2.10)$$

We know that the movement of rigid bodies (Material points) is governed by the Newton's second law,

$$\sum \mathbf{F} = m \mathbf{a}, \quad (2.11)$$

or, equivalently,

$$\sum \mathbf{F} = m \frac{d\mathbf{u}}{dt}, \quad (2.12)$$

that is a of first order ODE if we write it in terms of the velocity \mathbf{u} of a body. A generalization for a fluid is carried out by taking into account that a fluid is a material that is deformed continuously under the presence of forces. In fact, the fluids acquire the shape of the container where they are and do not have a preferred configuration. Fluids can be found in nature as liquid, gas and plasma state. Hence, to describe mathematically the flow of a fluid, we are going to consider a fluid as a set of particles (material points) and we are going to apply Newton's second law to describe their individual movement.

In a context of fluid dynamics, it is possible to describe the properties of the fluid particles, that is, position, velocity, density, temperature, etc. The process of determining these instantaneous properties is difficult. This is know as Lagrangian description. On the other hand, the Eulerian description uses a fixed frame of reference, and the particles that pass through a point assume the properties of this particular point.

In what follows, we are going to adapt the above discussion to Newton's second law. Firstly, we define the operator material derivative, when applied to a property of a particle

of the medium that moves with velocity \mathbf{u} , give us as a result the total derivative in relation to the time of the property of that particle in movement, the expression is given by:

$$\left. \frac{d}{dt} \right|_{\text{Lagrangian}} = \frac{\partial}{\partial t} + \frac{\partial}{\partial x} \frac{dx}{dt} + \frac{\partial}{\partial y} \frac{dy}{dt} + \frac{\partial}{\partial z} \frac{dz}{dt} = \frac{D}{Dt}, \quad (2.13)$$

or using a vector notation,

$$\frac{D(\cdot)}{Dt} = \frac{\partial(\cdot)}{\partial t} + (\mathbf{u} \cdot \nabla)(\cdot). \quad (2.14)$$

Then, dividing by a volume V , Newton's second law (2.12) for each fluid particle is written as

$$\rho \left(\frac{\partial \mathbf{u}}{\partial t} + \mathbf{u} \cdot \nabla \mathbf{u} \right) = \sum \mathbf{f}. \quad (2.15)$$

The forces acting on the fluid particles can be divided in two types: field forces, that have remote action, for example, gravity, electromagnetic forces, etc., by example $\mathbf{f}_f = \rho \mathbf{g}$, and surface forces \mathbf{f}_s , that are related to contact, for example, friction. Hence the forces acting on the fluid particle can be written as:

$$\sum \mathbf{f} = \mathbf{f}_s + \mathbf{f}_f. \quad (2.16)$$

Finally, the angular momentum equation can also be derived in terms of first principles [4]. In the case of Newtonian fluids, the angular momentum equation implies the symmetry of stress tensor (see Section 2.3). For the case of magnetic fluids, the angular momentum equation is still a matter of discussion [44, 33] and, we will postpone the derivation of this equation to Chapter 3.

2.3 Stress Tensors

From the mechanics of continuum media, we can write the surface forces as,

$$\mathbf{f}_s = \nabla \cdot \boldsymbol{\sigma}, \quad (2.17)$$

with $\boldsymbol{\sigma}$ being the stress tensor of the fluid. Replacing Eq. (2.17) in Eq. (2.15) and (2.16), we obtain

$$\rho \frac{D\mathbf{u}}{Dt} = \nabla \cdot \boldsymbol{\sigma} + \rho \mathbf{g}, \quad (2.18)$$

which is known as the Cauchy equation describing the motion of the fluid.

Equations for $\boldsymbol{\sigma}$ describes the material and they are called constitutive equations. They are proposed based in experimental observations and theoretical hypotheses. Written in another reference system a constitutive equation must not change its form, this condition is known as material frame indifference (MFI) and a constitutive equations satisfying the MFI principle are called objective.

For a Newtonian and incompressible fluids, the stress tensor $\boldsymbol{\sigma}$ is given by,

$$\boldsymbol{\sigma} = -p\mathbf{I} + \eta (\nabla\mathbf{u} + (\nabla\mathbf{u})^t), \quad (2.19)$$

where p is the pressure and \mathbf{I} is the identity tensor, forming the isotropic part of the stress tensor and the second term on right-hand side, is the deviatoric part of the stress tensor where η is the dynamic viscosity of the fluid and the superscript t indicates the transpose of a tensor quantity, associated with the shear stresses acting over the material.

By taking the Newton's second law (2.15) with (2.16) in consideration and by developing the divergence of (2.19) with the aid of the continuity equation (2.10), we can find

$$\rho \left(\frac{\partial\mathbf{u}}{\partial t} + \mathbf{u} \cdot \nabla\mathbf{u} \right) = \nabla p + \eta \nabla^2\mathbf{u} + \rho\mathbf{g}. \quad (2.20)$$

This is the Navier-Stokes equation. This equation represents the conservation law of momentum of a fluid flowing in a given domain. In (2.20), we have three equations, in x , y and z -directions, however we have four variables, three from velocity components u , v and w and the pressure p to be determined, hence in order to close the full system we are going to require one additional equation: the mass conservation equation. So that, the flow of a fluid is governed by the following system of partial differential equations,

$$\begin{cases} \rho \left(\frac{\partial\mathbf{u}}{\partial t} + \mathbf{u} \cdot \nabla\mathbf{u} \right) = \nabla p + \eta \nabla^2\mathbf{u} + \rho\mathbf{g}, \\ \nabla \cdot \mathbf{u} = 0. \end{cases} \quad (2.21)$$

CHAPTER 3

MAGNETISM AND MAGNETIC FLUIDS

In this Chapter, we will present the main results about the fluid that is part of this study.

3.1 Ferrofluids

Ferrofluids are colloidal suspension of nano-sized ferromagnetic particles dispersed in a non-magnetic base liquid, that usually is a Newtonian fluid [30, 33]. They have a dark appearance and the ferro-magnetic particles are typically magnetite, cobalt, etc., with an average diameter of 10 nanometers. The base liquid can be oil, mineral oil, ester or kerosene [33].

For ferrofluids to be suitable for practical applications, they must be stable in relation to the formation of aggregates due to the attractive forces between the particles. The interaction between the particles occurs by several mechanisms, among them are: the van der waals forces and the magnetic force due to the interaction between the dipole moments of the particles. Short-range forces create aggregates in the suspension. To avoid this, a thin sheet of surfactant is applied on the surface of the magnetic particle, which acts as a repellent layer, preventing the formation of aggregates [21]. On the other hand, there are magnetoreological suspensions (SMR) synthesized as magnetizable microparticles, dispersed in a non-magnetizable base fluid. This class of magnetic suspensions is different from other ferrofluids due to the microscale size of the particles. In this way, SMR are not subject to the Brownian movement that is induced by molecular thermal agitation, so they are more unstable in relation to the formation of aggregates and with greater magnetic memory [14].

According to [33], the stability of a ferrofluid is preserved when the thermal energy kT associated with the Brownian movement is greater than or equal to the magnetic energy $\mu_0 M_d H v_p$, where k is the Boltzmann constant, T is the fluid temperature, μ_0 is the magnetic permeability of the vacuum, M_d is the magnetization of the solid part constituted by the particles, H is the intensity of the magnetic field and v_p is the volume of the particle. The maximum diameter of the spherical particles that satisfy the stability condition is determined by the following expression:

$$d \leq \left(\frac{6kT}{\pi\mu_0 M_d H} \right)^{1/3}, \quad (3.1)$$

which means that to guarantee the stability of a magnetic suspension, the magnetic particles must be small, for example approximately 10 nm.

The practical applications of fluid dynamics in engineering, until the last decades, were restricted to systems in which the magnetic and electric fields did not intervene. However, the combination of magnetic fields in polarized fluids attracted the attention of the scientific community for its promising applications in various areas of knowledge, see [36].

3.2 The Magneto-static Limit of Maxwell's Equations

3.2.1 The Maxwell's Equations

The Maxwell's equations are a set of four partial differential equations that govern electromagnetic theory that related electrical and magnetic quantities [18]. These quantities are given by: the electric displacement vector \mathbf{D}_e , the free charge density ρ_e , the intensity vector or density of magnetic flux vector \mathbf{B} , with Tesla units [T], the current density or current flux vector \mathbf{J} , the electric field vector \mathbf{E} and the intensity of magnetic field \mathbf{H} .

The equations are given by Gauss's Law of the electricity, Gauss's law of the magnetism, Ampère's law and Faraday's law, which are given by:

$$\begin{aligned} \nabla \cdot \mathbf{D}_e &= \rho_e && \text{Maxwell Gauss's First Law} \\ \nabla \cdot \mathbf{B} &= 0 && \text{Maxwell Gauss's Second's Law} \\ \nabla \times \mathbf{H} &= \mathbf{J} + \frac{\partial \mathbf{D}_e}{\partial t} && \text{Ampère's Law} \\ \nabla \times \mathbf{E} &= -\frac{\partial \mathbf{B}}{\partial t} && \text{Faraday's Law} \end{aligned}$$

3.2.2 The Magnetostatic Limit

In the context of ferrohydrodynamics, only the magnetic quantities are considered and the electrical quantities are not involved when a magnetic fluid is flowing, that is, the free

current density \mathbf{J} , the electric displacement \mathbf{D}_e and the applied electric field \mathbf{E} are zero. These simplifications correspond to the magnetostatic limit of the Maxwell's equations [33, 59], and generates the following set of equations:

$$\frac{\partial \mathbf{B}}{\partial t} = \mathbf{0}, \quad (3.2)$$

$$\nabla \cdot \mathbf{B} = 0, \quad (3.3)$$

$$\nabla \times \mathbf{H} = \mathbf{0}. \quad (3.4)$$

3.3 The Boundary Conditions

In this section, the conditions that must be satisfied by the magnetic vector fields in the interface between two media with different magnetic properties will be determined.

Consider two fluids with different magnetic properties called fluids 1 and 2 and the interface between them, as an example two magnetic permeabilities μ_1 and μ_2 respectively for each fluid. Let's consider an infinitesimal volume containing part of the domain of the *fluid*₁, the interface and the *fluid*₂. We are going to analyze the flux of the magnetic induction field \mathbf{B} and the applied field \mathbf{H} , so that we can understand what happens across the boundary that divides the two media.

In order to determine the condition for the magnetic induction \mathbf{B} , consider a cylindrical volume δV , in which the upper and lower face forms a disk of radius r , height ϵ and total area δS . Consider the vector fields \mathbf{B}_1 and \mathbf{B}_2 crossing the regions of *fluid*₁ and *fluid*₂ respectively, as the Fig. (3.1) shows.

Applying Gauss's theorem to volume δV and vector field \mathbf{B} , we obtain an equivalent expression for the closed surface as follow,

$$0 = \int_{\delta V} \nabla \cdot \mathbf{B} dV = \oint_{\delta S} \mathbf{B} \cdot \hat{\mathbf{n}} dS, \quad (3.5)$$

in which $\hat{\mathbf{n}}$ is the exterior normal vector to the surface. From Maxwell's equations in the magneto-static limit, Eq. (3.3), the analysis is reduced to calculate the normal component of \mathbf{B} on the upper, lower and lateral faces.

$$\oint_{\delta S} \mathbf{B} \cdot \hat{\mathbf{n}} dS = \oint_{\text{lateral Area}} \mathbf{B} \cdot \hat{\mathbf{n}} dS + \oint_{\text{Upper Area}} \mathbf{B}_2 \cdot \hat{\mathbf{n}} dS + \oint_{\text{Lower Area}} \mathbf{B}_1 \cdot \hat{\mathbf{n}} dS. \quad (3.6)$$

Calculating the close integral of the lateral side:

$$\oint_{\text{lateral Area}} \mathbf{B} \cdot \hat{\mathbf{n}} dS \leq \oint_{\text{lateral Area}} |\mathbf{B} \cdot \hat{\mathbf{n}}| dS = \oint_{\text{lateral Area}} 1 dS |\mathbf{B}| |\hat{\mathbf{n}}| \cos(\theta) = 2\pi r \epsilon |\mathbf{B}|.$$

We are going to consider ϵ small in order to approximate our geometry to the interface so that we can neglect the lateral influence of the magnetic induction \mathbf{B} . Geometrically, the

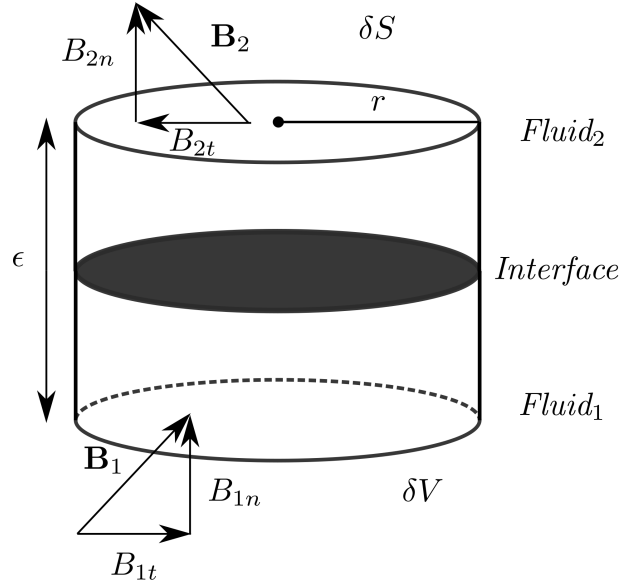


Figure 3.1: The sketch represents the cylindrical infinitesimal volume δV in the interface between two magnetic fluids, $fluid_1$ and $fluid_2$ with their respective magnetic induction field \mathbf{B}_1 and \mathbf{B}_2 .

normal vector is in the same direction of \mathbf{B}_2 and in the opposite direction of \mathbf{B}_1 .

$$\int_{\delta S} \mathbf{B} \cdot \hat{\mathbf{n}} dS = \int_{\text{Upper Area}} \mathbf{B}_2 \cdot \hat{\mathbf{n}} dS - \int_{\text{Lower Area}} \mathbf{B}_1 \cdot \hat{\mathbf{n}} dS, \quad (3.7)$$

Again, from the geometry we consider both faces are the disk of radius r and doing ϵ tend to zero the contribution of this integral is negligible, we can express,

$$\int_{\text{Upper Area}} (B_{2n} - B_{1n}) dS = 0. \quad (3.8)$$

This leave us to conclude that the normal components of \mathbf{B}_1 and \mathbf{B}_2 have to maintain continuity in the interface:

$$B_{1n} = B_{2n}. \quad (3.9)$$

An equivalent expression is given by:

$$(\mathbf{B}_1 - \mathbf{B}_2) \cdot \hat{\mathbf{n}} = 0. \quad (3.10)$$

In order to determine the condition for the applied magnetic \mathbf{H} , we use the Stokes's Theorem to a closed orientated curve C and the applied magnetic field \mathbf{H} , as the Fig. (3.2) shows. In this expression the integral over the closed contour is zero by using the magneto-static limit Eq. (3.4) for the applied magnetic field \mathbf{H} . Using Stokes theorem, we obtain that:

$$0 = \int_S (\nabla \times \mathbf{H}) \cdot \hat{\mathbf{n}} dS = \oint_C \mathbf{H} \cdot \hat{\mathbf{t}} dC. \quad (3.11)$$

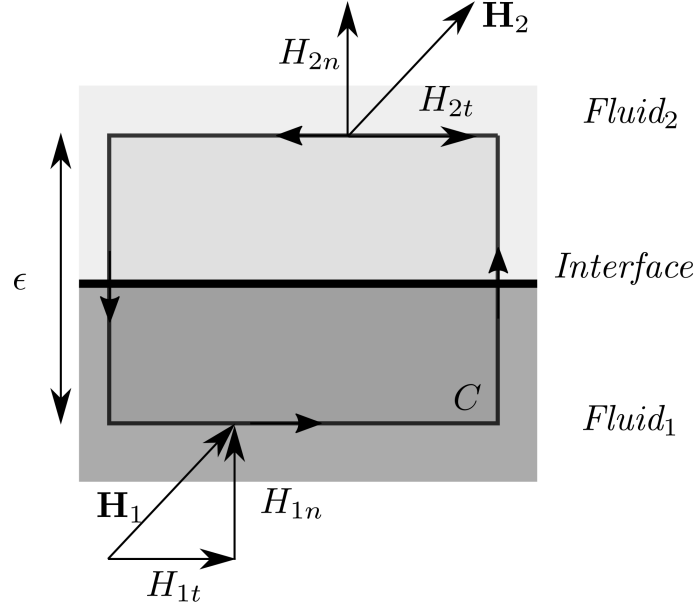


Figure 3.2: The sketch represents the closed orientated path in the interface between two magnetic fluids, $fluid_1$ and $fluid_2$ with their respective applied magnetic fields \mathbf{H}_1 and \mathbf{H}_2 .

The analysis is reduced to calculate the tangential component of \mathbf{H} on the upper, lower and lateral faces.

$$\oint_C \mathbf{H} \cdot \hat{\mathbf{t}} dC = \int_{\text{lateral sides}} \mathbf{H} \cdot \hat{\mathbf{t}} dC - \int_{\text{Upper side}} \mathbf{H}_2 \cdot \hat{\mathbf{t}} dC + \int_{\text{Lower side}} \mathbf{H}_1 \cdot \hat{\mathbf{t}} dC. \quad (3.12)$$

From the orientation of the curve the orientation of \mathbf{H}_2 in the tangential direction is negative and for \mathbf{H}_1 it is maintained positive. Calculating the integral in the lateral faces, we get

$$\int_{\text{lateral sides}} \mathbf{H} \cdot \hat{\mathbf{t}} dC \leq \int_{\text{lateral sides}} |\mathbf{H} \cdot \hat{\mathbf{t}}| dC = \int_{\text{lateral sides}} 1 dC |\mathbf{H}| |\hat{\mathbf{t}}| |\cos(\theta)| = 2|\mathbf{H}|\epsilon. \quad (3.13)$$

By the geometry of our contour, as we tend ϵ to zero, and we can neglect the contribution of the integral in Eq. (3.13) and we obtain:

$$\int_C (H_{2t} - H_{1t}) dC = 0 \quad (3.14)$$

that let us conclude,

$$H_{1t} = H_{2t}. \quad (3.15)$$

Or an equivalent expression can be,

$$\hat{\mathbf{n}} \times (\mathbf{H}_1 - \mathbf{H}_2) = 0. \quad (3.16)$$

Therefore, the boundary magnetic conditions are given by the continuity of the normal induction Eq. (3.10) and tangential applied field Eq. (3.16).

3.4 The Magnetization

In this section, we are going to define a local mean property of ferrofluids, the magnetization in the macroscopic sense. For this we are going to define the magnetic dipole moment or also called the magnetic moment, which comes from the nano-scale properties of the diluted particles in a colloidal magnetic suspension. We follow the development made by [6].

The magnetic dipole moment \mathbf{m} is defined by considering a close path with transversal area ΔA , with an electric current flux I constant. By definition, the magnetic dipole moment associated to this path, is given by

$$\mathbf{m} = I\Delta A \hat{\mathbf{n}}, \quad (3.17)$$

in which $\hat{\mathbf{n}}$ is the unitary normal vector to ΔA , defined by the direction of the electric current. Let's consider the magnetic dipole moments distributed in homogeneous statistically form and independent of the material volume δV , made up of a sufficiently large number of magnetic particles, in this form the mean value of dipole moments in δV has small variations in the scale ΔV . Then, by the ergodicity hypothesis, the volumetric mean value of the dipole moments is equivalent to the mean of the probability distribution associated to the dipoles moments of the particles in δV . Thus, the magnetic moments mean volumetric value distributed in δV is defined as,

$$\langle \mathbf{m} \rangle(\mathbf{x}, t) = \lim_{\delta V' \rightarrow \delta V} \frac{1}{\delta V'} \int_{\delta V'} \mathbf{m}(\mathbf{y}, t) dV, \quad (3.18)$$

where \mathbf{x} is a fixed position in the material volume δV , and \mathbf{y} is a mobile position inside of the infinitesimal volume, that allows to calculate the mean local property value, being able to be in the base fluid or particle domain, as in Fig. (3.3).

To avoid temporal dependence in (3.18), we consider a volumetric mean for a determined time t of equilibrium or permanent regime.

Now, as in Fig. (3.3), we can decompose the volume δV as the union of two sets, the first containing the base fluid and the second containing the volume of the magnetic particles. Let's consider N the number of magnetic particles in δV with particle volume v_p . Splitting the integral (3.18) in two integrals, one over the base fluid part δV_{fluid} and the other in over the magnetic particles,

$$\langle \mathbf{m} \rangle(\mathbf{x}) = \lim_{\delta V' \rightarrow \delta V} \frac{1}{\delta V'} \left(\int_{\delta V_{\text{fluid}}} \mathbf{m}(\mathbf{y}) dV + \int_{\sum_{k=1}^N v_p^k} \mathbf{m}(\mathbf{y}) dV \right). \quad (3.19)$$

The first integral takes into account the carrier fluid and since it is not magnetizable, $\mathbf{m}(\mathbf{y}) = 0$ for each $\mathbf{y} \in \delta V_{\text{fluid}}$. Therefore, the magnetization is concentrated in the magnetic

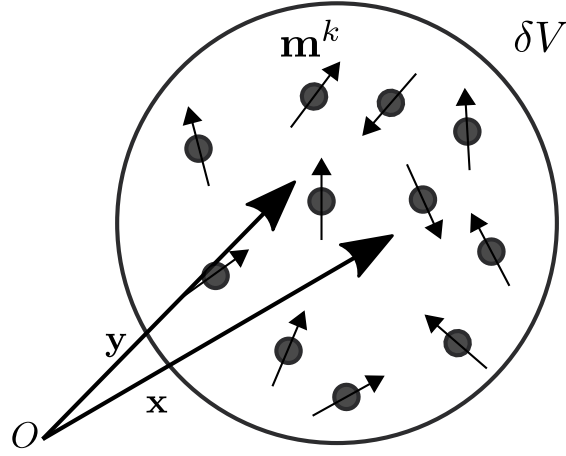


Figure 3.3: Figure shows a representation of a volume δV of a magnetic suspension, with the magnetic nano-particles k has associated a dipole moment \mathbf{m}^k represented by a vector.

particles and is given by:

$$\langle \mathbf{m} \rangle(\mathbf{x}) = \lim_{\delta V' \rightarrow \delta V} \frac{1}{\delta V'} \int_{\sum_{k=1}^N v_p^k} \mathbf{m}(\mathbf{y}) dV. \quad (3.20)$$

Considering that the particle k has a dipole moment \mathbf{m}^k as in Fig. (3.3), and that all magnetic particles have the same v_p :

$$\langle \mathbf{m} \rangle(\mathbf{x}) = \frac{1}{\delta V} \sum_{k=1}^N \mathbf{m}^k v_p, \quad (3.21)$$

the summation can be converted into a mean if we divide it by N . Consequently, defining $N/\delta V$ as being the particles density number n and the magnetisation at \mathbf{x} can be given by:

$$\langle \mathbf{m} \rangle(\mathbf{x}) = n v_p \bar{\mathbf{m}}, \quad (3.22)$$

where $\bar{\mathbf{m}}$ is the mean value of the dipole moments, and is given by:

$$\bar{\mathbf{m}} = \frac{1}{N} \sum_{k=1}^N \mathbf{m}^k. \quad (3.23)$$

Alternatively, $\phi = n v_p$ is the volumetric fraction of the particles in δV .

We can now define the local magnetization \mathbf{M} of a ferrofluid as being given by the mean moment of dipole of the particles divided by the volume v_p , that is:

$$\mathbf{M} := \frac{\langle \mathbf{m} \rangle}{v_p} = n \bar{\mathbf{m}}, \quad (3.24)$$

where $\bar{\mathbf{m}}$ is the component of the mean magnetic moment per particle along the field direction.

If the mean value $\langle \mathbf{m} \rangle$ is zero, that is, each particle is aligned in a different direction, then $\mathbf{M} = 0$. If all the particles are aligned in the direction of the field, then the magnetization of the suspension reaches the saturation of magnetization \mathbf{M}_s . In this case,

$$\mathbf{M}_s = n\bar{\mathbf{m}}_s, \quad (3.25)$$

We define the magnetization of the solid material \mathbf{M}_d , composed by the particles.

$$\mathbf{M}_d = \frac{\bar{\mathbf{m}}_s}{v_p}, \quad (3.26)$$

now combining this equation with (3.24), we have:

$$\mathbf{M}_s = n\bar{\mathbf{m}}_s = nv_p\mathbf{M}_d = \phi\mathbf{M}_d,$$

from where we obtain:

$$\mathbf{M}_s = \phi\mathbf{M}_d. \quad (3.27)$$

Since a magnetic fluid is a suspension of magnetic particles, it is convenient to define the saturation magnetization of the medium as a function of both the magnetization solid material \mathbf{M}_d , as well as the volumetric fraction ϕ of suspended magnetic particles, as in Eq. (3.27) and we can infer that the saturation of magnetization of the continuous liquid medium corresponds to a percentage of the magnetization of the suspended magnetic solid.

3.5 The magnetization of a Ferrofluid

3.5.1 The equilibrium Magnetization

The magnetization of equilibrium describes the state of a magnetizable medium at rest, where all the magnetic dipole moment of the particle suspended in the base fluid were oriented partially in the direction of the applied magnetic field and reach a permanent regime. When the magnetic dipole moments of the suspension are totally orientated in the direction of the applied magnetic field, the magnetization of the medium reach its maximum value, named the magnetization of saturation \mathbf{M}_s , as in Eq. (3.27). In this manner, the magnetization of equilibrium is limited by the magnetization of saturation, $M_0 \leq M_s$.

The mean of the magnetic dipole moments $\langle \mathbf{m} \rangle$ can be theoretically calculated from the angular density function of probability P_θ , such that for a collection of N particles with independent magnetic dipole moments, the number of particles in the configuration between θ and $\theta + d\theta$ is given by the probability $P_\theta d\theta$, with θ the angle that a determined vector magnetic moment \mathbf{m} of a particle causes the applied field \mathbf{H} . Thus, considering that the mean $\bar{\mathbf{m}}$ satisfies the previous conditions and from of the discrete definition of $\bar{\mathbf{m}}$ expressed

in equation (3.23), the mean of standard probability in integral form is given by Rosensweig [33]:

$$\bar{\mathbf{m}} = \hat{e}_H \int_0^\theta (m \cos \theta) P_\theta(\theta) d\theta. \quad (3.28)$$

where $\hat{e}_H = \mathbf{H}/|\mathbf{H}|$. For magnetic moments with independent orientations, a normalized probability density function $P(\theta)$, with $\int P(\theta) d\theta = 1$ in all the interval θ , is typically a distribution given by McQuarrie (1976) with exponential factor of Boltzmann:

$$P(\theta) = \frac{1}{2} \sin \theta \exp\left(-\frac{E}{kT}\right). \quad (3.29)$$

In this context, E corresponds to the energy needed to misalign the magnetic dipole moment \mathbf{m} of its alignment parallel, or preferential, with the magnetic field applied \mathbf{H} .

Being $dE = T_m d\theta$ and $T_m = mH \sin \theta$ the intensity of the magnetic torque per unit of particle volume. The intensity of the magnetic dipole moments is considered m equal for all suspended particles, however, due to variations in orientation of m of each particle, it is necessary that the calculation of the average probability given by equation (3.28) is performed for arbitrary orientations. The given integral solution in (3.28), for the probability density $P(\theta)$ of magnetic dipole moments independent orientations, results in:

$$\bar{\mathbf{m}} = \mathbf{m} (\coth \alpha_h - \alpha_h^{-1}) = \mathbf{m} \mathcal{L}(\alpha_h). \quad (3.30)$$

where the Langevin function $\mathcal{L}(\alpha)$ being the average result, coming from the condition that the magnetic dipole moments of the suspended particles were not necessarily oriented towards the applied magnetic field.

The dimensionless parameter

$$\alpha_h = mH/kT, \quad (3.31)$$

represents the ratio between the magnetic forces $F_m \sim mH/l$ and Brownian forces $F_B \sim kT/l$, where l is a characteristic suspension length scale, for example, the diameter of the suspended particles. Overall, the equilibrium magnetization of a magnetic fluid is well described by the Langevin equation, as shown by Odenbach [30]:

$$\frac{M_0}{M_s} = \coth \alpha_h - \alpha_h^{-1} = \mathcal{L}(\alpha_h). \quad (3.32)$$

Substituting Eq. (3.27) in (3.32), provides:

$$\frac{M_0}{M_d} = \phi \mathcal{L}(\alpha_h). \quad (3.33)$$

From an analysis of equation (3.31) it is possible to infer that $\alpha_h \gg 1$ describes the case in which the external field dominates the movement of the particles, which do not present relevant response to the thermal fluctuations of the Brownian movement and remain aligned

towards the applied field. If $\alpha_h \ll 1$ the suspension has a magnetization very small due to the influence of the Brownian forces and the magnetic moments have a distribution of random orientations. In such cases, it is possible to represent the Langevin function by a Taylor series around α_h in the form,

$$\mathcal{L}(\alpha_h) = \frac{\alpha_h}{3} - \frac{\alpha_h^3}{45} + \frac{2\alpha_h^5}{945} + \dots, \quad (3.34)$$

with the limit $\mathcal{L}(\alpha_h) \approx \alpha_h/3$ representing the condition of fluid paramagnetism.

This last expression is the model for the equilibrium magnetization of Langevin.

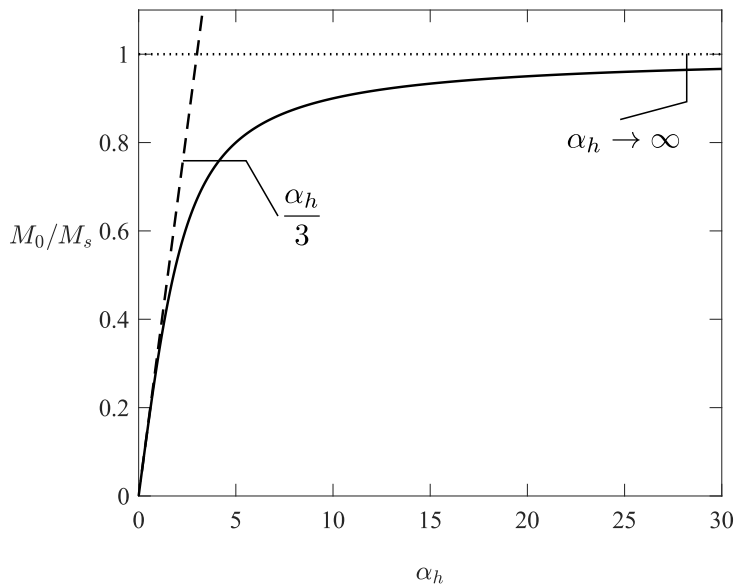


Figure 3.4: Figure shows the Langevin function (solid-line) and the equilibrium magnetization values plotted for small values of α_h , with the asymptotic solution for $\alpha_h \ll 1$: $M_0/\phi M_d = \alpha_h/3$ in a regime paramagnetic.

3.6 The Magnetic Relaxation Time

The magnetic relaxation time τ is another physical parameter, which is the time scale in which the material relaxes until it reaches its equilibrium magnetization \mathbf{M}_0 .

The *Brownian* relaxation time, τ_B , that involve the rotation of the magnetic particle together with its fixed dipole moment and is given by

$$\tau_B = \frac{3\eta_0 \bar{v}_p}{k_B T}. \quad (3.35)$$

In this expression, \bar{v}_p is the total particle volume, including the surfactant layer that avoids the formation of aggregates, η_0 is the viscosity of the carrier fluid, k_B is the Boltzmann constant and T is the absolute temperature of the fluid.

The *Néel* relaxation time, τ_N , whose dipole moment rotates freely relative to the particle and is given by:

$$\tau_N = f_0^{-1} \exp\left(\frac{K v_p}{k_B T}\right). \quad (3.36)$$

In this expression, K is the anisotropic constant of the particle, f_0 is the *Lamour* frequency of the magnetic moment and its value is approximately 10^9 s^{-1} , and represents a phenomenon of quantum characteristic, this time scale is out of the scope of continuum mechanics.

From both expression (3.35) and (3.36), it is clear that for a smaller particles the Néel time is much smaller than the Brownian time $\tau_N \ll \tau_B$, but considering a larger particles, the Brownian time is much less than the Néel time, that is $\tau_b \ll \tau_n$, as shown in Fig. (3.5). When the $\tau_n \approx \tau_B$, the effective relaxation time τ_{eff} is given by:

$$\frac{1}{\tau_{\text{eff}}} = \frac{1}{\tau_B} + \frac{1}{\tau_N}. \quad (3.37)$$

In Fig. (3.5), the magnetic relaxation times are shown for the following data: $\eta_0 = 0.1 \text{ Pa s}$, 2 nm surfactant layer, absolute temperature $T = 300 \text{ K}$ and anisotropic constant $K_s = 100 \text{ kJ/m}^3$ and $K_s = 10 \text{ kJ/m}^3$

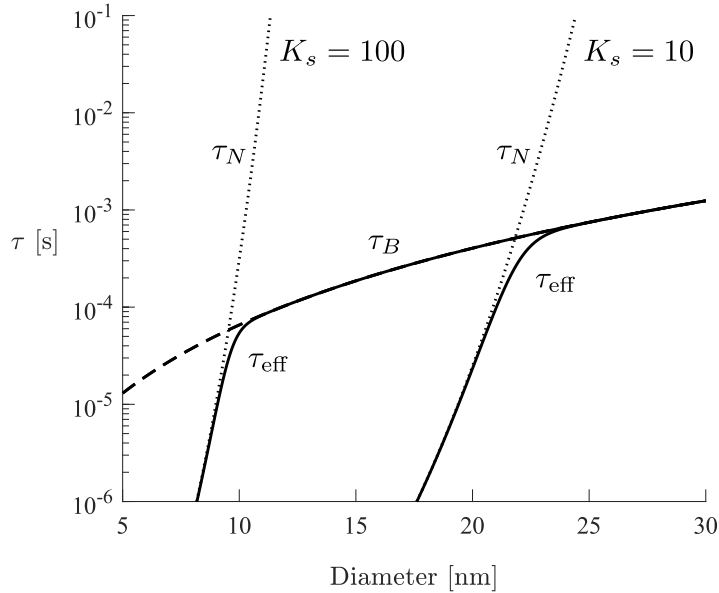


Figure 3.5: Figure shows Néel, Brownian and effective relaxation time using the formulas Eqs. (3.36), (3.35) and (3.37).

3.6.1 Out of the Equilibrium

In this section, we comment on some works in the direction of finding an evolution magnetization equation for a magnetic fluid flow. Initially, we must say that until today this is an open problem, and several works are on the way to consolidate this equation. Its derivation requires both experimental and theoretical knowledge in the topic of the continuum mechanics.

The first attempts were done by Shliomis in the works of (1967), (1968) and (1972) initially these works do not take the term of equilibrium magnetization that was deduced in Section (3.5.1). Later, we have the work of Felderhof (1999) in which the equilibrium magnetization term already intervenes and is valid for an incompressible fluid and an external applied fields of low intensity:

The model for the evolution equation was proposed by Shliomis (1974),

$$\frac{D\mathbf{M}}{Dt} = \boldsymbol{\Omega} \times \mathbf{M} + \frac{1}{\tau}(\mathbf{M}_0 - \mathbf{M}). \quad (3.38)$$

where τ is the magnetization relaxation time and \mathbf{M}_0 is the equilibrium magnetization and $\boldsymbol{\Omega} = \frac{1}{2}\nabla \times \mathbf{u}$. If this equation do not have the first term in the right-hand side, the referred differential indicates a growing as the function $\exp(-t/\tau)$ and the limit when time goes the function is close to the equilibrium magnetization \mathbf{M}_0 .

Later, it was proposed by Shliomis (2001),

$$\frac{\partial \mathbf{M}}{\partial t} + \mathbf{u} \cdot \nabla \mathbf{M} = -\frac{1}{\tau}(\mathbf{M} - \mathbf{M}_0) + \boldsymbol{\Omega} \times \mathbf{M} - \frac{\mu_0}{6\phi}(\mathbf{M} \times \mathbf{H}) \times \mathbf{M}. \quad (3.39)$$

In general, this equation is accepted by the scientific community, because it brings the most important phenomena when considering the flow of a magnetic fluid. The third term incorporates the viscous magnetic torques into the equation proposed by Felderhof (1999). The proposed equations for the evolution of magnetization described by the above equations were developed for an equivalent Brownian magnetic relaxation time τ_B . For an equivalent Néel magnetic relaxation time τ_N , the determination of the magnetization requires that the rotational speed effects of the internal magnetic dipole moment to the particle must be incorporated through an additional angular momentum balance equation, see [45].

3.7 The Magnetic Stress Tensor

The magnetic stress tensor, or the Maxwell stress tensor, provides a quantitative description of the field forces and also the surface forces density present in the magnetic fluid. Since ferrofluids are a colloidal suspension of magnetic nano-particles in a base fluid, this

behavior can be quantitatively described as the combination between the Newtonian part and the Magnetic part of the suspension.

$$\boldsymbol{\sigma} = \boldsymbol{\sigma}_h + \boldsymbol{\sigma}_m, \quad (3.40)$$

where $\boldsymbol{\sigma}_h$ is the tensor that incorporates the behavior of the Newtonian fluid and $\boldsymbol{\sigma}_m$ the Maxwell stress tensor, the latter incorporating the magnetic behavior of the nano-particles found in the colloidal suspension.

The next steps are in the direction of finding an expression for Maxwell's tensor of tensors $\boldsymbol{\sigma}_m$.

We consider a set V of magnetic dipoles around a point in the domain space. Brown's theorem [5] states that the distribution dipoles set in V is equivalent to a density distribution ρ_V and is given by:

$$\rho_V = -\mu_0 \nabla \cdot \mathbf{M}, \quad (3.41)$$

Once \mathbf{H} is a force per pole unit, the local density of force \mathbf{f} is:

$$\mathbf{f} = \rho_V \mathbf{H}. \quad (3.42)$$

This generates a magnetic force, where ρ_V is the magnetic dipole density. From the constitutive equation for the magnetic induction \mathbf{B} ,

$$\mathbf{B} = \mu_0 (\mathbf{H} + \mathbf{M}), \quad (3.43)$$

this expression together with the Maxwell's equation in the magnetostatic limit Eq. (3.3) leaves us to express the magnetic force density ρ_V in the following form,

$$\mu_0 \nabla \cdot \mathbf{H} = -\mu_0 \nabla \cdot \mathbf{M} = \rho_V. \quad (3.44)$$

Substituting ρ_V in Eq.(3.42), we deduce that:

$$\mathbf{f} = \mu_0 \mathbf{H}(\nabla \cdot \mathbf{H}), \quad (3.45)$$

and using vector identities in Eq. (3.45), it is possible to express it as:

$$\mathbf{f} = \nabla \cdot \left(-\frac{\mu_0 H^2 \mathbf{I}}{2} + \mu_0 \mathbf{H}\mathbf{H} \right). \quad (3.46)$$

This implies that the Maxwell stress tensor is given by,

$$\boldsymbol{\sigma}_m = -p_m \mathbf{I} + \mu_0 \mathbf{H}\mathbf{H}, \quad (3.47)$$

where $p_m = \mu_0 H^2/2$ is the magnetic pressure. It must be noticed that in a non-polarized media, where there is no magnetization, the magnetic induction \mathbf{B} takes the form $\mathbf{B} = \mu_0 \mathbf{H}$, which allows us to generalize the Maxwell stress tensor as;

$$\boldsymbol{\sigma}_m = -p_m \mathbf{I} + \mathbf{B}\mathbf{H}, \quad (3.48)$$

or since μ_0 is a constant, it can be manipulated to get $\mu_0 \mathbf{H}\mathbf{H} = \mathbf{H}(\mu_0 \mathbf{H})$ in Eq. (3.47), leaving us to modify (3.45) in order to obtain a second version of the Maxwell stress tensor,

$$\boldsymbol{\sigma}_m = -p_m \mathbf{I} + \mathbf{H}\mathbf{B}. \quad (3.49)$$

3.8 The Equations of Motion of a Ferrofluid

In this section, the equation for a magnetic fluid flow will be deduced. Let's consider an incompressible, barotropic and magnetic fluid flow described by the Cauchy equation given in (2.18). Substituting (3.40) in Eq. (2.18), we get:

$$\rho \frac{D\mathbf{u}}{Dt} = \nabla \cdot (\boldsymbol{\sigma}_h + \boldsymbol{\sigma}_m) + \rho \mathbf{g}. \quad (3.50)$$

The hydrodynamic part is well known and is given by the following expression:

$$\nabla \cdot \boldsymbol{\sigma}_h = \nabla \cdot (-p\mathbf{I}) + 2\mu \nabla \cdot \mathbf{D}, \quad (3.51)$$

where p is the pressure and \mathbf{D} is the deformation tensor, using Gibbs notation on the right-hand side of Eq.(3.51) allows to obtain:

$$\nabla \cdot \boldsymbol{\sigma}_h = -\nabla p + \mu \nabla^2 \mathbf{u}. \quad (3.52)$$

In order to complete the expression in Eq. (3.50), we develop the divergence of the magnetic stress tensor $\nabla \cdot \boldsymbol{\sigma}_m$, for this, we use the two formulation: **BH** and **HB** presented in Eq. (3.48) and Eq. (3.49) respectively.

Formulation BH

First, we start with the divergence of the magnetic stress tensor $\boldsymbol{\sigma}_m$ using the formulation **BH** in Eq. (3.48), which after some vector calculations is given by:

$$\nabla \cdot \boldsymbol{\sigma}_m = \mu_0 (\mathbf{M} \cdot \nabla) \mathbf{H}. \quad (3.53)$$

By consequence, the modified NSE for magnetic fluid flows for the formulation **BH** of the magnetic stress tensor is given by:

$$\rho \left(\frac{\partial \mathbf{u}}{\partial t} + \mathbf{u} \cdot \nabla \mathbf{u} \right) = -\nabla p + \eta \nabla^2 \mathbf{u} + \mu_0 (\mathbf{M} \cdot \nabla) \mathbf{H}. \quad (3.54)$$

The effect of the magnetic part is present in this equation in the term $\mu_0 (\mathbf{M} \cdot \nabla) \mathbf{H}$, which is known as the Kelvin force.

Formulation HB

We are going to take the divergence of $\boldsymbol{\sigma}_m$ using the formulation **HB** in Eq. (3.49),

$$\nabla \cdot \boldsymbol{\sigma}_m = \mu_0 [(\mathbf{H} \cdot \nabla) \mathbf{M} + \mathbf{M}(\nabla \cdot \mathbf{H}) + \mathbf{H}(\nabla \cdot \mathbf{H})] \quad (3.55)$$

Using the vector identity

$$\nabla \times (\mathbf{A} \times \mathbf{B}) = \mathbf{A}(\nabla \cdot \mathbf{B}) - \mathbf{B}(\nabla \cdot \mathbf{A}) + (\mathbf{B} \cdot \nabla)\mathbf{A} - (\mathbf{A} \cdot \nabla)\mathbf{B},$$

with $\mathbf{A} = \mathbf{M}$ and $\mathbf{B} = \mathbf{H}$,

$$\nabla \times (\mathbf{M} \times \mathbf{H}) = \mathbf{M}(\nabla \cdot \mathbf{H}) - \mathbf{H}(\nabla \cdot \mathbf{M}) + (\mathbf{H} \cdot \nabla)\mathbf{M} - (\mathbf{M} \cdot \nabla)\mathbf{H}. \quad (3.56)$$

Maintaining the first and third term of the right-hand side,

$$\mathbf{M}(\nabla \cdot \mathbf{H}) + (\mathbf{H} \cdot \nabla)\mathbf{M} = \mathbf{H}(\nabla \cdot \mathbf{M}) + (\mathbf{M} \cdot \nabla)\mathbf{H} + \nabla \times (\mathbf{M} \times \mathbf{H}). \quad (3.57)$$

Replacing this expression in Eq. (3.55) and using the information of the divergence of the magnetic induction Eq. (3.3)

$$\nabla \cdot \boldsymbol{\sigma}_m = \mu_0(\mathbf{M} \cdot \nabla)\mathbf{H} + \mu_0 \nabla \times (\mathbf{M} \times \mathbf{H}). \quad (3.58)$$

The second in the case of the formulation \mathbf{HB} , is given by the expression

$$\rho \left(\frac{\partial \mathbf{u}}{\partial t} + \mathbf{u} \cdot \nabla \mathbf{u} \right) = -\nabla p + \eta \nabla^2 \mathbf{u} + \mu_0(\mathbf{M} \cdot \nabla)\mathbf{H} + \mu_0 \nabla \times (\mathbf{M} \times \mathbf{H}). \quad (3.59)$$

In this expression can be identified the presence of the Kelvin force and the other magnetic contribution is given by $\mu_0 \nabla \times (\mathbf{M} \times \mathbf{H})$, known as the Torque force. Comparing both expressions (3.54) and (3.59), it is clear that the second formulation brings an additional magnetic term and incorporates different mechanisms of interaction of the magnetic fluid with the applied field.

Lack of symmetry of Maxwell stress tensor

In this section, we are going to study the influence of internal torques on the stress tensor symmetry for fluids that react polarly. In order to do this, we consider the balance of the angular momentum \mathbf{L} of a fluid particle, what is given by,

$$\frac{D\mathbf{L}}{Dt} = \sum \mathbf{T}, \quad (3.60)$$

where $\sum \mathbf{T}$ is representing the sum of torques that acts over a volume δV , which is assumed to be infinitesimal. Taking $\delta \mathbf{L} = (\mathbf{x} \times \rho \mathbf{u})dV$ what implies

$$\mathbf{L} = \int_V \mathbf{x} \times \rho \mathbf{u} dV. \quad (3.61)$$

By substituting (3.61) in (3.60),

$$\frac{D}{Dt} \left(\int_V \mathbf{x} \times (\rho \mathbf{u}) dV \right) = \sum \mathbf{T}, \quad (3.62)$$

in expression (3.62), mathematically it is required that the derived material be inserted into the integrand. This is done due to a consequence of the Reynolds Transport Theorem and the continuity equation (2.10) applied on the right-hand side of Eq. (3.62), which gives:

$$\frac{D}{Dt} \int_V \rho(\mathbf{x} \times \mathbf{u}) dV = \int_V \rho \frac{D}{Dt} (\mathbf{x} \times \mathbf{u}) dV. \quad (3.63)$$

We consider the contribution of the torque forces as a combination of field torques \mathbf{T}_v and surfaces torques \mathbf{T}_s , as follows:

$$\sum \mathbf{T} = \sum \mathbf{T}_s + \sum \mathbf{T}_v. \quad (3.64)$$

Now, using Eq. (3.64) and (3.63) into Eq. (3.62) yields

$$\int_V \rho \frac{D}{Dt} (\mathbf{x} \times \mathbf{u}) dV = \sum \mathbf{T}_s + \sum \mathbf{T}_v, \quad (3.65)$$

with surface torques given by:

$$\sum \mathbf{f}_s = \int_S \hat{\mathbf{n}} \cdot \boldsymbol{\sigma} dS = \int_S \hat{\mathbf{t}} dS. \quad (3.66)$$

Developing the terms involved in the right hand side of Eq. (3.65)

$$\sum \mathbf{T}_s = \int_S \mathbf{x} \times (\hat{\mathbf{n}} \cdot \boldsymbol{\sigma}) dS = \int_S \mathbf{x} \times \hat{\mathbf{t}} dS, \quad (3.67)$$

with the traction $\hat{\mathbf{t}} = \hat{\mathbf{n}} \cdot \boldsymbol{\sigma}$, and field torques given by:

$$\sum \mathbf{T}_v = \int_V (\mathbf{x} \times (\rho \mathbf{g}) + \rho \mathbf{T}^m) dV. \quad (3.68)$$

It must be observed that the term $\rho \mathbf{g}$ is related with the torque associated to the gravitational forces per unit by mass and the term $\rho \mathbf{T}^m$ corresponds to the inner magnetic torque of a magnetic fluid as a reaction to an external magnetic field per unit by mass.

Substituting Eqs. (3.67)-(3.68) in (3.65),

$$\int_V \rho \frac{D}{Dt} (\mathbf{x} \times \mathbf{u}) dV = \int_S \mathbf{x} \times \hat{\mathbf{t}} dS + \int_V (\mathbf{x} \times (\rho \mathbf{g}) + \rho \mathbf{T}^m) dV. \quad (3.69)$$

Using Gibbs notation to express the integrand of the first term on the right-hand side,

$$\begin{aligned} \mathbf{x} \times \hat{\mathbf{t}} &= \mathbf{x} \times (\hat{\mathbf{n}} \cdot \boldsymbol{\sigma}), \\ &= \xi_{ijk} x_j n_l \sigma_{kl} e_i. \end{aligned}$$

Note that $\xi_{ijk} x_j \sigma_{kl} = T_{il}$,

$$\int_S \mathbf{x} \times \hat{\mathbf{t}} dS = \int_S T_{il} n_l e_i dS = \int_S \mathbf{T} \cdot \hat{\mathbf{n}} dS. \quad (3.70)$$

Now, if we develop the expression $\hat{\mathbf{n}} \cdot \mathbf{T}^t$,

$$\begin{aligned}\hat{\mathbf{n}} \cdot \mathbf{T}^t &= n_i e_i \cdot (T_{jk} e_j e_k)^t, \\ &= n_i T_{ik} e_k,\end{aligned}$$

with this we proved $\mathbf{T} \cdot \hat{\mathbf{n}} = \hat{\mathbf{n}} \cdot \mathbf{T}^t$. This simplification we can write Eq. (3.67) as follow,

$$\begin{aligned}\int_S \mathbf{x} \times (\hat{\mathbf{n}} \cdot \boldsymbol{\sigma}) dS &= \int_S \mathbf{T} \cdot \hat{\mathbf{n}} dS, \\ &= \int_S \hat{\mathbf{n}} \cdot \mathbf{T}^t dS, \\ &= \int_V \nabla \cdot \mathbf{T}^t dV,\end{aligned}$$

in this expression we used the Divergence theorem applied to field \mathbf{T}^m over a infinitesimal volume V . Now, we develop the integrand of this expression,

$$\begin{aligned}\nabla \cdot \mathbf{T}^t &= \frac{\partial}{\partial x_i} e_i \cdot (T_{jk} e_j e_k)^t, \\ &= \frac{\partial}{\partial x_i} e_i \cdot T_{jk} e_k e_j, \\ &= \frac{\partial}{\partial x_i} T_{jk} e_k e_i \cdot e_j, \\ &= \frac{\partial}{\partial x_i} T_{ik} e_k,\end{aligned}$$

which in turn we can write it in the following form,

$$\begin{aligned}\frac{\partial}{\partial x_i} T_{ik} e_k &= \frac{\partial}{\partial x_i} \xi_{ijk} x_j \sigma_{pk}, \\ &= \xi_{ijk} \frac{\partial}{\partial x_i} (x_j \sigma_{pk}), \\ &= \xi_{ijk} \left(\frac{\partial x_j}{\partial x_i} \sigma_{pk} + x_j \frac{\partial \sigma_{pk}}{\partial x_i} \right), \\ &= \xi_{ijk} \left(\delta_{ji} \sigma_{pk} + x_j \frac{\partial \sigma_{pk}}{\partial x_i} \right), \\ &= \xi_{ijk} \delta_{ji} \sigma_{pk} + \xi_{ijk} x_j \frac{\partial \sigma_{pk}}{\partial x_i}, \\ &= \boldsymbol{\epsilon} : \boldsymbol{\sigma} + \mathbf{x} \times (\nabla \cdot \boldsymbol{\sigma}),\end{aligned}$$

where $\boldsymbol{\epsilon}$ is third order Levi-Civita permutation tensor and $\boldsymbol{\sigma}$ is the second order stress tensor. Finally we obtain,

$$\int_S \mathbf{x} \times (\hat{\mathbf{n}} \cdot \boldsymbol{\sigma}) dS = \int_V (\boldsymbol{\epsilon} : \boldsymbol{\sigma} + \mathbf{x} \times (\nabla \cdot \boldsymbol{\sigma})) dV. \quad (3.71)$$

Next step, we write Eq. (3.69) replacing the equivalent term of the right-hand side,

$$\int_V \rho \frac{D}{Dt} (\mathbf{x} \times \mathbf{u}) dV = \int_V \boldsymbol{\epsilon} : \boldsymbol{\sigma} + \mathbf{x} \times (\nabla \cdot \boldsymbol{\sigma}) dV + \int_V (\mathbf{x} \times (\rho \mathbf{g}) + \rho \mathbf{T}^m) dV, \quad (3.72)$$

placing all terms on the left hand side of the equation, we get

$$\int_V \left[\rho \frac{D}{Dt} (\mathbf{x} \times \mathbf{u}) - \boldsymbol{\epsilon} : \boldsymbol{\sigma} - \mathbf{x} \times (\nabla \cdot \boldsymbol{\sigma}) - (\mathbf{x} \times (\rho \mathbf{g}) + \rho \mathbf{T}^m) \right] dV = 0, \quad (3.73)$$

Here, we apply the Du Bois-Raymond lemma to the integrand over an arbitrary infinitesimal volume V , and develop the integrand of the integral by expanding the term $\rho \frac{D}{Dt} (\mathbf{x} \times \mathbf{u})$

$$\rho \left(\mathbf{x} \times \frac{D\mathbf{u}}{Dt} \right) + \rho \left(\frac{D\mathbf{x}}{Dt} \times \mathbf{u} \right) - \boldsymbol{\epsilon} : \boldsymbol{\sigma} - \mathbf{x} \times (\nabla \cdot \boldsymbol{\sigma}) - (\mathbf{x} \times (\rho \mathbf{g}) + \rho \mathbf{T}^m) = 0 \quad (3.74)$$

in this expression we must note that $D\mathbf{x}/Dt$ and \mathbf{u} are parallel what implies that the second term is canceled, and grouping terms involving the cross product with \mathbf{x}

$$\mathbf{x} \times \left(\rho \frac{D\mathbf{u}}{Dt} - \nabla \cdot \boldsymbol{\sigma} - \rho \mathbf{g} \right) - \boldsymbol{\epsilon} : \boldsymbol{\sigma} - \rho \mathbf{T}^m = 0. \quad (3.75)$$

Note that the term between parentheses is the Cauchy equation (2.18) implying that this term is zero and therefore we obtain the final version of the angular momentum equation:

$$\boldsymbol{\epsilon} : \boldsymbol{\sigma} + \rho \mathbf{T}^m = 0, \quad (3.76)$$

Now, we are going to prove that the presence of the internal torques generated by an external magnetic field breaks the symmetry of the stress tensor for magnetic fluids. In order to do this we are going to expand the term

$$\boldsymbol{\epsilon} : \boldsymbol{\sigma} = (\sigma_{23} - \sigma_{32})e_1 + (\sigma_{31} - \sigma_{13})e_2 + (\sigma_{12} - \sigma_{21})e_3, \quad (3.77)$$

In the expression (3.76), we can infer that if the $\mathbf{T}^m = 0$ then $\sigma_{23} = \sigma_{32}$, $\sigma_{31} = \sigma_{13}$ and $\sigma_{21} = \sigma_{12}$, that implies the symmetry of the stress tensor $\boldsymbol{\sigma} = \boldsymbol{\sigma}^t$ as it is the case of stress tensors for Newtonian fluids. Now, we consider the case in which there is a magnetic contribution of an external magnetic field expressed by $\mathbf{T}^m \neq 0$, which implies

$$\boldsymbol{\sigma} \neq \boldsymbol{\sigma}^t \quad (3.78)$$

which can be read as the stress tensor no longer being symmetrical in the presence of an external magnetic field in the case that we work with a magnetic fluid.

Part II

Stability of plane parallel flows of magnetic fluids

CHAPTER 4

INTRODUCTION

The problem of hydrodynamic stability was formulated for the first time in the nineteenth century, in the theoretical works by Helmholtz [41], Lord Kelvin [42] and Rayleigh [47]. The first experimental work on this subject was made by Osborne Reynolds in [49], who performed an experiment of a fluid flowing in a pipe. By using a tracer, he observed and characterized the flow transition from the laminar to a turbulent regime. The contribution of Reynolds's work was the association of this transition phenomenon to a dimensionless parameter, which would later be known as the Reynolds number. This dimensionless parameter can be understood as the relation between inertial and viscous forces acting on a moving fluid particle. He showed that the laminar flow breaks down when the dimensionless parameter exceeds critical value, and that the turbulence quickly arrives. If the Reynolds number is below 2000, this corresponds to a laminar regime flow, if the Reynolds number is above 4000, this indicates a turbulent regime flow and between 2000 and 4000 it is known as a flow in the transition regime. Due to the precision of the equipment these numbers have changed as the years have passed.

At the same time, Rayleigh [47] studied the parallel flows stability in the inviscid limit. The most important result of this period is the *Rayleigh's Theorem*, which establishes a necessary condition for the stability of the flow based on the existence of an inflection point of the velocity profile. This condition applied to plane Poiseuille flow immediately indicates flow stability. Hence viscosity should be the cause of a linear instability. Later, Fjørtoft [29] found a stronger necessary criterion for instability.

Later, the work of Orr [50] and Sommerfeld [53], in which hydrodynamic stability has been studied within the scope of viscous fluids, were published. These works defined the basis for the linear stability analysis of flows through the well-known Orr-Sommerfeld equa-

tion (OSE). For small Reynolds numbers, the plane Poiseuille flow is stable, but Heisenberg [55] proposed that it is unstable for large Reynolds numbers. He did not arrive at a critical value beyond which instability begins, but he calculated four points of the neutral curve of stability using an heuristic method to approximate the OSE. Several works would follow, in which the methods of asymptotic analysis for this equation were applied [56, 57]. The first numerical work to solve the Equation was due to Thomas [26], he used finite differences to approximate the derivatives of OSE. He confirmed the instability of the plane Poiseuille predicted by Heisenberg and found the critical values $Re = 5780$ and $\alpha = 1.026$. Later, Orzag [15] used approximation by means of Chebyshev polynomials to find accurate critical values for the Reynolds number $Re_c = 5772.22$ and $\alpha_c = 1.02056$.

The original application conceived by Papell [32] involves pumping magnetic fluid through pipes with the aid of magnetic fields. Some studies of similar setups have already been carried out in [34] (see also references therein). In fact, in [34] thorough experimental and numerical studies of the flow of ferrofluids in a pipe in the presence of an applied magnetic field has been carried out for both laminar and turbulent regimes. The aim of the work was to characterize the pressure drop as a function of the magnetic field properties, the frequency of an oscillatory applied field being the crucial parameter of the study. The work also assessed the role laminar and turbulent regimes on the measurements. However, there was no mention about the transition between these regimes in this work.

In [45], the authors studied the 2D planar-Couette magnetic fluid flow when an applied magnetic field is imposed transverse to the flow direction as in a previous study by [62] who also studied the effect of a parallel magnetic field. It was observed a dissipation effect when the applied magnetic field is time independent, but with spatially varying fields the mid-plane symmetry was broken. Imposing periodic boundaries conditions the system of velocity and spin evolution equation is solved. Considering a slow flow, it was found theoretically and numerically that the flow can be destabilized by a spatially varying magnetic field and this is related to the spatial gradient of the external field.

In [44], the authors have investigated the 3D unidirectional state flow of a sheared ferrofluid between two parallel plates when an applied magnetic field is imposed transversally to the direction of the flow. In this numerical approach, the authors used the modified Navier-Stokes equation, the magnetization evolution equation and the spin evolution equation. With a time independent magnetic field, it is reported a dissipative effect on the flow, while a time dependent or rotating transversal field show more control of the flow. The authors emphasize that a next step is this study is to perform a complete stability analysis and it is in this direction that our work goes. We note that in these two studies the authors place micro-electro-mechanical systems as a favorable scenario for the applications of these results.

CHAPTER 5

OVERVIEW OF THE BASIC RESULTS OF HYDRODYNAMIC STABILITY

In this chapter, we are going to review the principal results of the theory of hydrodynamics stability, following the literature [7, 25]. We will use the same concepts for a typical ODE to study this case concerning to a fluid flowing. We follow the following steps:

- Identify the equilibrium point.
- Perturb and linearize the the system around the equilibrium point.
- Find a governing equation for the perturbations of the system.
- Obtain the eigenvalues of the system.
- Study the linear stability of the system.

5.1 The Base State

Consider a flow between two parallel plane plates as in Fig. (5.1) separated by a distance $2l$. Consider an incompressible fluid in which the flow velocity is given by $\mathbf{u} = [u, v, 0]^t$, the density of the fluid ρ and its dynamic viscosity is η .

The fluid flow is described by the continuity equation (2.10) and the Navier-Stokes equation (2.20). However, due to the considerable number of parameters that involve the study of the flow of a fluid, it is advisable to reduce the amount of these parameters by

forming groups of dimensionless parameters. This is known as the Pi-Buckingham Theorem. In order to do this, we use typical scales of all variables involved in our problem;

$$\mathbf{x} \sim L; \quad \mathbf{u} \sim U; \quad t \sim L/U; \quad p \sim \rho U^2, \quad (5.1)$$

we are able to built dimensionless variables,

$$\mathbf{u}^* = \frac{\mathbf{u}}{U}; \quad \mathbf{x}^* = \frac{\mathbf{x}}{L}; \quad t^* = \frac{tU}{L}; \quad p^* = \frac{p}{\rho U^2}, \quad (5.2)$$

This kind of scale is known as Bernoulli scale. Substituting in the Navier-Stokes equation (2.20) and dropping the asterisk we get

$$\frac{\partial \mathbf{u}}{\partial t} + \mathbf{u} \cdot \nabla \mathbf{u} = -\nabla p + \frac{1}{Re} \nabla^2 \mathbf{u} + \frac{1}{Fr^2} \mathbf{g}, \quad (5.3)$$

and the unchanged continuity equation (2.10),

$$\nabla \cdot \mathbf{u} = 0, \quad (5.4)$$

where, Re is the Reynolds number and is given by,

$$Re = \frac{\rho U L}{\eta}. \quad (5.5)$$

Each problem has its characteristics and a set of specific dimensionless parameters can be defined. The NSE equations can be scaled in several forms, however, this allows comparison between different fluid flows. For two flows, if they have identical dimensionless parameters, then these flow are called dynamically similar.

In this section we are going to construct a base state based on the hypotheses of steady fully developed uni-directional flow. The steady-state flow refers to the condition where the fluid properties at any single point in the system do not change over time, this is $\partial(\cdot)/\partial t = 0$, in which the dot represents a fluid property. We first clarify the notion of fully developed velocity field: we say that a flow is fully developed when velocity does not change along the flow direction as shown in Fig. (5.1). This leads us to establish a first simplification,

$$\frac{\partial u}{\partial x} = 0. \quad (5.6)$$

Due to (5.6) we have, from continuity equation (5.4), that $\partial v/\partial y = 0$, this is, v is constant along the y direction. Since $v = 0$ on the plates (no-slip condition), we can conclude that the component of the velocity field is identically zero and we can express the velocity field as

$$\mathbf{u} = u(y) \hat{e}_x, \quad (5.7)$$

which is consistent with the hypotheses of uni-directionality. In addition, Eq. (5.7) leads us to establish that convective transport of linear momentum will be absent in this limit, $\mathbf{u} \cdot \nabla \mathbf{u} = 0$.

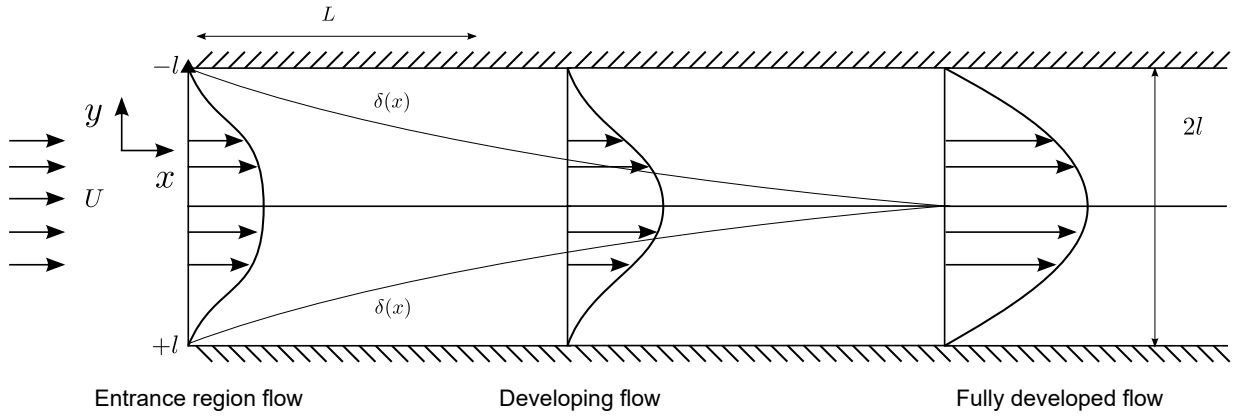


Figure 5.1: Sketch of a fully developed flow between two parallel plates with the thickness of the hydrodynamic boundary layer $\delta = \delta(x)$.

Considering the restrictive conditions obtained above and applying them to Eq. (5.3), gives us the following set of equations, in the x -direction:

$$\frac{\partial^2 u}{\partial y^2} = Re \frac{\partial p}{\partial x}, \quad (5.8)$$

and in the y -direction

$$\frac{\partial p}{\partial y} = -\frac{1}{Fr^2}g. \quad (5.9)$$

Now, we can integrate (5.9) in relation to y , which gives:

$$p = -\frac{1}{Fr^2}gy + c(x). \quad (5.10)$$

It can be inferred, by Eq. (5.9) that there is no change in the horizontal component of the pressure, however there is a change in its vertical component. It should be noted that the pressure in (5.9). By deriving (5.10) in relation to x :

$$\frac{\partial p}{\partial x} = c'(x). \quad (5.11)$$

This indicates that the $\partial p/\partial x$ is a function that depends exclusively on x . By consequence, since the left-hand side of (5.8) depends on y , both $\partial^2 u/\partial y^2$ and $\partial p/\partial x$ take a constant value, we consider the last one as,

$$\frac{\partial p}{\partial x} = \frac{p_0 - p_L}{L} = -G, \quad (5.12)$$

where G is a positive constant. In order to find the velocity profile we integrate two times (5.8):

$$u(y) = -Re G \frac{y^2}{2} + c_1 y + c_2, \quad (5.13)$$

where c_1 e c_2 are constants to be found from the no slip boundary conditions, $u(\pm 1) = 0$, which implies that $c_2 = Re G/2$ and that $c_1 = 0$. We obtain the velocity profile, where the sub-index b indicates the base state,

$$u^b(y) = \frac{Re G}{2} (1 - y^2). \quad (5.14)$$

By taking $Re G/2 = 1$ as in [7], we can normalize the *Poiseuille* parabolic velocity profile.

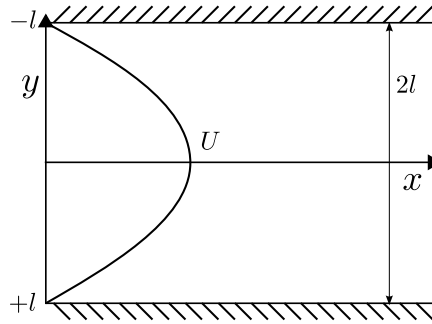


Figure 5.2: Sketch of the Poiseuille flow profile $u^b(y)$ between two rigid parallel plates.

5.2 The Linear Stability Problem

In order to analyze the flow stability, we impose a small perturbation on the base state solution as in Fig. (5.3),

$$\mathbf{u} = \mathbf{u}^b + \mathbf{u}', \quad p = p^b + p'. \quad (5.15)$$

We consider the unidirectional three-dimensional problem in which the base flow is given by $\mathbf{u}^b = u^b(y) \hat{e}_x$ with $y \in [-1, +1]$ and u^b being the Poiseuille velocity profile (5.14).

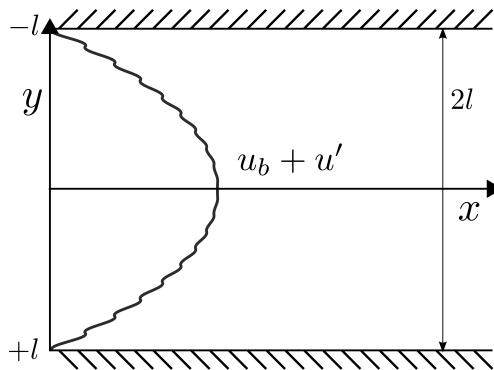


Figure 5.3: Sketch of the Poiseuille flow profile between two rigid parallel plates when a small disturbance is introduced.

The perturbations in the x and z directions are considered as plane waves with associated wave number given by α and β respectively, both real numbers since the solutions are required to be bounded as $x, y \rightarrow \pm\infty$, and the frequency ω which is a complex number associated with the grow or decay of the variable $t \in [0, +\infty)$. The amplitude of these perturbations are expressed here by a tilde, depending on the variable y . We can write the perturbations as:

$$\mathbf{u}'(\mathbf{x}, t) = (\tilde{u}(y), \tilde{v}(y), \tilde{w}(y)) \exp i(\alpha x + \beta z - \omega t), \quad (5.16)$$

and the disturbed pressure,

$$p'(\mathbf{x}, t) = \tilde{p}(y) \exp(i(\alpha x + \beta z - \omega t)). \quad (5.17)$$

We note that a derivative with respect to spatial variable x corresponds to a multiplication of the disturbed variable by a factor $i\alpha$ the disturbed variable, while a derivative with respect to z corresponds to multiply by $i\beta$ the disturbed variable.

Substituting the disturbed variables Eqs. (5.16) into the continuity Eq. (2.10), we get:

$$i\alpha\tilde{u}(y) + D\tilde{v}(y) + i\beta\tilde{w}(y) = 0, \quad (5.18)$$

where $D = d/dy$ represents the differential operator with respect to the variable y of the unknown amplitude function. We will use this expression in a later step, so we write it as follow

$$i(\alpha\tilde{u} + \beta\tilde{w}) + D\tilde{v} = 0. \quad (5.19)$$

which is valid for $y \in [-1, 1]$. The propagation vector \mathbf{k} is given by (α, β) , its magnitude k is the wave number being given by

$$k = (\alpha^2 + \beta^2)^{\frac{1}{2}}. \quad (5.20)$$

From the propagation frequency ω , we can define the velocity propagation of the perturbations $c = c_r + ic_i$ as being

$$c = \frac{\omega}{k} = \frac{\omega}{\sqrt{\alpha^2 + \beta^2}}. \quad (5.21)$$

By replacing the Eqs. (5.16)-(5.17) into the NSE (5.3) and keeping the notation d/dy for the derivative of a base state function, in this case the Poiseuille profile flow Eq. (5.14), we have the corresponding perturbed equations for the NSE in the x -direction:

$$i\alpha(u^b - c)\tilde{u} + \tilde{v}\frac{du^b}{dy} = -i\alpha\tilde{p} + \frac{1}{Re} (D^2 - k^2) \tilde{u}, \quad (5.22)$$

then in the y -direction

$$i\alpha(u^b - c)\tilde{v} = -D\tilde{p} + \frac{1}{Re} (D^2 - k^2) \tilde{v}, \quad (5.23)$$

and in the z -direction

$$i\alpha(u^b - c)\tilde{w} = -i\beta\tilde{p} + \frac{1}{Re} (D^2 - k^2) \tilde{w}. \quad (5.24)$$

This system of equations contains four unknown functions \tilde{u} , \tilde{v} , \tilde{w} , \tilde{p} and the system considers four equations (5.19) and (5.22)-(5.24). In order to reduce the system we differentiate Eq. (5.22) with respect to x , that is to say multiply Eq. (5.22) by $i\alpha$ and take the derivative of Eq. (5.24) with respect to z , i.e. multiply by $i\beta$. Once these steps are done we will add both expressions and use the continuity Eq. (5.19) for the disturbed variables to obtain:

$$i\alpha(u^b - c)(i\alpha\tilde{u} + i\beta\tilde{w}) + i\alpha\tilde{v}\frac{du^b}{dy} = -k^2\tilde{p} + \frac{1}{Re} (D^2 - k^2) (i\alpha\tilde{u} + i\beta\tilde{w}), \quad (5.25)$$

note that we are basically taking the divergence of the perturbed NSE. We eliminate \tilde{u} , \tilde{w} to leave the Eq. (5.23) in terms of \tilde{v} by using Eq. (5.19), Eq. (5.25) is rewritten only in terms of \tilde{v} :

$$-i\alpha(u^b - c)D\tilde{v} + i\alpha\tilde{v}\frac{du^b}{dy} = -k^2\tilde{p} - \frac{1}{Re} (D^2 - k^2) D\tilde{v}. \quad (5.26)$$

This equation contains \tilde{v} and \tilde{p} . In order to obtain an expression containing one of the variables we take the derivative of Eq. (5.26) with respect to y , that is,

$$-i\alpha(u^b - c)D^2\tilde{v} + i\alpha\tilde{v}\frac{d^2u^b}{dy^2} = -k^2D\tilde{p} - \frac{1}{Re} (D^2 - k^2) D^2\tilde{v}. \quad (5.27)$$

we can use the resulting equation to eliminate the term $D\tilde{p}$ from Eq. (5.23), which after some algebraic manipulations can be written as:

$$-i\alpha(u^b - c) (D^2 - k^2) \tilde{v} + i\alpha\tilde{v}\frac{d^2u^b}{dy^2} = -\frac{1}{Re} (D^2 - k^2) (D^2 - k^2) \tilde{v}. \quad (5.28)$$

Dividing by $i\alpha$, we obtain

$$\frac{1}{i\alpha Re} (D^2 - k^2)^2 \tilde{v} - (u^b - c) (D^2 - k^2) \tilde{v} + \frac{d^2u^b}{dy^2} \tilde{v} = 0. \quad (5.29)$$

This last expression is called the Orr-Sommerfeld equation (OSE) and is the starting point for hydrodynamic stability studies of flows between parallel plates. Eq. (5.29) is a fourth order ODE in \tilde{v} , and so for the system to be closed we need four boundary conditions. For our case, where the flow is given by Fig. (5.2), comprised between two parallel plates, the condition of no-slip implies that:

$$\tilde{v}(-1) = \tilde{v}(+1) = 0. \quad (5.30)$$

The other two conditions are obtained from the zero-shear condition:

$$D\tilde{v}(-1) = D\tilde{v}(+1) = 0. \quad (5.31)$$

Eq. (5.29) describes the evolution of the amplitude of the perturbations $\tilde{v}(y)$ of the velocity profile for a given choice of Re , α , β and the parabolic profile $u^b(y)$. Depending on the combination of the parameters, it is possible for the velocity c to assume complex values, see Eq. (5.21). If this happens, and $c_i > 0$, the amplitude of the disturbance will grow over time and the disturbance will be called the temporarily unstable.

We define the following Orr-Sommerfeld differential operator \mathcal{L}_{OS} as follows:

$$\mathcal{L}_{OS} = \frac{i}{\alpha Re} (D^2 - \alpha^2)^2 + (u^b - c)(D^2 - \alpha^2) - \frac{d^2 u^b}{dy^2}, \quad (5.32)$$

with D denoting a differentiation of the perturbations with respect to y , allowing us to write Eq. (5.29) in the following form,

$$\mathcal{L}_{OS} \tilde{v} = 0. \quad (5.33)$$

In the following, we will discuss some technical results that allow us to evaluate the stability of the flow from OSE (5.29).

5.2.1 The Theorem of Squire

The problem of linear stability was presented and it consider the OSE (5.29) together with the boundary conditions (5.30)-(5.31). For a given α , k , Re and the base state $u^b(y)$ it is possible to establish whether the flow is stable or not by analyzing the exponential part of the disturbed ansatz (5.16)

$$\exp(-ikct) = \exp(-ikc_r t) \exp(kc_i t). \quad (5.34)$$

where the c is expressed in complex form $c = c_r + ic_i$. The above expression indicates that $\exp(-ikc_r t)$ is the oscillatory part of the disturbances and $\exp(kc_i t)$ is the term that give us information about the stability: if c_i takes negative values this corresponds to a stable mode and if c_i takes positive values and the exponential grows on time that indicates an unstable mode.

Theorem 5.1 (Squire's theorem) *If a growing 3D disturbance can be found at a given Reynolds number, then a 2D growing disturbance exist at a lower Reynolds number.*

Proof: Let's consider a velocity base state $u^b(y)$. Consider an unstable 3D disturbance with Reynolds number Re_{3D} and a wave-number $(\alpha_{3D}, \beta_{3D})$ with $k_{3D}^2 = \alpha_{3D}^2 + \beta_{3D}^2$. The corresponding associated OSE solution with c , \tilde{v} and $c_i > 0$ is given by:

$$\frac{1}{i\alpha_{3D} Re_{3D}} (D^2 - k_{3D}^2)^2 \tilde{v} = \left((u^b - c)(D^2 - k_{3D}^2) - \frac{d^2 u^b}{dy^2} \right) \tilde{v}. \quad (5.35)$$

Now consider a 2D disturbance with Reynolds number Re_{2D} and a wave-number $(\alpha_{2D}, 0)$, that is, $\beta_{2D} = 0$ and consequently $k_{2D} = \alpha_{2D}$, then the corresponding 2D OSE solution is:

$$\frac{1}{i\alpha_{2D} Re_{2D}} (D^2 - \alpha_{2D}^2)^2 \tilde{v} = \left((u^b - c)(D^2 - \alpha_{2D}^2) - \frac{d^2 u^b}{dy^2} \right) \tilde{v}. \quad (5.36)$$

Comparing Eqs. (5.35) and (5.36), they will be the same if $k_{3D} = \alpha_{2D}$ and $\alpha_{2D} Re_{2D} = \alpha_{3D} Re_{3D}$, which provides:

$$Re_{2D} = \frac{\alpha_{3D}}{k_{3D}} Re_{3D}, \quad (5.37)$$

from these conditions, we found the same growing solution Eq. (5.35) with c , \tilde{v} and $c_i > 0$.

Hence it can be establish that for an unstable 3D disturbance at Re_{3D} with α_{3D} , β_{3D} , $k_{3D}^2 = \alpha_{3D}^2 + \beta_{3D}^2$, there exists an unstable 2D disturbance at Re_{2D} with $\alpha_{2D} = k_{3D}$.

Finally shown that $Re_{2D} \leq Re_{3D}$. In fact, since $k_{3D}^2 = \alpha_{3D}^2 + \beta_{3D}^2$, we have $k_{3D} \geq \alpha_{3D}$ or $\alpha_{3D}/k_{3D} \leq 1$, and replacing this expression into Eq. (5.37), we get $Re_{2D} \leq Re_{3D}$. Therefore, we can conclude that a 2D disturbance is unstable for a Reynolds number lower than a Reynolds number for a 3D disturbance.

It is shown through Squire's theorem (1933), that a disturbance in the form of a wave propagating obliquely in relation to the flow, is more stable than in the case of a disturbance that propagates parallel to the flow, which means that the minimum Re critical value for instability occurs in the case of a two-dimensional disturbance spreading along the flow direction.

With this additional information, we can write the Eq. (5.29) in the form of a differential operator \mathcal{L}_{OS} , this is, the Orr-Sommerfeld operator, acting over a an amplitude $\tilde{v} = \tilde{v}(y)$,

$$\mathcal{L}_{OS} \tilde{v} \equiv \left(\frac{1}{i\alpha Re} (D^2 - \alpha^2)^2 - (u^b - c)(D^2 - \alpha^2) + \frac{d^2 u^b}{dy^2} \right) \tilde{v} = 0. \quad (5.38)$$

This expression can be expressed by a dispersion relation

$$\mathcal{D}(\alpha, Re, u^b(y); c) = 0, \quad (5.39)$$

for a a given α , Re and a velocity profile $u^b(y)$, getting and eigenvalue c associated to an eigenvector \tilde{v} .

5.3 The inviscid limit

We will consider the non-viscous theoretical case, that is, assuming the extreme case when $Re \rightarrow \infty$ in Eq. (5.29).

$$(u^b - c)(D^2 - \alpha^2)\tilde{v} - \frac{d^2 u^b}{dy^2} \tilde{v} = 0. \quad (5.40)$$

This equation is called the Rayleigh's Equation and is a second order ODE. In this way, we need only two boundary conditions: the no-slip condition on each wall $\tilde{v}(\pm 1) = 0$. The case in which $Re \rightarrow \infty$ is said to be *Singular*, since Re^{-1} is multiplying the largest order derivative of Eq. (5.29).

From Eq. (5.40) we can determine some stability criteria of the flow at small perturbations. We shall now present the classical results of the inviscid theory.

Theorem 5.2 (Rayleigh's inflection point Theorem) *Suppose u^b and $\frac{du^b}{dy}$ are continuous functions with $y \in [-1, +1]$.*

A necessary condition, but not sufficient, for inviscid instability is that the base flow has a inflection point.

Proof: Let's suppose an inviscid unstable flow, i.e., $Re \rightarrow \infty$ and $c_i > 0$. In addition, we suppose that \tilde{v} is a non-trivial solution of the OS's equation, that is, \tilde{v} is not identically zero.

If $u^b(y) - c = 0$, we must note that $u^b(y)$ takes real values and $c = c_r + ic_i$ takes complex, then $u^b(y) = c$ implies $c_i = 0$. This leads us to a contradiction with first assumption $c_i > 0$. Therefore,

$$u^b(y) - c \neq 0 \quad (5.41)$$

Dividing (5.40) by (5.41),

$$D^2\tilde{v} - \alpha^2\tilde{v} - \frac{\tilde{v}}{u^b - c} \frac{d^2u^b}{dy^2} = 0, \quad (5.42)$$

Note that if \tilde{v} is a solution of (5.40), then its complex conjugate \bar{v} also it is going to be a solution of (5.40). Multiplying (5.42) by \bar{v} ,

$$\bar{v}D^2\tilde{v} - \alpha^2|\tilde{v}|^2 - \frac{|\tilde{v}|^2}{u^b - c} \frac{d^2u^b}{dy^2} = 0, \quad (5.43)$$

and integrating in the interval $[-1, +1]$, yields:

$$\int_{-1}^{+1} \bar{v}D^2\tilde{v}dy - \int_{-1}^{+1} \alpha^2|\tilde{v}|^2dy - \int_{-1}^{+1} \frac{|\tilde{v}|^2}{u^b - c} \frac{d^2u^b}{dy^2}dy = 0, \quad (5.44)$$

where $|\tilde{v}|^2 = \tilde{v}\bar{v}$. Integrating by parts the first term on the LHS of (5.44),

$$D\tilde{v}\bar{v} \Big|_{-1}^{+1} - \int_{-1}^{+1} (|D\tilde{v}|^2 + \alpha^2|\tilde{v}|^2) dy - \int_{-1}^{+1} \frac{|\tilde{v}|^2}{u^b - c} \frac{d^2u^b}{dy^2}dy = 0. \quad (5.45)$$

First term on LHS of (5.45) cancels using boundary conditions. Note that $|D\tilde{v}|^2 = D\tilde{v}D\bar{v}$;

$$- \int_{-1}^{+1} (|D\tilde{v}|^2 + \alpha^2|\tilde{v}|^2) dy - \int_{-1}^{+1} \frac{|\tilde{v}|^2}{u^b - c} \frac{d^2u^b}{dy^2}dy = 0. \quad (5.46)$$

Here, we consider the complex conjugate of $u^b - c$,

$$u^b - \bar{c} = u^b - (c_r - ic_i) = u^b - c_r + ic_i.$$

Using this expression, by multiplying on the numerator and denominator of the second term of LHS, gives us

$$- \int_{-1}^{+1} (|D\tilde{v}|^2 + \alpha^2|\tilde{v}|^2) dy - \int_{-1}^{+1} \frac{(u^b - c_r + ic_i)|\tilde{v}|^2}{|u^b - c|^2} \frac{d^2u^b}{dy^2} dy = 0. \quad (5.47)$$

In this expression we can extract its real part,

$$- \int_{-1}^{+1} (|D\tilde{v}|^2 + \alpha^2|\tilde{v}|^2) dy - \int_{-1}^{+1} \frac{(u^b - c_r)|\tilde{v}|^2}{|u^b - c|^2} \frac{d^2u^b}{dy^2} dy = 0, \quad (5.48)$$

and its complex part:

$$c_i \int_{-1}^{+1} \frac{|\tilde{v}|^2}{|u^b - c|^2} \frac{d^2u^b}{dy^2} dy = 0. \quad (5.49)$$

In this equation, as $c_i > 0$, the expression with integral must be zero. We are going to denote the integrand of (5.49) by f , and we note that f is a continuous function.

In the following, we show that $f = 0$.

By contradiction, i.e., $\exists y_0 \in (-1, 1)$ such that $f(y_0) > 0$ without of generality, then

$$0 = \int_{-1}^{+1} f(y) dy > \int_{B_\epsilon(y_0)} f(y) dy > 0, \quad (5.50)$$

the first inequality comes from continuity of f , ($\forall y \in B_\epsilon(y_0)$ without of generality $f(y) > 0$). Where the left and right side of this expression leads us to a contradiction

From (5.41),

$$\frac{d^2u^b}{dy^2} |\tilde{v}|^2 = 0 \quad \forall y \in (-1, +1). \quad (5.51)$$

Since $\tilde{v} \neq 0$, i.e., $\exists y^*$ such that $\tilde{v}(y^*) \neq 0$, then satisfying (5.51)

$$\frac{d^2u^b}{dy^2}(y^*) = 0. \quad (5.52)$$

Therefore, $\exists y^* \in (-1, 1)$ such that $\frac{d^2u^b}{dy^2}(y^*) = 0$.

Now, regarding the real part of Eq. (5.44), we can state the following result:

Theorem 5.3 (Fjørtoft's Theorem) *Assume that u^b and $\frac{du^b}{dy}$ are continuous with $y \in [-1, +1]$. Then a necessary condition for instability is*

$$\frac{d^2u^b}{dy^2}(u^b - u_c) < 0, \quad (5.53)$$

for some $y \in [-1, +1]$ and where u_c is a flow velocity at the inflection point.

Proof: Consider an Eq. (5.48), as follows:

$$\int_{-1}^{+1} \frac{(u^b - c_r)|\tilde{v}|^2}{|u^b - c|^2} \frac{d^2 u^b}{dy^2} dy = - \int_{-1}^{+1} (|D\tilde{v}|^2 + k^2|\tilde{v}|^2) dy. \quad (5.54)$$

Using the Rayleigh's inflection point Theorem, we obtain the existence of a point y_c in which $d^2 u(y_c)/dy^2 = 0$ and $u_c = u(y_c)$ and we have that the integral in (5.49) is equal to zero, then we add to the left-hand side the expression,

$$(c_r - u_c) \int_{-1}^{+1} \left(\frac{|\tilde{v}|^2}{|u^b - c|^2} \right) \frac{d^2 u^b}{dy^2} dy = 0. \quad (5.55)$$

We can cancel the value of c_r and we obtain,

$$\int_{-1}^{+1} \left(\frac{(u^b - u_c)|\tilde{v}|^2}{|u^b - c|^2} \right) \frac{d^2 u^b}{dy^2} dy = - \int_{-1}^{+1} (|D\tilde{v}|^2 + k^2|\tilde{v}|^2) dy. \quad (5.56)$$

In this case, the integral on the left-hand side takes negatives values which indicates that $\frac{d^2 u^b}{dy^2} (u^b - u_c)$ must be negative for some $y \in [-1, +1]$.

Starting from this result, and applying it to the specific case of flows of a symmetric base profile, we present the following corollary, without proof:

Corollary 5.4 (Result of Tollmien) *For a symmetric profile in a channel, the existence of an inflection point $\frac{d^2 u^b}{dy^2} = 0$ is not only necessary, but is also sufficient for instability.*

For a Poiseuille flow profile between parallel plates, we have $u^b(y) = 1 - y^2$, with $y \in [-1, +1]$, as in Eq. (5.14) with $d^2 u^b(y)/dy^2 = -2 \neq 0$, $\forall y \in [-1, +1]$. That is, the flow profile has no inflection point, and then, by the Rayleigh inflection point theorem, we can conclude that it is stable in the inviscid limit. This result clearly violates the Reynolds experimental observations and therefore indicates that the instability of parallel outflows must be associated in some way with finite Reynolds numbers, i.e., viscosity is also a destabilizing factor in high Reynolds number flows.

5.4 Numerical Solution of the Orr-Sommerfeld Stability Problem

In this section, we present the numerical method based on finite differences to solve the generalized eigenvalue problem given by the Orr-Sommerfeld equation (5.29) with the boundary conditions (5.30)-(5.31), following [7, 8].

The Orr-Sommerfeld equation can be recast into the form of an eigenvalue problem given by

$$\left(\frac{1}{i\alpha Re} (D^2 - \alpha^2)^2 - u^b (D^2 - \alpha^2) + \frac{d^2 u^b}{dy^2} \right) \tilde{v} = -c (D^2 - \alpha^2) \tilde{v}. \quad (5.57)$$

With the finite difference technique, the differential operator \mathcal{L}_{OS} in Eq. (5.38) is approximated by matrix operators, where A and B are matrices and c is the eigenvalue of the problem to be found, as follows:

$$A\tilde{v} = cB\tilde{v}. \quad (5.58)$$

We use second-order central differences to approximate the second and fourth-order derivatives that appear on left-hand side of Eq. (5.57), that is:

$$D^2\tilde{v}_n \approx \frac{\tilde{v}_{n-1} - 2\tilde{v}_n + \tilde{v}_{n+1}}{h^2}, \quad (5.59)$$

and

$$D^4\tilde{v}_i \approx \frac{\tilde{v}_{i-2} - 4\tilde{v}_{i-1} + 6\tilde{v}_i - 4\tilde{v}_{i+1} + \tilde{v}_{i+2}}{h^4}. \quad (5.60)$$

In order to impose the boundary conditions $\tilde{v} = 0$ and $D\tilde{v} = 0$ in $y = \pm 1$, we consider a partition of the domain interval $[-1, +1]$ in $N + 1$ mesh points $\{\tilde{v}_1, \dots, \tilde{v}_{N+1}\}$ with a step-size $h = 2/N$. The boundaries establish that $\tilde{v}_1 = 0 = \tilde{v}_{N+1}$ and $D\tilde{v}_1 = 0 = D\tilde{v}_{N+1}$, that is, $\tilde{v}_0 = \tilde{v}_2$ and $\tilde{v}_{N+1} = \tilde{v}_{N-1}$. Then, for example, the discretization for the node $i = 2$ is given by,

$$D^4\tilde{v}_2 \approx \frac{7\tilde{v}_2 - 4\tilde{v}_3 + \tilde{v}_4}{h^4}, \quad (5.61)$$

An analogous result can be derived for the node $i = N$.

The finite differences for the interior nodes $i = 3, \dots, N - 1$, we use centered finite differences following the formula (5.60) getting a system of $N - 1$ equations for $N - 1$ unknowns. The matrix A is pentadiagonal and the matrix B is tridiagonal. Next, we present the coefficients for both matrices, for the matrix A we have:

$$A = \begin{pmatrix} \check{a}_1 & a_2 & a_3 & & 0 \\ a_2 & a_1 & \ddots & \ddots & \\ a_3 & \ddots & \ddots & \ddots & a_3 \\ & \ddots & \ddots & a_1 & a_2 \\ 0 & & a_3 & a_2 & \check{a}_1 \end{pmatrix}, \quad (5.62)$$

where the components of the matrix A are given by:

$$\check{a}_1 = \left(-u^b \alpha^2 - \frac{d^2 u^b}{dy^2} + \frac{i\alpha^3}{Re} \right) - \frac{2}{h^2} \left(u^b - \frac{2i\alpha}{Re} \right) + \frac{7}{i\alpha Re h^4}, \quad (5.63)$$

$$a_1 = \left(-u^b \alpha^2 - \frac{d^2 u^b}{dy^2} + \frac{i\alpha^3}{Re} \right) - \frac{2}{h^2} \left(u^b - \frac{2i\alpha}{Re} \right) + \frac{6}{i\alpha Re h^4}, \quad (5.64)$$

$$a_2 = \frac{1}{h^2} \left(u^b - \frac{2i\alpha}{Re} \right) - \frac{4i}{\alpha Re h^4}, \quad \text{and} \quad a_3 = \frac{1}{i\alpha Re h^4}, \quad (5.65)$$

where the $\tilde{\alpha}_1$ satisfying the condition (5.61). The matrix B is given by:

$$B = \begin{pmatrix} b_1 & b_2 & & 0 \\ b_2 & \ddots & \ddots & \\ & \ddots & \ddots & b_2 \\ 0 & & b_2 & b_1 \end{pmatrix}, \quad (5.66)$$

and their components being

$$b_1 : -\left(\frac{2}{h^2} + \alpha^2\right), \quad \text{and } b_2 : \frac{1}{h^2}. \quad (5.67)$$

We solve the generalized eigenvalue problem Eq. (5.58) using EIG MatLab function. The EIG function of A and B returns a diagonal matrix of generalized eigenvalues and a full matrix whose columns are the corresponding eigenvectors.

The problem of hydrodynamic stability was represented by a dispersion equation Eq. (5.39), in it are the parameters that are part of our problem and normally generate a 3D graph as Fig. (5.4), which is difficult to interpret. For this reason we will analyze adequate combinations of parameters in 2D.

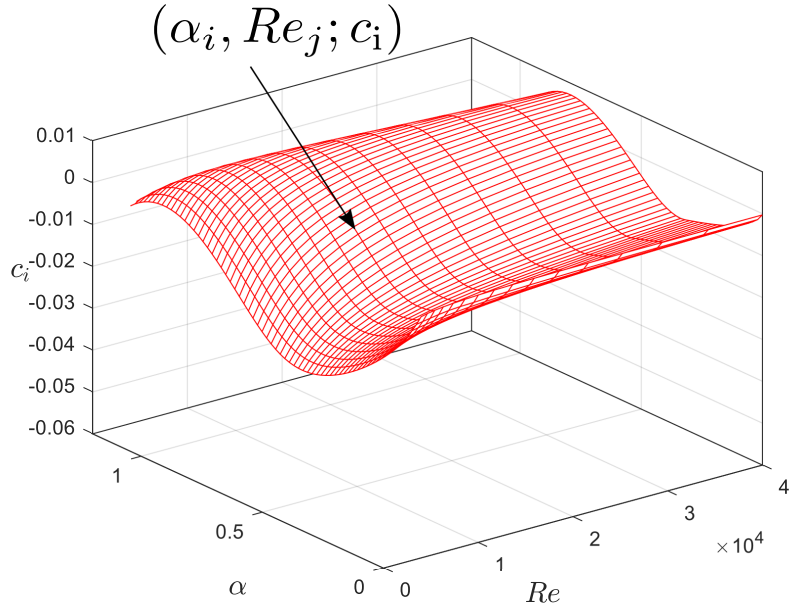


Figure 5.4: An example of a dispersion relation obtained from the Orr-Sommerfeld equation for a partition of α and Re numbers in m and n parts respectively and an specific node $(\alpha_i, Re_j; c_i)$.

According to our discretization procedure will take m elements to partition the interval α_{\min} and α_{\max} and n elements for the interval Re_{\min} to Re_{\max} . Initially, we take an α and

go through all the Reynolds numbers parallel to the axis of the abscissa, as in Figure 3, then we go to the next number of α and continue with the process. In each case we calculate the minimum value of the complex part of the set of eigenvalues obtained and it is this value which will represent the node (α_i, Re_j) as shown in Fig. (5.5).

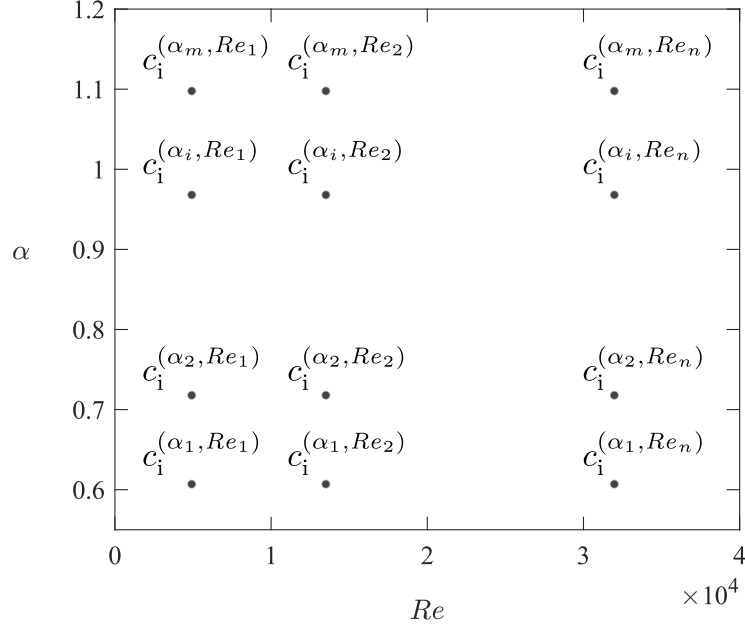


Figure 5.5: A graphical scheme of the discretized parameter space α Vs. Re . The iterative process starts with α_{\min} and solves the eigenvalue problem for all Re in the chosen range. Once these steps are finished, another value of α is taken until $\alpha = \alpha_{\max}$.

In Fig. (5.5), we obtain a total of $m \times n$ points $(\alpha_i, Re_j; c_i)$, which form a discretised representation of the surface defined by the dispersion relation, as shown in Fig. (5.4) and in it three options for values of c_i : $c_i < 0$, $c_i = 0$ and $c_i > 0$. With these results, we can identify a curve with $c_i = 0$ that divides the α Vs. Re plane into two regions, one inside in which the values $c_i > 0$ and another outside with $c_i < 0$.

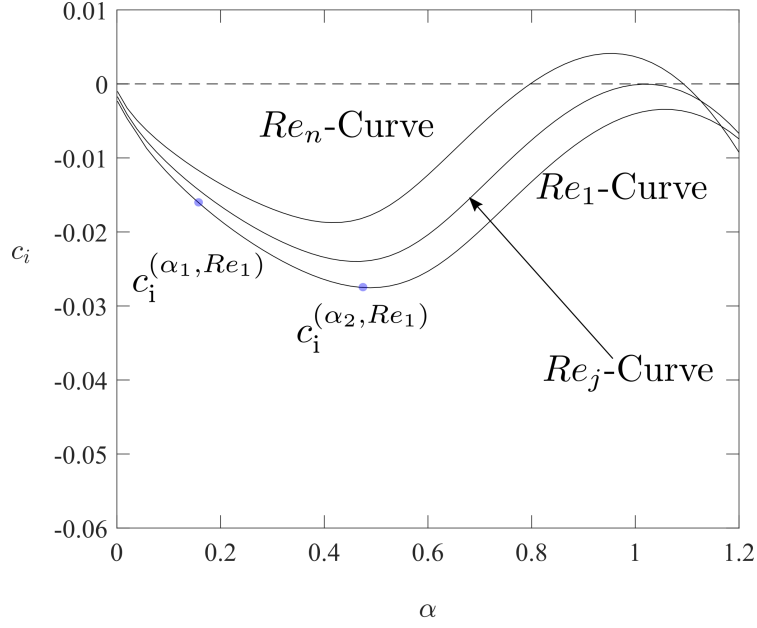


Figure 5.6: Growth rates as functions of the wave number of the disturbances for different values of Re . Note that we show three different possibilities of configurations: stable, marginally stable and unstable configurations.

To obtain the graph of c_i Vs. α , we consider the set of points $\{(\alpha_i, Re_j; c_i) \mid 1 \leq i \leq m, 1 \leq j \leq n\}$ obtained in Fig. (5.6). By fixing the Reynolds number, we take the α points and their corresponding c_i from the bottom to the top parallel to the ordinates axis. In this way, we obtain the Re_j -Curves in the c_i Vs. α plane, as in Fig. (5.5). Note that for small α , the values of c_i are negative (stability region) and hence the curve does not pass from the line $c_i = 0$. If we increase α , the constant Re vertical line will cross modes for which $c_i = 0$ and $c_i > 0$, that is, unstable modes. These results are shown in Fig. (5.6).

In the following Fig. (5.7), some contour lines are shown for the bifurcation diagram, for various values of c_i . We observe that c_i negatives are in the outer region and positive values of c_i are in the inner region defined by the curve $c_i = 0$, which we call the marginal stability curve. Even more, we can see that as these curves approach the marginal curve they decrease their value.

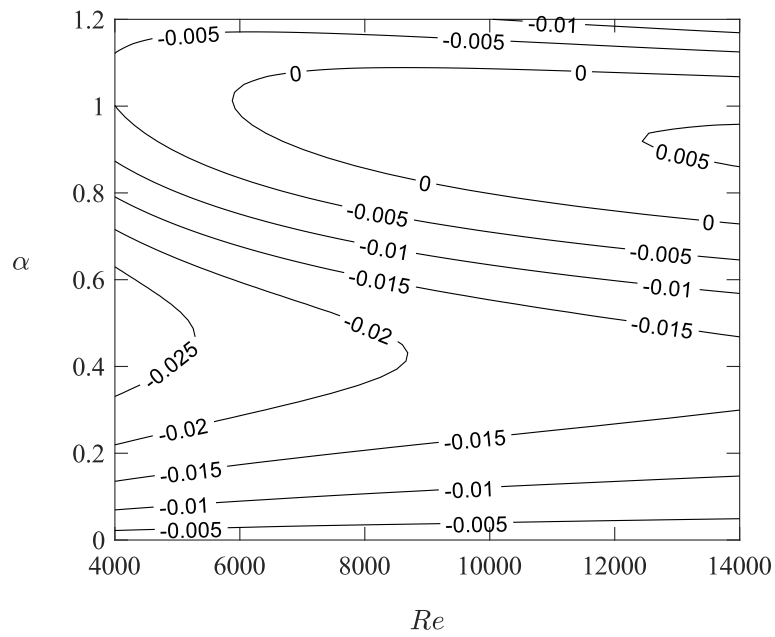


Figure 5.7: Bifurcation diagram with contour lines for different values of c_i evaluated in (α_i, Re_j) for $N = 128$, $Re \in [4000, 14000]$ and $\alpha \in [0, 1.2]$ taking $n_\alpha = 64$ and $n_{Re} = 32$.

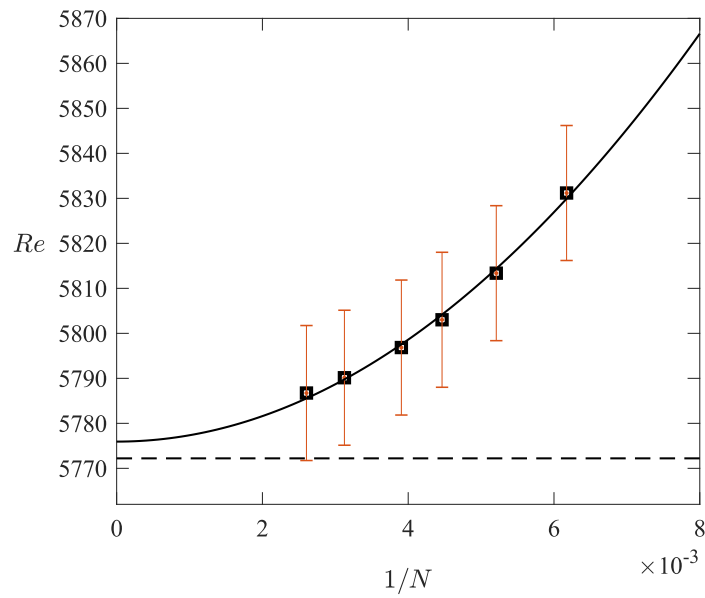


Figure 5.8: This diagram shows the numerical error produced by the finite difference method using $N = 162, 192, 224, 256, 320, 384$ points in the mesh and its correspondents critical values Re_c . Solid-line indicates the fitted curve and the limit $h = 0$ found the numerical critical value $Re = 5775.94$. Dash-line indicates the critical Reynolds number in $Re = 5772.22$, finding an error less than 1%. The error-bars indicate a 0.5% confidence interval on the obtained value of Re .

CHAPTER 6

STABILITY OF SYMMETRIC MAGNETIC FLUIDS

In this chapter, we are going to present two cases of hydrodynamic stability for symmetric magnetic fluids. The first of them, for the case of magnetic fluids in the superparamagnetic limit and the second for a magnetic fluid considering the Kelvin force in the modified Navier-Stokes equation together with an evolution magnetization equation.

We consider a two-dimensional flow of between two rigid parallel plates separated by a distance of $2l$. The horizontal direction is denoted by x and the vertical by y and all the components of the magnetic vector quantities are denoted by subscripts 1 for horizontal and 2 for vertical components. The horizontal and vertical components of the velocity field are denoted by u and v , respectively.

Following [12], Eqs. (3.54), (2.10), (3.3), (3.4), (3.43) and (3.39) are made dimensionless by assuming that the typical length scale is l , the typical velocity scale U is the average velocity on the channel and a typical applied field intensity H_0 as the appropriate scale for the applied field and the magnetization of the magnetic fluid. Therefore, a typical scale for the induction field is $\mu_0 H_0$. As a result, Eqs.(11.33), (3.4) and (3.3) remain unchanged in dimensionless variables and we obtain:

$$\frac{\partial \mathbf{u}}{\partial t} + \mathbf{u} \cdot \nabla \mathbf{u} = -\nabla p + \frac{1}{Re} \nabla^2 \mathbf{u} + C_{pm} \mathbf{M} \cdot \nabla \mathbf{H}, \quad (6.1)$$

and

$$\frac{\partial \mathbf{M}}{\partial t} + \mathbf{u} \cdot \nabla \mathbf{M} = \frac{1}{\tau^*} (\chi_0 \mathbf{H} - \mathbf{M}) + \frac{1}{2} (\nabla \times \mathbf{u}) \times \mathbf{M}, \quad (6.2)$$

where

$$Re = \frac{\rho U l}{\eta}, \quad C_{pm} = \frac{\mu_0 H_0^2}{\rho U^2}, \quad \text{and} \quad \tau^* = \frac{\tau U}{l}, \quad (6.3)$$

are, respectively, the Reynolds number of the flow, the magnetic pressure coefficient and the dimensionless magnetization relaxation time. Finally, Eq. (3.43) becomes simply

$$\mathbf{B} = \mathbf{H} + \mathbf{M}. \quad (6.4)$$

The boundary conditions for this problem are no-slip velocities at the parallel walls, that is,

$$\mathbf{u}(x, \pm 1) = \mathbf{0}, \quad (6.5)$$

and continuity of normal magnetic induction and tangential magnetic field the interface, that is,

$$\mathbf{n} \cdot \mathbf{B}|_{y=\pm 1} = 0, \quad \mathbf{n} \times \mathbf{H}|_{y=\pm 1} = \mathbf{0}, \quad (6.6)$$

where \mathbf{n} stands for the normal outward vector of the boundaries.

6.1 Super-Paramagnetic Case

Considering the modified Navier-Stokes equation with Kelvin force. Let's address the super-para-magnetic case by taking the limit $\tau^* = 0$ in the dimensionless evolution equation,

$$\mathbf{M} = \chi_0 \mathbf{H}, \quad (6.7)$$

where the magnetization \mathbf{M} is aligned with the applied field \mathbf{H} with constant χ_0 . Equation (6.7) is the constitutive equation for the magnetization of a superparamagnetic magnetic fluid. In this limit, the magnetization of the fluid does not depend on the velocity field. The Kelvin force in Eq. (6.1) is now written as $\chi_0 \mathbf{H} \cdot \nabla \mathbf{H}$ and, because \mathbf{H} and \mathbf{M} are collinear, there are no magnetic torques in the system and the last term on the RHS in Eq. (6.1) is identically zero. Magnetic forces are only present if there is a gradient of magnetic field.

We introduce the disturbed variables and write the new system keeping the first order disturbances, as follows:

$$\begin{aligned} \frac{\partial \mathbf{u}'}{\partial t} + \mathbf{u}^b \cdot \nabla \mathbf{u}' + \mathbf{u}' \cdot \nabla \mathbf{u}^b = & -\nabla p' + \frac{1}{Re} \nabla^2 \mathbf{u}' \\ & + \chi_0 C_{pm} (\mathbf{H} \cdot \nabla \mathbf{H}' + \mathbf{H}' \cdot \nabla \mathbf{H}), \end{aligned} \quad (6.8)$$

Following the standard derivation of the Orr-Sommerfeld equation in Section (5.2), we take the divergence of Eq. (6.8) in \mathbf{u}' ,

$$\begin{aligned} \frac{\partial \nabla \cdot \mathbf{u}'}{\partial t} + \nabla \cdot [\mathbf{u}^b \cdot \nabla \mathbf{u}' + \mathbf{u}' \cdot \nabla \mathbf{u}^b] = & -\nabla^2 p' + \frac{1}{Re} \nabla^2 \nabla \cdot \mathbf{u}' \\ & + \chi_0 C_{pm} \nabla \cdot (\mathbf{H} \cdot \nabla \mathbf{H}' + \mathbf{H}' \cdot \nabla \mathbf{H}). \end{aligned} \quad (6.9)$$

The second term on the left-hand side can be written as follows,

$$\nabla \cdot (\mathbf{u}^b \cdot \nabla \mathbf{u}' + \mathbf{u}' \cdot \nabla \mathbf{u}^b) = 2 \frac{du^b}{dy} \frac{\partial v'}{\partial x}. \quad (6.10)$$

The perturbation of the incompressibility fluid equation (2.10) produces an equivalent expression for the disturbed variables, substituting this expression in Eq. (6.9), the first term on the left-hand side and the second term on right-hand side are canceled. We can express the Laplacian of the disturbed pressure in Eq. (6.9) as;

$$\nabla^2 p' = -2 \frac{du^b}{dy} \frac{\partial v'}{\partial x} + \chi_0 C_{pm} \nabla \cdot (\mathbf{H} \cdot \nabla \mathbf{H}' + \mathbf{H}' \cdot \nabla \mathbf{H}). \quad (6.11)$$

Now, taking the Laplacian of the component in the y -direction of Eq. (6.8),

$$\frac{\partial \nabla^2 v'}{\partial t} + \nabla^2 \left(u^b \frac{\partial v'}{\partial x} \right) = -\frac{\partial \nabla^2 p'}{\partial y} + \frac{1}{Re} \nabla^4 v' \quad (6.12)$$

$$+ \chi_0 C_{pm} \nabla^2 \left(H_1 \frac{\partial H'_2}{\partial x} + H_2 \frac{\partial H'_2}{\partial y} + H'_1 \frac{\partial H_2}{\partial x} + H'_2 \frac{\partial H_2}{\partial y} \right). \quad (6.13)$$

By substituting Eq. (6.11) in Eq. (6.12), we get:

$$\begin{aligned} \frac{\partial \nabla^2 v'}{\partial t} + \nabla^2 \left(u^b \frac{\partial v'}{\partial x} \right) &= -\frac{\partial}{\partial y} \left[-2 \frac{du^b}{dy} \frac{\partial v'}{\partial x} + \chi_0 C_{pm} \nabla \cdot (\mathbf{H} \cdot \nabla \mathbf{H}' + \mathbf{H}' \cdot \nabla \mathbf{H}) \right] \\ &+ \frac{1}{Re} \nabla^4 v' + \chi_0 C_{pm} \nabla^2 \left(H_1 \frac{\partial H'_2}{\partial x} + H_2 \frac{\partial H'_2}{\partial y} + H'_1 \frac{\partial H_2}{\partial x} + H'_2 \frac{\partial H_2}{\partial y} \right). \end{aligned} \quad (6.14)$$

Developing the Laplacian on the left-hand side and the derivative with respect to the y variable on the right-hand side:

$$\begin{aligned} - \left(\left(\frac{\partial}{\partial t} + u^b \frac{\partial}{\partial x} \right) \nabla^2 v' - \frac{d^2 u^b}{dy^2} \frac{\partial v'}{\partial x} - \frac{1}{Re} \nabla^4 v' \right) &= \frac{\partial}{\partial y} [\chi_0 C_{pm} \nabla \cdot (\mathbf{H} \cdot \nabla \mathbf{H}' + \mathbf{H}' \cdot \nabla \mathbf{H})] \\ &- \chi_0 C_{pm} \nabla^2 \left(H_1 \frac{\partial H'_2}{\partial x} + H_2 \frac{\partial H'_2}{\partial y} + H'_1 \frac{\partial H_2}{\partial x} + H'_2 \frac{\partial H_2}{\partial y} \right). \end{aligned} \quad (6.15)$$

On the left-hand side of this expression, we have the Orr-Sommerfeld operator, which for $C_{pm} = 0$ takes the solution of the known case of OSE. We can write it as:

$$\mathcal{L}_{OS} \hat{v} = \chi_0 C_{pm} \frac{\partial}{\partial y} [\nabla \cdot (\mathbf{H} \cdot \nabla \mathbf{H}' + \mathbf{H}' \cdot \nabla \mathbf{H})] \quad (6.16)$$

$$- \chi_0 C_{pm} \nabla^2 \left(H_1 \frac{\partial H'_2}{\partial x} + H_2 \frac{\partial H'_2}{\partial y} + H'_1 \frac{\partial H_2}{\partial x} + H'_2 \frac{\partial H_2}{\partial y} \right). \quad (6.17)$$

yielding:

$$\mathcal{L}_{OS} \hat{v} = \chi_0 C_{pm} \frac{\partial}{\partial x} \left(\frac{\partial ((\mathbf{H} \cdot \nabla) H'_1 + (\mathbf{H}' \cdot \nabla) H_1)}{\partial y} - \frac{\partial ((\mathbf{H} \cdot \nabla) H'_2 + (\mathbf{H}' \cdot \nabla) H_2)}{\partial x} \right). \quad (6.18)$$

This last expression can be considered as the stability analysis equation for the superparamagnetic case (6.7).

Because of the unidirectionality of the flow, the only permissible magnetic fields are such that $H_1^b = H_1^b(y)$ and $H_2^b = H_2^b(y)$.

$$\mathcal{L}_{OS} \tilde{v} = \chi_0 C_{pm} i\alpha \left[\left(\frac{dH_1^b}{dy} i\alpha + \frac{dH_2^b}{dy} D \right) \tilde{H}_1 + \left(\frac{dH_1^b}{dy} D - \frac{dH_2^b}{dy} i\alpha \right) \tilde{H}_2 \right]. \quad (6.19)$$

Note that, now, the RHS of Eq.(6.19) does not contain any \tilde{v} -dependence. In fact, the RHS is a non-homogeneous forcing term and, therefore, does not affect the eigenvalues and eigenfunctions of the differential operator \mathcal{L}_{OS} . We then conclude that the stability of the flow is not affected by the presence of magnetic fields in this case and the critical Re_c is identical to the hydrodynamical case. Therefore, the stability of the plane parallel Poiseuille flow of a magnetic fluid can only be affected by an applied magnetic field if the magnetization of the fluid depends on the flow velocity.

6.2 Base State: Kelvin force

The flow of a ferrofluid in the presence of a magnetic field is described by the continuity equation (2.10), the modified Navier-Stokes equation (3.54), Maxwell's equations (3.3), and (3.4) and the magnetization evolution equation (3.38), as in [33]. The system of equations is written in terms of its components, given by:

$$\frac{\partial u}{\partial x} + \frac{\partial v}{\partial y} = 0, \quad (6.20)$$

$$\frac{\partial u}{\partial t} + u \frac{\partial u}{\partial x} + v \frac{\partial u}{\partial y} = -\frac{\partial p}{\partial x} + \frac{1}{Re} \left(\frac{\partial^2 u}{\partial x^2} + \frac{\partial^2 u}{\partial y^2} \right) + C_{pm} \left(M_1 \frac{\partial H_1}{\partial x} + M_2 \frac{\partial H_1}{\partial y} \right), \quad (6.21)$$

$$\frac{\partial v}{\partial t} + u \frac{\partial v}{\partial x} + v \frac{\partial v}{\partial y} = -\frac{\partial p}{\partial y} + \frac{1}{Re} \left(\frac{\partial^2 v}{\partial x^2} + \frac{\partial^2 v}{\partial y^2} \right) + C_{pm} \left(M_1 \frac{\partial H_2}{\partial x} + M_2 \frac{\partial H_2}{\partial y} \right), \quad (6.22)$$

$$\frac{\partial M_1}{\partial t} + u \frac{\partial M_1}{\partial x} + v \frac{\partial M_1}{\partial y} = -\frac{1}{\tau^*} (M_1 - M_{01}) - \frac{1}{2} M_2 \left(\frac{\partial v}{\partial x} - \frac{\partial u}{\partial y} \right), \quad (6.23)$$

$$\frac{\partial M_2}{\partial t} + u \frac{\partial M_2}{\partial x} + v \frac{\partial M_2}{\partial y} = -\frac{1}{\tau^*} (M_2 - M_{02}) + \frac{1}{2} M_1 \left(\frac{\partial v}{\partial x} - \frac{\partial u}{\partial y} \right), \quad (6.24)$$

$$\frac{\partial H_2}{\partial x} - \frac{\partial H_1}{\partial y} = 0, \quad (6.25)$$

$$\frac{\partial B_1}{\partial x} + \frac{\partial B_2}{\partial y} = 0, \quad (6.26)$$

$$B_1 = H_1 + M_1, \quad B_2 = H_2 + M_2. \quad (6.27)$$

We first clarify the notion of fully developed velocity and magnetic field: we say that a flow is fully developed when velocity does not change along the flow direction. This leads us to establish a first simplification,

$$\frac{\partial u}{\partial x} = 0, \quad \frac{\partial M_1}{\partial x} = 0. \quad (6.28)$$

Due to (6.28) we have, from continuity equation (6.20), that $\partial v/\partial y = 0$, this is, v is constant along the y direction. Since $v = 0$ on the plates (impenetrability condition), we can conclude that component of the velocity field is identically null and we can express the velocity field as

$$\mathbf{u} = u(y) \hat{e}_x. \quad (6.29)$$

This is consistence with the uni-directional hypotheses. If the ratio between the length L in the flow direction and the distance that separates the plates $2l$ is small, this is $l \ll L$, the continuity equation (2.10) allows us to write $V \ll U$, where U, V are the typical scales of u, v respectively and by consequence $\partial v/\partial y = 0$, this is, v is a constant in the perpendicular direction to the flow and since $v = 0$ in the plates, v is identically null, as derived previously. This analysis leads us to establish that convective transport of linear momentum will be absent in this limit, $\mathbf{u} \cdot \nabla \mathbf{u} = 0$.

From the uni-directional condition, we assume that both \mathbf{H} and \mathbf{B} have the following form:

$$\mathbf{H} = (H_1(y), H_2(y)), \quad \mathbf{B} = (B_1(y), B_2(y)). \quad (6.30)$$

where function components H_1, H_2, B_1 e B_2 depend only on variable y as (5.7). In this case, we impose that the fields satisfy Maxwell's equations (3.3) and (3.4). Equation (3.3) provides $dB_2/dy = 0$, then B_2 is constant and Equation (3.4) indicates that $dH_1/dy = 0$, then H_1 is also constant. With these additional simplification, the magnetic fields can be expressed by,

$$\mathbf{H} = (H_1, H_2(y)), \quad \mathbf{B} = (B_1(y), B_2), \quad (6.31)$$

where H_1 and B_2 are constants. We note that the magnetization field \mathbf{M} is obtained from dimensional Eq. (6.4). Now, we are in conditions to establish the velocity profile and magnetic base states.

Considering the restrictive conditions obtained above and applying them to Eqs. (6.21)-(6.24), gives us the following set of equations:

$$\frac{\partial^2 u}{\partial y^2} = Re \frac{\partial p}{\partial x}, \quad (6.32)$$

$$\frac{\partial p}{\partial y} = C_{pm} M_2 \frac{\partial H_2}{\partial y}, \quad (6.33)$$

$$0 = -\frac{1}{\tau^*} (M_1 - M_{01}) + \frac{1}{2} M_2 \frac{\partial u}{\partial y}, \quad (6.34)$$

$$0 = -\frac{1}{\tau^*} (M_2 - M_{02}) - \frac{1}{2} M_1 \frac{\partial u}{\partial y}. \quad (6.35)$$

We emphasize that the first coordinate of \mathbf{H} in (6.31) is constant and cancels the corresponding component of the Kelvin force, that is, there is no influence of the magnetic force in the horizontal component flow direction. There is a change in the pressure along the vertical direction due to the dependence of M_2 and the derivative of H_2 on y .

6.2.1 The velocity base state

Let consider steady-state, uni-directional and fully developed flow. From Eqs. (6.32)-(6.33) we obtain;

$$\frac{\partial^2 u}{\partial y^2} = Re \frac{\partial p}{\partial x}, \quad (6.36)$$

$$\frac{\partial p}{\partial y} = C_{pm} M_2 \frac{\partial H_2}{\partial y}. \quad (6.37)$$

In these equation, no-magnetic influence of Kelvin force is observed in the horizontal direction of Navier-Stokes equation, but it is present in the vertical variation of the pressure and, we note that the term on the left hand side of (6.37) depends on the y variable. From this, we can integrate (6.37) in relation to y , getting:

$$p = C_{pm} \int M_2(y) \frac{\partial H_2(y)}{\partial y} dy + c(x). \quad (6.38)$$

It can be inferred that there is no change in the horizontal component of the pressure, however there is a change in its vertical component. It should be noted that the pressure in (6.37) contains partial derivatives in the two components and that the integration in relation to one of them derives in the inclusion of a function of the other variable, added in (6.38) as $c(x)$. By deriving (6.38) in relation to x :

$$\frac{\partial p}{\partial x} = c'(x). \quad (6.39)$$

This indicates that the $\partial p / \partial x$ is a function that depends exclusively on x . By consequence, since the left hand side of (6.36) depends on y , $\partial p / \partial x$ is constant and we consider it as,

$$\frac{\partial p}{\partial x} = \frac{p_0 - p_L}{L} = -G. \quad (6.40)$$

In order to find the velocity profile we integrate two times (6.36):

$$u(y) = -Re G \frac{y^2}{2} + c_1 y + c_2, \quad (6.41)$$

where c_1 e c_2 are constants to be found with the no slip boundary conditions, $u(\pm 1) = 0$, which implies that $c_2 = Re G / 2$ and that $c_1 = 0$ and, we obtain the velocity profile, where the subscript b indicates the base state,

$$u^b(y) = 1 - y^2. \quad (6.42)$$

By taking $Re G / 2 = 1$ as in [7], we can conclude that the velocity profile, for the magnetic fields (6.31) that satisfies the Maxwell's equations, is the parabolic velocity profile of *Poiseuille*.

6.2.2 The magnetic base state

In order to find the magnetic base state, we consider Eqs. (6.34)-(6.35)

$$\frac{1}{\tau^*}(M_1 - \chi_0 H_1) - \frac{1}{2}M_2 \frac{\partial u}{\partial y} = 0, \quad (6.43)$$

$$\frac{1}{\tau^*}(M_2 - \chi_0 H_2) + \frac{1}{2}M_1 \frac{\partial u}{\partial y} = 0, \quad (6.44)$$

where the linear approximation for the equilibrium magnetization \mathbf{M}_0 is assumed,

$$\mathbf{M}_0 = \chi_0 \mathbf{H}. \quad (6.45)$$

In the system of equations above we want to compute functions $M_1 = M_1(y)$ and $M_2 = M_2(y)$, and it should be noted that the component of H_1 of the applied magnetic field is constant and that the second component depends on the variable y , this is $H_2 = H_2(y)$. In this case, we use Eq. (6.27), which gives:

$$H_2(y) = B_2 - M_2(y), \quad (6.46)$$

where B_2 is constant. With this consideration we have a linear system of equations

$$M_1 - \frac{1}{2}\tau^* \frac{du^b(y)}{dy} M_2 = \chi_0 H_1, \quad (6.47)$$

$$\frac{1}{2}\tau^* \frac{du^b(y)}{dy} M_1 + (1 + \chi_0)M_2 = \chi_0 B_2. \quad (6.48)$$

with unknown M_1, M_2 and constant values of H_1, B_2 , which give us some scenarios to be studied.

Therefore, the solution of the linear system (6.47)-(6.48) for M_1 is given by:

$$M_1(y) = \frac{\chi \left((1 + \chi)H_1 + \frac{\tau^*}{2} \frac{du^b(y)}{dy} B_2 \right)}{1 + \chi + \left(\frac{\tau^*}{2} \frac{du^b(y)}{dy} \right)^2}, \quad (6.49)$$

and for M_2 is;

$$M_2(y) = \frac{\chi \left(B_2 - \frac{\tau^*}{2} \frac{du^b(y)}{dy} H_1 \right)}{1 + \chi + \left(\frac{\tau^*}{2} \frac{du^b(y)}{dy} \right)^2}. \quad (6.50)$$

These functions (6.49)-(6.50) are the components in the horizontal and vertical direction respectively of the magnetic base state \mathbf{M}^b .

Some scenarios have been studied following the references [44, 62], where the conditions $H_1^b = 1$ and $B_2^b = 0$ were used, getting

$$M_1^b(y) = \frac{\chi(1 + \chi)}{1 + \chi + (y\tau^*)^2}, \quad M_2^b(y) = \frac{\chi y \tau^*}{1 + \chi + (y\tau^*)^2},$$

and for $H_1^b = 0$ and $B_2^b = 1$, we have:

$$M_1^b(y) = \frac{-\chi y \tau^*}{1 + \chi + (y \tau^*)^2}, \quad M_2^b(y) = \frac{\chi}{1 + \chi + (y \tau^*)^2}.$$

With these expressions, we can determine the functions $H_2^b(y)$ and $B_1^b(y)$ from Eq. (6.27). As an example, if we take $\chi_0 = 1$, $H_1^b = 1$ and $B_2^b = 0$, the magnetization base states are presented in Fig. (6.1) for different values of τ^* . We note that for very small values of τ^* , the magnetization base state is almost undisturbed by the flow.

6.3 The Stability Equations

6.3.1 Linear stability analysis

The stability of the flow is based on the temporal evolution of small disturbances introduced in the system [25]. This is done by perturbing all the variables of the problem around the base state in Section (6.2.1) and Section (6.2.2)

$$\mathbf{u} = \mathbf{u}^b + \mathbf{u}', \quad p = p^b + p', \quad \mathbf{H} = \mathbf{H}^b + \mathbf{H}', \quad \mathbf{M} = \mathbf{M}^b + \mathbf{M}', \quad (6.51)$$

that is, writing

$$\mathbf{u} = (u^b(y) + u'(x, y), v'(x, y)) \quad \text{and} \quad p = p^b(x, y) + p'(x, y), \quad (6.52)$$

for the hydrodynamical variables, and

$$\mathbf{H} = (H_1^b + H_1'(x, y), H_2^b(y) + H_2'(x, y)), \quad (6.53)$$

$$\mathbf{B} = (B_1^b(y) + B_1'(x, y), B_2^b + B_2'(x, y)), \quad (6.54)$$

for the applied magnetic field and magnetic induction, respectively, and

$$\mathbf{M} = (M_1^b(y) + M_1'(x, y), M_2^b(y) + M_2'(x, y)), \quad (6.55)$$

for the magnetization of the magnetic fluid. All the variables with a ' symbol denote perturbations. We assume that the perturbations are small and, therefore, after substituting the variables above on the governing equations, they can be linearized by retaining only linear terms in perturbations. Therefore, we obtain:

$$\frac{\partial u'}{\partial t} + u^b \frac{\partial u'}{\partial x} + v' \frac{du^b}{dy} = -\frac{\partial p'}{\partial x} + \frac{1}{Re} \nabla^2 u' + C_{pm} \left(M_1^b \frac{\partial H_1'}{\partial x} + M_2^b \frac{\partial H_1'}{\partial y} + M_2' \frac{dH_1^b}{dy} \right), \quad (6.56)$$

$$\frac{\partial v'}{\partial t} + u^b \frac{\partial v'}{\partial x} = -\frac{\partial p'}{\partial y} + \frac{1}{Re} \nabla^2 v' + C_{pm} \left(M_1^b \frac{\partial H_2'}{\partial x} + M_2^b \frac{\partial H_2'}{\partial y} + M_2' \frac{dH_2^b}{dy} \right), \quad (6.57)$$

$$\frac{\partial M_1'}{\partial t} + u^b \frac{\partial M_1'}{\partial x} + v' \frac{dM_1^b}{dy} = \frac{(\chi_0 H_1^b - M_1')}{\tau^*} + \frac{1}{2} \left(-\frac{\partial v'}{\partial x} M_2^b + \frac{\partial u'}{\partial y} M_2^b + \frac{du^b}{dy} M_2' \right), \quad (6.58)$$

$$\frac{\partial M_2'}{\partial t} + u^b \frac{\partial M_2'}{\partial x} + v' \frac{dM_2^b}{dy} = \frac{(\chi_0 H_2^b - M_2')}{\tau^*} + \frac{1}{2} \left(\frac{\partial v'}{\partial x} M_1^b - \frac{\partial u'}{\partial y} M_1^b - \frac{du^b}{dy} M_1' \right), \quad (6.59)$$

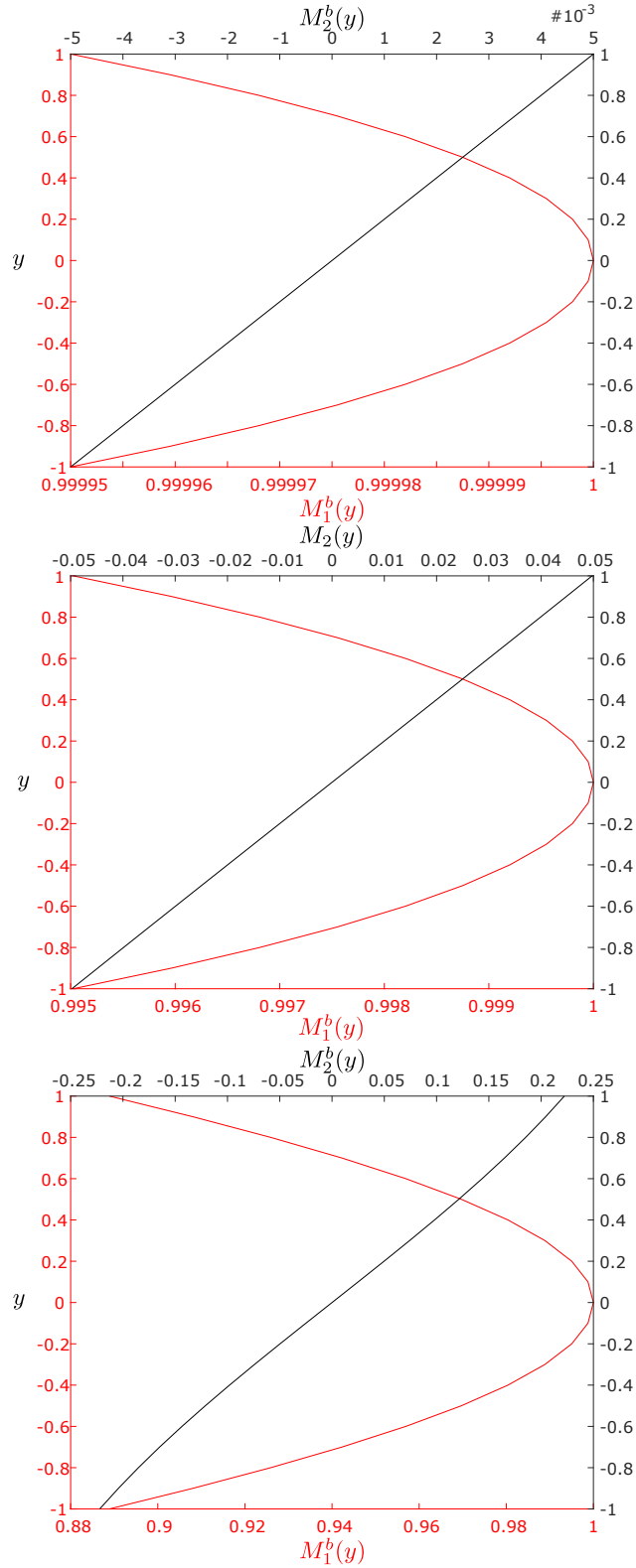


Figure 6.1: Magnetization base states for $\chi_0 = 1$, $H_1^b = 1$ and $B_2^b = 0$, calculated from Eqs. (6.49), (6.50). The red-line represents $M_1^b(y)$ and the black-line represents $M_2^b(y)$. The top graph was obtained for $\tau^* = 10^{-2}$, the center one for $\tau^* = 10^{-1}$ and the bottom one for $\tau^* = 0.5$.

as well as

$$\frac{\partial u'}{\partial x} + \frac{\partial v'}{\partial y} = 0, \quad (6.60)$$

and

$$\frac{\partial B'_1}{\partial x} + \frac{\partial B'_2}{\partial y} = 0, \quad (6.61)$$

$$\frac{\partial H'_2}{\partial x} - \frac{\partial H'_1}{\partial y} = 0. \quad (6.62)$$

Now, considering that the perturbations are of the form of plane waves

$$\Gamma'(x, y, t) = \tilde{\Gamma}(y)e^{i\alpha(x-ct)}, \quad (6.63)$$

where $\Gamma'(x, y, t)$ is a generic function representing any of the perturbation variables and $\tilde{\Gamma}(y)$ its amplitude, $i = \sqrt{-1}$, α is the wave number of the perturbations and c is their propagation velocity. Therefore, with this ansatz, differentiations with respect to x are now replaced by a multiplication by $i\alpha$ and differentiations with respect to time are now replaced by a multiplication by $-i\alpha c$. Substituting Eq.(6.63) in the linearized equations, and performing some algebraic manipulations (see Appendix A for more details), we obtain the following equation for the amplitudes of the vertical velocity perturbations:

$$\mathcal{L}_{OS}\tilde{v} = C_{pm} \left[i\alpha \frac{dM_2^b}{dy} D\tilde{H}_1 - \alpha^2 \frac{dM_1^b}{dy} \tilde{H}_1 + \alpha^2 \frac{dH_2^b}{dy} \tilde{M}_2 \right], \quad (6.64)$$

where \mathcal{L}_{OS} is the Orr-Sommerfeld differential operator, defined in (5.32). Considering that the perturbed version of Eq. (3.2) gives, in terms of amplitudes of perturbations,

$$\tilde{H}_1 = -\tilde{M}_1 \quad \text{and} \quad \tilde{H}_2 = -\tilde{M}_2, \quad (6.65)$$

and taking into account Eq.(6.61), then Eq.(6.64) can be further simplified to

$$\mathcal{L}_{OS}\tilde{v} = C_{pm} i\alpha \frac{dM_1^b}{dy} \tilde{M}_1. \quad (6.66)$$

Furthermore, the perturbations of the magnetization evolution equations are:

$$(\mathcal{A} + 2c\alpha^2)\tilde{M}_1 = \mathcal{B}\tilde{M}_2 - \left(M_2^b(D^2 - \alpha^2) + 2i\alpha \frac{dM_1^b}{dy} \right) \tilde{v}, \quad (6.67)$$

$$(\mathcal{A} + 2c\alpha^2)\tilde{M}_2 = -\mathcal{B}\tilde{M}_1 + \left(M_1^b(D^2 - \alpha^2) - 2i\alpha \frac{dM_2^b}{dy} \right) \tilde{v}, \quad (6.68)$$

where the functions \mathcal{A} and \mathcal{B} are given by:

$$\mathcal{A} = 2 \left(\frac{i\alpha(1 + \chi_0)}{\tau^*} - \alpha^2 u^b \right) \quad \text{and} \quad \mathcal{B} = i\alpha \frac{du^b}{dy}. \quad (6.69)$$

Equations (6.66)-(6.68) form a system of three coupled linear ODEs for the unknowns amplitudes $\tilde{v}(y)$, $\tilde{M}_1(y)$ and $\tilde{M}_2(y)$ and the unknown propagation velocity c . In fact, c

is the eigenvalue of this system of equations for a given wave number α . If $c = c_r + ic_i$ is a complex number with positive complex part c_i then, from Eq. (6.63), the disturbance with wave number α grows exponentially in time and the system is said to be unstable. Therefore, in order to understand the stability of this system, we need to calculate the eigenvalue c . In the section below, we present the numerical method used to achieve that goal.

6.3.2 Numerical solution

The solution of the system composed by Eqs.(6.66)-(6.68) is carried out numerically via a second order finite difference method [25]. We discretize the interval $[-1, 1]$ in the y -direction in $N + 1$ mesh points separated by a step size $\Delta y = 2/N$ so that the coordinate of each point is given by $y^j = (j - 1)\Delta y - 1$. The amplitudes at the mesh points are $\tilde{v}(y^j) = \tilde{v}^j$, $\tilde{M}_1(y^j) = \tilde{M}_1^j$ and $\tilde{M}_2(y^j) = \tilde{M}_2^j$, for $j = 1, \dots, N + 1$.

The boundary conditions for the amplitudes of the perturbations are $\tilde{v}^1 = \tilde{v}^{N+1} = 0$, $D\tilde{v}^1 = D\tilde{v}^{N+1} = 0$, $\tilde{M}_1^1 = \tilde{M}_1^{N+1} = 0$ and $\tilde{M}_2^1 = \tilde{M}_2^{N+1} = 0$. With this approach, we obtain a system of $3(N - 1)$ equations for the $3(N - 1)$ unknowns \tilde{v}^j , \tilde{M}_1^j and \tilde{M}_2^j , $j = 2, \dots, N$. The resulting system of equations can be rearranged into a generalized eigenvalue problem in matrix form as:

$$P\tilde{w} = cQ\tilde{w}, \quad (6.70)$$

where $\tilde{w} = (\tilde{v}^2, \dots, \tilde{v}^N, \tilde{M}_1^2, \dots, \tilde{M}_1^N, \tilde{M}_2^2, \dots, \tilde{M}_2^N)^T$ and the matrices P and Q are block coefficient matrices obtained from the discretized set of equations. The matrices involved in the generalized eigenvalue problem presented in Eq. (6.70) are given by the block matrices

$$P = \begin{bmatrix} P_{11} & P_{12} & 0 \\ P_{21} & P_{22} & P_{23} \\ P_{31} & P_{32} & P_{33} \end{bmatrix} \text{ and } Q = \begin{bmatrix} Q_1 & 0 & 0 \\ 0 & Q_2 & 0 \\ 0 & 0 & Q_3 \end{bmatrix}. \quad (6.71)$$

The matrix P_{11} is the standard pentadiagonal matrix obtained in the purely hydrodynamical stability problem as in Section (5.4). The matrix P_{21} is tridiagonal, whereas P_{12} is diagonal, and their elements are given by:

$$\{P_{21}\}_{j,j+1} = \{P_{21}\}_{j,j-1} = \frac{M_2^b}{\Delta y^2}, \quad (6.72)$$

$$\{P_{21}\}_{j,j} = -\left(\frac{2}{\Delta y^2} + \alpha^2\right) M_2^b + 2i\alpha \frac{dM_1^b}{dy}, \quad (6.73)$$

$$\{P_{12}\}_{j,j} = -i\alpha C_{pm} \frac{dM_1^b}{dy}. \quad (6.74)$$

The matrix P_{31} is also tridiagonal, with elements given by:

$$\{P_{31}\}_{j,j+1} = \{P_{31}\}_{j,j-1} = -\frac{M_1^b}{\Delta y^2}, \quad (6.75)$$

$$\{P_{31}\}_{j,j} = \left(\frac{2}{\Delta y^2} + \alpha^2\right) M_1^b + 2i\alpha \frac{dM_2^b}{dy}. \quad (6.76)$$

The other matrices in the matrix P are diagonal matrices with elements given by:

$$\{P_{22}\}_{j,j} = \{P_{33}\}_{j,j} = \mathcal{A}, \quad \{P_{23}\}_{j,j} = -\{P_{32}\}_{j,j} = -\mathcal{B}, \quad (6.77)$$

with \mathcal{A} and \mathcal{B} as in Eq.(6.69).

The matrix Q_1 is the standard tridiagonal matrix obtained in the purely hydrodynamical stability problem as in Section (5.4), whereas the matrices Q_2 and Q_3 are diagonal matrices, with elements given by

$$\{Q_2\}_{j,j} = \{Q_3\}_{j,j} = -2\alpha^2. \quad (6.78)$$

We note that the base state functions appearing in the above matrix components are evaluated at y^j .

Equation (6.70) is implemented in MatLab with the EIG routine, which gives as results the eigenvalues c and the eigenvectors \tilde{w} of Eq. (6.70). We have checked our algorithm by determining the critical Reynolds number for the onset of instability of the purely hydrodynamical problem, Re_c^h (see definition and further details about the critical Reynolds number in Section 6.4.1), for which $C_{pm} = 0$. We find $Re_c^h = 5775.94$, which gives an error of less than 1% when compared with the reference value of $Re_c^h = 5772.22$ given in [25].

6.4 Results

In the following, we present the results that were obtained for the linear stability analysis of the plane Poiseuille flow for four different base state magnetic fields. We consider a horizontal applied field, for which we assume $H_1^b = \pm 1$ and $B_2^b = 0$, and a vertical applied field, for which we assume $H_1^b = 0$ and $B_2^b = \pm 1$. Note, however, that the applied fields are not strictly horizontal or vertical, as there are non-zero y -dependent components $H_2^b(y)$ and $B_1^b(y)$. Since these are small, as can be inferred from Fig.6.1, therefore the applied fields are almost horizontal and vertical, respectively, and we have opted to keep this nomenclature. Finally, we also assume that $\chi_0 = 0.513$ to obtain the results presented in this section. This is the typical value of magnetic susceptibility for the experiments performed in [31], which is within the range for χ_0 given in [62]. All results presented in this Section were obtained for $N = 256$. For this choice of N , the error in the estimated value of Re_c^h is under 1%.

6.4.1 Horizontal applied magnetic field

We consider here the case of an external horizontal applied magnetic field given by $H_1^b = 1$ and $B_2^b = 0$. For a given configuration of the parameters Re , C_{pm} , χ_0 , τ^* and α , we solve Eq.(6.70) and find the $3(N - 1)$ eigenvalues $c = c_r + ic_i$ of the system. In Fig.6.2, we plot some of the eigenvalues obtained for one particular set of parameters and we observe that all but one of the eigenvalues of the system have negative imaginary part c_i : this eigenvalue is the one with the largest c_i and will be called, from now on, as the critical eigenvalue. Because the critical eigenvalue in this case has a positive imaginary part, we conclude that the flow is unstable for the values of the parameters used to generate Fig.6.2.

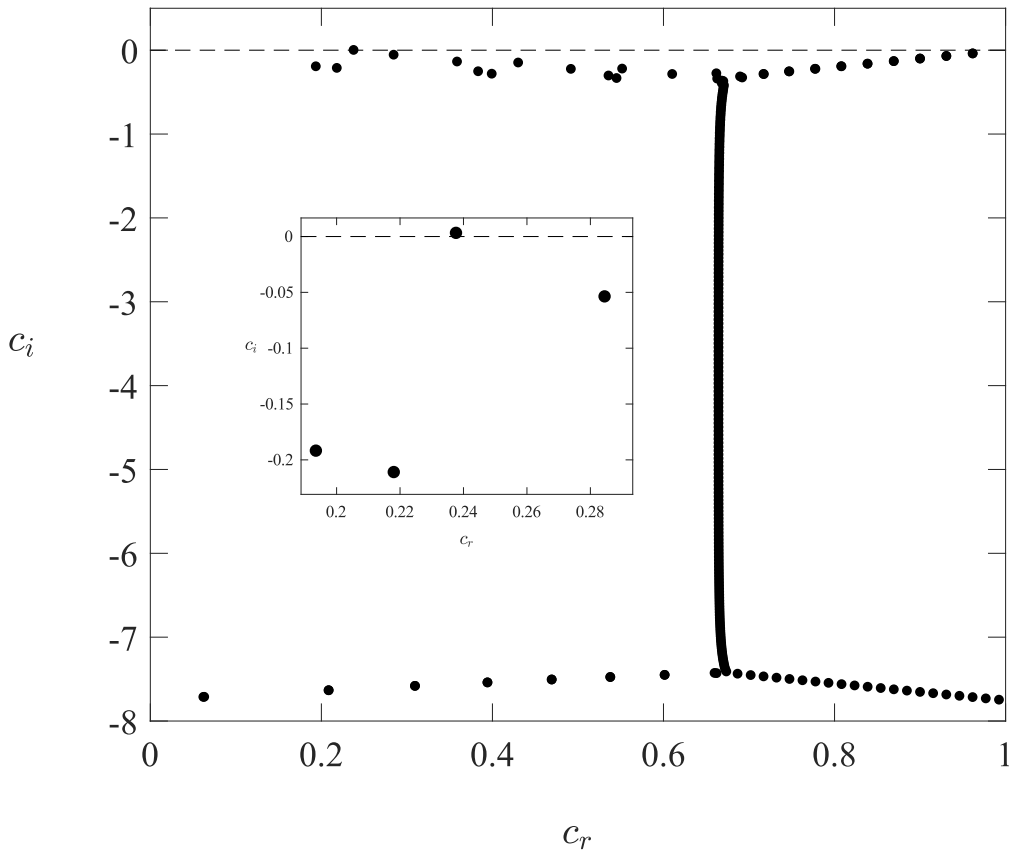


Figure 6.2: The eigenvalues with the smallest absolute complex part of the system Eq.(6.70) plotted on the complex plane, obtained for $Re = 8619.5$, $C_{pm} = 5 \times 10^6$, $\chi_0 = 0.513$, $\tau^* = 10^{-2}$ and $\alpha = 0.9807$. The applied magnetic field is horizontal, with $H_1^b = 1$ and $B_2^b = 0$ and $N = 256$. The insert shows the unstable eigenvalue with positive c_i above the dashed line $c_i = 0$. All the other eigenvalues of the system have very large negative values of c_i .

If we now collect the imaginary part of the critical eigenvalue for different values of wave number α , we construct a dispersion relation for this problem, which is presented in Fig.6.3. For values of Re : $Re_1 = 1000$, $Re_2 = 1951.3$, $Re_3 = 4101.1$, the critical eigenvalues have negative imaginary part and, therefore, the flows are stable. As the value of Re increases, there is an increase in the value of c_i and, for a given critical Re_c , there will be an α_c for which $c_i = 0$. This is called the neutral growth mode. Any further increase in Re will lead to a critical eigenvalue having positive c_i for a certain range of α . Consequently, the flow is unstable under these conditions.

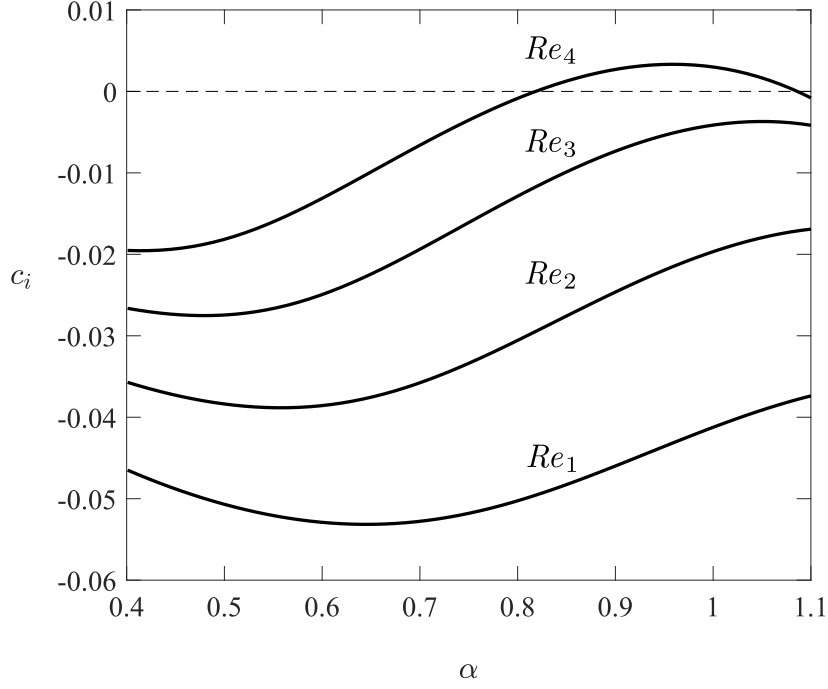


Figure 6.3: The complex part of the critical eigenvalue as a function of the wave number α for different values of Re : $Re_1 = 1000$, $Re_2 = 1951.3$, $Re_3 = 4101.1$ and $Re_4 = 8619.5$. The other parameters are the same as the ones used in Fig.6.2.

The results in Fig.6.3 can be consolidated into a stability diagram in which all the wave numbers α of the neutral growth modes are plotted for different values of Re . This plot is presented in Fig.6.4, which was obtained for different values of the magnetic parameter C_{pm} . The value of Re_c^h , for which $C_{pm} = 0$, is presented in Fig.6.4 as the dashed vertical line. The solid lines represent the values of α for which $c_i = 0$ at a given C_{pm} . The points lying inside these lines represent unstable modes for which $c_i > 0$ and the points lying outside denote stable modes, $c_i < 0$. We can observe that there is a decrease in the value of the minimum Re_c for which a neutral mode is achieved when C_{pm} increases. This indicates that the flow is destabilized by the presence of the applied field. The observed decrease in Re_c is of around 1700 for the range of C_{pm} tested in this case, which represents only a reduction

of around 30% on Re_c for a significant change of C_{pm} over two orders of magnitude. In fact, the values of C_{pm} for any change at all on the instability of the flow to be perceived are actually very high, starting at the order of 10^6 . For lower values, only insignificant changes on Re_c are observed. This is due to the fact that the base state magnetization of the fluid is very little affected by the applied field when τ^* is small, with a τ^{*2} also appearing in the perturbation equations, namely multiplying C_{pm} in Eq.(6.66). In this case, the fluid behaves almost as a superparamagnetic magnetic fluid, in which limit the magnetic field does not affect the hydrodynamic instability, as discussed in 6.7.

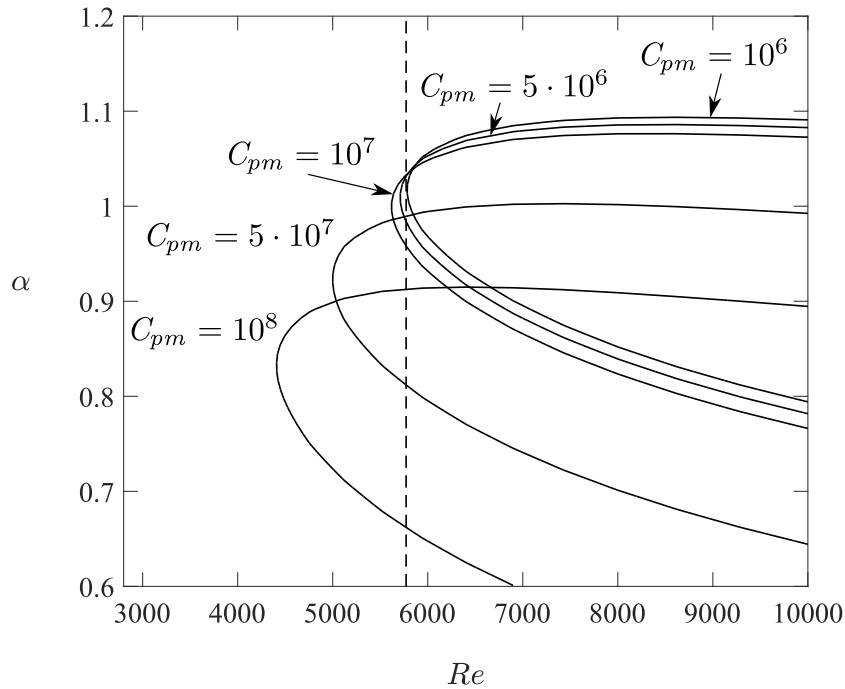


Figure 6.4: The stability diagram showing α of the neutral growth disturbances as a function of Re , for different values of the magnetic parameter C_{pm} . The dashed vertical line represents the value of Re_c^h . The other parameters are the same as the ones used in Fig.6.2.

The influence of τ^* on Re_c is presented in Fig.6.5, where the critical values of Re_c were computed for different values of τ^* . We observe that the values required to detect an observable change in Re_c grow significantly with the decrease of τ^* . It is interesting to note, nevertheless, that the decay rate of Re_c with C_{pm} seems to be a power-law of the type C_{pm}^γ , with a decay rate γ that is fairly independent on the value of τ^* , at least for the few values tested in this work: $\gamma = -0.1593$ for $\tau^* = 10^{-2}$, $\gamma = -0.1541$ for $\tau^* = 5.5 \times 10^{-3}$, and $\gamma = -0.1627$ for $\tau^* = 10^{-3}$.

Finally, if we invert the sign of the horizontal applied magnetic field, i.e. $H_1^b = -1$, we observe no change on the results presented here for $H_1^b = 1$. In fact, by inverting the sense of the applied field, the magnetization of the fluid also changes sign, both the base

state and the perturbations. Since the sign of the RHS of Eq.(6.66) remains unchanged, the stability results also remain unchanged.

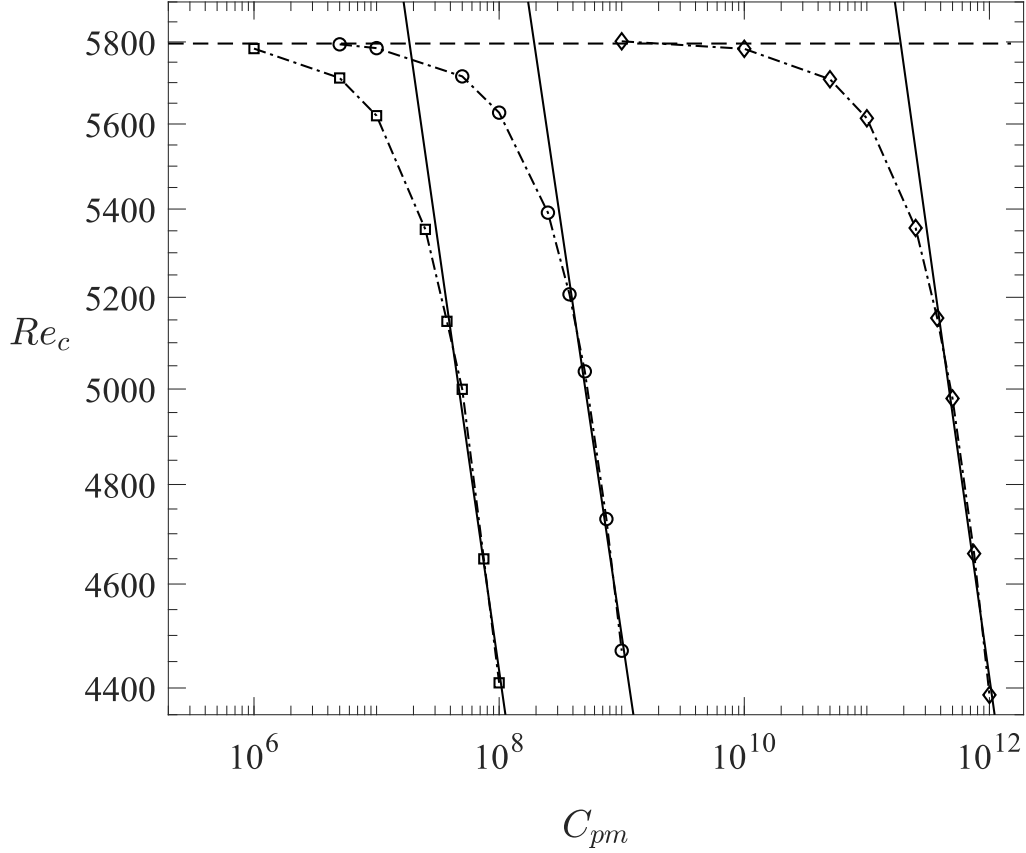


Figure 6.5: Influence of the dimensionless relaxation time τ^* on the value of Re_c , for different values of the magnetic parameter C_{pm} . From left to right, the curves were determined for $\tau^* = 10^{-2}$, 5.5×10^{-3} and 10^{-3} , respectively. The dashed horizontal line represents the value of Re_c^h . The heavy lines represent the power-law fit of the results (see text for details). The other parameters are the same as the ones used in Fig.6.2. Note the results are plotted in a log-log scale.

6.4.2 Vertical applied magnetic field

We consider now the case of a vertical applied magnetic field given by $H_1^b = 0$ and $B_2^b = 1$. The stability diagram for this problem is presented in Fig.6.6 and the stability behavior is now different from the one observed for the case of the horizontal applied magnetic field: the flow is stabilized as the value of C_{pm} increases. As before, the same change of two orders of magnitude of C_{pm} results in an increase of about 30% on the value of Re_c .

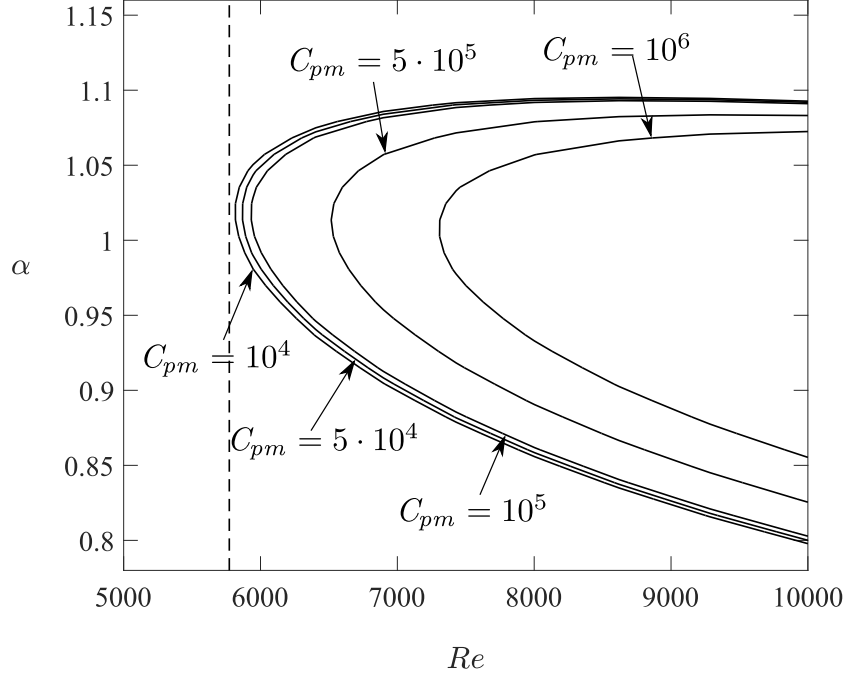


Figure 6.6: The stability diagram showing α of the neutral growth disturbances as a function of Re , for different values of the magnetic parameter C_{pm} for the vertical applied magnetic field. The dashed vertical line represents the value of Re_c^h . The other parameters are the same as the ones used in Fig.6.2.

The influence of τ^* on the increase of Re_c is presented in Fig.6.7 and it is now observed that the increase in Re_c is significantly affected by τ^* , contrary to the results presented in Fig.6.5 for the horizontal applied magnetic field. For $\tau^* = 10^{-2}$, the rate of increase is $\gamma = 0.1638$. It changes to $\gamma = 0.1634$ for $\tau^* = 5.5 \times 10^{-3}$ and assumes the value of $\gamma = 0.0706$ when $\tau^* = 10^{-3}$. Note that when τ^* decreases to 0, the system should recover a superparamagnetic-like behavior (see 6.7) and, therefore, the value of Re_c for all values of C_{pm} should be Re_c^h . Therefore, the slower growth for $\tau^* = 10^{-3}$ is already a manifestation of this asymptotic limit, which seems to occur faster in the vertical case than in the horizontal case. Finally, similarly to the case of a horizontal applied field, no changes were observed when the results were calculated for $B_2^b = -1$.

6.5 Discussion and final remarks

In this work, we have performed a linear stability analysis of the plane parallel flow of a magnetic fluid in the presence of an applied magnetic field. The results indicate that the flows are made more unstable when the applied magnetic field is horizontal, whereas

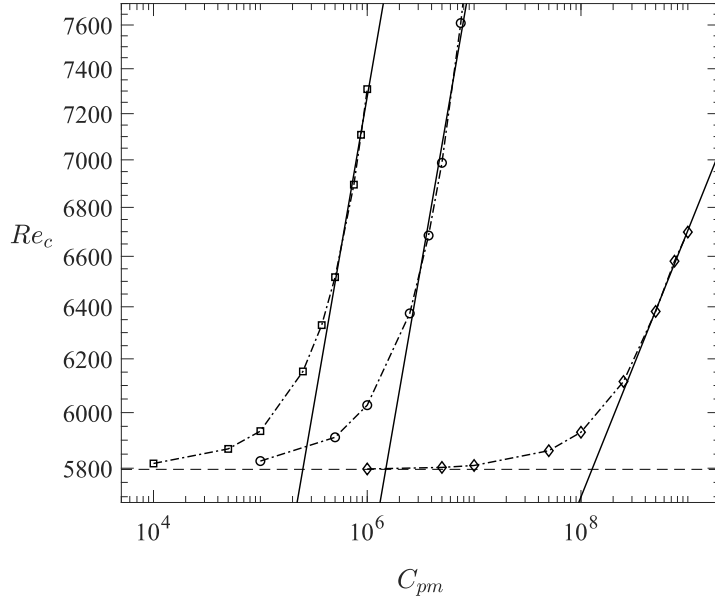


Figure 6.7: Influence of the dimensionless relaxation time τ^* on the value of Re_c , for different values of the magnetic parameter C_{pm} . From left to right, the curves were determined for $\tau^* = 10^{-2}$, 5.5×10^{-3} and 10^{-3} , respectively. The dashed horizontal line represents the value of Re_c^h . The heavy lines represent the power-law fit of the results (see text for details). The other parameters are the same as the ones used in Fig.6.2. Note the results are plotted in a log-log scale.

a stabilization of the flow is achieved for a vertically applied magnetic field. However, the values of the magnetic pressure coefficients that were needed to generate an observable difference on the stability of the flows are very large, far beyond the range observed the experimental setup of [34]. In the case of the largest intensity of applied magnetic field in a turbulent flow in [34], the parameters used in the present work would be $C_{pm} \approx 1.2$ and $Re \approx 3100$. Similarly, in [46] values of $C_{pm} \sim 1 - 5$ (called Ma in their work) were enough to generate the interfacial instabilities.

We believe that the reasons for the range of C_{pm} obtained in this work is so far from the ones mentioned above can be the following. The first one is directly due to the choice of the relaxation time appearing in the magnetization evolution equation. We have chosen to use the range $\tau^* \sim 10^{-3} - 10^{-2}$, which seems to be reasonable for the most common magnetic fluids flowing in normal laboratory conditions [34, 71, 31]. However, if we choose slightly larger particles of a few μm in diameter, the relaxation times might be larger than the ones used here and the influence of the magnetic field on the flow can be more significant, as the base state magnetization will be further away from equilibrium and the RHS of Eq.(6.66) will have a larger weight on the eigenvalues of the stability problem. A quick test of our code with $\tau^* = 10^{-1}$ indicates that $C_{pm} \sim 10^2$ are enough to produce observable change on

the stability of the flow in the case of a vertical applied magnetic field. This range is already closer to the experimental observed values. On the other hand, it is not clear whether the model of the magnetization evolution used in this work is adequate to produce reliable estimates for a real case scenario in which magnetic fluids have such large relaxation times.

The second reason, and most likely the most relevant one, can be that the transition to turbulence in a pipe flow of a magnetic fluid is not affected when magnetic torques are not present on the fluid, that is, when the fluid behaves as a symmetric and/or superparamagnetic magnetic fluid. The extremely large C_{pm} obtained in this work indicate that the transition of the flow will follow its normal hydrodynamical course. In this sense, our results have a strong similarity with Rayleigh's inviscid instability criterion. His work has shown that inertia by itself is not enough to destabilize a Poiseuille flow, since its velocity profile has no inflection point and, by experience, these flows are unstable. A conclusion of the results presented here are, therefore, that the Kelvin force can (and does) change the route of the flow to the base state, but that does not change the rheology of the fluid nor the inner structure of the base state in a way as to significantly alter the stability of the flow.

6.6 Future directions

In this section, we are going to discuss the next steps in this investigation. We want to study the full magnetic problem that considers the torque force in the modified Navier-Stokes equation and the precessional term in the magnetization evolution equation.

As in the Section 6.2, the flow of a ferrofluid in the presence of a magnetic field is described by the continuity equation (6.79), the modified Navier-Stokes equation (6.80) and this time considering the torque force, Maxwell's equations (6.82, 6.83) and the magnetization evolution equation (6.81) with precessional term, as in [52]. These equations in dimensionless form are described by:

$$\nabla \cdot \mathbf{u} = 0, \quad (6.79)$$

$$\frac{\partial \mathbf{u}}{\partial t} + \mathbf{u} \cdot \nabla \mathbf{u} = -\nabla p + \frac{1}{Re} \nabla^2 \mathbf{u} + C_{pm} (\mathbf{M} \cdot \nabla) \mathbf{H} + \frac{C_{pm}}{2} \nabla \times (\mathbf{M} \times \mathbf{H}), \quad (6.80)$$

$$\frac{\partial \mathbf{M}}{\partial t} + \mathbf{u} \cdot \nabla \mathbf{M} = -\frac{1}{\tau^*} (\mathbf{M} - \mathbf{M}_0) + \boldsymbol{\Omega} \times \mathbf{M} - \frac{C_{pm} Re}{6\phi} (\mathbf{M} \times \mathbf{H}) \times \mathbf{M}, \quad (6.81)$$

$$\nabla \times \mathbf{H} = \mathbf{0}, \quad (6.82)$$

$$\nabla \cdot \mathbf{B} = 0, \quad \text{with} \quad \mathbf{B} = \mathbf{H} + \mathbf{M}, \quad (6.83)$$

In order to perform the linear stability analysis we need to determinate the base state for the velocity and magnetic fields. The velocity base state is based on the hypotheses of steady fully developed uni-directional flow in the presence of and external applied magnetic field.

The velocity base state

Let consider steady-state, uni-directional and fully developed flow. From Eq. (6.80), we obtain:

$$\frac{\partial^2 u}{\partial y^2} = Re \frac{\partial p}{\partial x} - \frac{C_{pm}}{2} \frac{\partial (M_1 H_2 - M_2 H_1)}{\partial y}, \quad (6.84)$$

$$\frac{\partial p}{\partial y} = C_{pm} M_2 \frac{\partial H_2}{\partial y}. \quad (6.85)$$

In Eq. (6.85), because there is not explicit dependency of x -variable in the term $(M_1 H_2 - M_2 H_1)$ this equation does not change and only we have modification of the Eq. (6.84) compared to the previous case in Section 6.2.

We note that if there is no magnetic contribution, that is $C_{pm} = 0$, we recover the parabolic profile of Poiseuille, as in Eq. (5.14). Therefore, we expect a non-symmetric profile as a result of magnetic contribution.

The magnetic base state

In order to find the magnetic base state, we consider Eq. (6.81) in both x and y components:

$$0 = -\frac{1}{\tau^*} (M_1 - \chi_0 H_1) + \frac{1}{2} M_2 \frac{du}{dy} - \frac{C_{pm} Re}{6\phi} (M_1 H_2 - M_2 H_1) M_2, \quad (6.86)$$

$$0 = -\frac{1}{\tau^*} (M_2 - \chi_0 H_2) - \frac{1}{2} M_1 \frac{du}{dy} + \frac{C_{pm} Re}{6\phi} (M_1 H_2 - M_2 H_1) M_1, \quad (6.87)$$

where the equilibrium magnetization is approximated by $\mathbf{M}_0 = \chi_0 \mathbf{H}$.

In the system of equations above we want to compute functions $M_1 = M_1(y)$ and $M_2 = M_2(y)$, and it should be noted that the component of H_1 of the applied magnetic field is constant and that the second component depends on the variable y , this is $H_2 = H_2(y)$. In this case, we use constitutive equation for the magnetic induction \mathbf{B} , that is:

$$H_2(y) = B_2 - M_2(y), \quad (6.88)$$

where B_2 constant. With this consideration we obtain a non-linear system of equations,

$$\frac{M_1}{\tau^*} - \frac{1}{2} \frac{du}{dy} M_2 = \frac{\chi_0 H_1}{\tau^*} - \frac{C_{pm} Re}{6\phi} (M_1 (B_2 - M_2) - M_2 H_1) M_2, \quad (6.89)$$

$$\frac{1}{2} \frac{du}{dy} M_1 + \frac{(1 + \chi_0) M_2}{\tau^*} = -\frac{\chi_0 B_2}{\tau^*} + \frac{C_{pm} Re}{6\phi} (M_1 (B_2 - M_2) - M_2 H_1) M_1. \quad (6.90)$$

Observe that this system have M_1, M_2 unknowns functions of y and H_1 and B_2 constants. At the same time, if we consider non-magnetic contribution $C_{pm} = 0$, then we recover the explicit expressions for M_1 and M_2 obtained in Eq. (6.49) and (6.50).

In future works, we intend to solve the system of partial differential equations formed by Eq s (6.84), (6.89) and (6.90) to obtain the velocity and magnetic base states, then we can perform the stability analysis with similar arguments as in Section (6.3.1). There are already results about the calculation of the base states, for example in [43], where the authors found that the base state slightly loses symmetry as an effect of a uniform magnetic field, and this will be the direction that our investigation.

CHAPTER 7

CONCLUSION AND FUTURE DIRECTIONS

In this part of thesis, we studied the linear stability analysis for a two-dimensional flow of symmetrical magnetic fluids between two rigid parallel plates. We have presented the set of equations that govern this problem and that are formed by: the continuity equation, the Navier-Stokes equations modified by the magnetic forces, the magnetization evolution equation proposed by Shliomis [52] and Maxwell's equations.

Linear stability analysis was performed for an applied magnetic field proposed by [46, 62], and the base state of both flow and magnetization were identified. Therefore, by introducing a small disturbance on the base states, it was possible to find an Orr-Sommerfeld type differential equation involving information about the magnetization of the fluid. The critical parameters controlling the magnetic effects on the flow were identified as the magnetic pressure constant and the dimensionless magnetization relaxation time. Subsequently, the numerical approach to solve the extended generalized eigenvalue problem using finite differences was presented.

The marginal stability curves were found for two cases: for an applied magnetic field in the flow direction and for an applied magnetic field perpendicular to the flow direction. Our results have shown that for high intensity magnetic fields the flow behavior is affected by the magnetic effects. For a field in the flow direction, a decrease in the critical Reynolds number was identified, which indicates an advance on the onset of the instability. For a field transversal to the flow direction, the results show an increase of the critical Reynolds number, which indicates a stabilization of the system. For low intensity fields, no change

on the stability has been observed. This is the case of the magnetic fluids present in the industry where the average diameter of the magnetic particles is 10 nanometers, which provides a very short magnetic relaxation time.

In future works, we plan to study the influence of magnetic torques on this problem. Preliminary results have shown that the base state for the flow is no longer Poiseuille's parabolic profile and this, in addition to the influence of the precessional term in the magnetization evolution equation, can bring a new dynamics to the stability problem. On the other hand, we intend to study this problem for magnetorheological fluids which present an average magnetic particle diameter of order micrometers, and which allows us to consider considerably longer magnetic relaxation times.

Part III

Long-wave approximation of Plateau-Rayleigh instability of magnetic fluids

CHAPTER 8

INTRODUCTION

The Plateau-Rayleigh instability has attracted the attention of the scientific community for the last centuries. If we consider a liquid cylinder and introduce a small disturbance on the radius, they grow due to surface tension and cause the breakup into drops and satellite drops. This phenomenon is part of our daily life, for example, when a jet of tap falls downwards into the sink or when honey falls down by its own weight, and a vast list of industrial applications. Among the industrial application we can mention, the atomization, inkjet printing, drug delivery, fuel injection, as quoted in [73, 74, 75].

One of the promising applications of ferrofluids that is under implementation is in the jet printing industry as mentioned in [72]. Due to the nano size of the ferromagnetic particles and their magnetic response, it is possible to use them to give security to documents that are printed on paper, for example: as an additional security measure in passports or to leave a magnetic impression on books that can be read later by a magnetic reader in libraries.

In [61], there is a complete treatment of liquid jet problems, which happen on a small and large scales. These effects are related to the surface tension due to the cohesive intermolecular forces that promote jet rupture. Among applications are aerosol, agricultural irrigation, jet engine technology. The liquid jets involve the study of the free surface, hydrodynamic stability and the formation of singularities that lead to the rupture of the drop. The jets are an ideal scenario to observe liquid properties such as surface tension, viscosity and non-Newtonian rheology, at the same time, other studies are directed to study the jet dynamics of the jet in front of the effect of temperature in the system or considering a surrounding fluid with different characteristics.

We first mention the Rayleigh's work for inviscid fluids [47] in which a dispersion equa-

tion is found that relates instability to the terms of the cylinder radius, surface tension and liquid density. Later, Rayleigh also incorporated the viscosity on the dynamics of the perturbations [48], that result is a classic reference and many authors mention this work for the viscous case.

In order to find new models, several works were developed. For instance, in Eggers and Dupont's work [64], the authors studied the viscous Plateau-Rayleigh problem, and they used the Taylor's series in the radial direction and truncated it to obtain a reduced model of the Navier-Stokes equations, retaining the leading orders of the equations in the radial and axial directions. The obtained one-dimensional equations facilitates the study of the Plateau-Rayleigh problem, both of the stability and of the numerical aspect, and a study of the pinch-off is also made. The authors reproduce examples with high-viscosity fluids, which agree very well with previous experiments [76].

In the work of Balmforth and *al.* [65], the authors assumed the long wavelengths hypothesis, this is the cylinder radius is much less than the wavelength of the disturbances, and this introduces a small parameter that allows to find an asymptotic approximation of the Navies-Stokes equations for viscoplastic fluids, in which the Herschel-Bulkley model is used.

Among the works involving ferrofluids, we can cite the work of Rosensweig [33]. It presents a compendium of problems on the stability of ferrofluids. Among them, one that is of our interest is the problem of a inviscid magnetic liquid jet, in which the short wavelengths hypothesis is assumed. The equations that govern this problem are the same for an inviscid fluid, but the magnetic effect is taken into account by considering a modified magnetic pressure. In this analysis, the velocity of the jet motion is considered to be small, so that the effect of the surrounding liquid on the disintegration of the jet may be neglected. An uniform field is applied to the jet positioned co-axially to the cylinder. Basically, we must solve a Laplace equation for the magnetic potential and satisfy the magnetic boundary conditions, both in the normal and tangential direction. As a result of this stability analysis, the authors present a dispersion relationship involving the frequency, the wave number, the applied magnetic field and the magnetic permeability of the fluid. The analysis lead to conclude that, in the absence of the field, the Rayleigh classic result is recovered, indicating the onset of instability when the wavelength of the disturbance exceeds the perimeter of the jet. The authors [33, 61] conclude that in theory the jet can be stabilized using a longitudinal magnetic field. This approach is also quoted in [61].

In the work of Entov and *al.* [66], the authors studied the jet stability of magnetorheological fluids, for this, they use a power-law model for the stress tensor in which various approaches could be studied, for example, shear-thinning or shear-thickening or simply Newtonian, together with Maxwell's magnetic stress tensor at the super-paramagnetic limit, where the long-wavelength hypothesis was assumed. The evolution equations for the mag-

netic liquid jet are given by the continuity equation and the conservation of liquid flux. The magnetic effect can be seen in two places: one of them is in the viscosity, where the rheology has a small modification as an effect of the magnetic field applied to the fluid. The other place is in the modified pressure in the form of an additional magnetic pressure. The magnetic field flux is taken constant, where the magnetic applied field is inversely proportional to the square of the free boundary radius, thus evolving the boundary close to zero provides a high magnetic field that increases viscosity. In this work, a numerical study about the pinch-off is also carried out and the breakup time is estimated. The authors were able to conclude that the magnetic effect changes significantly the viscosity due to the non-Newtonian rheological approach. this magneto-viscous effect slows down the capillary breakup and shifts the most unstable wavelength, and leads it to long waves corresponding to small wave-number. In the other hand, the effect of the magnetic pressure counteracts the capillary pressure, emulating a kind of elastic behavior. From the linear stability analysis, it can be concluded that a high enough magnetic field can prevent the breakup completely.

In Furlani and Hanchak's work [69], they present a numerical study to predict the instability and breakup of a viscous liquid jet of a Newtonian fluid. In this new approach, the authors use the method of lines (MOL) to transform the one-dimensional system of partial differential presented in [61] to a system of ordinary differential equations using a staggered uniform mesh for the discretisation of the spatially dependent variables of the jet. Two problems were studied to demonstrate the method: an infinite micro-thread Newtonian fluid and a driven-nozzle liquid jet. The authors confirm their results with other works that involve other numerical methods and verify that this numerical approach allows ease of implementation and is faster computationally, they enable a quick analysis of the jet parameters, of the breakup and of the satellite drop formation.

This work will take the follow direction: initially, we are going to establish the classic result of the Plateau-Rayleigh instability, first for a inviscid case and then for a viscous fluid. Next, we will formulate the Plateau-Rayleigh instability for the limit of long wavelengths and we will compare our results with the short wavelength theories. We continue with the analysis of superparamagnetic magnetic inviscid fluid for long wavelengths and compare the linear stability results with the work cited in [33]. We also present the superparamagnetic viscous fluid case and compare this result with [66], both the linear stability and the pinch-off analysis. Finally, we present the full magnetic fluid model, in which we consider the magnetization evolution equation of Shliomis [52].

8.1 General framework for the Rayleigh-Plateau instability

In 1873, Joseph Plateau [63] characterized this instability through experimental observation, built on the work of Savart. He identified the instability arose when the liquid column length exceeded the cylinder diameter of about approximately 3.13 [63]. Later, Lord Rayleigh corroborated the Plateau's work and gave a theoretical explanation of this physical observation.

The behavior of this phenomena derives from the existence of a small perturbation in any physical system. All real flows have some external disturbances that can be considerable non-negligible and that will increase exponentially in unstable systems. In general this deformation of the cylindrical column, sometimes called varicose perturbation, is presented as a series of periodic sinusoidal displacement, as in Fig. (8.2). In this case, for certain wavelengths, the perturbation waves will grow larger in time.

In this configuration, when the displacement amplitude increases, the liquid column will no longer have a constant radius of curvature. From the problem geometry and considering short times or small lengths, the jet is a cylinder with an axial curvature radius $1/R_0$ and longitudinal curvature radius equal to zero. In Fig. (8.1), the perturbed cylinder has areas with positive curvature and others with negative curvature. The pinched sections have higher pressure, this is $1/R$ is greater, and the bulging sections (belly region) have lower pressure, producing a fluid flow as a result of the effect of the pressure gradient. The internal flux causes the growth of the displacement amplitude which initiates the formation of the droplets and they form when the pinched section ruptures and the *belly* areas transform into a sequence of small droplets.

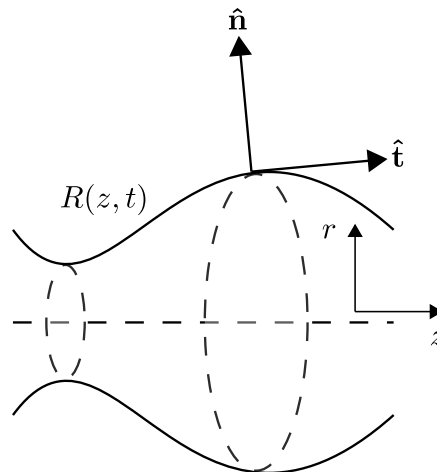


Figure 8.1: A diagram showing the configuration of the free surface in cylindrical coordinates. The horizontal dashed line represents the axis of symmetry in $r = 0$.

This is described by the momentum equation along the radial direction

$$\rho \left(\frac{\partial u}{\partial t} + u \frac{\partial u}{\partial r} + w \frac{\partial u}{\partial z} \right) = -\frac{\partial p}{\partial r} + \mu \left(\frac{\partial^2 u}{\partial r^2} + \frac{1}{r} \frac{\partial u}{\partial r} - \frac{u}{r^2} + \frac{\partial^2 u}{\partial z^2} \right), \quad (8.1)$$

then in axial direction

$$\rho \left(\frac{\partial w}{\partial t} + u \frac{\partial w}{\partial r} + w \frac{\partial w}{\partial z} \right) = -\frac{\partial p}{\partial z} + \mu \left(\frac{\partial^2 w}{\partial r^2} + \frac{1}{r} \frac{\partial w}{\partial r} + \frac{\partial^2 w}{\partial z^2} \right), \quad (8.2)$$

and the continuity equation,

$$\frac{\partial u}{\partial r} + \frac{\partial w}{\partial z} + \frac{u}{r} = 0. \quad (8.3)$$

where u and w are the radial and the axial velocities.

The boundary conditions, calculated at the free surface of the jet which is related to the mean curvature, express the relation between the pressure difference, across the free surface with the normal stress is given by

$$\hat{\mathbf{n}}^t \cdot \boldsymbol{\Sigma} \cdot \hat{\mathbf{n}} = -\sigma \kappa, \quad (8.4)$$

where $\boldsymbol{\Sigma}$ is the stress tensor, κ is the mean curvature of the free surface, here defined as $\nabla \cdot \hat{\mathbf{n}}$, σ is the surface tension and $\hat{\mathbf{n}}$ is the unit normal vector to the free surface, which points from the inside to the exterior of the cylinder as shown the Fig.(8.1). If we consider the external zone to be empty (vacuum), then the tangential stresses along the surface of the jet can be equated to zero

$$\hat{\mathbf{n}}^t \cdot \boldsymbol{\Sigma} \cdot \hat{\mathbf{t}} = \mathbf{0}, \quad (8.5)$$

where $\hat{\mathbf{t}}$ is the tangent vector to the free surface, define by $r = R(z, t)$, again as shown in Fig. (8.1).

Finally, the kinematic condition at the free surface requires that a particle at the free surface to remain there so that $F(r, z, t) = r - R(z, t)$ must satisfy:

$$\frac{DF}{Dt} = 0, \quad (8.6)$$

this can be also expressed as,

$$\frac{\partial R}{\partial t} + w \frac{\partial R}{\partial z} = u, \quad (8.7)$$

The effect of the pressure inside the cylindrical liquid jet is a function of the curvature of the surface, which is given by the Young-Laplace equation, as it can be seen in [67]:

$$p = \sigma \left(\frac{1}{R_1} + \frac{1}{R_2} \right). \quad (8.8)$$

It is also written as (see Appendix II.4),

$$p = \sigma \left(\frac{1}{R \left(1 + \left(\frac{\partial R}{\partial z} \right)^2 \right)^{\frac{1}{2}}} - \frac{\frac{\partial^2 R}{\partial z^2}}{\left(1 + \left(\frac{\partial R}{\partial z} \right)^2 \right)^{\frac{3}{2}}} \right). \quad (8.9)$$

The Young-Laplace equation gives an expression for the pressure difference over an interface between two fluids terms of the surface tension coefficient σ and the principal radii of curvature R_1 and R_2 .

8.2 The Plateau-Rayleigh Instability

8.2.1 The Inviscid Case

In this section, we present the classical result of the Plateau and Rayleigh about the instability of a cylindrical fluid jets due the surface tension, for this purpose we follow the references [7, 9].

Consider a column of fluid of radius R_0 with density ρ in which we neglect its viscosity μ and the effects of gravity g , this case is commonly called inviscid flow. The pressure inside the column is assumed to be constant p_0 and it is calculated by balancing the normal stress at the boundary. We also assume zero external pressure which yields,

$$p_0 = \frac{\sigma}{R_0}. \quad (8.10)$$

Note that from Eq. (8.9) the radii of curvature R_1 is R_0 and the R_2 takes infinite value for cylindrical column configuration.

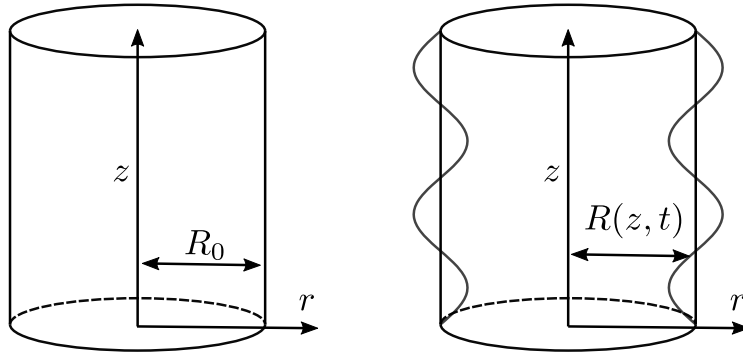


Figure 8.2: On the left-hand side, we have the unperturbed cylinder of radius R_0 (base state). On the right-hand side, the perturbed cylinder in which the surface is given by $R = R(z, t)$.

The base state consider the radius constant R_0 of the unperturbed cylinder, as on the left-side of Fig. (8.2) and we consider the radial perturbed state in the right-hand side of Fig. (8.2), as follows:

$$R = R_0 + \varepsilon e^{(\omega t + ikz)}, \quad (8.11)$$

where $\varpi \in \mathbb{C}$ is the frequency and k is the wave-number and ε is a small perturbation such that $\varepsilon \ll R_0$. By the axial symmetry R does not depend on θ , that is, R is a function depending on z and t .

The governing equations of a inviscid fluid in cylindrical coordinates are given by the axial and radial components equation, the latter is

$$\rho \left(\frac{\partial u}{\partial t} + u \frac{\partial u}{\partial r} + w \frac{\partial u}{\partial z} \right) = -\frac{\partial p}{\partial r}, \quad (8.12)$$

and in the axial component,

$$\rho \left(\frac{\partial w}{\partial t} + u \frac{\partial w}{\partial r} + w \frac{\partial w}{\partial z} \right) = -\frac{\partial p}{\partial z}, \quad (8.13)$$

these two equations together with the continuity equation in cylindrical coordinates (8.3) form the system of partial differential equations that governs the nonlinear problem.

8.2.2 The stability analysis

We consider the following ansatz for the disturbed variable:

$$(u', w', p') = (U(r), W(r), P(r))e^{(\varpi t + ikz)}, \quad (8.14)$$

where u' is the radial velocity, w' is the axial velocity and p' is the pressure of the perturbations. We substitute these perturbations in Eqs. (8.12)-(8.13) and retain only $\mathcal{O}(\varepsilon)$ terms, that is, we consider only the linear terms in perturbations. Keeping the terms of order $\mathcal{O}(\varepsilon)$ in Eq. (8.12) yields,

$$\rho \frac{\partial u'}{\partial t} = -\frac{\partial p'}{\partial r}, \quad (8.15)$$

and substituting in Eq. (8.13) provides,

$$\rho \frac{\partial w'}{\partial t} = -\frac{\partial p'}{\partial z}. \quad (8.16)$$

We note that a temporal derivative of the ansatz Eq. (8.14) contributes a factor of ϖ , while a spatial derivative contributes with a factor of ik with $i = \sqrt{-1}$ and a radial derivative implies a derivative of the amplitude function. Substituting the ansatz Eq. (8.14) in Eqs.(8.15)-(8.16), provides for Eq. (8.15),

$$\rho \varpi U(r) = -\frac{dP(r)}{dr}, \quad (8.17)$$

while for Eq. (8.16),

$$\rho \varpi W(r) = -ikP(r). \quad (8.18)$$

Developing the incompressibility Eq. (8.3), keeping the terms order $\mathcal{O}(\varepsilon)$ and substituting the ansatz perturbations Eq. (8.14)

$$\frac{dU}{dr} + ikZ(r) + \frac{U(r)}{r} = 0. \quad (8.19)$$

Solving the system of Eqs.(8.17)-(8.18) and (8.19) by deriving Eq.(8.18) in relation to radial component

$$\rho\varpi \frac{dW}{dr} = -ik \frac{dP}{dr}, \quad (8.20)$$

then, we substitute the derivative dP/dr by the expression in Eq. (8.17)

$$\rho\varpi \frac{dW}{dr} = ik\rho\varpi U. \quad (8.21)$$

Simplifying $\rho\varpi$, and taking the radial taking the radial derivative of Eq. (8.19), we get

$$\frac{d^2U}{dr^2} + ik \frac{dW}{dr} + \frac{d}{dr} \left(\frac{U(r)}{r} \right) = 0. \quad (8.22)$$

Expanding the radial derivative of the third term of the left hand side

$$\frac{d^2U}{dr^2} + ik \frac{dW}{dr} + \frac{1}{r} \frac{dU}{dr} - \frac{U}{r^2} = 0, \quad (8.23)$$

Multiplying by r^2 and substituting the term dW/dr using Eq. (8.21)

$$r^2 \frac{d^2U}{dr^2} + (ik)^2 r^2 U + r \frac{dU}{dr} - R = 0, \quad (8.24)$$

Factorizing the terms involving the amplitude R

$$r^2 \frac{d^2U}{dr^2} + r \frac{dU}{dr} - (1 + (kr)^2)U = 0, \quad (8.25)$$

The expression above is the modified Bessel equation of order 1 with factor kr [2], whose solution is a linear combination of the modified Bessel functions of first and second kind $I_1(kr)$ and $K_1(kr)$ respectively. In order to main regularity of solution, we note that $K_1(kr) \rightarrow 0$ as $kr \rightarrow 0$, allowing us to access the solution of $U(r)$,

$$U(r) = C I_1(kr), \quad (8.26)$$

where C is a constant to be found. By using Eq. (8.17) and replacing the solution of the Bessel equation (8.26),

$$\frac{dP(r)}{dr} = -\rho\varpi C I_1(kr), \quad (8.27)$$

and by using the Bessel functions identity $I'_0(\xi) = I_1(\xi)$ [2], and integrating we have

$$P(r) = -\frac{\rho\varpi}{k} C I_0(kr), \quad (8.28)$$

8.2.2.1 Boundary conditions

The kinematic condition (8.7) on the free surface for the perturbed variables (8.11) and (8.14) indicates,

$$\frac{\partial R}{\partial t} = u, \quad (8.29)$$

which is valid at the boundary $r = R_0$. Introducing the ansatz (8.14) in expression above, allows us to obtain:

$$\varepsilon\varpi e^{(\varpi t+ikz)} = U(R_0)e^{(\varpi t+ikz)}. \quad (8.30)$$

Replacing $U(R_0)$ from Eq. (8.26), gives us,

$$\varepsilon\varpi = CI_1(kR_0), \quad (8.31)$$

from where we can determine the value of the constant C as,

$$C = \frac{\varepsilon\varpi}{I_1(kR_0)}. \quad (8.32)$$

We replace the value of C in the expression of $U(r)$ in Eq. (8.26), as follows;

$$U(r) = \frac{\varepsilon\varpi}{I_1(kR_0)}I_1(kr), \quad (8.33)$$

and substituting the value of C in Eq. (8.28), we get a final expression for P ,

$$P(r) = -\frac{\varepsilon\rho\varpi^2}{kI_1(kR_0)}I_0(kr). \quad (8.34)$$

The boundary conditions requires a normal stress balance at the free surface,

$$p_0 + p' = \sigma\nabla \cdot \hat{\mathbf{n}}. \quad (8.35)$$

We write the curvature as in Eq. (8.9), where R_1 and R_2 are the principal radii of curvature on the free surface. The expression for R_1 contains a square root involving a derivative of the free surface that contributes to the stability analysis with terms $\mathcal{O}(\varepsilon^2)$ and we discard that term, then terms $\mathcal{O}(1)$ and $\mathcal{O}(\varepsilon)$ are maintained with the free surface R . Substituting (8.11) and using the binomial expansion to develop $R_1 = R$, yields:

$$\frac{1}{R_1} = \frac{1}{R_0} - \frac{\varepsilon}{R_0^2}e^{(\varpi t+ikz)}. \quad (8.36)$$

Now, we find a expression for R_2 , which is related with the second derivative of R

$$\frac{1}{R_2} = \varepsilon k^2 e^{(\varpi t+ikz)}. \quad (8.37)$$

Substituting Eq.(8.36) and (8.37) into Eq. (8.35) yields;

$$p_0 + p' = \frac{\sigma}{R_0} - \frac{\varepsilon\sigma}{R_0^2}(1 - (kR_0)^2)e^{(\varpi t+ikz)}, \quad (8.38)$$

here we use the expression for p_0 from Eq. (8.10),

$$\frac{\sigma}{R_0} + p' = \frac{\sigma}{R_0} - \frac{\varepsilon\sigma}{R_0^2}(1 - (kR_0)^2)e^{(\varpi t+ikz)}, \quad (8.39)$$

Canceling the first terms in both sides and substituting p' by its respective expression in Eq. (8.34)

$$P(r)e^{(\varpi t+ikz)} = -\frac{\varepsilon\sigma}{R_0^2}(1 - (kR_0)^2)e^{(\varpi t+ikz)}, \quad (8.40)$$

we obtain the following expression for $P(r)$:

$$P(r) = -\frac{\varepsilon\sigma}{R_0^2}(1 - (kR_0)^2), \quad (8.41)$$

substituting the expression of P by using Eq. (8.34) and evaluating at $r = R_0$,

$$-\frac{\varepsilon\rho\varpi^2 I_0(kR_0)}{kI_1(kR_0)} = -\frac{\varepsilon\sigma}{R_0^2}(1 - (kR_0)^2). \quad (8.42)$$

Isolating the ϖ^2 term, we finally obtain:

$$\varpi^2 = \frac{\sigma k R_0 I_1(kR_0)}{\rho R_0^3 I_0(kR_0)}(1 - (kR_0)^2), \quad (8.43)$$

which is expressed in dimensionless form using $\bar{\varpi} = \varpi\sqrt{\rho R_0^3/\sigma}$ and $\bar{k} = kR_0$, providing:

$$\bar{\varpi}^2 = \frac{\bar{k} I_1(\bar{k})}{I_0(\bar{k})}(1 - \bar{k}^2). \quad (8.44)$$

This expression is called *Dispersion Equation*. This is a relation between the frequency ϖ and the wave-number k and it is possible to conclude the following: if $kR_0 < 1$, then $\varpi^2 = a$ with $a \in \mathbb{R}^+$, which implies that $\varpi = \sqrt{a} > 0$ and getting a factor of $e^{\sqrt{a}t}$ in the considered ansatz producing an unstable state as the time goes by. If $kR_0 > 1$, then $\varpi^2 = -a$ with $a \in \mathbb{R}^+$, implying $\varpi = i\sqrt{a}$ and giving us a factor of $e^{i\sqrt{a}t}$ in the ansatz yielding a stable (oscillatory) state as time evolves.

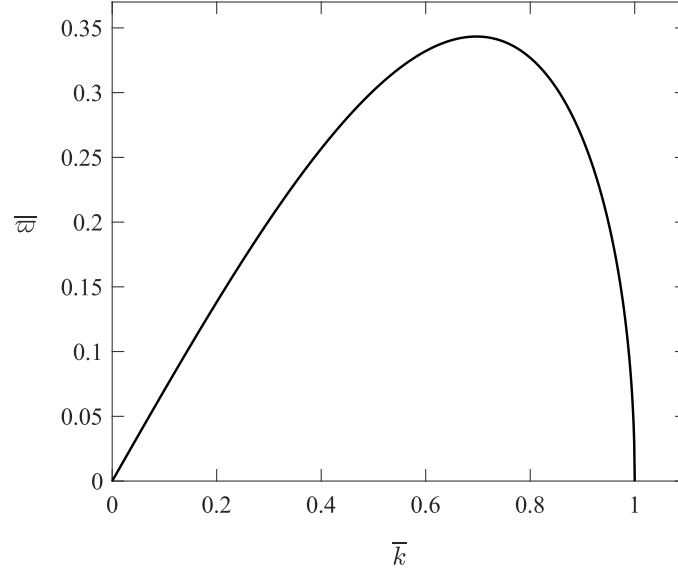


Figure 8.3: Figure shows the growth rate $\bar{\varpi} = \varpi\sqrt{\rho R_0^3/\sigma}$ as a function of the wave number $\bar{k} = kR_0$ for a cylinder liquid jet in the inviscid limit.

The representation of this kind of instability is shown in Fig. (8.3). With this, the liquid jet is unstable when the wavelength are larger than $2\pi R_0$, this is, if $kR_0 < 1$, then $(kR_0)^{-1} > 1$ and multiplying by $2\pi R_0$, yields $\lambda > 2\pi R_0$. If $kR_0 > 1$, then $(kR_0)^{-1} < 1$ and multiplying by $2\pi R_0$, yields $\lambda < 2\pi R_0$ getting stable modes.

The equation (8.44) is valid short and long wave-lengths, but a particular limit of our interest is taken when we consider long wave-lengths, for this the recall the limit of the Bessel function $I_\alpha(x)$ and $\Gamma(n) = (n - 1)!$;

$$I_\alpha(x) = \sum_{n=0}^{+\infty} \frac{(-1)^n}{n!\Gamma(n + \alpha + 1)} \left(\frac{x}{2}\right)^\alpha \stackrel{x \rightarrow 0}{\approx} \frac{1}{\Gamma(\alpha + 1)} \left(\frac{x}{2}\right)^\alpha \quad (2)$$

Taking $\alpha = 0$ and $\alpha = 1$, provides;

$$I_0(x) \stackrel{x \rightarrow 0}{\rightarrow} 1, \quad I_1(x) \stackrel{x \rightarrow 0}{\rightarrow} \frac{x}{2}. \quad (8.45)$$

By replacing this information in Eq. (8.44), we get:

$$\overline{\omega}^2 = \frac{\overline{k}^2}{2}(1 - \overline{k}^2), \quad (8.46)$$

this equation will be invoked throughout this work.

8.2.3 The Viscous Case

In this subsection, we present the result of the Plateau-Rayleigh instability for a viscous fluid flow.

After presenting the result for the inviscid instability, Rayleigh in 1982 [48] extended his work regarding Plateau-Rayleigh instability for viscous fluid flows, as a result of his work he found a dispersion relation involving the wave number k and the frequency ϖ , however, he used the ansatz proportional to $\exp(i\varpi t - ikz)$, which produced a complex expression that involves the Bessel functions of first and second order, from which it is difficult to draw conclusions. In general, the scientific community refers to this result, but they only use an asymptotic approximation of it, in the limit of very large viscosity in comparison to inertia [61], which can be expressed in the following form

$$i\varpi = -\frac{\sigma}{2R_0\eta} \frac{1 - (kR_0)^2}{1 + (kR_0)^2(1 + (J_0(ikR_0)/J'_0(ikR_0)^2))}. \quad (8.47)$$

Later, the work of Chandrasekhar in 1961 [9] approached the problem using a different ansatz: proportional to $\exp(\varpi t + ikz)$, which allowed the use of Bessel functions I_0 , I_1 and its derivatives, getting

$$\varpi = -\frac{\sigma}{2R_0\eta} \frac{1 - (kR_0)^2}{1 + (kR_0)^2(1 - (I_0(kR_0)/I_1(kR_0)^2))}, \quad (8.48)$$

again this approach is valid for a very viscous flow.

Later, Eggers and Dupont's work came [64], in which they used a linear approximation around $w = 0$ and $R = R_0$ leads us to find the following dispersion relation in non-dimensional form,

$$\varpi^2 = \frac{\sigma(kR_0)^2}{2\rho R_0^3}(1 - (kR_0)^2) - \frac{3\eta(kR_0)^2}{\rho R_0^2}\varpi. \quad (8.49)$$

in this equation, if we consider the viscosity $\eta = 0$, then we recover the inviscid limit Eq. (8.44) when $k \rightarrow \infty$. This limit is called *the strong viscous limit*. The Eq. (8.49) has been reported in [9, 64].

CHAPTER 9

LONG WAVES APPROXIMATION OF THE PLATEAU-RAYLEIGH INSTABILITY

9.1 The Long-Wave Approximation

The problem of determining the time evolution of the fluid jet is nonlinear because: first, the Navier-Stokes equations that govern the fluid flow are nonlinear. Second, the boundary conditions to be applied at the free surface of the jet are nonlinear and third, the surface of the jet is a free surface, in the sense that its position must be found as a part of the solution technique. These all make part of a nonlinear free boundary value problem.

The assumption of the long wave-lengths approximation, or sometimes called slender fluid jet, in which one of the typical length scales is smaller (very much smaller) than the others leads to a significant simplification of the problem. In fact, it becomes possible to regard the flow as essentially one dimensional and to obtain a closed coupled set of equations for the evolution of the velocity and the free surface, see by example [65].

In this work, we assume that the initial radius of the cylinder R_0 is much less than the wavelength λ , that is, $R_0 \ll \lambda$. By doing this, we introduce a small parameter in our problem given by:

$$\epsilon = \frac{R_0}{\lambda} \ll 1, \tag{9.1}$$

then the re-scale radial position is $r = \epsilon \bar{r}$.

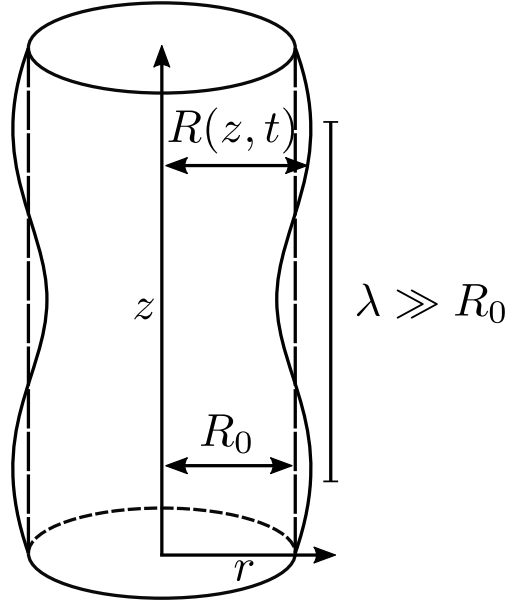


Figure 9.1: Geometry of the problem, the long-wave limit is characterized by using long wavelengths compared to the initial radius R_0 .

9.2 The inviscid case

In this Section, we consider the Navier-Stokes equations in cylindrical coordinates for an incompressible inviscid fluid: first we enunciate the equation in the radial direction

$$\rho \left(\frac{\partial u}{\partial t} + u \frac{\partial u}{\partial r} + w \frac{\partial u}{\partial z} \right) = - \frac{\partial p}{\partial r}, \quad (9.2)$$

then the equation in the axial direction

$$\rho \left(\frac{\partial w}{\partial t} + u \frac{\partial w}{\partial r} + w \frac{\partial w}{\partial z} \right) = - \frac{\partial p}{\partial z}, \quad (9.3)$$

and the continuity equation in cylindrical coordinates

$$\frac{1}{r} \frac{\partial (ru)}{\partial r} + \frac{\partial w}{\partial z} = 0. \quad (9.4)$$

The velocity field is given by $\mathbf{u} = (u, 0, w)$, and due that there is not movement in the θ -component we do not consider the equation in θ -direction. The pressure is given by p from Eq (8.9).

In Fig. (9.1), the initial cylinder radius is R_0 and the radial function depends only on z and t variables. The variable λ is the wave-length, and in this case it is being analyzed the case of long wave-lengths, this case is also known as long-wave limit, i.e. $R_0 \ll \lambda$, this hypotheses generates small parameter $\epsilon = R_0/\lambda \ll 1$ as in Eq. (9.1). Under this observations also is assumed that,

$$r \rightarrow \epsilon r, \quad u \rightarrow \epsilon u, \quad \frac{\partial}{\partial r} \rightarrow \epsilon^{-1} \frac{\partial}{\partial r}, \quad u \ll w. \quad (9.5)$$

Which these modification we re-scale the Eq. (9.2)-(9.3) and (9.4). From re-scaling Eq. (9.3):

$$\rho \left(\frac{\partial w}{\partial t} + \epsilon u \frac{1}{\epsilon} \frac{\partial w}{\partial r} + w \frac{\partial w}{\partial z} \right) = -\frac{\partial p}{\partial z}, \quad (9.6)$$

then after cancellation of parameter ϵ we maintain the initial Eq. (9.2). This indicates that Eq. (9.3) does not change with this limit. But with Eq. (9.2)

$$\rho \left(\epsilon \frac{\partial u}{\partial t} + \epsilon^2 u \frac{1}{\epsilon} \frac{\partial u}{\partial r} + \epsilon w \frac{\partial u}{\partial z} \right) = -\frac{1}{\epsilon} \frac{\partial p}{\partial r} \quad (9.7)$$

simplifying and putting the ϵ term in the left-hand side yields

$$\rho \epsilon^{-2} \left(\frac{\partial u}{\partial t} + u \frac{\partial u}{\partial r} + w \frac{\partial u}{\partial z} \right) = -\frac{\partial p}{\partial r}. \quad (9.8)$$

The last equation changes in relation to Eq. (9.2) and in order to scale this expression, it has to be assumed that $\partial p / \partial r = 0$ or that p is independent of r , implying that the p -function depends only on z and t , that is, $p = p(z, t)$. Regarding Eq. (9.3) indicates no dependency on variable r , then we can conclude that $w = w(z, t)$, and through the project we are going to assume that w does not depend on r . Also there is no change with the continuity equation (9.4), once we replace the proposed scale

$$\frac{\epsilon^2}{\epsilon^2 r} \frac{\partial(ru)}{\partial r} + \frac{\partial w}{\partial z} = 0, \quad (9.9)$$

and after simplify the ϵ 's we get the unchanged Eq. (9.4). Integrating Eq. (9.4) with respect to $r \in [0, R]$:

$$\int \frac{\partial(ru)}{\partial r} dr + \int r \frac{\partial w}{\partial z} dr = 0, \quad (9.10)$$

we remark that the w -function does not depend on r , getting

$$u = -\frac{R}{2} \frac{\partial w}{\partial z}. \quad (9.11)$$

Using the boundary condition,

$$\frac{\partial R}{\partial t} + w \frac{\partial R}{\partial z} = u. \quad (9.12)$$

substituting u from Eq. (9.11) in the last expression provides,

$$2R \left(\frac{\partial R}{\partial t} + w \frac{\partial R}{\partial z} \right) + R^2 \frac{\partial w}{\partial z} = 0, \quad (9.13)$$

when the first term is written as a second time derivative of the square of R and the second and third terms are condensed as a second spatial derivative of wR , as follows

$$\frac{\partial(R^2)}{\partial t} + \frac{\partial(R^2 w)}{\partial z} = 0. \quad (9.14)$$

Regarding Eq. (9.3), we note that w does not depend on r and hence the r -derivative is neglected, getting the expression

$$\rho \left(\frac{\partial w}{\partial t} + w \frac{\partial w}{\partial z} \right) = -\frac{\partial p}{\partial z}. \quad (9.15)$$

The equations (9.14), (9.3) and (8.9) form the reduced system of partial differential equations in terms of R and w for the problem of Plateau-Rayleigh in the long-wave limit.

9.2.1 The stability analysis

For the stability analysis, we solve the system of partial differential equations Eqs. (9.14) and (9.15) by considering the following perturbations for R and w ,

$$R \approx R_0 + \varepsilon R_1, \quad w \approx \varepsilon W_1, \quad (9.16)$$

in which the disturbed parameters R_1 and W_1 are given by:

$$R_1, W_1 \propto \exp(\varpi t + ikz). \quad (9.17)$$

In this expressions, we consider the perturbation of the cylinder of the free boundary R , and the third component of the velocity field, also the typical ansatz is taken as the previous Section (8.2.1).

In order to find the stability expression, we first introduce the above perturbations (9.16) in Eq. (9.14)

$$\frac{\partial(R_0 + \varepsilon R_1)^2}{\partial t} + \frac{\partial(\varepsilon W_1(R_0 + \varepsilon R_1)^2)}{\partial z} = 0, \quad (9.18)$$

and keeping the terms of order ε , $\mathcal{O}(\varepsilon)$, we obtain:

$$2R_0\varpi R_1 + ikW_1R_0^2 = 0. \quad (9.19)$$

Regarding Eq.(9.15), the expression of p is given by Eq. (8.9), in which the expression $(\partial R/\partial z)^2$ together with the perturbation $R_0 + \varepsilon R_1$ yield a expression of order $\mathcal{O}(\varepsilon)$, and it is neglected in this approximation. By introducing the above perturbations on the momentum w -equation, we get

$$\rho \left(\varepsilon \frac{\partial W_1}{\partial t} + \varepsilon^2 W_1 \frac{\partial W_1}{\partial z} \right) = -\sigma \frac{\partial}{\partial z} \left(\frac{1}{R_0 + \varepsilon R_1} - \frac{\partial^2(R_0 + \varepsilon R_1)}{\partial z^2} \right), \quad (9.20)$$

when the second term of $\mathcal{O}(\varepsilon^2)$ on the left side is neglected and the second term on the right side contains a constant R_0 is also canceled,

$$\rho \varepsilon \frac{\partial W_1}{\partial t} = -\sigma \frac{\partial}{\partial z} \left(\frac{1}{R_0 + \varepsilon R_1} - \varepsilon \frac{\partial^2 R_1}{\partial z^2} \right), \quad (9.21)$$

developing with binomial expansion the first term on the right side provides

$$\rho \varepsilon \frac{\partial W_1}{\partial t} = -\sigma \frac{\partial}{\partial z} \left(\frac{1}{R_0} \left(1 - \varepsilon \frac{R_1}{R_0} \right) - \varepsilon \frac{\partial^2 R_1}{\partial z^2} \right), \quad (9.22)$$

and eliminating the inner parentheses on the right-hand side and the corresponding time derivative of the ansatz on the left-hand side provides a factor of ϖ ,

$$\rho \varepsilon \varpi W_1 = -\sigma \frac{\partial}{\partial z} \left(\frac{1}{R_0} - \varepsilon \frac{R_1}{R_0^2} - \varepsilon \frac{\partial^2 R_1}{\partial z^2} \right), \quad (9.23)$$

distributing the z -derivative on the parentheses, replacing an spatial derivative that provides a factor of ik , placing the $-\varepsilon ik$ factor outside the parentheses, and then we simplify the ε term, taking the denominator of R_0^2 outside of the parentheses, provides:

$$\rho\varpi W_1 = \frac{\sigma ik}{R_0^2} (1 - (kR_0)^2) R_1. \quad (9.24)$$

From Eqs. (9.18) and (9.24), substituting W_1 and maintaining the growth-rate kR_0 in the expression, we get:

$$\varpi^2 = \frac{\sigma(kR_0)^2}{2\rho R_0^3} (1 - (kR_0)^2), \quad (9.25)$$

which in dimensionless form is given by:

$$\bar{\varpi}^2 = \frac{\bar{k}^2}{2} (1 - \bar{k}^2). \quad (9.26)$$

The Eq. (9.26) is know as the *dispersion relation* equation for the stability of a liquid jet considering the long wave-lengths approximation. If we take the limit $kR_0 \rightarrow 0$ and replace

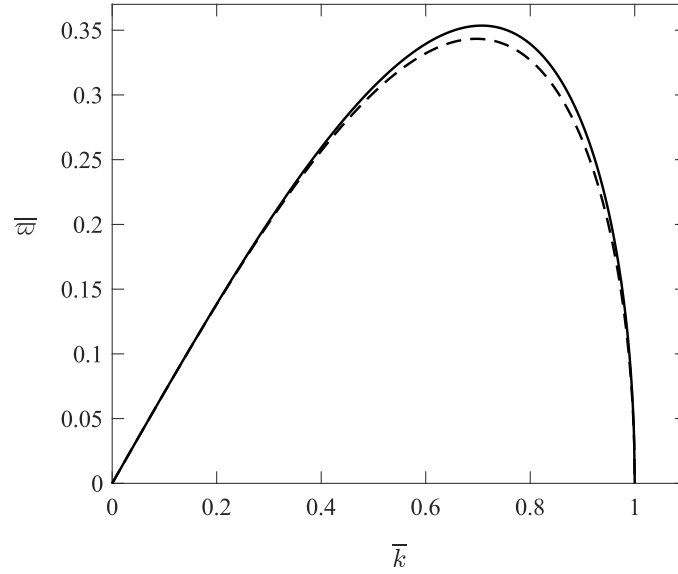


Figure 9.2: Figure shows the growth rate $\bar{\omega} = \varpi\sqrt{\rho R_0^3/\sigma}$ as a function of the wave number $\bar{k} = kR_0$ for an inviscid cylinder liquid jet in the long wavelength approximation (solid-line) compared with the classical dispersion relation of the Plateau-Rayleigh instability (dashed-line).

the approximate value of Bessel functions I_0 and I_1 into the Eq. (8.44), allows us to find the Eq. (9.26) for the long wave-lengths limit.

9.3 The viscous case

We consider the following governing equations in cylindrical coordinates for a viscous incompressible fluid: The equation in the radial direction is

$$\rho \left(\frac{\partial u}{\partial t} + u \frac{\partial u}{\partial r} + \hat{w} \frac{\partial u}{\partial z} \right) = -\frac{\partial p}{\partial r} + \eta \left(\frac{\partial}{\partial r} \left(\frac{1}{r} \frac{\partial(ru)}{\partial r} \right) + \frac{\partial^2 u}{\partial z^2} \right), \quad (9.27)$$

and the equation in the axial direction is given by

$$\rho \left(\frac{\partial \hat{w}}{\partial t} + u \frac{\partial \hat{w}}{\partial r} + \hat{w} \frac{\partial \hat{w}}{\partial z} \right) = -\frac{\partial p}{\partial z} + \eta \left(\frac{1}{r} \frac{\partial}{\partial r} \left(r \frac{\partial \hat{w}}{\partial r} \right) + \frac{\partial^2 \hat{w}}{\partial z^2} \right), \quad (9.28)$$

and we maintain the continuity equation that is given by Eq. (9.4).

$$\frac{1}{r} \frac{\partial(ru)}{\partial r} + \frac{\partial \hat{w}}{\partial z} = 0. \quad (9.29)$$

The velocity field is given by $\mathbf{u} = (u, 0, \hat{w})$, the pressure p and the viscosity η and due that we do not have movement in the θ -component we do not consider the equation in θ -direction.

In Fig. (9.1), radius of the initial cylinder is R_0 and the radius function depends only on z and t variables. The variable λ is wave-length, and in this case it is being analyzed the case of long wave limit, i.e. $\lambda \gg R_0$. Under this modifications also is assumed that $r \rightarrow \epsilon r$, $u \rightarrow \epsilon u$ and $\partial/\partial r \rightarrow \epsilon^{-1} \partial/\partial r$, also $u \ll w$. Which these modification we have to re-scale the above equations.

We start by re-scaling Eq. (9.28):

$$\rho \left(\frac{\partial \hat{w}}{\partial t} + \epsilon u \frac{1}{\epsilon} \frac{\partial \hat{w}}{\partial r} + \hat{w} \frac{\partial \hat{w}}{\partial z} \right) = -\frac{\partial p}{\partial z} + \eta \left(\frac{\epsilon^{-2}}{r} \frac{\partial}{\partial r} \left(r \frac{\partial \hat{w}}{\partial r} \right) + \frac{\partial^2 \hat{w}}{\partial z^2} \right). \quad (9.30)$$

This indicates that Eq. (9.30) must to be balanced in order to maintain the same scale. In order to do this we introduce,

$$\hat{w} = w(z, t) + \epsilon^2 w_2(r, z, t), \quad (9.31)$$

Replacing this expression into Eq. (9.30), note that the factor ϵ^{-2} on the right-hand side is simplified by the new expansion of w , we get;

$$\rho \left(\frac{\partial w}{\partial t} + w \frac{\partial w}{\partial z} \right) = -\frac{\partial p}{\partial z} + \eta \left(\frac{1}{r} \frac{\partial}{\partial r} \left(r \frac{\partial w_2}{\partial r} \right) + \frac{\partial^2 w}{\partial z^2} \right). \quad (9.32)$$

But introducing the scale in Eq. (9.27), yields

$$\rho \left(\epsilon \frac{\partial u}{\partial t} + \epsilon u \frac{\partial u}{\partial r} + \epsilon w \frac{\partial u}{\partial z} \right) = -\frac{1}{\epsilon} \frac{\partial p}{\partial r} + \eta \left(\frac{1}{\epsilon} \frac{\partial}{\partial r} \left(\frac{1}{r} \frac{\partial}{\partial r} (ru) \right) + \epsilon \frac{\partial^2 u}{\partial z^2} \right). \quad (9.33)$$

In order to scale this expression, $\partial p/\partial r = 0$ it seems to be same order of viscous term, $\partial^2 u/\partial z^2$ term is order epsilon but other term it is order $\mathcal{O}(\epsilon^{-1})$. Due to leading order of $u \approx -\frac{r}{2} \frac{\partial w}{\partial z}$, it has to be assumed that $\partial p/\partial r = 0$ or p is independent of r , then $p = p(z, t)$. Regarding Eq. (9.28) indicates no dependency of variable r , then we can conclude that $w = w(z, t)$, and through the project we are going to assume w not depending of r . Also there is no change with the continuity equation (9.29). Integrating Eq. (9.29) for $r \in [0, R]$, and calculating as the previous section, we get Eq. (9.14).

Now, we are going to find the boundary conditions, normal and tangent stress condition at the free surface, given by the normal boundary condition

$$\hat{\mathbf{n}}^t \cdot \boldsymbol{\Sigma} \cdot \hat{\mathbf{n}} = -\sigma\kappa, \quad (9.34)$$

and the tangencial boundary condition,

$$\hat{\mathbf{n}}^t \cdot \boldsymbol{\Sigma} \cdot \hat{\mathbf{t}} = 0, \quad (9.35)$$

The stress tensor fo axysymmetric incompressible jet expressed in cylindrical coordinates is given by;

$$\boldsymbol{\Sigma} = \begin{pmatrix} 2\frac{\partial u}{\partial r} & 0 & \frac{\partial w}{\partial r} + \frac{\partial u}{\partial z} \\ 0 & 2\frac{u}{r} & 0 \\ \frac{\partial w}{\partial r} + \frac{\partial u}{\partial z} & 0 & 2\frac{\partial w}{\partial z} \end{pmatrix}, \quad (9.36)$$

with $\boldsymbol{\Sigma} = -p\mathbf{I} + 2\eta\mathbf{D}$, where \mathbf{D} being the Strain-rate tensor given by

$$\mathbf{D} = \frac{\nabla u + \nabla u^t}{2}.$$

The Normal stress at the free surface is given by;

$$\hat{\mathbf{n}} = \left(1, 0, -\epsilon \frac{\partial R}{\partial z}\right) / \sqrt{1 + \epsilon^2 \left(\frac{\partial R}{\partial z}\right)^2},$$

and tangent stress at the free surface is given by

$$\hat{\mathbf{t}} = \left(\epsilon \frac{\partial R}{\partial z}, 0, 1\right) / \sqrt{1 + \epsilon^2 \left(\frac{\partial R}{\partial z}\right)^2}.$$

Finding the normal stress expression using the Eq. (9.34),

$$p - \eta \left(2\frac{\partial u}{\partial r} - 2\epsilon \frac{\partial R}{\partial z} \left(\frac{\partial w}{\partial r} + \frac{\partial u}{\partial z}\right) + 2\epsilon^2 \left(\frac{\partial R}{\partial z}\right)^2 \frac{\partial w}{\partial z}\right) = \sigma \left(\frac{1}{R} - \frac{\partial^2 R}{\partial z^2}\right). \quad (9.37)$$

From normal stress condition Eq. (9.37), eliminating term of order $\mathcal{O}(1)$, and from continuity Equation Eq. (9.29) of a value of $u = -\frac{r\partial w}{2\partial z}$, as in Eq. (9.11), then the pressure is given by;

$$p = \sigma \left(\frac{1}{R} - \frac{\partial^2 R}{\partial z^2}\right) - \eta \frac{\partial w}{\partial z}. \quad (9.38)$$

Now, using the Eq. (9.35) to find a expression for the tangential stress;

$$\left(1 + \epsilon^2 \left(\frac{\partial R}{\partial z}\right)^2\right) \epsilon \left(\frac{\partial w_2}{\partial r} + \frac{\partial u}{\partial z}\right) + 2\epsilon \frac{\partial R}{\partial z} \left(\frac{\partial u}{\partial r} - \frac{\partial w}{\partial z}\right) = 0. \quad (9.39)$$

Keeping terms of order $\mathcal{O}(\epsilon)$,

$$\frac{\partial w_2}{\partial r} = -2 \frac{\partial R}{\partial z} \left(\frac{\partial u}{\partial r} - \frac{\partial w}{\partial z}\right) - \frac{\partial u}{\partial z}, \quad (9.40)$$

and using the expression $u = -\frac{r}{2} \frac{\partial w}{\partial z}$,

$$\frac{\partial w_2}{\partial r} = 3 \frac{\partial R}{\partial z} \frac{\partial w}{\partial z} + \frac{R}{2} \frac{\partial^2 w}{\partial z^2}. \quad (9.41)$$

We consider the momentum reduced Eq.(9.28) ;

$$\rho \left(\frac{\partial w}{\partial t} + w \frac{\partial w}{\partial z}\right) = -\frac{\partial p}{\partial z} + \eta \left(\frac{1}{r} \frac{\partial}{\partial r} \left(r \frac{\partial w_2}{\partial r}\right) + \frac{\partial^2 w}{\partial z^2}\right), \quad (9.42)$$

substituting the Eq. (9.38) in this equation

$$\rho \left(\frac{\partial w}{\partial t} + w \frac{\partial w}{\partial z}\right) + \sigma \frac{\partial}{\partial z} \left(\frac{1}{R} - \frac{\partial^2 R}{\partial z^2}\right) - \eta \frac{\partial^2 w}{\partial z^2} = \eta \left(\frac{1}{r} \frac{\partial}{\partial r} \left(r \frac{\partial w_2}{\partial r}\right) + \frac{\partial^2 w}{\partial z^2}\right), \quad (9.43)$$

multiplying by r this equation, each term is affected but it is simplified with the denominator of the first term on the right-hand side,

$$r \left[\rho \left(\frac{\partial w}{\partial t} + w \frac{\partial w}{\partial z}\right) + \sigma \frac{\partial}{\partial z} \left(\frac{1}{R} - \frac{\partial^2 R}{\partial z^2}\right) - \eta \frac{\partial^2 w}{\partial z^2}\right] = \eta \left(\frac{\partial}{\partial r} \left(r \frac{\partial w_2}{\partial r}\right) + r \frac{\partial^2 w}{\partial z^2}\right), \quad (9.44)$$

integrating this expression for $0 \leq r \leq R$, we note that both w and R do not depend on r , adding similar terms $\partial^2 w / \partial z^2$ that appear in both sides replacing the term $\partial w_2 / \partial z$ by using Eq. (9.41), and eliminating the inner parentheses on the right-hand side, provides:

$$\frac{R^2}{2} \left[\rho \left(\frac{\partial w}{\partial t} + w \frac{\partial w}{\partial z}\right) + \sigma \frac{\partial}{\partial z} \left(\frac{1}{R} - \frac{\partial^2 R}{\partial z^2}\right)\right] = \eta \left(3R \frac{\partial R}{\partial z} \frac{\partial w}{\partial z} + \frac{R^2}{2} \frac{\partial^2 w}{\partial z^2} + R^2 \frac{\partial^2 w}{\partial z^2}\right), \quad (9.45)$$

adding similar terms involving $\partial^2 w_2 / \partial z^2$, multiplying by $2/R^2$ and factorizing 3, then condensing the notation of the parentheses on the left-side,

$$\rho \left(\frac{\partial w}{\partial t} + w \frac{\partial w}{\partial z}\right) + \sigma \frac{\partial}{\partial z} \left(\frac{1}{R} - \frac{\partial^2 R}{\partial z^2}\right) = \frac{3\eta}{R^2} \frac{\partial}{\partial z} \left(R^2 \frac{\partial w}{\partial z}\right), \quad (9.46)$$

finally, we get the momentum equation for the jet dynamics by placing the term of pressure on the left side,

$$\rho \left(\frac{\partial w}{\partial t} + w \frac{\partial w}{\partial z}\right) = -\sigma \frac{\partial}{\partial z} \left(\frac{1}{R} - \frac{\partial^2 R}{\partial z^2}\right) + \frac{3\eta}{R^2} \frac{\partial}{\partial z} \left(R^2 \frac{\partial w}{\partial z}\right), \quad (9.47)$$

The stability analysis

Let consider the following system of partial differential equations consisting of Eqs. (9.14) and (9.47). In order to find the dispersion equation we consider perturbation as follows

$$R \approx R_0 + \varepsilon R_1, \quad w \approx \varepsilon W_1, \quad (9.48)$$

where R_0 is the initial radius of the cylinder and R_1 and W_1 are the corresponding disturbs, which we assume to take the form

$$R_1, W_1 \propto \exp(\varpi t + ikz), \quad (9.49)$$

where $i = \sqrt{-1}$.

We start our analysis by substituting the above perturbations into the Eq. (9.14)

$$\frac{\partial[(R_0 + \varepsilon R_1)^2]}{\partial t} + \frac{\partial[\varepsilon W_1(R_0 + \varepsilon R_1)^2]}{\partial z} = 0, \quad (9.50)$$

developing the time and spatial partial derivatives, we keep terms $\mathcal{O}(\varepsilon)$, which provides:

$$2R_0 R_1 \varpi + ik W_1 R_0^2 = 0, \quad (9.51)$$

this expression is the relation between disturbs R_1 and W_1 , in it also are involved the initial radius and k and w ,

$$W_1 = -\frac{2\varpi}{ikR_0} R_1. \quad (9.52)$$

Considering the pressure p as in Eq. (8.9), we solve the Eq. (9.47), by analyzing by parts. First, we introduce the perturbations, as follows

$$\begin{aligned} \rho \left(\varepsilon \frac{\partial W_1}{\partial t} + \varepsilon^2 W_1 \frac{\partial W_1}{\partial z} \right) &= -\sigma \frac{\partial}{\partial z} \left(\frac{\varepsilon R_1}{R_0^2} - \varepsilon \frac{\partial^2 R_1}{\partial z^2} \right) \\ &+ \frac{3\eta}{R_0^2} \frac{\partial}{\partial z} \left((R_0 + \varepsilon R_1)^2 \varepsilon \frac{\partial W_1}{\partial z} \right). \end{aligned} \quad (9.53)$$

some terms are neglected as the second term of the left-hand side which is order $\mathcal{O}(\varepsilon^2)$, while the second term on the right-hand side contains R^2 in the denominator and it is used the binomial expansion to maintain R_0^2 . here we keep the terms order $\mathcal{O}(\varepsilon)$ for the complete expression

$$\rho \varepsilon \frac{\partial W_1}{\partial t} = -\sigma \left(-\frac{\varepsilon}{R_0^2} \frac{\partial R_1}{\partial z} - \varepsilon \frac{\partial^3 R_1}{\partial z^3} \right) + 3\varepsilon \eta \frac{\partial^2 W_1}{\partial z^2}, \quad (9.54)$$

where the time derivative contributes with a factor ε multiplying the amplitude W_1 while an spatial derivative contributes with ik multiplying the amplitude, applying this we get

$$\rho \varepsilon \varpi W_1 = -\sigma \left(-ik\varepsilon \frac{R_1}{R_0^2} - \varepsilon (ik)^3 R_1 \right) + 3\varepsilon \eta (ik)^2 W_1, \quad (9.55)$$

leaving the εik factor outside the parentheses, simplifying the ε , and substituting the amplitude W_1 from Eq. (9.52), allows us to obtain:

$$\frac{-2\rho R_1}{ikR_0}\varpi^2 = \frac{\sigma ik}{R_0^2} (1 - (kR_0)^2) R_1 - 3\eta k^2 \frac{-2R_1}{ikR_0}\varpi, \quad (9.56)$$

after some algebraic manipulations,

$$\varpi^2 = \frac{\sigma(kR_0)^2}{2\rho R_0^3} (1 - (kR_0)^2) - 3\frac{\eta}{\rho} k^2 \varpi. \quad (9.57)$$

From Eqs. (9.52) and (9.24), substituting W_1 , we get;

$$\varpi^2 = \frac{\sigma(kR_0)^2}{2\rho R_0^3} (1 - (kR_0)^2) - \frac{3\eta(kR_0)^2}{\rho R_0^2} \varpi. \quad (9.58)$$

which in dimensionless form is given by:

$$\overline{\varpi}^2 = \frac{\overline{k}^2}{2} (1 - \overline{k}^2) - \frac{3}{Re} \overline{k}^2 \overline{\varpi}, \quad (9.59)$$

where the Reynolds number Re is given by:

$$Re = \frac{\sqrt{\rho\sigma R_0}}{\eta} = Oh^{-1}, \quad (9.60)$$

the last being the inverse of the Ohnesorge number Oh , that is the relation between the viscous and the capillary forces. The above Eq. (9.59) is known as the *dispersion relation* equation for the stability of a viscous liquid jet in the long wave-length approximation. If we neglect the viscous term in Eq. (9.59), we recover the inviscid dispersion relation given by Eq. (9.26).

In Fig. (9.3), We observe that the growth rates are reduced when the Reynolds number decreases, this is because the viscosity mechanism maintains the streamlines and prevents them from deforming. We don't observe cutoff of the wave numbers set values.

9.3.1 Numerical approach to the nonlinear regimes

We consider the slender jet approximation of the Plateau-Rayleigh instability problem. These equations consider the evolution equation for velocity field $w = w(z, t)$

$$\frac{\partial w}{\partial t} + w \frac{\partial w}{\partial z} = -\frac{1}{\rho} \frac{\partial p}{\partial z} + 3\frac{\eta}{\rho} \frac{1}{R^2} \frac{\partial}{\partial z} \left(R^2 \frac{\partial w}{\partial z} \right), \quad (9.61)$$

and the equation for the evolution of the surface $R(z, t)$,

$$\frac{\partial}{\partial t} (R^2) + \frac{\partial}{\partial z} (R^2 w) = 0, \quad (9.62)$$

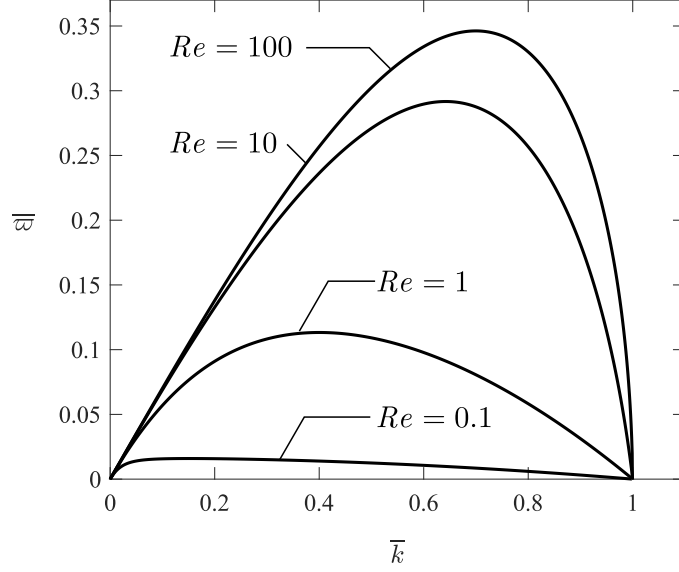


Figure 9.3: Figure shows the growth rate $\bar{\omega} = \varpi \sqrt{\rho R_0^3 / \sigma}$ as a function of the wave-number $\bar{k} = kR_0$ for several values of $Re = 0.1, 1, 10, 100$, for a viscous cylinder liquid jet assuming the long wavelength limit.

where the parameters involved in these equations are the density ρ , the viscosity η and the surface tension coefficient σ for the pressure equation (8.9).

$$p = \sigma \left(R^{-1} \left(1 + \left(\frac{\partial R}{\partial z} \right)^2 \right)^{-\frac{1}{2}} - \frac{\partial^2 R}{\partial z^2} \left(1 + \left(\frac{\partial R}{\partial z} \right)^2 \right)^{-\frac{3}{2}} \right). \quad (9.63)$$

The asymptotic approximation strictly applied generates a pressure term as in Eq. (9.47), but in order to bring more information about the term that plays an important role in this non-linear behavior, we keep the full pressure term (8.9), as previous works did [65, 66, 69].

Our problem presents a considerable amount of physical parameters, so we are going to consider characteristic scales to dimensionless the above set of equations. We consider the capillary velocity v_c to scale the velocity w , and for the radius the initial jet radius R_0 and for the time scale the capillary t_c , as follow

$$w \sim v_c = \sqrt{\sigma / \rho R_0}, \quad z \sim R_0, \quad t \sim t_c = \frac{R_0}{v_c} = \sqrt{\rho R_0^3 / \sigma} \quad (9.64)$$

which in dimensionless form takes the form $t^* = t/t_c$. With these dimensionless parameters the system of equations that govern the jet dynamics are given by

$$\frac{\partial w}{\partial t} + w \frac{\partial w}{\partial z} = -\frac{\partial p}{\partial z} + \frac{3}{Re} \frac{1}{R^2} \frac{\partial}{\partial z} \left(R^2 \frac{\partial w}{\partial z} \right), \quad (9.65)$$

The dimensionless evolution equation (9.62) for the surface $R(z, t)$ remains unchanged and the scaled pressure equation it is expressed without the coefficient of surface tension in Eq.(9.63). Because we are concentrated in study the pinch-off we solve numerically the system (9.63)-(9.65) above and we consider a steady cylinder and a perturbation of the free surface as the initial condition

$$R(z, 0) = R_0(1 + \delta \cos(kz)), \quad (9.66)$$

where $\delta \ll 1$ and the wavenumber k is given by

$$k = \frac{2\pi}{\lambda}, \quad (9.67)$$

in which λ is the wavelength and our computational domain, which partitioned in n mesh points. We assume periodic boundary conditions,

$$R_0 = R_{n-1}, \quad R_1 = R_n, \quad R_2 = R_{n+1}. \quad (9.68)$$

We use with $\delta = 0.05$ corresponding to a 5% of the initial radius as mentioned in [69]. We discretize the system (9.62)-(9.65) and solve resorting the method of lines (MOL), which consist in transform the partial differential equations in a system of ordinary differential equations as proposed by [69], where the spatial derivatives are written as finite differences.

We start with the kinematic condition (9.62), which can be written as

$$2R \frac{\partial R}{\partial t} = - \frac{\partial}{\partial z} (R^2 w), \quad (9.69)$$

following [69], the discretization for the n points in the mesh ($1 \leq i \leq n$) are given by

$$\frac{dR_i}{dt} = - \frac{R_{i+1/2}^2 w_i - R_{i-1/2}^2 w_{i-1}}{2R_i \Delta z}, \quad (9.70)$$

where the half-points of R are given by

$$R_{i+\frac{1}{2}} = \frac{R_i + R_{i+1}}{2}, \quad R_{i-\frac{1}{2}} = \frac{R_i + R_{i-1}}{2}.$$

By replacing these expressions in (9.70), we get

$$\frac{\partial R_i}{\partial t} = - \frac{(R_i + R_{i+1})^2 w_i - (R_i + R_{i-1})^2 w_{i-1}}{8R_i \Delta z}, \quad (9.71)$$

yielding n differential equations for each mesh point i for ($1 \leq i \leq n$). In what follows, we present the ODE for each node. We start with node $i = 1$,

$$\frac{\partial R_1}{\partial t} = - \frac{(R_1 + R_2)^2 w_1 - (R_1 + R_0)^2 w_0}{8R_1 \Delta z}, \quad (9.72)$$

where the values of R_0 and w_0 are ghost values out of the domain mesh points, for this we consider periodical boundary conditions by replacing the values of R_{n-1} and w_{n-1} respectively. Then we consider the intermediate points for $i = 2, \dots, n-1$ using the Eq. (9.71).

We note that in equation for $i = n$ appears the term R_{n+1} , out of the mesh domain, but we changes its values by the corresponding periodic value R_2 , getting the equation exactly equal to $\partial R_1/\partial t$, that is,

$$\frac{\partial R_n}{dt} = \frac{\partial R_1}{dt}. \quad (9.73)$$

Now, we discretize the momentum Eq. (9.61), for this equation we first discretize the advective term,

$$\text{Advection}_i = -(w_i^+ d_i^- + w_i^- d_i^+), \quad (9.74)$$

where

$$w_i^+ = \max(w_i, 0), \quad w_i^- = \min(w_i, 0),$$

with

$$d_i^+ = \frac{w_{i+1} - w_i}{\Delta z}, \quad d_i^- = \frac{w_i - w_{i-1}}{\Delta z}.$$

We note that for $i = 1$ we need to consider the boundary conditions due to the presence of the ghost value w_0 .

The equation for the pressure(9.63) is discretized by

$$\text{Pressure}_i = \frac{C_{i+1} - C_i}{\Delta z}. \quad (9.75)$$

with centered finite difference for C_{i+1}

$$C_i = \frac{1}{R_i A_i^{1/2}} - \frac{R_{i+1} - 2R_i + R_{i-1}}{\Delta z^2 A_i^{3/2}}, \quad (9.76)$$

with A_i also is given by the centered approximation

$$A_i = \left(1 + \left(\frac{R_{i+1} - R_{i-1}}{2\Delta z} \right)^2 \right), \quad (9.77)$$

valid for $i = 1, \dots, n$ and again as the previous remarks, the boundary points yield the R_0 and R_{n+1} terms which must be changed with the boundary conditions (9.68).

The contribution of the viscous term is given by

$$\text{Viscous}_i = \frac{1}{R_{i+1/2}^2} \frac{R_{i+1}^2(w_{i+1} - w_i) - R_i^2(w_i - w_{i-1})}{\Delta z^2}. \quad (9.78)$$

when $R_{i+1/2}$ is introduced as above

$$\text{Viscous}_i = \frac{4}{(R_{i+1} + R_i)^2} \frac{R_{i+1}^2(w_{i+1} - w_i) - R_i^2(w_i - w_{i-1})}{\Delta z^2}. \quad (9.79)$$

then, substituting the advection, pressure and viscous expressions in the discretized momentum equation (9.61), it takes the following form

$$\frac{dw_i}{dt} = -(w_i^+ d_i^- + w_i^- d_i^+) - \frac{C_{i+1} - C_i}{\Delta z} + \frac{12}{Re} \frac{R_{i+1}^2(w_{i+1} - w_i) - R_i^2(w_i - w_{i-1})}{(R_{i+1} + R_i)^2 \Delta z^2}, \quad (9.80)$$

valid for $i = 2, \dots, n - 1$. Then for $i = 1$ we have

$$\frac{dw_1}{dt} = -(w_1^+ d_1^- + w_1^- d_1^+) - \frac{\mathcal{C}_2 - \mathcal{C}_1}{\Delta z} + \frac{12 R_2^2 (w_2 - w_1) - R_1^2 (w_1 - w_0)}{Re (R_2 + R_1)^2 \Delta z^2},$$

where the term w_0 must be changed by the periodic boundary condition w_{n-1} . Finally, for $i = n$ have to maintain valid the boundary conditions which led to establish that

$$\frac{\partial w_n}{dt} = \frac{\partial w_1}{dt}. \quad (9.81)$$

Once the system of differential equation is establish we use the MatLab function *Ode23t* to solve the system formed by (8.9) and (9.65), subject to initial condition (9.66) and boundary conditions (9.68). For our test cases we use data published by [70] and [69], the first one used a Galerkin finite element method to study the instability of an axisymmetric, incompressible Newtonian liquid cylinder and the second one presented a numerical model to predict the breakup of viscous micro-jets of Newtonian fluid using the method of lines (MOL) to achieve its objective, this is the direction we took. In the Table (9.1), we compare the scaled breakup time with the data from [70] and [69], taking in consideration that our code used 500 mesh points and took less than a minute to run.

Table 9.1: Comparison of the scaled breakup time of the numerical model with [69, 70] and our code.

Re	k	<i>Ashgriz et al.</i>	<i>Furlani et al.</i>	<i>Our code</i>
200	0.2	25.2	25	24.87
	0.45	12.9	12.6	12.63
	0.7	10	9.7	9.71
	0.9	14.5	11	11
10	0.2	26.7	27.9	27.48
	0.45	14.3	14.3	14.35
	0.7	11.6	11.4	11.47
	0.9	14.8	14.4	14.39
0.1	0.2	230.6	227	234.86
	0.45	243.6	238	245.79
	0.7	311.9	305	312.58
	0.9	628.2	634	627.51

In Fig.(9.4), we observed that for smaller Re , the growth rates are decreasing, this means that, it will take more time to evolve the growth, that is, breakup times become larger. For large Re , Fig. (9.4) shows that as the Re is increased the break-up time converges to a critical value and this corresponds to the inviscid case break-up time.

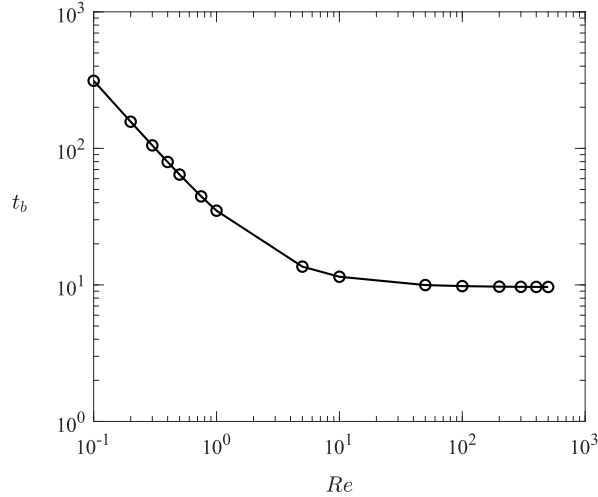


Figure 9.4: Figure shows the time break-up against Reynolds numbers $Re = 0.1, 0.2, 0.3, \dots, 300, 400, 500$ in loglog scale with $N = 500$ and $k = 0.7$.

We compare our results with [69] by extracting data using web resources, see Fig. (9.5). We used $Re = 200, 0.1$ and wavenumbers $k = 0.45, 0.7$. From that, we observe a very good agreement of the nonlinear shapes near break-up time obtained in our code with those presented in [69]. Note that, the break-up time can not be measured very accurately because of the MatLab subroutine used in this work. This routine, *Ode23t*, which uses trapezoidal method with adaptive time step, does not allow a the user the time step and we have to rely on its built in criteria to reach as close as possible to the singularity. Furthermore, the data from [69] was extracted artisanally and there are also fluctuations on the values. However, despite all that, the agreement is excellent.

In Fig. (9.6), we analyze the sensitivity of the profiles close to the singularity for $Re = 200$ for different mesh sizes $N = 135, 270$ and 540 . As mentioned before the agreement is very good and gets better as we increase the number of points in the mesh. The error-bars show a range of 9% of the initial radius of the undisturbed profile. It is only near high curvature regions that the differences become noticeable. For smaller Re viscosity prevents the formation of large curvature regions and excellent agreement with the results of [69] is obtained even for a modest number of points, see Fig. (9.7).

We have reproduced the results cited in [69] for the viscous case, for this we have taken wave numbers $0.2, 0.45, 0.7$ and 0.9 together with Reynolds numbers $Re = 0.1, 10, 200$. As a computational domain we use only a wavelength λ and periodic boundary conditions. From the Fig.(9.3) for the viscous case, we observe that when the Reynolds number is increased, the stability curve becomes more flattened, this indicates that the viscosity delays instability and the breakup time is slowed down. Fixing the wavelengths, we observe that as

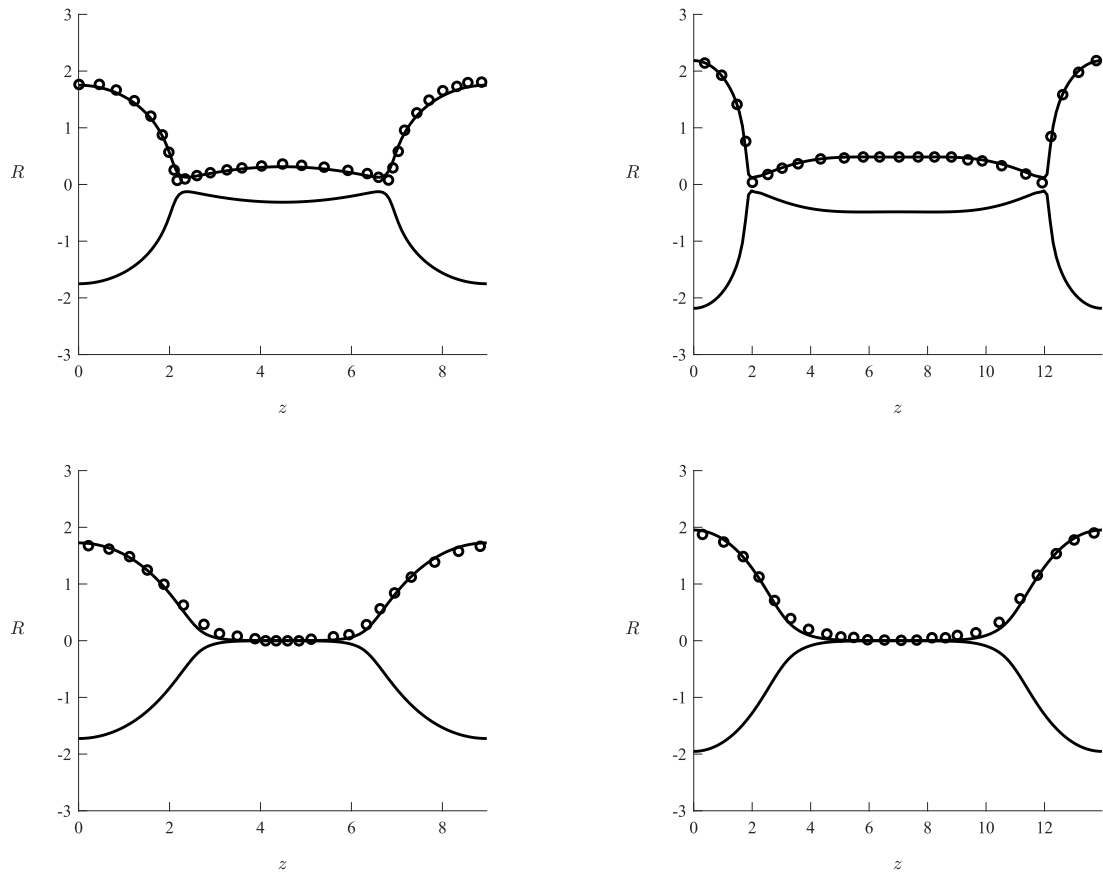


Figure 9.5: Figure shows the comparison between the shape of the free-surface at pinch-off (clock-wise from top left) of [69] (circles) and our result (solid-line) for: $Re = 200, k = 0.7$; $Re = 200, k = 0.45$; $Re = 0.1, k = 0.45$; $Re = 0.1, k = 0.7$.

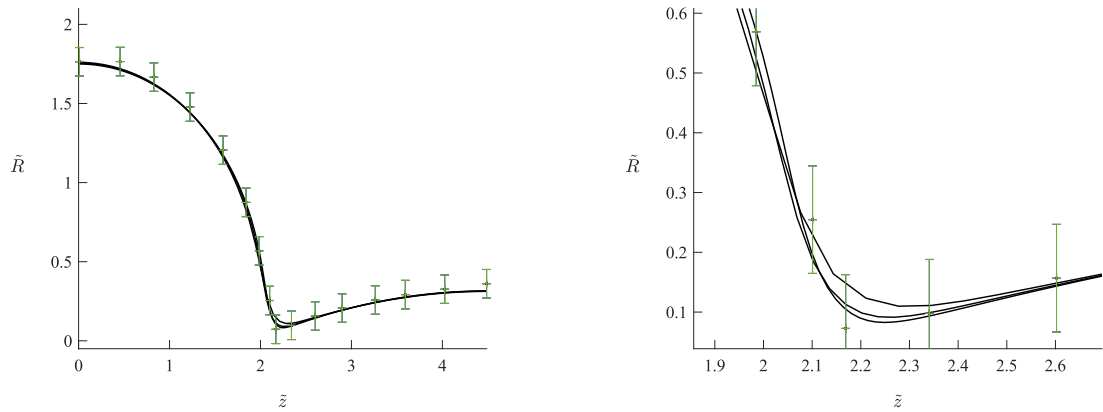


Figure 9.6: Figure (left) shows the data sensibility taken from [69] with an error 0.09 of the radius. The pinch-off profiles was calculated for $N = 135$, $N = 270$ and $N = 540$; for $Re = 200$ and $k = 0.7$. Figure (right) shows the data sensibility close the pinch-off near the time breakup.

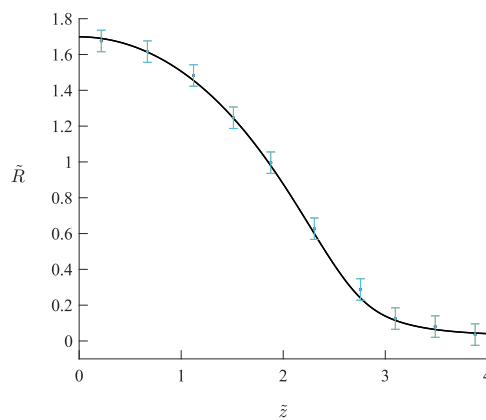


Figure 9.7: Figure shows the data sensibility taken from [69] with an error 0.06 of the radius with the pinch-off profiles for $N = 135$, $N = 270$ and $N = 540$; for $Re = 0.1$ and $k = 0.70$.

the Reynolds number grows the neck bed becomes smaller and thus delaying the break-up, this can be observed in Table (9.1).

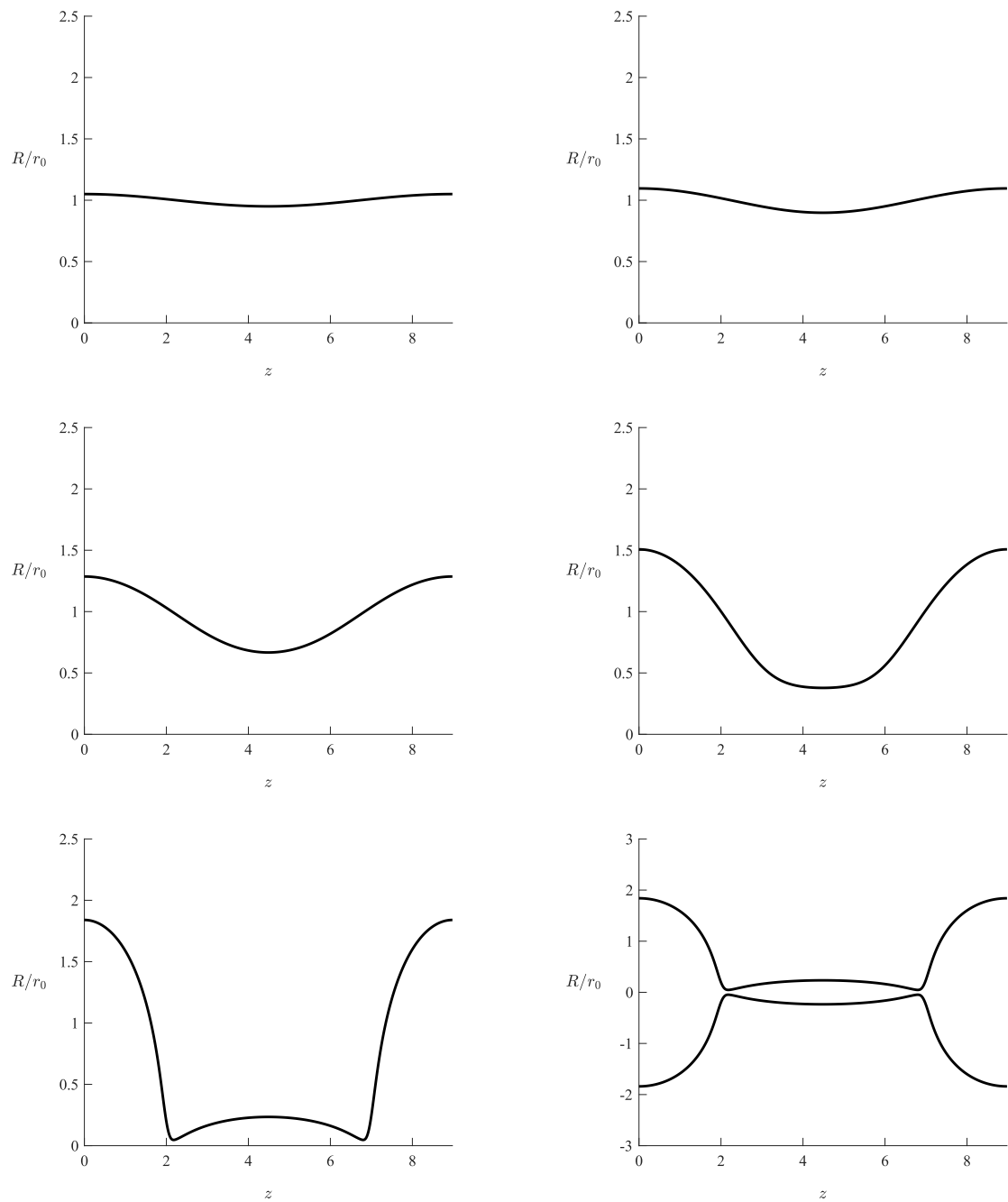


Figure 9.8: Figure shows the evolution of the surface until the break-up, the Reynolds number $Re = 10$ and the wavenumber $k = 0.7$ for $t = 0, 4, 8, 10, 11.4$. Last figure shows the state of the cylinder evolution shortly before the break-up.

In Fig. (9.8), we present a evolution of the surface for $Re = 10$ and $k = 0.7$. Initially, we start with top left figure with time $t = 0$, and continue with the top right figure, then

for $t = 8$ we have the the middle left figure and then right figure for $t = 0$, finally for $t = 11.4$ the surface was deformed until a moment before the breakup. The bottom right graph shows the last figure reflected through the z -axis, obtaining the configuration of the cylinder deformed until a moment before break-up.

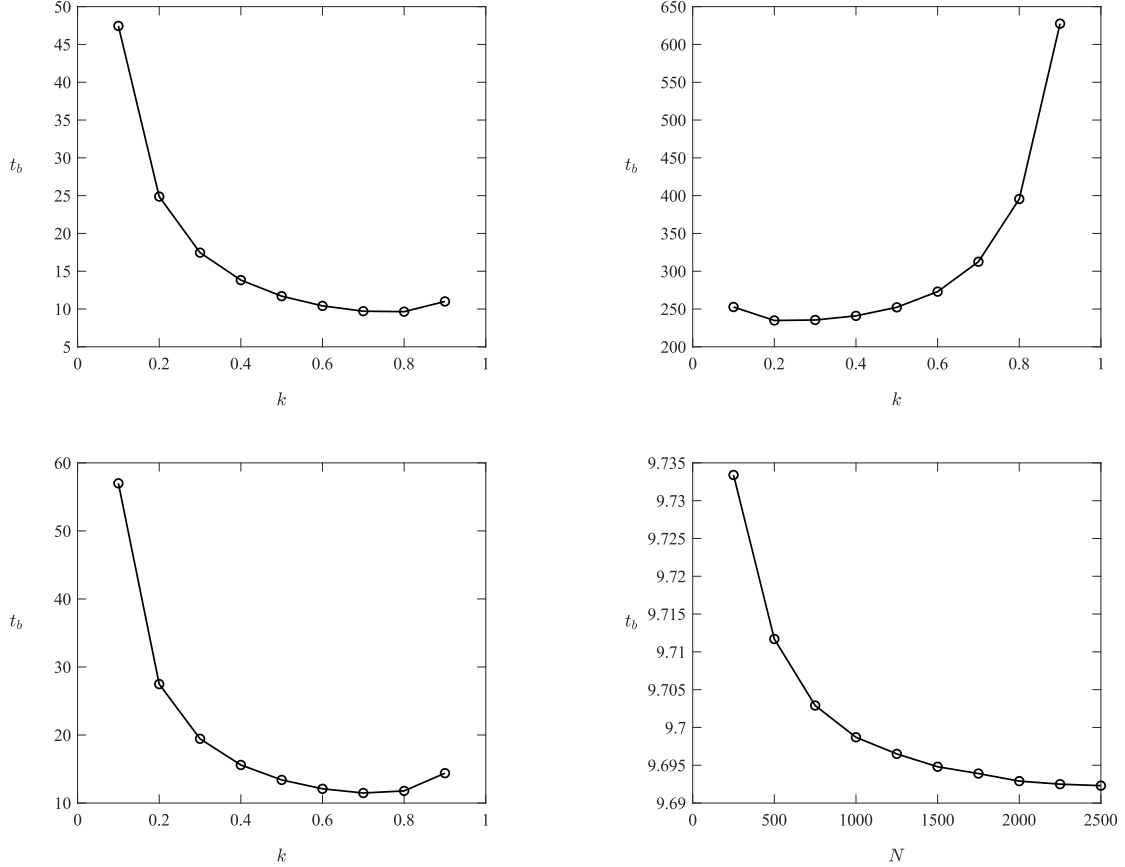


Figure 9.9: The top figures show the break-up time dependence on the wave number of the disturbance for $Re = 200$ (top left) and $Re = 0.1$ (top right). Both results were obtained for $N = 500$. Bottom left graph shows the break-up time of mode $k = 0.7$ as a function of Re for $N = 500$. Finally, bottom right graph shows the mesh dependence of the break-up time for $k = 0.7$ and $Re = 10$.

We observed in Fig. (9.3), that as Re decreases the maximum value of the growth rate takes smaller values and with it k also decreases. In Fig. (9.9), left figures consider $Re = 200$ and $Re = 10$, and k small, that is long waves, it takes more time to break-up. For k near 1, those modes correspond to very small growth rates and then they take longer to evolve. The figure on the top right, shows a case in which the viscosity term is considerable, $Re = 0.1$. Note the much larger break-up times obtained in these cases. Now, shorter waves can take almost 3 times as long to break-up as the longer waves. Bottom right graph shows the mesh dependence of the break-up time for fixed value of $k = 0.7$ and $Re = 200$, we observe

that as the number of mesh points is increased the break-up time converges. Our standard mesh of 500 points overestimated the break-up time by less than 1%.

CHAPTER 10

THE PLATEAU-RAYLEIGH INSTABILITY FOR SUPER-PARAMAGNETIC FLUIDS

10.1 The inviscid Super-paramagnetic Case

In this section we are going to analyze the case of a inviscid incompressible magnetic fluid. The governing equations are given by the momentum equations in the radial direction

$$\rho \left(\frac{\partial u}{\partial t} + u \frac{\partial u}{\partial r} + w \frac{\partial u}{\partial z} \right) = -\frac{\partial p}{\partial r}, \quad (10.1)$$

and the momentum equation in the axial direction

$$\rho \left(\frac{\partial w}{\partial t} + u \frac{\partial w}{\partial r} + w \frac{\partial w}{\partial z} \right) = -\frac{\partial p}{\partial z}, \quad (10.2)$$

and the continuity equation in cylindrical coordinates

$$\frac{1}{r} \frac{\partial(ru)}{\partial r} + \frac{\partial w}{\partial z} = 0. \quad (10.3)$$

For the case of a ferrofluid, we must satisfy the magneto-static limit of the Maxwell's equations, for this we recall expressions Eq. (3.3) and (3.4): where the constitutive equation for the magnetic induction is given by Eq. (3.43). Eq. (3.4) indicates that there exists a function ψ defining \mathbf{H} .

In this case, we consider an uniform magnetic applied field H_0 in the z -direction, that is:

$$\mathbf{H} = H_0 \hat{e}_z + \nabla \psi. \quad (10.4)$$

With this applied magnetic field, magnetism is presented in the treatment of the boundary condition. We remark that the magnetic applied field satisfies Maxwell's Eqs. (3.4)-(3.3). Since we are assuming the super-paramagnetic hypotheses, in which the magnetization is aligned with the applied magnetic field \mathbf{H} , that is:

$$\mathbf{M} = \chi_0 \mathbf{H}, \quad (10.5)$$

the magnetic induction takes the form

$$\mathbf{B} = \mu \mathbf{H}, \quad (10.6)$$

then Eq. (3.3) implies that ψ must satisfy Laplace's equation in Cartesian coordinates, $\nabla^2 \psi = 0$. In cylindrical coordinates, which is our environment, Laplace's equation without the θ -component is

$$\frac{1}{r} \frac{\partial}{\partial r} \left(r \frac{\partial \psi}{\partial r} \right) + \frac{\partial^2 \psi}{\partial z^2} = 0. \quad (10.7)$$

In order to perform the *long-wave approximation* as the previous cases, we replace r by ϵr and evaluating that limit in Laplace's equation (10.7), gives us:

$$\frac{\epsilon^{-2}}{r} \frac{\partial}{\partial r} \left(r \frac{\partial \psi}{\partial r} \right) + \frac{\partial^2 \psi}{\partial z^2} = 0. \quad (10.8)$$

The above equation must be balanced due the presence of the ϵ^{-2} parameter, in order to do that we assume a expansion for ψ as follows:

$$\psi = \Psi(z, t) + \epsilon^2 \psi_2(r, z, t). \quad (10.9)$$

In this expression Ψ is a function only of z and t while ψ_2 depends also on r . With this modification the Eq. (10.8) is balanced and takes the following form:

$$\frac{1}{r} \frac{\partial}{\partial r} \left(r \frac{\partial \psi_2}{\partial r} \right) + \frac{\partial^2 \Psi}{\partial z^2} = 0. \quad (10.10)$$

Now, it is possible to find an expression for ψ_2 in terms of Ψ in Eq. (10.10) by leaving it on the left-hand side: and multiplying by r and integrating with relation to r , which provides:

$$r \frac{\partial \psi_2}{\partial r} = -\frac{r^2}{2} \frac{\partial^2 \Psi}{\partial z^2} + c_1, \quad (10.11)$$

where c_1 is a constant and dividing by r , again integrating with relation to r , we obtain:

$$\psi_2 = -\frac{r^2}{4} \frac{\partial^2 \Psi}{\partial z^2} + c_1 \ln(r) + c_2, \quad (10.12)$$

where c_1 and c_2 are constants (both independents of r) to be found. In order to maintain regularity inside the cylinder, we note that when $r \rightarrow 0$, we have $\ln(r) \rightarrow \infty$, indicating that we must cancel the logarithm coefficient, that is, $c_1 = 0$, yielding:

$$\psi_2 = -\frac{r^2}{4} \frac{\partial^2 \Psi}{\partial z^2} + c_2, \quad (10.13)$$

with this modification, Eq. (10.9) for ψ provides:

$$\psi = \Psi(z, t) - \epsilon^2 \frac{r^2}{4} \frac{\partial^2 \Psi}{\partial z^2} + \epsilon^2 c_2(z, t). \quad (10.14)$$

Now, we impose the boundary condition that must be satisfied in the interface. First, the normal boundary condition (3.10) is expressed by:

$$\mu \hat{\mathbf{n}} \cdot \nabla \psi_1 = \mu_0 \hat{\mathbf{n}} \cdot \nabla \psi_2, \quad (10.15)$$

and the tangential boundary condition (3.16) is written as:

$$\hat{\mathbf{t}} \cdot \nabla \psi_1 = \hat{\mathbf{t}} \cdot \nabla \psi_2, \quad (10.16)$$

Sub-index 1 and 2 indicate the cylinder inside and outside region respectively in which $\hat{\mathbf{n}}$ is the unitary normal vector to the free surface and $\hat{\mathbf{t}}$ is the unitary tangent vector to the free surface. Taking $F(r, z, t) = r - R(z, t) = 0$, the normal vector is given by

$$\hat{\mathbf{n}} = \frac{\nabla F}{|\nabla F|}. \quad (10.17)$$

where the nabla operator ∇ must be scaled taking into account the long wavelength limit:

$$\nabla = \left(\epsilon^{-1} \frac{\partial}{\partial r}, 0, \frac{\partial}{\partial z} \right). \quad (10.18)$$

Applying the nabla operator to the free surface F , provides the unitary normal vector:

$$\hat{\mathbf{n}} = \left(1, 0, -\epsilon \frac{\partial R}{\partial z} \right) / \left(1 + \epsilon^2 \left(\frac{\partial R}{\partial z} \right)^2 \right)^{\frac{1}{2}}, \quad (10.19)$$

Now, we compute the tangent unitary vector which is orthogonal to the normal vector,

$$\hat{\mathbf{t}} = \left(\epsilon \frac{\partial R}{\partial z}, 0, 1 \right) / \left(1 + \epsilon^2 \left(\frac{\partial R}{\partial z} \right)^2 \right)^{\frac{1}{2}}. \quad (10.20)$$

Thus the Eq. (10.15) is given by the expression

$$\mu \left(1, 0, -\epsilon \frac{\partial R}{\partial z} \right) \cdot \left(\epsilon^{-1} \frac{\partial \psi}{\partial r}, 0, \frac{\partial \psi}{\partial z} \right) = \mu_0 \left(1, 0, -\epsilon \frac{\partial R}{\partial z} \right) \cdot \left(\frac{\partial \psi}{\partial \xi}, 0, \frac{\partial \psi}{\partial z} \right), \quad (10.21)$$

in this expression the denominator of the normal vector was simplified because it is the same in both sides, and after making the dot product

$$\mu \left(\epsilon^{-1} \frac{\partial \psi}{\partial r} - \epsilon \frac{\partial R}{\partial z} \frac{\partial \psi}{\partial z} \right) = \mu_0 \left(\frac{\partial \psi}{\partial \xi} - \epsilon \frac{\partial R}{\partial z} \frac{\partial \psi}{\partial z} \right). \quad (10.22)$$

The tangential boundary Eq. (10.16) is given by

$$\left(\epsilon \frac{\partial R}{\partial z}, 0, 1 \right) \cdot \left(\epsilon^{-1} \frac{\partial \psi}{\partial r}, 0, \frac{\partial \psi}{\partial z} \right) = \left(\epsilon \frac{\partial R}{\partial z}, 0, 1 \right) \cdot \left(\frac{\partial \psi}{\partial \xi}, 0, \frac{\partial \psi}{\partial z} \right), \quad (10.23)$$

in this expression the denominator of the tangential vector is simplified in both sides and developing the dot product we get the expression for the tangential boundary condition

$$\frac{\partial R}{\partial z} \frac{\partial \psi}{\partial r} + \frac{\partial \psi}{\partial z} = \epsilon \frac{\partial R}{\partial z} \frac{\partial \psi}{\partial \xi} + \frac{\partial \psi}{\partial z}, \quad (10.24)$$

Now, we are going to figure out the expression for the pressure across the boundary. Following the Rosenzweig's reference [33], the pressure is given by:

$$p + p_m + p_n = p_0 + p_c, \quad (10.25)$$

where the p_m is given by:

$$p_m = \mu_0 \int_0^H M dH, \quad (10.26)$$

and from $B = \mu_0(H + M)$ with $B = \mu H$, allows us to obtain

$$p_m = \mu_0 \int_0^H M dH = \int_0^H (\mu - \mu_0) H dH = \frac{1}{2}(\mu - \mu_0) H^2, \quad (10.27)$$

and $p_n = \frac{1}{2}\mu_0 M_n^2$ and p_0 is the environmental pressure and $p_c = \sigma \mathcal{H}$ the mean curvature of the boundary. With these expressions we have:

$$p + \frac{1}{2}(\mu - \mu_0) \int_0^H M dH = \sigma \mathcal{H} = \sigma \left(\frac{1}{R} - \frac{\partial^2 R}{\partial z^2} \right). \quad (10.28)$$

10.1.1 The case of a magnetically impermeable outer region

In order to find a solution for our problem we are going to assume the vacuum permeability $\mu_0 = 0$, which implies that the right-hand side of Eq. (10.22) is neglected, that is:

$$\mu \left(\epsilon^{-1} \frac{\partial \psi}{\partial r} - \epsilon \frac{\partial R}{\partial z} \frac{\partial \psi}{\partial z} \right) = 0, \quad \text{at } r = R, \quad (10.29)$$

then substituting ψ by its expression in Eq. (10.14) and multiplying by $2R$, we get,

$$\frac{\partial^2 \Psi}{\partial z^2} R^2 + 2R \frac{\partial R}{\partial z} \left(H_0 + \frac{\partial \Psi}{\partial z} \right) = 0, \quad (10.30)$$

which allows us to obtain:

$$\frac{\partial}{\partial z} \left(R^2 \left(H_0 + \frac{\partial \Psi}{\partial z} \right) \right) = 0, \quad (10.31)$$

and solving one derivative on the last differential equation, the expression between parentheses is equal to a constant C , which is independent of z and evaluating in $t = 0$, C takes the initial values of $C = R_0^2 H_0$, then we can express the applied field in the following form:

$$H_0 + \frac{\partial \Psi}{\partial z} = R_0^2 H_0 R^{-2}, \quad (10.32)$$

which is inversely proportional to the square of the free surface. Substituting the last expression Eq.(10.32) in Eq. (10.28) yields:

$$p = \sigma \left(\frac{1}{R} - \frac{\partial^2 R}{\partial z^2} \right) - \frac{1}{2} \mu R_0^4 H_0^2 R^{-4}. \quad (10.33)$$

With the expression for the pressure Eq. (10.33), we replace this equation into the Eq. (10.2), which is treated as the previous Section.

$$\rho \left(\frac{\partial w}{\partial t} + w \frac{\partial w}{\partial z} \right) = - \frac{\partial}{\partial z} \left(\sigma \left(\frac{1}{R} - \frac{\partial^2 R}{\partial z^2} \right) - \frac{1}{2} \mu R_0^4 H_0^2 R^{-4} \right), \quad (10.34)$$

introducing the partial derivative with relation to z in the parentheses and developing the derivative of R^{-4} , we have

$$\rho \left(\frac{\partial w}{\partial t} + w \frac{\partial w}{\partial z} \right) = - \sigma \frac{\partial}{\partial z} \left(\frac{1}{R} - \frac{\partial^2 R}{\partial z^2} \right) - \frac{2 \mu R_0^4 H_0^2}{R^5} \frac{\partial R}{\partial z}. \quad (10.35)$$

In order to present this expression in dimensionless form, we consider the scales used in 9.64, where v_c is the capillary velocity, R_0 is the initial jet radius and t_c is the time scale,

$$w \sim v_c = \sqrt{\sigma/\rho R_0}, \quad z \sim R_0, \quad t \sim t_c = \frac{R_0}{v_c} = \sqrt{\rho R_0^3/\sigma},$$

calling the dimensionless magnetic pressure parameter

$$C_{pm} = \frac{\mu R_0 H_0^2}{\sigma}, \quad (10.36)$$

this parameter can be understood as the relation between the magnetic pressure (resistance magnetic force) and the driving forces. By substituting the above scale we arrive to the dimensionless version of Eq. (10.35)

$$\frac{\partial w}{\partial t} + w \frac{\partial w}{\partial z} = - \frac{\partial}{\partial z} \left(\frac{1}{R} - \frac{\partial^2 R}{\partial z^2} \right) - \frac{2 C_{pm}}{R^5} \frac{\partial R}{\partial z}. \quad (10.37)$$

The stability analysis

In this subsection, we are going to perform the stability analysis for the inviscid super-paramagnetic case. For this, we consider the following perturbations

$$R \approx R_0 + \varepsilon R_1, \quad w \approx \varepsilon W_1, \quad (10.38)$$

where the disturbed variables are given by

$$R_1, W_1 \propto \exp(\varpi t + ikz) \quad (10.39)$$

Now, we introduce the ansatz above into Eq. (10.34), provides

$$\rho \varepsilon \varpi W_1 = - \frac{\partial}{\partial z} \left(\sigma \left(\frac{1}{R_0} \left(1 - \varepsilon \frac{R_1}{R_0} \right) - \varepsilon \frac{\partial^2 R_1}{\partial z^2} \right) - \frac{1}{2} \mu \frac{R_0^4 H_0^2}{R_0^4} \left(1 - 4 \varepsilon \frac{R_1}{R_0} \right) \right). \quad (10.40)$$

Introducing the spatial z -derivative into the parenthesis on the right hand side of the last equation and keeping the terms of order $\mathcal{O}(\varepsilon)$, we get:

$$\rho\varepsilon\varpi W_1 = - \left(\sigma \left(-\frac{\varepsilon}{R_0^2} \frac{\partial R_1}{\partial z} - \varepsilon \frac{\partial^3 R_1}{\partial z^3} \right) + 2\varepsilon\mu \frac{H_0^2}{R_0} \frac{\partial R_1}{\partial z} \right). \quad (10.41)$$

after simplifying by a term ε , and manipulating

$$\rho\varpi W_1 = \frac{\sigma ik}{R_0^2} (1 - (kR_0)^2) R_1 - 2\mu(ik) \frac{H_0^2}{R_0} R_1. \quad (10.42)$$

The relation between W_1 and R_1 is given by Eq. (9.52) and solution for $W_1 = -2\frac{R_1}{ikR_0}\varpi$:

$$-2\frac{\rho R_1}{ikR_0}\varpi^2 = \frac{\sigma ik}{R_0^2} (1 - (kR_0)^2) R_1 - 2\mu(ik) \frac{H_0^2}{R_0} R_1. \quad (10.43)$$

Simplifying R_1 and isolating ϖ , yields

$$\varpi^2 = \frac{\sigma(kR_0)^2}{2\rho R_0^3} (1 - (kR_0)^2) - \frac{\mu(kR_0)^2 H_0^2}{\rho R_0^2}. \quad (10.44)$$

Obtaining the *Dispersion relation* for the inviscid superparamagnetic case with magnetic applied field of magnitude H_0 and magnetic permeability μ .

$$\varpi^2 = \frac{\sigma(kR_0)^2}{2\rho R_0^3} (1 - (kR_0)^2) - \frac{\mu(kR_0)^2 H_0^2}{\rho R_0^2}. \quad (10.45)$$

which in dimensionless form is:

$$\overline{\varpi}^2 = \frac{\overline{k}^2}{2} (1 - \overline{k}^2) - C_{pm} \overline{k}^2. \quad (10.46)$$

If we consider non-magnetic influence, $C_{pm} = 0$, we recover the dispersion relation for a inviscid fluid for long wave-lengths previously found in Eq. (9.26). A graph of the dimensionless quantity $\overline{\varpi} = \varpi/\sqrt{\rho R_0^3/\sigma}$ as a function of $\overline{k} = kR_0$ in terms of $C_{pm} = 0.01, 0.1, 5/4\pi$, is shown in Fig. (10.1), in it we can observe that the growth $\overline{\varpi}$ decreases its value when C_{pm} increases, and also the range of values for the wave number \overline{k} moves to zero. It can be inferred that the magnetization stabilize the system and that a C_{pm} sufficiently strong can stabilize completely the growth rates.

In what follows, we cite the result mentioned in [33], where the author has commented a result from Tartakov (1975), in which he has studied the stability of fluid cylinders. His point of departure was the same equations of momentum and magnetic fluid as us, with the term of viscosity neglected and assuming that the gravitational force is absent. With the same technique used in Section 8.2.1, for an inviscid fluid for wave-lengths without restriction, Bessel's equation must be solved for an uniform applied magnetic field in the axial direction of the cylinder. Noting that the magnetostatic limit of the Maxwell's equations indicates

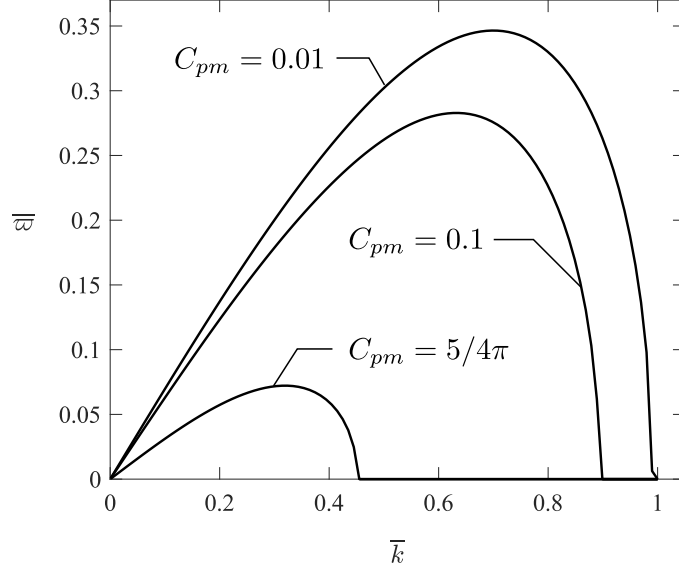


Figure 10.1: Figure shows the dispersion Eq. (10.46) of the dimensionless quantity $\bar{\omega} = \varpi \sqrt{\rho R_0^3 / \sigma}$ as a function of $\bar{k} = kR_0$ for the magnetic parameters $C_{pm} = 0.01, 0.1, 5/4\pi$.

that Laplace's equation must be solved, both inside and outside of the cylinder, and the matching condition is concentrated in the treatment of the magnetic boundary normal condition, he concluded that the magnetic effect is concentrated in the pressure term, getting the following dispersion relation

$$\varpi^2 = \frac{\sigma k I_1(kR_0)}{\rho R_0^2 I_0(KR_0)} (1 - (kR_0)^2) - \frac{k^2 H_0^2 (\mu - \mu_0)^2 I_1(kR_0) K_0(kR_0)}{\rho [\mu I_1(kR_0) K_0(kR_0) + \mu_0 I_0(kR_0) K_1(kR_0)]}. \quad (10.47)$$

This expression was found using the ansatz $\exp(i(\varpi t + kz))$, given a result with the sign changed, but after a change of variable of the frequency, we get Eq. (10.47). The first term on the right-hand side is related to the capillary pressure that brings instability to the system, the second term is related to the magnetic effect and counteracts to the capillary pressure, stabilizing the system [33].

If we consider no magnetic effect in Eq. (10.47), this is $H_0 = 0$, we recover the first case solution Eq. (8.44). Next, we use the long wavelength limit, i.e. kR_0 goes to zero together with $\mu_0 = 0$ and considering the Bessel functions limits $I_0(x) \xrightarrow{x \rightarrow 0} 1$ and $I_1(x) \xrightarrow{x \rightarrow 0} \frac{x}{2}$ we obtain the dispersion relation Eq. (10.46). From Eq. (10.46), we can conclude that both terms, the capillary pressure and the magnetic term counteracts, in fact, if

$$\frac{\mu H_0^2}{\rho R_0^2} \geq \frac{\sigma}{2\rho R_0^3}, \quad (10.48)$$

indicates that a magnetic parameter $\mu R_0 H_0^2 / \sigma \geq 1/2$ enables to stabilize the system.

10.1.2 The case of a magnetically permeable outer region

In this subsection, we are going to consider the magnetic permeability not equal to zero, for this purpose we consider Eq. (10.14) and the normal boundary condition Eq. (10.22):

$$\mu \left(-\epsilon \frac{\partial^2 \Psi}{\partial z^2} \frac{R}{2} - \epsilon \frac{\partial R}{\partial z} \left(H_0 + \frac{\partial \Psi}{\partial z} \right) \right) = \mu_0 \left(\frac{\partial \psi}{\partial \xi} - \epsilon \frac{\partial R}{\partial z} \frac{\partial \psi}{\partial z} \right). \quad (10.49)$$

The left hand-side corresponds to ψ inside the cylinder and the right-hand side corresponds to the outside region, where $\nabla \psi^{\text{out}} = (\partial \psi / \partial \xi, 0, \partial \psi / \partial z)$. For the outer solution we must satisfy also the Laplace's equation, where the radius in the surrounding media is ξ ($r \rightarrow \epsilon$) with $\xi = \epsilon R$, which in cylindrical coordinates is:

$$\xi^{-1} \frac{\partial}{\partial \xi} \left(\xi \frac{\partial \psi}{\partial \xi} \right) + \frac{\partial^2 \psi}{\partial z^2} = 0. \quad (10.50)$$

In order to find a solution for Eq. (10.50), we take the Fourier Transform, yielding:

$$\psi^o \rightarrow \mathcal{F}(k) = \hat{\psi}(\xi, k) \quad \text{with} \quad \hat{\psi} = [\beta I_0(k\xi) + \alpha K_0(k\xi)], \quad (10.51)$$

where I_0 and K_0 are the modified Bessel functions of first and second kind respectively. In order to satisfy regularity $\beta = 0$, because when $k\xi \rightarrow 0$, $I_0(k\xi) \rightarrow 0$. It is important to note that the Fourier transform and its inverse are given by:

$$\mathcal{F}(k) = \int_{-\infty}^{+\infty} \psi_z e^{-ikz} dz, \quad \mathcal{F}^{-1}(z) = (2\pi)^{-1} \int_{-\infty}^{+\infty} \hat{\psi}(z) e^{ikz} dk. \quad (10.52)$$

In order to avoid sign problems, we are going to use:

$$\hat{\psi} = \alpha(k) K_0(k\xi). \quad (10.53)$$

for the match condition $\hat{\psi} \rightarrow \alpha K_0(k\xi)$, with $\xi = \epsilon R$, that means $\hat{\Psi} = \hat{\psi}$ at $\xi = 0$.

$$\alpha = \frac{\hat{\Psi}}{\ln(\epsilon^{-1})}. \quad (10.54)$$

In the above equation $K_0(\varsigma) \approx -\ln(\varsigma/2)$ and we applied that to $K_0(k\xi)$ with $\xi = \epsilon R$. In order to find a expression from the normal boundary condition in Eq. (10.15), We calculate $\partial \psi / \partial \xi$ for the exterior solution through the inverse Fourier transform and the properties of the modified Bessel function of the second kind (see the details in appendix) with $K_1 = -K_0' = 1/\varsigma$, note that $K_0 \approx -\ln \frac{\varsigma}{2}$, giving us:

$$\frac{\partial \psi}{\partial \xi} = -\frac{\Psi}{\epsilon R \ln(\epsilon^{-1})}. \quad (10.55)$$

Substituting $\partial \psi / \partial \xi$ in Eq. (10.15):

$$\left(-\frac{\partial^2 \Psi}{\partial z^2} \frac{R}{2} - \frac{\partial R}{\partial z} \left(H_0 + \frac{\partial \Psi}{\partial z} \right) \right) \Big|_{r=R} = \frac{\mu_0}{\epsilon \mu} \left(\frac{\partial \psi}{\partial \xi} \Big|_{\xi \rightarrow O(\epsilon)} - \epsilon \frac{\partial R}{\partial z} \frac{\partial \psi}{\partial z} \right). \quad (10.56)$$

In this expression in order to find a solution we are going to take $\mu_0 = \hat{\mu}_0 \epsilon^2 \ln(\epsilon^{-1})$.

$$\left(-\frac{\partial^2 \Psi}{\partial z^2} \frac{R}{2} - \frac{\partial R}{\partial z} \left(H_0 + \frac{\partial \Psi}{\partial z} \right) \right) \Big|_{r=R} = -\frac{\hat{\mu}_0 \epsilon^2 \ln(\epsilon^{-1})}{\epsilon \mu} \frac{\Psi}{R \epsilon \ln(\epsilon^{-1})}. \quad (10.57)$$

Making simplifications and multiplying by $-2R$, we get:

$$\left(\frac{\partial^2 \Psi}{\partial z^2} R^2 + 2R \frac{\partial R}{\partial z} \left(H_0 + \frac{\partial \Psi}{\partial z} \right) \right) = 2 \frac{\hat{\mu}_0}{\mu} \Psi. \quad (10.58)$$

This expression can be reduced to:

$$\frac{\partial}{\partial z} \left(R^2 \left(H_0 + \frac{\partial \Psi}{\partial z} \right) \right) = 2 \frac{\hat{\mu}_0}{\mu} \Psi. \quad (10.59)$$

Now, we have to solve the following problem.

$$p = \sigma \left(\frac{1}{R} - \frac{\partial^2 R}{\partial z^2} \right) - \frac{1}{2} \mu H^2, \quad (10.60)$$

$$\frac{\partial}{\partial z} \left(R^2 \left(H_0 + \frac{\partial \Psi}{\partial z} \right) \right) = 2 \frac{\hat{\mu}_0}{\mu} \Psi, \quad (10.61)$$

$$\rho \left(\frac{\partial w}{\partial t} + w \frac{\partial w}{\partial z} \right) = -\frac{\partial p}{\partial z}, \quad (10.62)$$

$$\frac{\partial(R^2)}{\partial t} + \frac{\partial(wR^2)}{\partial z} = 0, \quad (10.63)$$

The stability analysis

With the following perturbations and considering ε how our disturbing parameter:

$$R \approx R_0 + \varepsilon R_1, \quad w \approx \varepsilon W_1, \quad H \approx H_0 + \varepsilon H_1, \quad (10.64)$$

with the disturbed variables,

$$R_1, W_1, H_1 \propto \exp(\varpi t + ikz), \quad (10.65)$$

with $i = \sqrt{-1}$. Combining Eq. (10.60) with Eq. (10.62) and introducing perturbed expressions, then keeping terms order ε , provides:

$$\rho \varpi W_1 = \sigma \frac{(ik)}{R_0^2} (1 - (R_0 k)^2) R_1 + \mu (ik) H_0 H_1. \quad (10.66)$$

This expression involves term W_1 , R_1 and H_1 , then we proceed to obtain W_1 in terms of R_1 from Eq. (10.63),

$$W_1 = \frac{-2\varpi}{ikR_0} R_1, \quad (10.67)$$

and then H_1 is obtained from Eq. (10.61) deriving in z and using the relation $H_1 = \partial \Psi_1 / \partial z$, which gives:

$$H_1 = \frac{-2R_0 H_0 k^2}{2(\hat{\mu}_0/\mu) + (R_0 k)^2} R_1, \quad (10.68)$$

Replacing W_1 from Eq. (10.67) and H_1 from Eq. (10.68) in Eq. (10.66):

$$\varpi^2 = \frac{\sigma(kR_0)^2}{2\rho R_0^3} (1 - (kR_0)^2) - \frac{\mu H_0^2 (kR_0)^4}{\rho R_0^2 (2(\hat{\mu}_0/\mu) + (kR_0)^2)}, \quad (10.69)$$

This expression is the dispersion relation for the super-paramagnetic full case, and we must note that taking $H_0 = 0$, this is, non-magnetic influence, we recover the Eq. (9.26) and taking $\hat{\mu}_0 = 0$, then we get the Eq. (10.46). The dimensionless expression is given by:

$$\bar{\varpi}^2 = \frac{\bar{k}^2}{2} (1 - \bar{k}^2) - \frac{C_{pm} \bar{k}^4}{(2(\hat{\mu}_0/\mu) + \bar{k}^2)}, \quad (10.70)$$

where the dimensionless quantity $\bar{\varpi} = \varpi \sqrt{\rho R_0^3 / \sigma}$ and $\bar{k} = kR_0$. Again, we note that $C_{pm} = 0$ recovers the case inviscid case Eq. (9.26) for long wavelengths and taking $\hat{\mu}_0 = 0$ recovers the previous inviscid superparamagnetic case reported in Eq. (10.46). In fact, comparing both magnetic terms in Eq. (10.46) and Eq. (10.70), it is possible to obtain

$$C_{pm} \bar{k}^2 \geq \frac{C_{pm} \bar{k}^4}{(\hat{\mu}_0/\mu) + \bar{k}^2},$$

and considering that the capillary term is the same in both cases, allows us to conclude that the $\bar{\varpi}$ for the case $\mu_0 = 0$ is less or equal to $\bar{\varpi}$ for the case $\mu_0 \neq 0$, getting:

$$\bar{\varpi}_{\mu=0}^2 \leq \bar{\varpi}_{\mu \neq 0}^2,$$

and because the magnetic permeability of a fluid is much greater than the vacuum magnetic permeability, the term $\hat{\mu}_0/\mu$ appears to be very small, indicating that the superparamagnetic case with $\mu_0 = 0$ adequately approximates the case $\mu_0 \neq 0$. In Fig. (10.2), two cases are observed: the solid-line considers $\mu_0 = 0$ and the dotted-line represents $\mu_0 \neq 0$, in which the dotted-line is greater than the solid-line but this value depends on $\hat{\mu}_0/\mu$, if it is very small, there will be no changes.

10.2 The viscous magnetic case

In this section we consider the magnetic viscous liquid cylinder, in the superparamagnetic limit. This study must basically a combination for the previous results of Section 9.3 and Section 10.1. In this analysis, we also consider an applied magnetic field orthogonal to the cylinder surface and in the axial direction.

The governing equations are given by the momentum equations in the radial direction

$$\rho \left(\frac{\partial u}{\partial t} + u \frac{\partial u}{\partial r} + w \frac{\partial u}{\partial z} \right) = -\frac{\partial p}{\partial r} + \eta \left(\frac{\partial}{\partial r} \left(\frac{1}{r} \frac{\partial(ru)}{\partial r} \right) + \frac{\partial^2 u}{\partial z^2} \right) + \text{Magnetic terms}, \quad (10.71)$$

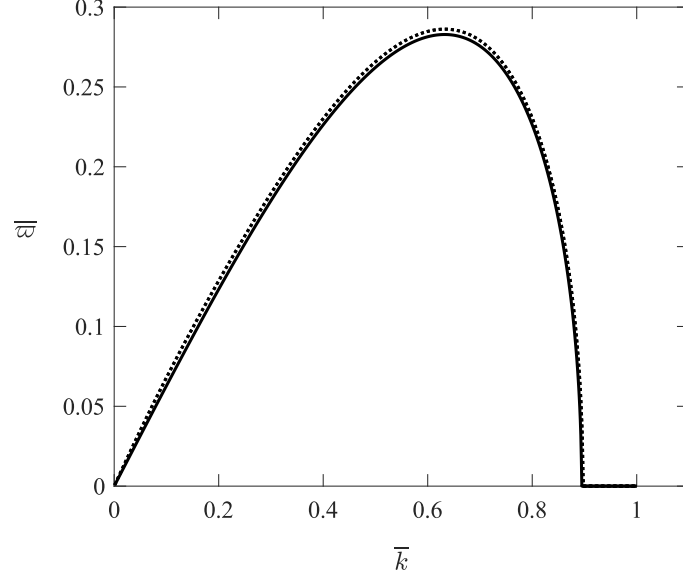


Figure 10.2: Figure shows the comparison between the case $\mu_0 = 0$ (solid-line) and the case $\mu_0 \neq 0$ (dotted-line), both using the value of $C_{pm} = 0.1$ and $\hat{\mu}_0/\mu = 0.01$.

and the momentum equation in the axial direction

$$\rho \left(\frac{\partial w}{\partial t} + u \frac{\partial w}{\partial r} + w \frac{\partial w}{\partial z} \right) = -\frac{\partial p}{\partial z} + \eta \left(\frac{1}{r} \frac{\partial}{\partial r} \left(r \frac{\partial w}{\partial r} \right) + \frac{\partial^2 w}{\partial z^2} \right) + \text{Magnetic terms}, \quad (10.72)$$

in which the magnetic terms are representing the Kelvin force, $\mathbf{M} \cdot \nabla \mathbf{H}$, with viscosity η and the continuity equation (9.29) in cylindrical coordinates that does not change.

For this reduced case, we assume the magneto-static limit of the Maxwell's equations (3.4) and (3.3), which is given by $\mathbf{M} = \chi \mathbf{H}$, and where the magnetic induction takes the form $\mathbf{B} = \mu_0(1 + \chi) \mathbf{H} = \mu \mathbf{H}$. As the Section 10.1, Eq. (3.3) indicates that exists a function ψ such that $\mathbf{H} = -\nabla \psi$. By Eq. (3.4), we have to satisfy the Laplace's equation in cylindrical coordinates. We note that the applied magnetic field is given by a uniform field in the axial direction of the cylinder $\mathbf{H} = (0, 0, H_0) = H_0 \hat{z}$, and with this assumption the Kelvin force in the Eqs. (10.71) and (10.72) is neglected as the previous case analyzed in Section 10.1. With these simplifications, the system of equation that govern the viscous magnetic problem are reduced to those of the viscous case, the momentum equations (9.27) and (9.28) and the unchanged continuity equation (9.29). This indicates that the magnetic effect is transferred to the treatment of the free surface and that the reduced equations that govern this problem, in the long wavelength limit, are exactly the same than the viscous case.

The analysis continues with the magnetic boundary condition that must satisfy Eqs. (10.15) and (10.16) and the Laplacian equation that must be solved inside and outside the cylinder,

again as in the previous Section 10.1 and considering the modified magnetic pressure quoted by [33].

$$p = \sigma \left(\frac{1}{R} - \frac{\partial^2 R}{\partial z^2} \right) - \frac{1}{2} \mu H^2, \quad (10.73)$$

$$\frac{\partial}{\partial z} \left(R^2 \left(H_0 + \frac{\partial \Psi}{\partial z} \right) \right) = 2 \frac{\hat{\mu}_0}{\mu} \Psi, \quad (10.74)$$

$$\rho \left(\frac{\partial w}{\partial t} + w \frac{\partial w}{\partial z} \right) = - \frac{\partial p}{\partial z} + \frac{3\eta}{R^2} \frac{\partial}{\partial z} \left(R^2 \frac{\partial w}{\partial z} \right), \quad (10.75)$$

$$\frac{\partial(R^2)}{\partial t} + \frac{\partial(wR^2)}{\partial z} = 0, \quad (10.76)$$

The stability analysis

In this section, we present the dispersion relation derived from the linear stability analysis for viscous magnetic cylinder under a uniform magnetic coaxially applied to the jet.

The perturbations of the jet radius, velocity and the magnetic field are looked in the form

$$R \approx R_0 + \varepsilon R_1, \quad w \approx \varepsilon W_1, \quad H \approx H_0 + \varepsilon H_1, \quad (10.77)$$

with ε being the parameter of perturbation and the disturbed variables

$$R_1, W_1, H_1 \propto \exp(\varpi t + ikz). \quad (10.78)$$

the calculation of the dispersion relation follows directly from the combination of the cases studied of the Subsecs. 9.3 and 10.1.1 for the viscous and the inviscid superparamagnetic approximations respectively, and takes the following form

$$\varpi^2 = \frac{\sigma(kR_0)^2}{2\rho R_0^3} (1 - (kR_0)^2) - \frac{3\eta(kR_0)^2}{\rho R_0^2} \varpi - \frac{\mu(kR_0)^2 H_0^2}{\rho R_0^2}. \quad (10.79)$$

The above expression is a relation between the frequency ϖ as a function of the wave-number k , given the fluid and magnetic parameters ρ density, R_0 initial radius, σ surface tension coefficient, η viscosity and μ magnetic permeability of the fluid. Usually expressed as a dispersion relation $\mathcal{D}(\varpi, k)$, we present the Eq. (10.79) with the dimensionless parameters $\bar{\varpi} = \varpi \sqrt{\rho R_0^3 / \sigma}$ and $\bar{k} = kR_0$, getting

$$\bar{\varpi}^2 = \frac{\bar{k}^2}{2} (1 - \bar{k}^2) - \frac{3}{Re} \bar{k}^2 \bar{\varpi} - C_{pm} \bar{k}^2, \quad (10.80)$$

where $Re = \sqrt{\rho \sigma R_0} / \eta$ is the Reynolds number considering the capillary velocity and $C_{pm} = \mu R_0 H_0^2 / \sigma$ is the magnetic parameter. Eq.(10.80) is a second order algebraic equation with linear term involving the viscosity term and independent term capturing the capillary and the magnetic pressure terms, this expression agrees with the dispersion relation of [66] where he took the entire magnetic pressure.

Following the previous analysis of stability, the capillary pressure brings instability to the system when $\tilde{k} = kR_0 \ll 1$. The viscosity term indicates that when viscosity is increased the Reynolds number Re decreased and the breakup time is delayed but it is reached, while the effect of the magnetic pressure prevents the breakup as the range of dimensional wave-numbers is decreased when the magnetic parameter is increased. We consider the graphs of the dimensionless quantity $\varpi \sqrt{\rho R_0^3 / \sigma}$ against kR_0 , for several values of the $Re = 0.1, 1, 10, 100$. In the Fig. (10.3) (Top), we take the magnetic parameter $C_{pm} = \mu R_0 H_0^2 / \sigma = 0.01$ and we observe that the magnetic effect it seems non dominant, against the viscosity and the diagram is flattened when viscosity is decreased, indicating lower growth rates, this in term of stability indicates that the breakup time involving the viscous and magnetic influence is greater than the viscous breakup time.

In the Fig. (10.3) (Middle), we take the magnetic parameter $C_{pm} = \mu_0 R_0 H_0^2 / \sigma = 0.1$ and we observe that the magnetic effect it seems dominant, against to the viscosity and the diagram is flattened when viscosity is decreased, but also the magnetic pressure shifted the curve to the line $kR_0 = 0$, indicating lower growth rates and less (ϖ, k) unstable modes.

In the Fig. (10.3) (Bottom), we take the magnetic parameter $C_{pm} = \mu_0 R_0 H_0^2 / \sigma = 5/4\pi$ and again we observe that the magnetic effect it seems dominant, against to the viscosity and the diagram is flattened when viscosity is decreased, but also the magnetic pressure shifted the curve to the line $kR_0 = 0$, indicating lower growth rates and less (ϖ, k) unstable modes.

10.2.1 Numerical approach to the nonlinear regimes

In this section, we are going to present the numerical solution to the nonlinear problem of Plateau-Rayleigh instability for superparamagnetic fluids. For that, we mention and compare our result with Entov et *al.*'s work in [66].

In [66], authors studied the one-dimensional theory of the capillary instability and the breakup of jets considering magneto-rheological fluids. They performed linear instability of the nonlinear jet profile using, similarly to us, the long-wave approximation. However, they used a phenomenological rheology modification of the viscosity due to the effect of the magnetic field. They concluded that the magnetic field can prevent the early breakup of the jet because of the formation of thin flat necks between droops that cannot deform due to the high packing of magnetic field lines. Furthermore, they have considered only the case in which the outer region is magnetically impermeable.

Let's consider the set of equations Eq. (9.62) and Eq. (10.37). The last one has the term $C_{pm} R^{-5} \partial R / \partial z$, which brings the information about the magnetic applied field. The discretization of all the terms in both equations remains the same as those used in Section (10.2.1). In this case, the discretization of the magnetic term in the w^i points of the

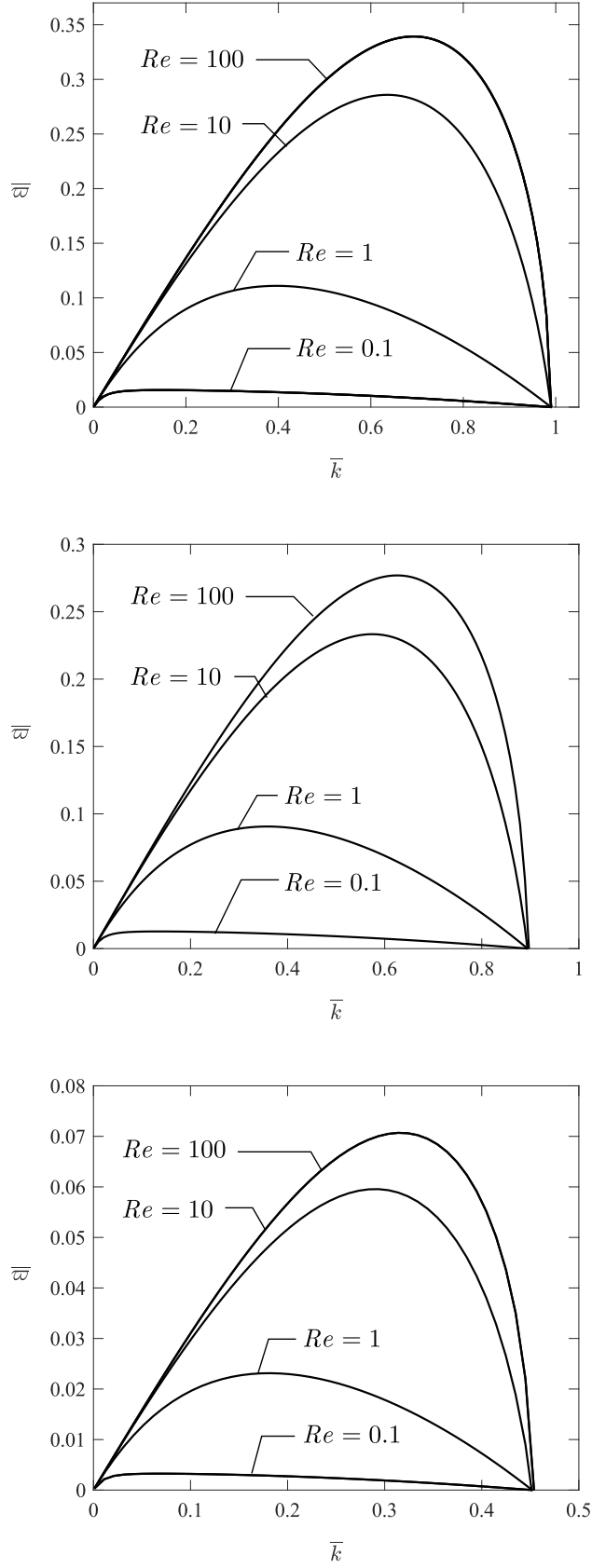


Figure 10.3: Graph of the dimensionless quantity $\bar{\omega} = \varpi \sqrt{\rho R_0^3 / \sigma}$ as a function of $\bar{k} = k R_0$ for various number Reynolds $Re = 0.1, 1, 10, 100$, with the magnetic parameter $C_{pm} = \mu_0 R_0 H_0^2 / \sigma = 0.01$ (Top figure), $C_{pm} = 0.1$ (Middle figure) and $C_{pm} = 5/4\pi$ (Bottom figure) with the long wavelength approximation.

staggered mesh is given by:

$$\frac{1}{R^5} \frac{\partial R}{\partial z} \Big|_i = \frac{R_{i+1} - R_i}{(0.5(R_{i+1} + R_i))^5}. \quad (10.81)$$

As we can observe from the results in Fig. (10.4) the steady states present a long flat neck connecting the two drops. The thickness of the necks increase significantly as we increase C_{pm} showing that when the magnetic field is more intense it becomes harder to pack the magnetic field lines along the necks.

As we increase the Re , the flow tends towards an inviscid regime. The shapes observed at steady state are similar to the ones shown before, with the exception of a pronounced neck near the drops for $Re = 200$. It seems that Re increases the magnetic effect needed to be stronger to stabilize the flow. It is interesting to notice that the evolution of the case $Re = 10$ already shows that the magnetic fields prevented the formation of satellite drops in the neck region. Details of this interaction still remain to be studied in further depth.

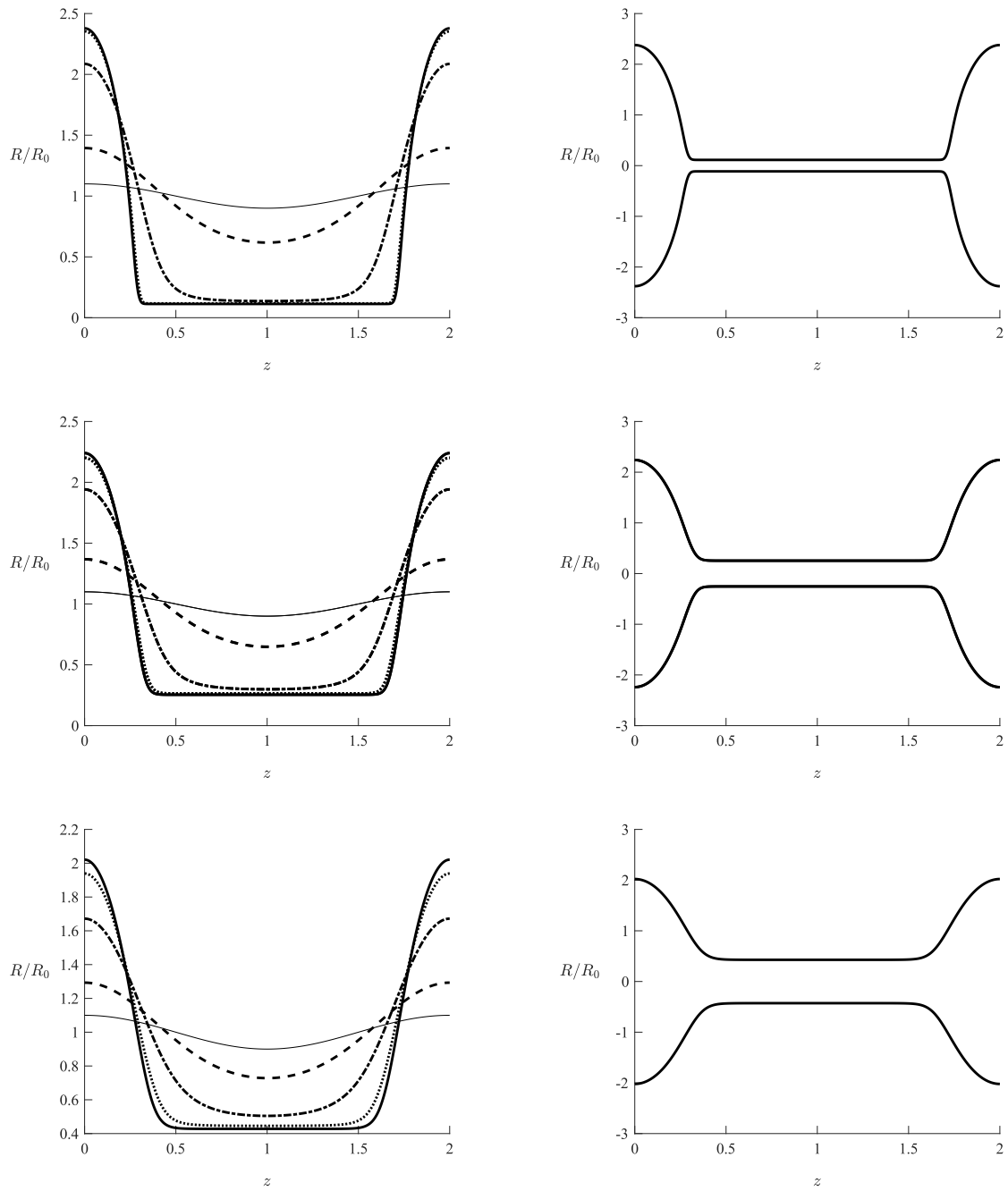


Figure 10.4: Figures show the free surface evolution at time $t = 0, 10, 15, 20, 24.8$, this last being the approximated scaled breakup time (left). Calculation was made for $Re = 0.1$ and $C_{pm} = 0.01$ (Top), $C_{pm} = 0.1$ (Middle) and $C_{pm} = 5/4\pi$ (Bottom) the breakup time curve is reflected through the axis OZ to replicate the pinch-off (right).

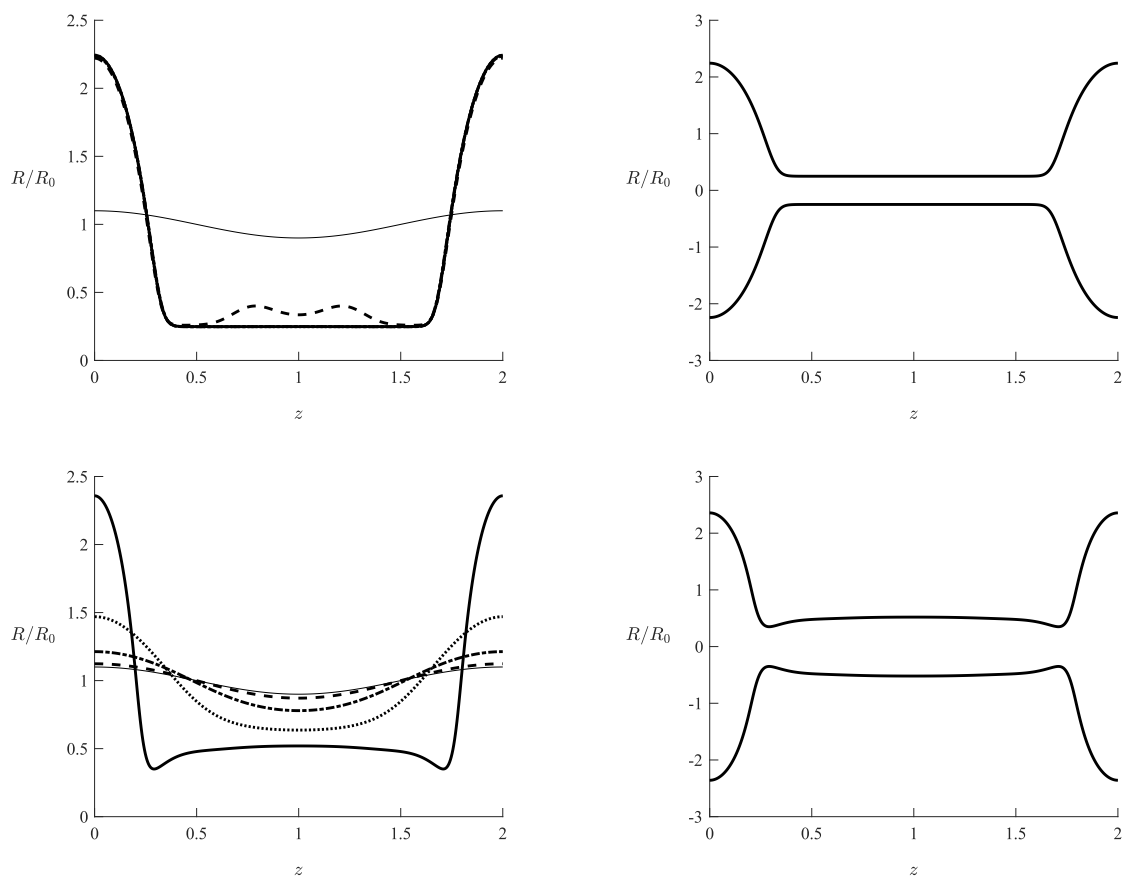


Figure 10.5: Figures show the free surface evolution at time $t = 0, 10, 15, 20, 24.8$, this last being the approximated scaled breakup time (left). Calculation was made for $Re = 10$ (Top) and $Re = 200$ (Bottom) with $C_{pm} = 0.1$ and the breakup time curve is reflected through the axis OZ to replicate the pinch-off (right).

CHAPTER 11

THE PLATEAU-RAYLEIGH INSTABILITY COUPLED WITH MAGNETIZATION

11.1 The full magnetic model

In this chapter we are going to present a study of the Plateau-Rayleigh instability for a magnetic fluid considering its coupling with an evolution equation for the magnetization. For that, we are going to consider the modified Navier-Stokes equation Eq. (3.59), where the **HB** formulation is used for the Maxwell stress tensor, we choose this formulation because it brings information about the magnetic forces, the Kelvin and Torque forces, due to the presence of magnetism in the system. At the same time, the magnetic evolution Eq. (3.39) according to Shliomis [52] is considered, together with an incompressible flow and the Maxwell's equations in the magnetostatic limit Eqs.(3.3)-(3.4). In order to find the solution of this problem, we are going to use the long wavelengths hypothesis Eq. (11.8), that allows us to simplify our set of equations and transform them into a simpler set of differential equations. Later, we will use this reduced set of partial differential equations to establish the dispersion relationship and proceed to the non-linear analysis. In this process we are going to recover the results that were obtained in the previous chapters.

11.1.1 Scaling arguments

Initially, we consider the modified Navier-Stokes equation (3.59), in which the stress tensor consider the Maxwell tensor with the the formulation **HB** as in Sub-Section (3.8),

which is given by

$$\boldsymbol{\Sigma} = -p\mathbf{I} + \eta \frac{(\nabla \mathbf{u} + \nabla \mathbf{u}^t)}{2} + \mu_0 \mathbf{H}\mathbf{B} - \frac{\mu_0 H^2}{2} \mathbf{I}, \quad (11.1)$$

where $\boldsymbol{\Sigma}$ and \mathbf{I} are second order tensors, \mathbf{M} and \mathbf{I} are first order tensors. The magnetic stress tensor is scaled with the same scale of the pressure.

Also, we consider a magnetization evolution Eq. (3.39):

$$\frac{\partial \mathbf{M}}{\partial t} + \mathbf{u} \cdot \nabla \mathbf{M} = \frac{(\mathbf{M}_0 - \mathbf{M})}{\tau} + \boldsymbol{\Omega} \times \mathbf{M} + \frac{\mu_0}{6\phi\eta} (\mathbf{M} \times \mathbf{H}) \times \mathbf{M}, \quad (11.2)$$

in which \mathbf{M} is the magnetization, μ_0 is the vacuum magnetic permeability, \mathbf{u} the velocity field, \mathbf{M}_0 is the magnetization equilibrium state, τ is the magnetic relaxation time, \mathbf{H} is the magnetic applied field, η is the viscosity and ϕ the volumetric fraction and

$$\boldsymbol{\Omega} = \frac{1}{2} \nabla \times \mathbf{u}, \quad (11.3)$$

For the magnetic fluid flow, we have a modified equation of the Navier-Stokes equations through the Maxwell stress tensor in the $\mathbf{H}\mathbf{B}$ formulation as in Section 3.49, given by:

$$\rho \frac{\partial \mathbf{u}}{\partial t} + \mathbf{u} \cdot \nabla \mathbf{u} = -\nabla p + \eta \nabla^2 \mathbf{u} + \mu_0 \mathbf{M} \cdot \nabla \mathbf{H} + \mu_0 \nabla \times (\mathbf{M} \times \mathbf{H}). \quad (11.4)$$

The system of equations (11.1), (11.2), (11.4) together with Maxwell's equations that we write them again here:

$$\nabla \times \mathbf{H} = \mathbf{0}, \quad \nabla \cdot \mathbf{B} = 0, \quad (11.5)$$

form the model we are going to follow to study the Plateau-Rayleigh problem. Due the large number of parameter involved we dimensionless the above equations, for this, we choose typical scales for flow and magnetic variables.

$$\mathbf{u} \sim v_c, \quad r \sim R_0, \quad z \sim L, \quad t \sim t_c, \quad \mathbf{M} \sim M_s, \quad \mathbf{H} \sim H_0, \quad p \sim \frac{\sigma}{R_0}. \quad (11.6)$$

By using the above scale the radial and axial components are given by $r = R_0 \check{r}$ and $z = L \check{z}$, where variables with the *check* symbols are the dimensionless parameters. By doing this, $\epsilon = R_0/L \ll 1$ is the small parameter assumed to reduce the system of equations above mentioned, then $w = v_c \check{w}$ and $u = \epsilon v_c \check{u}$, the time is given by $t = (L/v_c) \check{t}$ with $v_c = \sqrt{\sigma/\rho R_0}$. The magnetic stress tensor (11.1) inside of the cylinder is scaled with the same scale of the pressure, this is $\boldsymbol{\Sigma} = (\sigma/R_0) \check{\boldsymbol{\Sigma}}$ and the viscous and magnetic terms are scaled with pressure as well, getting

$$\check{\boldsymbol{\Sigma}} = -\check{p}\mathbf{I} + \frac{\eta}{v_c L} \frac{(\nabla \mathbf{u} + \nabla \mathbf{u}^t)}{2} + \check{\mathbf{H}}\check{\mathbf{M}} C_{pm} + \left(\check{\mathbf{H}}\check{\mathbf{H}} - \frac{\check{H}^2}{2} \mathbf{I} \right) C_{pm} \frac{H_0}{M_s}, \quad (11.7)$$

where the magnetic parameter C_{pm} is,

$$C_{pm} = \frac{\mu_0 R_0 M_s H_0}{\sigma}, \quad (11.8)$$

By using the Maxwell stress tensor, we obtain the corresponding modified Navier-Stokes equations for a magnetic fluid,

$$\frac{\partial \check{\mathbf{u}}}{\partial t} + \check{\mathbf{u}} \cdot \check{\nabla} \check{\mathbf{u}} = -\check{\nabla} \check{p} + \frac{1}{Re} \check{\nabla}^2 \check{\mathbf{u}} + (\check{\mathbf{M}} \cdot \check{\nabla} \check{\mathbf{H}} + \check{\nabla} \times (\check{\mathbf{M}} \times \check{\mathbf{H}})) C_{pm}. \quad (11.9)$$

The parameter C_{pm} in (11.8) is a relation between the resistance magnetic force and the capillary pressure, the viscous term is related to the Reynolds number $Re = \rho v_c L / \eta$ and again that is a relation between the inertial and the capillary pressure, $(\eta v_c / L) / (\sigma / R_0)$. For the vacuum Maxwell stress tensor, we put $\mathbf{M} = \mathbf{0}$ and $p = 0$, getting $\check{\Sigma} = \mathcal{O}(H_0^2 / (\sigma / R_0)) = \mathcal{O}(C_{pm} H_0 / M_s)$.

The normal component of \mathbf{B} and the tangential component of \mathbf{H} must be continuous across the boundary, for this purpose the Maxwell condition for the magnetic field in Eq. (11.5), indicates that there exists a potential ψ defining \mathbf{H} . We incorporate the co-axially applied magnetic field by taking $\mathbf{H} = H_0 \hat{z} + \nabla \psi$ as in previous sections. This condition must be satisfied everywhere, and then we consider the potential Φ for the exterior region.

The continuity of the normal induction field is given by Eq. (3.10), and expressed as

$$\mathbf{n} \cdot (\nabla \psi + \mathbf{M}) = \mathbf{n} \cdot \nabla \Phi, \quad (11.10)$$

in this expression \mathbf{n} is the normal unitary vector and we consider a non magnetizable medium in outside region. We scale the interior potential by using $\psi = H_0 L \check{\psi}$ and for the exterior potential $\Phi = H_0 L \check{\Phi} / \ln(1/\epsilon)$. The scaling if the above equation is given by, $[\Phi] = \epsilon^2 M_s L$ this is because \mathbf{M} scales with M_s and the ϵ factor comes from the normal vector, and the $[\Phi] \sim \ln(\epsilon R)$ then a derivative on the radial surrounding region is given by $[\Phi] \sim 1/\epsilon L$, giving the scale for $[\Phi]$ as above.

The continuity of the tangential magnetic field is given by Eq. (3.16) and it is expressed as

$$\mathbf{t} \cdot \nabla \psi = \mathbf{t} \cdot \nabla \Phi, \quad (11.11)$$

in this expression \mathbf{t} is the tangent unitary vector, the left hand side scales like H_0 the right hand side scales with $\ln(1/\epsilon)/L$, then $[\Phi] = H_0 L / \ln(1/\epsilon)$. Comparing the $[\Phi]$ in both continuity conditions we have

$$\frac{H_0}{M_s} = \epsilon^2 \ln(1/\epsilon), \quad (11.12)$$

this indicates that the vacuum Maxwell stress tensor is small, $\mathcal{O}(C_{pm} H_0 / M_s) \ll 1$. with this scale the continuity conditions take the following form

$$\mathbf{n} \cdot \check{\mathbf{M}} = \mathbf{n} \cdot \check{\nabla} \check{\Phi} \epsilon^2 \mathcal{S}, \quad \text{and} \quad \mathbf{t} \cdot \check{\nabla} \check{\psi} = \mathbf{t} \cdot \frac{\check{\nabla} \check{\Phi}}{\ln(1/\epsilon)}, \quad (11.13)$$

where the parameter $\mathcal{S} = H_0 / M_s \epsilon^2 \ln(1/\epsilon)$ and using Eq. (11.12) takes the value 1. In other hand, as the exterior potential $\Phi \sim f(z) \ln(\xi)$ with ξ being the external radius and regarding

the tangential continuity conditions (11.13), then the spatial derivative $\frac{\partial\Phi}{\partial z} \sim f'(z)\ln(\epsilon)$ with the leading order, then Eq. (11.13) provides

$$1 + H_z = \frac{1}{\ln(1/\epsilon)} \frac{\partial\Phi}{\partial z} \sim \frac{f'(z)\ln(\epsilon)}{-\ln(\epsilon)} = -f'(z), \quad (11.14)$$

this indicates that H_z is independent of r .

For the magnetic evolution equation (11.2), using the proposed scales takes the form,

$$\frac{\partial\check{\mathbf{M}}}{\partial\check{t}} + \check{\mathbf{u}} \cdot \nabla\check{\mathbf{M}} = \frac{(\check{\mathbf{M}}_0 - \check{\mathbf{M}})}{\mathcal{T}} + \check{\mathbf{\Omega}} \times \check{\mathbf{M}} + ((\check{\mathbf{M}} \times \check{\mathbf{H}}) \times \check{\mathbf{M}})\mathcal{N}, \quad (11.15)$$

with the magnetic parameters,

$$\mathcal{N} = \frac{\mu_0 L M_s H_0}{6\eta\phi v_c}, \quad (11.16)$$

and the scaled magnetic relaxation time being,

$$\mathcal{T} = \frac{v_c}{L}\tau, \quad (11.17)$$

with the equilibrium magnetization given by:

$$\check{\mathbf{M}}_0 = \mathcal{L}(\alpha) \frac{\check{\mathbf{H}}}{\check{H}}. \quad (11.18)$$

We also have to satisfy the Maxwell's equations (11.5), this is by taking $\mathbf{H} = H_0\hat{z} + \nabla\psi$, we must solve the Laplace's equation both inside and outside of the cylinder, as was done in the previous Section (10.2) and the condition of the magnetic induction takes the form,

$$\frac{H_0}{M_s} \nabla^2\psi + \nabla \cdot \mathbf{M} = 0. \quad (11.19)$$

which indicates that only must satisfy the divergence of the magnetization,

$$\nabla \cdot \mathbf{M} = 0. \quad (11.20)$$

The normal stress balance across the boundary must satisfy

$$\mathbf{n}^t \cdot \mathbf{\Sigma}^{\text{In}} \cdot \mathbf{n} - \mathbf{n}^t \cdot \mathbf{\Sigma}^{\text{Out}} \cdot \mathbf{n} = \mathcal{H}, \quad (11.21)$$

the full stress tensor consider the Newtonian fluid $\mathbf{\Sigma}^{\text{nf}}$ and the magnetic $\mathbf{\Sigma}^{\text{m}}$ parts and it can be write as $\mathbf{\Sigma} = \mathbf{\Sigma}^{\text{nf}} + \mathbf{\Sigma}^{\text{m}}$. From this expression, the Newtonian fluid stress tensor is equal to 9.36 and the magnetic stress tensor considering the product of the fields \mathbf{H} and \mathbf{M} of the Maxwell stress tensor Eq. (11.7) and is giving by asymmetric stress tensor

$$\mathbf{\Sigma}_{HM} = \begin{pmatrix} \epsilon^2 H_r M_r & 0 & \epsilon H_r M_z \\ 0 & 0 & 0 \\ \epsilon(1 + H_z)M_r & 0 & (1 + H_z)M_z \end{pmatrix}, \quad (11.22)$$

where the contribution of the Newtonian part to the normal stress across the boundary is the same as in the viscous case, this is $\mathbf{n}^t \cdot \Sigma^{\text{nf}} \cdot \mathbf{n} = p - 2\partial u/\partial r$, by doing this Eq.(11.21) is

$$p - 2\frac{\partial u}{\partial r} - \mathbf{n}^t \cdot (\Sigma_{HM}^{\text{In}} + \Sigma_{HH}^{\text{In}}) \cdot \mathbf{n} - \mathbf{n}^t \cdot \Sigma_{HH}^{\text{Out}} \cdot \mathbf{n} = \sigma\mathcal{H}, \quad (11.23)$$

here both interior and exterior normal stress tensor of **HH** are the same and they can be canceled, giving the following expression

$$p - 2\frac{\partial u}{\partial r} - \mathbf{n}^t \cdot \Sigma_{HM}^{\text{In}} \cdot \mathbf{n} = \mathcal{H}, \quad (11.24)$$

where we conclude that $\mathbf{n}^t \cdot \Sigma_{HM}^{\text{In}} \cdot \mathbf{n} = \mathcal{O}(\epsilon)^2$, see Appendix (II.4) and it is not retained in this expression, finding

$$p - 2\frac{\partial u}{\partial r} = \sigma\mathcal{H}. \quad (11.25)$$

The tangential stress across the boundary is given by

$$\mathbf{t}^t \cdot \Sigma^{\text{In}} \cdot \mathbf{n} = \mathbf{t}^t \cdot \Sigma^{\text{Out}} \cdot \mathbf{n}, \quad (11.26)$$

with a similar analysis for the normal stress the magnetic stress tensor is given by the symmetric part corresponding to the diadic product of **H** and the asymmetric part related to the diadic product of **H** and **M**,

$$\mathbf{t}^t \cdot (\Sigma_{HM}^{\text{In}} + \Sigma_{HH}^{\text{In}}) \cdot \mathbf{n} = \mathbf{t}^t \cdot \Sigma_{HH}^{\text{Out}} \cdot \mathbf{n}, \quad (11.27)$$

then both interior and exterior tangential stress contribution of the diadic **HH** are the same and they are neglected, and it must be confirmed that $\mathbf{t}^t \cdot \Sigma_{HM}^{\text{In}} \cdot \mathbf{n}$, as seen in Appendix (II.5).

To perform the long wave expansion, we first consider the dimensionless modified Navier-Stokes equation (11.9) in cylindrical coordinates and we remark that expression of the torque force must be write in cylindrical coordinates as well. The radial component of Eq. (11.9), that we consider without the check symbol, which is written as,

$$\begin{aligned} \epsilon \left(\frac{\partial u}{\partial t} + u \frac{\partial u}{\partial r} + w \frac{\partial u}{\partial z} \right) &= -\frac{1}{\epsilon} \frac{\partial p}{\partial r} + \frac{\epsilon}{Re} \nabla^2 u \\ &+ C_{pm} \epsilon \left(\left(M_r \frac{\partial}{\partial r} + M_z \frac{\partial}{\partial z} \right) H_r + \frac{\partial}{\partial z} (M_r(1 + H_z) - M_z H_r) \right), \end{aligned} \quad (11.28)$$

in this expression each r -derivative indicates that we have to multiply a factor of ϵ and the same happens with u component of the velocity field, also notice that the factor epsilon is multiplying the first component of **H** and **M**, this factor is factored so that it multiplies the entire magnetic term. In the left hand side the factor is factorized and by using the same reasoning as in Section 8.2.1 the viscous term has also the factor. The equation above indicates that $\partial p/\partial r = 0$, i.e., p is independent of r as deduced in the previous sections.

Now, the axial component equation of Eq. (11.9) is given by

$$\begin{aligned} \frac{\partial w}{\partial t} + u \frac{\partial w}{\partial r} + w \frac{\partial w}{\partial z} = -\frac{\partial p}{\partial z} + \frac{1}{Re} \nabla^2 w \\ - C_{pm} \left(\left(M_r \frac{\partial}{\partial r} + M_z \frac{\partial}{\partial z} \right) (1 + H_z) + \left(\frac{1}{r} \frac{\partial}{\partial r} (r(H_r M_z - M_r(1 + H_z))) \right) \right), \end{aligned} \quad (11.29)$$

in this equation factors of ϵ appears but it is simplified in the term $u\partial w/\partial r$, $M_r\partial/\partial r$ and the last magnetic term. How was deduced above the term $1+H_z$ and M_z and p are independents of r so we can conclude like the Section 8.2.1, that $w = w(z, t)$ is independent of r , that cancels the second term on the left-hand side, This is also an argument that has been used since the beginning of this study.

We continue to perform the expansion with Eq. (11.15), that we consider without the check symbol, by analyzing the radial equation

$$\begin{aligned} \frac{\partial M_r}{\partial t} + w \frac{\partial M_r}{\partial z} = \frac{(\mathcal{L}H_r - M_r)}{\mathcal{T}} \\ + \frac{M_z}{2} \left(\frac{\partial u}{\partial z} - \frac{\partial w_2}{\partial r} \right) \\ + \mathcal{N}M_z (M_r(1 + H_z) - M_z H_r), \end{aligned} \quad (11.30)$$

The above equation is presented with the factor ϵ already simplified, it was the contribution of H_r and M_r and present in the expansion of w through w_2 .

$$\begin{aligned} \frac{\partial M_z}{\partial t} + w \frac{\partial M_z}{\partial z} = \frac{(\mathcal{L}(1 + H_z) - M_z)}{\mathcal{T}} \\ - \epsilon^2 \frac{M_r}{2} \left(\frac{\partial u}{\partial z} - \frac{\partial w_2}{\partial r} \right) \\ - \epsilon^2 \mathcal{N}M_r (M_r(1 + H_z) - M_z H_r), \end{aligned} \quad (11.31)$$

with the two last term being $\mathcal{O}(\epsilon^2)$ and retained the terms $\mathcal{O}(1)$ from this equation, we get

$$\frac{\partial M_z}{\partial t} + w \frac{\partial M_z}{\partial z} = \frac{(\mathcal{L}(1 + H_z) - M_z)}{\mathcal{T}}, \quad (11.32)$$

we know that H_z is independent of r and Eq. (11.32) involves $1 + H_z$ and M_z leaving us to deduce that nothing indicates that there is a dependency on r , then both $1 + H_z$ and M_z are independents on r .

We continue our analysis by deriving the set of equations that govern the full magnetic problem, assuming the long wavelengths hypothesis. Let's consider the modified Navier-Stokes equations (11.9) with the magnetic contribution of the Kelvin and Torque forces. We also consider the magnetization evolution equation proposed by [52] in (11.15) and the Maxwell's equations together with the continuity equation and the jump conditions.

We start the analysis with the Navier-Stokes equations (11.9). As in the previous Section, from the incompressibility equation for the velocity field $\mathbf{u} = (u, 0, w)$, we maintain

$$u = -\frac{r}{2} \frac{\partial w}{\partial z}. \quad (11.33)$$

Considering that the pressure term as:

$$p = \left(\frac{1}{R} - \frac{\partial^2 R}{\partial z^2} \right) + \frac{2}{Re} \frac{\partial u}{\partial r}, \quad (11.34)$$

and combining Eq. (11.33) with Eq. (11.34) we got,

$$p = \left(\frac{1}{R} - \frac{\partial^2 R}{\partial z^2} \right) - \frac{1}{Re} \frac{\partial w}{\partial z}. \quad (11.35)$$

Now, we are going to use dimensionless w -equation of (11.9) without the check symbol, and taking the $\mathbf{H} = (H_r, 0, 1 + H_z)$ with the sub-index indicating the position vector component:

$$\begin{aligned} \frac{\partial w}{\partial t} + w \frac{\partial w}{\partial z} = & -\frac{\partial p}{\partial z} + \frac{1}{Re} \left(\frac{1}{r} \frac{\partial}{\partial r} \left(r \frac{\partial w_2}{\partial r} \right) + \frac{\partial^2 w}{\partial z^2} \right) \\ & + C_{pm} \left(\frac{1}{r} \frac{\partial}{\partial r} (r H_r M_z) + \frac{\partial}{\partial z} ((1 + H_z) M_z) \right). \end{aligned} \quad (11.36)$$

Substituting the expression we got for the pressure p from Eq. (11.35),

$$\begin{aligned} \frac{\partial w}{\partial t} + w \frac{\partial w}{\partial z} = & -\frac{\partial}{\partial z} \left(\frac{1}{R} - \frac{\partial^2 R}{\partial z^2} \right) \\ & + \frac{1}{Re} \left(\frac{1}{r} \frac{\partial}{\partial r} \left(r \frac{\partial w_2}{\partial r} \right) + 2 \frac{\partial^2 w}{\partial z^2} \right) \\ & + C_{pm} \left(\frac{1}{r} \frac{\partial}{\partial r} (r H_r M_z) + \frac{\partial}{\partial z} ((1 + H_z) M_z) \right). \end{aligned} \quad (11.37)$$

The denominator on third and fourth term on the right-hand side involve r and the other terms do not have dependency on r , then we can multiply by r and integrate by r in the interval $[0, R]$ and dividing by $R^2/2$, allows us to find

$$\begin{aligned} \frac{\partial w}{\partial t} + w \frac{\partial w}{\partial z} = & -\frac{\partial}{\partial z} \left(\frac{1}{R} - \frac{\partial^2 R}{\partial z^2} \right) \\ & + \frac{1}{Re} \left(\frac{2}{R} \frac{\partial w_2}{\partial r} \Big|_{r=R} + 2 \frac{\partial^2 w}{\partial z^2} \right) \\ & + C_{pm} \left(\frac{2}{R} H_r \Big|_{r=R} M_z + \frac{\partial}{\partial z} ((1 + H_z) M_z) \right). \end{aligned} \quad (11.38)$$

We have to find a expression for second term on the right-hand side which is evaluated at $r = R$, for that we find the viscous normal stress balance as in Eq. (11.24), which is given by:

$$\frac{\partial w_2}{\partial r} + \frac{\partial u}{\partial z} + 2 \frac{\partial R}{\partial z} \left(\frac{\partial u}{\partial z} - \frac{\partial w}{\partial z} \right) = 0, \quad \text{at } r = R. \quad (11.39)$$

Using Eq. (11.33) allows us to find a new expression for $\partial w_2/\partial r$ in terms of R and w , then substituting that expression in Eq. (11.38), and after further additional simplification in

the viscous term, gives us:

$$\begin{aligned} \frac{\partial w}{\partial t} + w \frac{\partial w}{\partial z} &= -\frac{\partial}{\partial z} \left(\frac{1}{R} - \frac{\partial^2 R}{\partial z^2} \right) \\ &+ \frac{3}{Re} \left(\frac{1}{R^2} \frac{\partial}{\partial z} \left(R^2 \frac{\partial w}{\partial z} \right) \right) \\ &+ C_{pm} \left(\frac{2}{R} H_r \Big|_{r=R} M_z + \frac{\partial}{\partial z} ((1 + H_z) M_z) \right). \end{aligned} \quad (11.40)$$

The last expression has H_r and $1 + H_z$ and both can be extracted from the magnetization evolution equation (11.15) in the radial direction and leaving out the check symbol. Using the scaled variables and dropping out higher order terms.

$$\frac{DM_r}{Dt} = \frac{(\chi H_r - M_r)}{\mathcal{T}} + \frac{M_z}{2} \left(\frac{\partial u}{\partial z} - \frac{\partial w_2}{\partial r} \right) + \mathcal{N} M_z (M_r (1 + h_z) - M_z H_r). \quad (11.41)$$

Where χ is given by the following expression:

$$\chi = \frac{\mathcal{L}(\xi H)}{H}. \quad (11.42)$$

Which \mathcal{L} is the *Langevin* function and it is given by $\mathcal{L}(\alpha_h) = \coth(\alpha_h) - \alpha_h^{-1}$, with $\xi = mH_0 K^{-1} T^{-1}$. The scaling process gives us $\nabla \cdot \mathbf{M} = 0$ in Eq. (11.20), which in cylindrical coordinates gives us:

$$M_r = -\frac{r}{2} \frac{\partial M_z}{\partial z}. \quad (11.43)$$

Replacing Eq. (11.43) in Eq. (11.41), then evaluating on $r = R$ and substituting u from Eq. (11.33), and substituting $\partial w_2 / \partial r$ from Eq. (11.39), and after some additional algebraic manipulations, give us:

$$\begin{aligned} \frac{D}{Dt} \left(-\frac{r}{2} \frac{\partial M_z}{\partial z} \right) \Big|_{r=R} &= \frac{1}{\mathcal{T}} \left(\chi H_r \Big|_{r=R} + \frac{R}{2} \frac{\partial M_z}{\partial z} \right) \\ &- \frac{3M_z}{4} \left(\frac{1}{R} \frac{\partial}{\partial z} \left(R^2 \frac{\partial w}{\partial z} \right) \right) + \frac{M_z R}{4} \frac{\partial^2 w}{\partial z^2} \\ &+ \mathcal{N} M_z \left(-\frac{R}{2} \frac{\partial M_z}{\partial z} (1 + H_z) - M_z H_r \Big|_{r=R} \right). \end{aligned} \quad (11.44)$$

Considering the expression on the left-hand side, it is possible to prove that:

$$\frac{D}{Dt} \left(-\frac{r}{2} \frac{\partial M_z}{\partial z} \right) \Big|_{r=R} = \frac{D}{Dt} \left(-\frac{R}{2} \frac{\partial M_z}{\partial z} \right), \quad (11.45)$$

then after substitute Eq. (11.45) in Eq. (11.44), and leaving the term $H_r \Big|_{r=R}$ on the left-hand side,

$$\begin{aligned} (\chi - \mathcal{N} \mathcal{T} M_z^2) H_r \Big|_{r=R} &= -\frac{R}{2} \frac{\partial M_z}{\partial z} \\ + \mathcal{T} \left(\frac{D}{Dt} \left(-\frac{R}{2} \frac{\partial M_z}{\partial z} \right) + \frac{3M_z}{4} \left(\frac{1}{R} \frac{\partial}{\partial z} \left(R^2 \frac{\partial w}{\partial z} \right) \right) - \frac{M_z R}{4} \frac{\partial^2 w}{\partial z^2} + \mathcal{N} M_z \frac{R}{2} \frac{\partial M_z}{\partial z} (1 + H_z) \right), \end{aligned} \quad (11.46)$$

then after multiplying Eq. (11.46) by $2/R$ and isolating H_r , we get:

$$\begin{aligned} (\chi - \mathcal{N}\mathcal{T}M_z^2) \frac{2}{R} H_r \Big|_{r=R} &= -\frac{\partial M_z}{\partial z} \\ + \mathcal{T} \left[\frac{2}{R} \frac{D}{Dt} \left(-\frac{R}{2} \frac{\partial M_z}{\partial z} \right) + \frac{3M_z}{2} \left(\frac{1}{R^2} \frac{\partial}{\partial z} \left(R^2 \frac{\partial w}{\partial z} \right) \right) - \frac{M_z}{2} \frac{\partial^2 w}{\partial z^2} + \mathcal{N}M_z \frac{\partial M_z}{\partial z} (1 + H_z) \right]. \end{aligned} \quad (11.47)$$

Now, we are going to find an expression for $1 + H_z$ from Eq. (11.32), which provides

$$1 + H_z = \frac{1}{\chi} \left(\mathcal{T} \frac{DM_z}{Dt} + M_z \right). \quad (11.48)$$

From the normal continuity conditions Eq. (11.13), and considering that $\hat{\mathbf{n}} = (1, 0, -\epsilon R_z)$ and $\mathbf{M} = (\epsilon M_r, 0, M_z)$, we obtain the following relation:

$$\frac{\partial}{\partial z} (R^2 M_z) = -2R \left(\frac{\partial \Phi}{\partial \xi} - \epsilon \frac{\partial R}{\partial z} \frac{\partial \Phi}{\partial z} \right) \epsilon, \quad (11.49)$$

but from the scaling analysis we know that:

$$\frac{\partial \Phi}{\partial \xi} (\epsilon R, z) \sim -\frac{\Phi}{\epsilon R \ln \epsilon^{-1}}, \quad (11.50)$$

and after substituting this expression in Eq. (11.49) and keeping term order ϵ , we get:

$$\frac{\partial}{\partial z} (R^2 M_z) = 2 \frac{\Phi}{\ln \epsilon^{-1}}, \quad (11.51)$$

then deriving with relation to z ,

$$\frac{\partial^2}{\partial z^2} (R^2 M_z) = \frac{2}{\ln \epsilon^{-1}} \frac{\partial \Phi}{\partial z}. \quad (11.52)$$

Now, it is possible to access to $\partial \Phi / \partial z$ through the tangential continuity condition Eq. (11.13),

$$\hat{\mathbf{t}} \cdot \mathbf{H} = \hat{\mathbf{t}} \cdot \frac{\nabla \Phi}{\ln \epsilon^{-1}}.$$

Note that $\hat{\mathbf{t}} = (\epsilon R_z, 0, 1)$ and maintaining terms order 1:

$$1 + H_z = \frac{1}{\ln \epsilon^{-1}} \frac{\partial \Phi}{\partial z}, \quad (11.53)$$

then, substituting this expression in Eq. (11.52), provides:

$$\frac{\partial^2}{\partial z^2} (R^2 M_z) = 2(1 + H_z). \quad (11.54)$$

With the last expression, we are able to propose the reduced set of equations that allows us to analyze the Plateau Rayleigh instability for long wavelengths. The set of equations are given by Eqs. (11.40), (9.14), (11.54), (11.47) and (11.48).

On the right hand side of Eq. (11.40), the capillary term, the viscous term, the magnetic contribution of the kelvin and the torque force are present: the term $(2/R)H_r$ at $r = R$ is given by the Eq. (11.47), which only involves terms with relation to w , R , M_z and $1 + H_z$, and because it is a large expression we write it in a separate equation. The Eq. (9.14) is kept unchanged. Although Eq. (11.48) has the material derivative of M_z this is a formula to calculate $1 + H_z$, and we are going to substitute $1 + H_z$ from Eq. (11.54) in all equations except in Eq. (9.14), this substitution allows us to obtain 3 partial differential equations involving w , R and M_z . After additional algebraic operations the equations for the free surface evolution Eq. (9.14) is given by:

$$\frac{\partial R}{\partial t} + w \frac{\partial R}{\partial z} = -\frac{R}{2} \frac{\partial w}{\partial z}, \quad (11.55)$$

then the magnetization evolution equation Eq. (11.48) takes the following form:

$$\frac{\partial M_z}{\partial t} + w \frac{\partial M_z}{\partial z} = \frac{1}{\mathcal{T}} \left(-M_z + \frac{\chi}{2} \frac{\partial^2}{\partial z^2} (R^2 M_z) \right), \quad (11.56)$$

and the z -direction momentum Eq. (11.40) is given by the following expression:

$$\begin{aligned} \frac{\partial w}{\partial t} + w \frac{\partial w}{\partial z} = & -\frac{\partial}{\partial z} \left(\frac{1}{R} - \frac{\partial^2 R}{\partial z^2} \right) + \frac{3}{Re} \left(\frac{1}{R^2} \frac{\partial}{\partial z} \left(R^2 \frac{\partial w}{\partial z} \right) \right) \\ & + \frac{C_{pm}}{\chi - \mathcal{N} M_z^2 \mathcal{T}} \left(-M_z \frac{\partial M_z}{\partial z} + \mathcal{T} \left[\frac{2M_z}{R} \frac{D}{Dt} \left(-\frac{R}{2} \frac{\partial M_z}{\partial z} \right) \right. \right. \\ & \left. \left. + \frac{3M_z^2 [R^2 w_z]_z}{2R^2} - \frac{M_z^2 w_{zz}}{2} + \frac{\mathcal{N} M_z^2}{2} \frac{\partial M_z}{\partial z} \frac{\partial^2}{\partial z^2} (R^2 M_z) \right] \right) \\ & + C_{pm} \frac{\partial}{\partial z} \left(\frac{M_z}{2} \frac{\partial^2}{\partial z^2} (R^2 M_z) \right). \end{aligned} \quad (11.57)$$

11.1.2 Limiting cases

In this sub-section we are going to validate the theoretical result obtained in equations (11.55), (11.56) and (11.57) with the previous model obtained in the Section (10.2). Certainly the case of $C_{pm} = 0$, the case in which there is no magnetic interaction with the flow, leads us to the viscous case as in Section (9.3). For the magnetic case, we are going to consider the superparamagnetic limit where $\mathcal{T} \rightarrow 0$, which allows us to access to the magnetization through the evolution equation (11.56) and (11.54), obtaining that the magnetization is proportional to the applied field and the proportionality constant is given by χ , i.e., $M_z = \chi(1 + H_z)$. With these considerations Eq. (11.57) reduces to:

$$\frac{\partial w}{\partial t} + w \frac{\partial w}{\partial z} = -\frac{\partial}{\partial z} \left(\frac{1}{R} - \frac{\partial^2 R}{\partial z^2} \right) + \frac{3}{Re} \left(\frac{1}{R^2} \frac{\partial}{\partial z} \left(R^2 \frac{\partial w}{\partial z} \right) \right) + \frac{C_{pm}}{2} \frac{\partial M_z^2}{\partial z},$$

remarking that the magnetic parameter C_{pm} for the full model content M_s which is χH_0 for the superparamagnetic case, allowing us to obtain the magnetic parameter of Section (9.3).

In other hand, Eq. (11.56) together with Eq. (11.54) allows to satisfy the superparamagnetic limit. An additional approximation can be tested by using Eq. (11.54) an its limit when $\mu_0 = 0$, which gives us $M_z = R^{-2}$ and replacing this term in the last expression,

$$\frac{\partial w}{\partial t} + w \frac{\partial w}{\partial z} = -\frac{\partial}{\partial} \left(\frac{1}{R} - \frac{\partial^2 R}{\partial z^2} \right) + \frac{3}{Re} \left(\frac{1}{R^2} \frac{\partial}{\partial z} \left(R^2 \frac{\partial w}{\partial z} \right) \right) - \frac{2 C_{pm}}{R^5} \frac{\partial R}{\partial z},$$

which is the same result of Eq. (10.37).

The equation (11.55) remains unchanged in all these cases since there are no magnetic terms involved in it.

11.1.3 Linear stability analysis.

In this subsection, we perform the linear stability analysis for the full magnetic problem to find the dispersion relation. To that end, we consider the following perturbed parameters:

$$R \approx 1 + \varepsilon R_1, \quad w \approx \varepsilon W_1, \quad M \approx \hat{M}_0 + \varepsilon M_1, \quad (11.58)$$

with $\hat{M}_0 = M_0/M_s$ and the disturbed variables being:

$$R_1, W_1, M_1 \propto \exp(\overline{\omega}t + i\bar{k}z), \quad (11.59)$$

in which, $\overline{\omega}$ is the wavelength and k is the wave number with $i = \sqrt{-1}$.

The system of equations to be solved consider the momentum equation Eq. (11.57), the magnetization evolution Eq. (11.48), the jump condition Eq. (11.56) and the surface evolution Eq. (11.55). The later, after introduce perturbed variables provides the following expression:

$$\varepsilon \frac{\partial R_1}{\partial t} + \varepsilon \frac{\partial W_1}{\partial z} = 0, \quad (11.60)$$

and replacing perturbed proportions,

$$2\overline{\omega}R_1 + (i\bar{k})W_1 = 0. \quad (11.61)$$

We continue the linear analysis with the equation of the evolution of magnetization (11.56) by introducing the perturbed variables, provides:

$$\mathcal{T} \left(\varepsilon \frac{\partial M_1}{\partial t} + \varepsilon \frac{\partial W_1}{\partial z} \hat{M}_0 \right) = \chi - \varepsilon M_1 + \frac{\chi}{2} \left(\varepsilon \frac{\partial^2 M_1}{\partial z^2} + 2\varepsilon \frac{\partial^2 R_1}{\partial z^2} \hat{M}_0 \right). \quad (11.62)$$

Retaining terms of $\mathcal{O}(\varepsilon)$ and replacing perturbed proportions:

$$\mathcal{T}(\overline{\omega}M_1 + (i\bar{k})W_1\hat{M}_0) = \chi - M_1 + \frac{\chi}{2} \left((i\bar{k})^2 M_1 + 2(i\bar{k})^2 R_1 \hat{M}_0 \right). \quad (11.63)$$

Now , we continue with the momentum Eq. (11.57) by substituting perturbed variables. The left-hand side and first two terms of the right-hand side of Eq. (11.57) are treated as previous

Section (9.3). We continue with the magnetic terms developing them independently and substituting on the final expression. We develop the term $M\partial M/\partial z$, obtaining:

$$\frac{1}{2} \frac{\partial(\hat{M}_0 + \varepsilon M_1)^2}{\partial z} = \varepsilon(i\bar{k})\hat{M}_0 M_1, \quad (11.64)$$

and continue with the following magnetic term of Eq. (11.57). Once we got the perturbations for all magnetic terms, we present the momentum w -equation (11.57) keeping terms order ε , which takes the following form:

$$\begin{aligned} \overline{\omega} W_1 &= (i\bar{k})(1 - \bar{k}^2)R_1 + \frac{3}{Re}(i\bar{k})^2 W_1 \\ &+ C_{pm} \left(\left(-(i\bar{k})M_1 M_0 + \mathcal{T} \left[-M_0 \overline{\omega}(i\bar{k})M_1 + \frac{3}{2}M_0^2(i\bar{k})^2 W_1 - \frac{M_0^2(i\bar{k})^2 W_1}{2} + \frac{\mathcal{N}M_0^3(i\bar{k})M_1}{\chi} \right] \right) \right. \\ &\left. \left(\frac{1}{\chi} + \frac{(M_0^2 + 2M_1 M_0)\mathcal{N}\mathcal{T}}{\chi^2} \right) + \frac{1}{\chi} (\mathcal{T}\overline{\omega}(i\bar{k})M_1 M_0 + 2(i\bar{k})M_1 M_0) \right), \end{aligned} \quad (11.65)$$

then grouping terms with W_1 , R_1 and W_1 , taking the following form:

$$\begin{aligned} W_1 \left(\overline{\omega} + \frac{3}{Re}\bar{k}^2 + \frac{C_{pm}\mathcal{T}\hat{M}_0\bar{k}^2}{1 + \mathcal{N}\hat{M}_0\mathcal{T}} \right) &= (i\bar{k})(1 - \bar{k}^2)R_1 \\ &+ (i\bar{k})C_{pm} \left(-\frac{1}{1 + \mathcal{N}\hat{M}_0\mathcal{T}} - \frac{\overline{\omega}\mathcal{T}}{1 + \mathcal{N}\hat{M}_0\mathcal{T}} - \frac{\mathcal{N}\hat{M}_0\mathcal{T}}{1 + \mathcal{N}\hat{M}_0\mathcal{T}} + \overline{\omega}\mathcal{T} + 2 \right) M_1, \end{aligned} \quad (11.66)$$

leaving the equation in terms of W_1 by replacing R_1 through Eq. (11.61) and M_1 with Eq. (11.63), allowing us to obtain:

$$\begin{aligned} \overline{\omega} \left[\overline{\omega} + \left(\frac{3}{Re} + \frac{C_{pm}\mathcal{T}\hat{M}_0}{1 + \mathcal{N}\hat{M}_0\mathcal{T}} \right) \bar{k}^2 \right] &= \frac{\bar{k}^2}{2}(1 - \bar{k}^2) \\ &- \left(1 + \frac{\overline{\omega}\mathcal{N}\hat{M}_0\mathcal{T}^2}{1 + \mathcal{N}\hat{M}_0\mathcal{T}} \right) \frac{\hat{M}_0^3\bar{k}^4 C_{pm}}{(2(\mathcal{T}\overline{\omega} + 1)\hat{M}_0 + \hat{M}_0^2\bar{k}^2)}. \end{aligned} \quad (11.67)$$

This expression is the relation dispersion for the full magnetic problem in term of $\overline{\omega}$ and \bar{k} , and now the magnetic parameters C_{pm} , Re , \mathcal{T} , \mathcal{N} appear, bringing information about the magnetization mechanism influencing the fluid flow. In it the following can be observed: on the left-hand side, the second term corresponds to the viscous term and then follows the term that is compared with the viscous term, this term is a magneto viscous modification due to the presence of magnetization in this problem. On the right-hand side, initially we have the capillary term and later we have the magnetic term that contains in the denominator $\overline{\omega}$, the new magnetic mode that makes the dispersion relation a third degree algebraic equation.

As it has been throughout this study, we are going to continue taking some particular limits that allow us to recover the previously studied cases: the first of these cases is the case $C_{pm} = 0$, in which we do not have magnetic interaction, for this case the left-hand

side recovers the quadratic term $\overline{\omega}^2$ and the viscous term, then on the right-hand side only contains the capillary term, thus obtaining the eq. (9.59).

We are going to evaluate the superparamagnetic case, when $\mathcal{T} \rightarrow 0$. In that case: the third term on the left-hand side is canceled and then on the right hand side, we obtain the superparamagnetic contribution equals to Eq. (10.70).

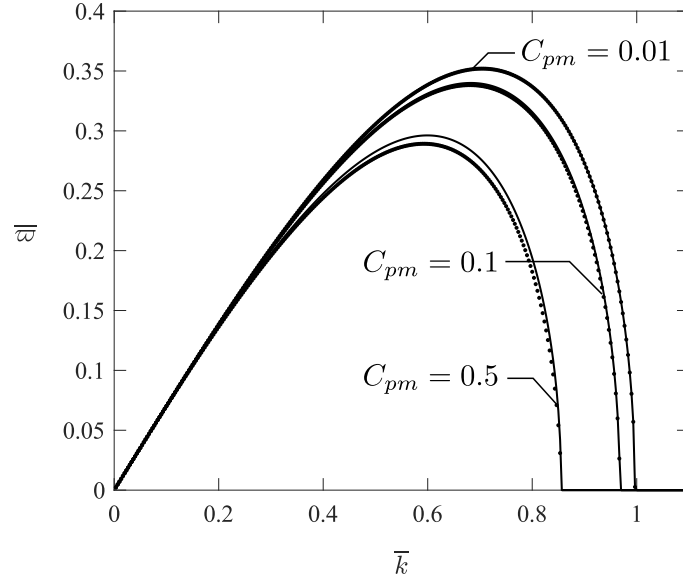


Figure 11.1: Figure shows the comparison between the cases $C_{pm} = 0.01, 0.1, 0.5$ with $\mathcal{T} = 0$ (solid-line) and $\mathcal{T} = 0.1$ (dotted-line), all using the value of $\mathcal{N} = 1$ and $Re \gg 1$.

In Fig. (11.1), three cases are shown using $C_{pm} = 0.01, 0.1, 0.5$ with $\mathcal{T} = 0, 0.1$. The solid-lines corresponds to the superparamagnetic case $\mathcal{T} = 0$ and the dotted-lines represents the cases in which there is a magnetic relaxation mechanism as a consequence of the interaction of the magnetization with the flow. Initially, low magnetic field (small C_{pm}), the magnetic relaxation effect is very small and instability is not affected, being similar to a superparamagnetic case. As we increase C_{pm} a more pronounced difference is observed on the growth rates. Surprisingly the relaxation mechanisms reduces the growth rate, up to 10% for $C_{pm} = 0.5$. It is not clear what is the physical mechanisms behind this stabilization of the flow, but we speculate that the enhanced magnetization of the fluid in the axial and radial directions could be behind a larger response of the fluid to the applied magnetic field.

In Fig. (11.2), we verified the influence of the magnetic parameter \mathcal{N} , which is related to the precessional term of the magnetic evolution equation (11.2), on the growth rates. We observed that as we increase \mathcal{N} growth rates increase. This indicates that the precessional term is dominating the dynamics of the magnetization, preventing it to adjust to the flow. In this case, the system behaves as if the fluid were superparamagnetic.

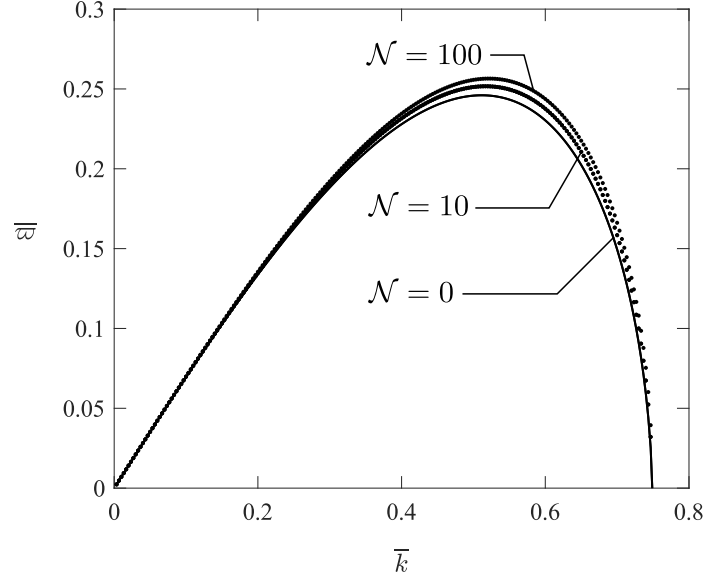


Figure 11.2: Figure shows the comparison between the cases $\mathcal{N} = 0$ (solid-line) and $\mathcal{N} = 10, 100$ (dotted-line), all using the value of $\mathcal{T} = 0.1$, $C_{pm} = 0.5$ and $Re \gg 1$.

There are still many parameters and cases to study in this model: the effect of the viscosity, via Re , has to be investigated in detail, as it will couple the flow field to the magnetization in different ways. Furthermore we still have to explore the nonlinear regimes in the full model and the asses the steady state shapes. This, among other are subject of our current studies.

CHAPTER 12

CONCLUSION AND FUTURE DIRECTIONS

In this part of thesis, we studied the Plateau-Rayleigh instability using the limit of long wavelengths for magnetic fluids. We have presented the set of equations that govern this problem and that are formed by: the continuity equation, the Navier-Stokes equations modified by the magnetic forces, the magnetization evolution equation proposed by Shliomis [52] and Maxwell's equations, in the presence of a uniform magnetic field applied in the axial direction.

Initially, the equations for the Plateau-Rayleigh instability were derived for the asymptotic limit of long waves, for both inviscid and viscous non-magnetic fluids, and the classical results of the problem were recovered. Thereafter, the super-paramagnetic problem was considered for both the inviscid and viscous cases. We have compared the inviscid problem with [33] and viscous problem with [66]. At the same time, we have obtained a simple numerical routine for the non-linear dynamics of drop breakup, following [69] and [66]. This work has contributed by adding information about the magnetic permeability of the exterior fluid to the cylinder. The results show that considering a magnetically permeable outer fluid is a small correction of the impermeable case, however, this small correction makes the system more unstable. From the analysis performed in this work, we found that the viscosity delays the cylinder breakup time, but the magnetism prevents completely the breakup of the cylinder if a magnetic field with an intensity sufficiently large is applied.

In addition, we consider a magnetic evolution equation proposed by Shliomis [52] where the torques are incorporated with the precessional term. Then this equation with the

modified Navier-Stokes equation, the continuity equation and Maxwell's equations are used to derive an asymptotic approximation for long waves. The linear stability analysis provides a third degree algebraic equation for the dispersion relation, where the additional degree brings information on the new magnetic mode. From our preliminary observations, the theory presented here seems to be a small correction of the super-paramagnetic case when the magnetic relaxation time is very small.

In future works, we plan to obtain the self-similar solution of the non-linear regimes. Furthermore, we intend to explore this problem for magnetorheological fluids which present and average magnetic particle diameter of order of micrometers, and which allows us to study the system for longer magnetic relaxation times.

BIBLIOGRAPHY

- [1] Acheson D.J., Elementary fluid dynamics. *Oxford: Clarendon Press.* (1990).
- [2] Abramowitz M. and Stegun I.A., Handbook of Mathematical function with formulas, graphs, and mathematical tables. *National bureau of standards applied mathematics series 55: tenth printing.* (1972).
- [3] Rutherford A., Vectors, Tensors and the Basic Equations of Fluid Mechanics. *Dover Books on Mathematics: Courier Corporation.* (2012).
- [4] Batchelor C.K., Batchelor G.K., An Introduction to Fluid Dynamics. *Cambridge University Press.* (2000).
- [5] Brown W.F., Electric and Magnetic Forces: A Direct Calculation. I *American Journal of Physics.* **19(5)**, (1951), 290–304.
- [6] Cunha F.R., Fundamentals of Magnetic Fluid Hydrodynamics. *Turbulence (Book Chapter), Poli-USP-ABCM.* (2012)
- [7] Drazin P.G. and Reid W.H., Hydrodynamic Stability. *Cambridge University Press.* (1981), 63–88.
- [8] Betchov R. and Criminale W.O., Stability of Parallel Flows. *Academic Press.* (1967), 74–96.
- [9] Chandrashekar S., Hydrodynamic and Hydromagnetic Stability. *Oxford University Press.* (1961).
- [10] Cowley M.D. and Rosensweig R.E., The Interfacial Stability of a Ferromagnetic Fluid, *Journal of Fluid Mechanics.* **30: 4**, (1967), 671–688.

- [11] Chen T.S. and Eaton T.E., Magneto-hydrodynamic Stability of the Developing Laminar Flow in a Parallel-Plate Channel, *Physics of Fluids*. **15:4**, (1972), 592–596.
- [12] Cunha F.R. and Sobral Y.D., Characterization of the Physical parameters in a Process of Magnetic Separation and Pressure-Driven Flow of a Magnetic Fluid. *Physica A*. **343**, (2004), 36–64.
- [13] Altmeyer S., Do Y., Lai Y.C. Transition to Turbulence in Taylor-Couette Ferrofluidic Flow, *Scientific Reports*. **5**, 10781, (2015).
- [14] Dang A., Ooi L., Fales J. and Stroeve P., Yield Stress Measurements of Magnetorheological Fluids in Tubes, *Industrial and Engineering Chemistry Research*. **39(7)**, (2000), 2269-2274.
- [15] Orzag S.A., Accurate Solution of the Orr-Sommerfeld Stability Equation. *Journal of Fluid Mechanics*. **50(4)**, (1971), 689–703.
- [16] Maxwell J.C., A Dynamical Theory of the Electromagnetic Field. *Philosophical Transactions of the Royal Society*. (1865).
- [17] Lübbe A.S., Alexiou C. and Bergemann C., Clinical Applications of Magnetic Drug Targeting. *The Journal Surgical Research*. **95(2)**, (2001), 200–206.
- [18] Grant I.S. and Phillips W.R., Electromagnetism. *John Wiley & Sons*. (2013).
- [19] Alexiou Ch., Schmid R., Jurgons R., Bergemann Ch., Arnold W. and Parak F.G., Targeted Tumor Therapy with "Magnetic Drug Targeting": Therapeutic Efficacy of Ferrofluid Bound Mitoxantrone. *Ferrofluids*. **594**, (2002).
- [20] Jordan A. et al, Presentation of a New Magnetic Field Therapy System for the Treatment of Human Solid Tumors With Magnetic Fluid Hyperthermia. *Journal of Magnetism and Magnetic Materials*. **225**, (2001), 118–126.
- [21] Jansons K., Determination of the Constitutive Equations for a Magnetic Fluid. *Journal of Fluid Mechanics*. **137**, (1983), 187–216.
- [22] Brusentsov N.A., Nikitin L.V., Brusentsova T.N., Kuznetsov A.A., Bayburtskiy F.S., Shumakov L.I. and Jurchenko N.Y., Magnetic fluid Hyperthermia of the Mouse Experimental Tumor. *Journal of Magnetism and Magnetic Materials*. **252**, (2002), 378–380.
- [23] Rümenapp Ch., Gleich B. and Haase A., Magnetic Nanoparticles in Magnetic Resonance Imaging and Diagnostics. *Pharmaceutical research*. **252**, (2012), 1165–1179.
- [24] Pankhurst Q., Jones S. and Dobson J., Applications of Magnetic Nanoparticles in Biomedicine: the story so far. *Journal of Physics D: Applied Physics*. **49**, (2016).

- [25] Schimid P. and Henningson D.S., Stability and Transition in Shear Flows. *Springer-Verlag*. (2001), 15–149.
- [26] Thomas L.H, The Stability of Plane Poiseuille Flows. *American Physical Society* **91:4**, (1953), 780–783.
- [27] Lidström P. Moving Regions in Euclidean Space and Reynolds’s Transport Theorem. *Mathematics and Mechanics of Solids*. **16(4)**, (2011), 366–380.
- [28] Lin C.C., The Theory of Hydrodynamic Stability. *Cambridge University Press*. (1955).
- [29] Fjørtoft R. *Geofysiske Publikasjoner*. **17:1**, (1950).
- [30] Odenbach S. Ferrofluids: Magnetically controllable fluids and their applications. *Springer-Verlag*. (2002).
- [31] Pereira I.D.O. Rheology of ferrofluids in shear flows. *MSc. dissertation, Universidade de Brasília*. November (2019).
- [32] Papell S.S. Low viscosity magnetic fluid obtained by the colloidal suspension of magnetic particles, US Patent number 3215572. *United States Patent Office*. October 9th (1963).
- [33] Rosensweig R.S., Ferrohydrodynamics. *Dover Publications Inc*. (1997), 76–79.
- [34] Schumacher K.R., Sellien I., Knoke G.S., Cader T., Finlayson B.A., Experiment and simulation of laminar and turbulent ferrofluid pipe flow in an oscillating magnetic field, *Physical Review E*. **67**, 026308, (2003).
- [35] Hart J.E. Ferromagnetic Rotating Couette flow: The Role of Magnetic Viscosity., *Journal of Fluid Mechanics*. **453**, (2002), 21–38.
- [36] Rinaldi C., Chaves A., Elborai S., He X., Zahn M. Magnetic fluid rheology and flows. *Current Opinion in Colloid & Interface Science*. **10**, 3-4, (2005), 141–157.
- [37] Trefethen L.N., Spectral Methods in MATLAB. *Society for Industrial Mathematics*. **10**, (2000).
- [38] Gottlieb D. and Orszag S.A., Numerical Analysis of Spectral Methods: Theory and Applications. *Society for Industrial and Applied Mathematics*. (1977), 144–145.
- [39] Ng B.S. and Reid W.H., On the Numerical Solution of the Orr-Sommerfeld Problem: Asymptotic Initial Condition for Shooting Methods. *Journal of Computational Physics*. **3**, (1979), 275–292.

- [40] Gersting J.M., Numerical Methods for Eigensystems: The Orr-Sommerfeld Problem as an Initial Value Problem. *Computers & Mathematics with Applications*. **6**, (1980), 167–174.
- [41] Helmholtz H., On Discontinuous Movements of Fluids. *Philosophical Magazine*. Series 4, **36**, (1868), 337–346.
- [42] Lord Kelvin (Thomson W.), Hydrokinetic solutions and observations. *Philosophical Magazine*. **42**, (1871), 362–377.
- [43] Luz G.M. and Cunha F.R., Flow of a non-symmetrical magnetic fluid between parallel plates. *Undergraduate final project, Universidade de Brasília*. (2018). Available online at: https://bdm.unb.br/bitstream/10483/24265/1/2018_GuilhermeDeMendoncaLuz_tcc.pdf
- [44] Korlie M. S., Mukherjee A., Nita B. G., Stevens J. G., Trubatch A. D. and Yecko P., Analysis of Flows of Ferrofluids Under Simple Shear. *Magnetohydrodynamics*. (2008).
- [45] Mukherjee, A., Vaidya, A. and Yecko, P., Laminar Shear in a Ferrofluid: Stability Studies. *Magnetohydrodynamics*. **49**, (2013), 505–511.
- [46] Yecko P. Stability of Layered Channel Flow of Magnetic Fluids. *Physics of Fluids*. **21**, 034102, 2009.
- [47] Lord Rayleigh (Strutt J.W.), On the Stability, or Instability, of Certain Fluid Motions. *Proceedings of the London Mathematical Society*. **11**, (1880), 57–70.
- [48] Lord Rayleigh (Strutt J.W.), On the Instability of a Cylinder of Viscous Liquid under Capillary Force. *Philosophical Magazine*. **34**, (1892), 145–154.
- [49] Reynolds O., An Experimental Investigation of the Circumstances which Determine whether the Motion of Water Shall be Direct or Sinuous, and of the Law of Resistance in Parallel Channels. *Philosophical Transactions of the Royal Society*. **174**, (1883), 935–982.
- [50] Orr W. M’F., The Stability or Instability of the Steady Motions of a Liquid. Part I. *Proceedings of the Royal Irish Academy*. A, **27**, (1907), 9–68.
- [51] Orr, W. M’F., The Stability or Instability of the Steady Motions of a Liquid. Part II. *Proceedings of the Royal Irish Academy*. A, **27**, (1907), 69–138.
- [52] Shliomis, M. I., Ferrohydrodynamics: Retrospective and Issues. *Ferrofluids: Magnetically Controllable Fluids and Their Applications*. Ed. Odenbach, Stefan: Springer Berlin Heidelberg. (2002), 85–111.

- [53] Sommerfeld A., Ein Beitrag zur hydrodynamische Erklärung der turbulenten Flüssigkeitsbewegungen. *Proceedings of the 4th International Congress of Mathematicians. III. Rome* (1908), 116–124.
- [54] Stiles P.J. and Blennerhassett P.J. Stability of cylindrical Couette Flow of a Radially Magnetized Ferrofluids in a Radial Temperature Gradient. *Journal of Magnetism and Magnetic Materials*. **122**, (1993), 207–209.
- [55] Heisenberg W., On Stability and Turbulence of Fluid Flows. *Translation from Annalen der Physik*. **74:15**, (1924), 577–627.
- [56] Tollmien W., Über die Entstehung der Turbulenz. 1. Mitteilung. *Nachrichten von der Gesellschaft der Wissenschaften zu Göttingen, Mathematisch-Physikalische Klasse*. (1929), 21–44.
- [57] Tollmien W., Asymptotische Integration der Störungsdifferentialgleichung ebener laminarer Strömungen bei hohen Reynoldsschen Zahlen. *Zeitschrift für Angewandte Mathematik und Mechanik*. **25/27**, (1947), 33–50, 70–83.
- [58] Lin C.C., On the Stability of Two-Dimensional Parallel Flows. Parts I-II-III. *Quarterly of Applied Mathematics*. **3**, 1945-46: 117–142, 218–234, 277–301.
- [59] Cunha F.R. and Couto H., A New Boundary Integral Formulation to Describe Three-Dimensional Motions of Interfaces Between Magnetic Fluids. *Applied Mathematics and Computation*. **199:1**, (2008), 70–83.
- [60] Vislovich A.N., Sinitsyn A.K., Tymanovich V.V., Instability of Plane-Parallel Couette Flow of a Magnetic Liquid in a Homogeneous Magnetic Field. *Magnitnaya Gidrodinamika*. **2**, (1984), 32–37.
- [61] Eggers J. and Villermaux E., Physics of Liquids Jets. *Reports on Progress in Physics*. **71**, 036601.
- [62] Zahn M. and Pioch L., Ferrofluid Flows in AC and Traveling Wave Magnetic Fields with Effective Positive, Zero or Negative Dynamic Viscosity. *Journal of Magnetism and Magnetic Materials*. **201:1**, (1999), 144–148.
- [63] Plateau J., Statique Expérimentale et Théorique des Liquides Soumis aux Seules Forces Moléculaires [Experimental and Theoretical Statics of Liquids Subject to Only Molecular Forces] (in French). *Paris, France: Gauthier-Villars*. **2**, (1873), 261.
- [64] Eggers J. and Dupont T. F., Drop Formation in a One-Dimensional Approximation of the Navier-Stokes equation. *Journal in Fluid Mechanics*. **262**, (1994), 205–221.

- [65] Balmforth N. J., Dubash N. and Slim A. C., Extensional Dynamics of Viscoplastic Filaments: I. Long-wave Approximation and the Rayleigh instability. *Journal of Non-Newtonian Fluid Mechanics*. **165**, (2010), 1139-1146.
- [66] Entov V. M., Barsoum M. and Shmarrayan L. E., On Capillary Instability of Jets of Magneto-Rheological Fluids. *Journal of Rheology*. **40:727**, (1996).
- [67] Do Carmo M. P., Differential Geometry of Curves and Surfaces. Revised and Updated Second Edition. *Courier Dover Publications*. (2016).
- [68] Hirsch M.W., Smale S. and Devaney R.L., Differential Equation, Dynamical Systems, and An Introduction to Chaos. *Elsevier Academic Press*. (2004).
- [69] Furlani E.P. and Hanchak M.S. Nonlinear Analysis of the Deformation and Breakup of the Viscous Microjets using the Method of Lines. *International Journal for Numerical Methods in Fluids*. **65**, (2011), 563-577.
- [70] Ashgriz N. and Mashayek F. Temporal Analysis of Capillary Jet Breakup. *Journal of Fluid Mechanics*. **291**, 163 (1995).
- [71] Rosa A.P. Microstructure and Magnetorheology of Ferrofluids in Shear: Theory and Simulation. *PhD thesis, Universidade de Brasília*. July (2018). Available online at: https://repositorio.unb.br/bitstream/10482/33751/1/2018_AdrianoPossebonRosa.pdf
- [72] Surajit S. Nanoprinting with Nanoparticles: Concept of a Novel Inkjet Printer with Possible Applications in Invisible Tagging of Objects. *Journal of Dispersion Science and Technology*. **25:4**, (2005), 523–528.
- [73] Basaran O. A. Small-Scale Free Surface Flows with Breakup: Drop Formation and Emerging Applications. *AIChE Journal*. **48(9)**, (2002), 1842–1848.
- [74] Utada A.S., Chu L.Y., Fernandez-Nieves A., Link D.R., Holtze C. and Weitz D.A. Dripping, Jetting, Drops, and Wetting: The Magic of Microfluidics. *Materials Research Society Bulletin*. **32**, (2007), 702-708.
- [75] Kaminski T.S., Scheler O., Garstecki P. Droplet Microfluidics for Microbiology: Techniques, Applications and Challenges. *Lab on a Chip*. **16(12)**, (2016), 2168–2187.
- [76] Goedde E. and Yuen M. Experiments on Liquid Jet Instability. *Journal of Fluid Mechanics*. **40(3)**, (1970), 495–511.

APPENDIX

APPENDIX A

In this appendix, we present the details to find an expression for the perturbation of the modified Navier-Stokes equations containing the Kelvin force and for the Magnetization evolution equation.

I.1 Perturbation of modified the Navier-Stokes equation

Let's consider the system of equations formed by the Eq. (6.56)-(6.57) together with the disturbed continuity equation (6.60) and the disturbed version of the Maxwell's equations in (6.61). We then continue with the same procedure done with the pure hydrodynamic stability section (5.2) to find the fundamental stability equation that governs this case.

The system formed by Eqs. (6.56)-(6.57) with the perturbed variables (6.51) is written in vector form:

$$\begin{aligned} \frac{\partial \mathbf{u}'}{\partial t} + \mathbf{u}^b \cdot \nabla \mathbf{u}' + \mathbf{u}' \cdot \nabla \mathbf{u}^b = & -\nabla p' + \frac{1}{Re} \nabla^2 \mathbf{u}' \\ & + C_{pm} (\mathbf{M} \cdot \nabla \mathbf{H}' + \mathbf{M}' \cdot \nabla \mathbf{H}), \end{aligned} \quad (1)$$

and the perturbed continuity equation Eq. (6.60) is rewritten here:

$$\frac{\partial u'}{\partial x} + \frac{\partial v'}{\partial y} = 0, \quad (2)$$

with the corresponding perturbed Maxwell's equations (6.61), that we write again,

$$\frac{\partial H'_2}{\partial x} - \frac{\partial H'_1}{\partial y} = 0, \quad (3)$$

$$\frac{\partial B'_1}{\partial x} + \frac{\partial B'_2}{\partial y} = 0, \quad \text{with } \mathbf{B}' = \mathbf{H}' + \mathbf{M}'. \quad (4)$$

Taking the divergence of Eq. (1) in \mathbf{u}' ,

$$\frac{\partial \nabla \cdot \mathbf{u}'}{\partial t} + \nabla \cdot [\mathbf{u}^b \cdot \nabla \mathbf{u}' + \mathbf{u}' \cdot \nabla \mathbf{u}^b] = -\nabla^2 p' + \frac{1}{Re} \nabla^2 \nabla \cdot \mathbf{u}' + \quad (5)$$

$$+ C_{pm} \nabla \cdot (\mathbf{M} \cdot \nabla \mathbf{H}' + \mathbf{M}' \cdot \nabla \mathbf{H}). \quad (6)$$

Second term on the left side can be written as,

$$\nabla \cdot [\mathbf{u}^b \cdot \nabla \mathbf{u}' + \mathbf{u}' \cdot \nabla \mathbf{u}^b] = 2 \frac{du^b}{dy} \frac{\partial v'}{\partial x}.$$

From Eq. (2), the Laplacian of pressure in Eq. (5) can be expressed by:

$$\nabla^2 p' = -2 \frac{du^b}{dy} \frac{\partial v'}{\partial x} + C_{pm} \nabla \cdot (\mathbf{M} \cdot \nabla \mathbf{H}' + \mathbf{M}' \cdot \nabla \mathbf{H}). \quad (7)$$

Now taking, the Laplacian of the component in direction y of Eq. (1),

$$\frac{\partial \nabla^2 v'}{\partial t} + \nabla^2 \left(u^b \frac{\partial v'}{\partial x} \right) = -\frac{\partial \nabla^2 p'}{\partial y} + \frac{1}{Re} \nabla^4 v' \quad (8)$$

$$+ C_{pm} \nabla^2 \left(M_1 \frac{\partial H'_2}{\partial x} + M_2 \frac{\partial H'_2}{\partial y} + M'_1 \frac{\partial H_2}{\partial x} + M'_2 \frac{\partial H_2}{\partial y} \right). \quad (9)$$

Substituting Eq. (7) in Eq. (8), we get:

$$\begin{aligned} \frac{\partial \nabla^2 v'}{\partial t} + \nabla^2 \left(u^b \frac{\partial v'}{\partial x} \right) &= -\frac{\partial}{\partial y} \left[-2 \frac{du^b}{dy} \frac{\partial v'}{\partial x} + C_{pm} \nabla \cdot (\mathbf{M} \cdot \nabla \mathbf{H}' + \mathbf{M}' \cdot \nabla \mathbf{H}) \right] \\ &+ \frac{1}{Re} \nabla^4 v' + C_{pm} \nabla^2 \left(M_1 \frac{\partial H'_2}{\partial x} + M_2 \frac{\partial H'_2}{\partial y} + M'_1 \frac{\partial H_2}{\partial x} + M'_2 \frac{\partial H_2}{\partial y} \right). \end{aligned} \quad (10)$$

Developing the Laplacian in the left hand side and the expression with derivative with respect to y in the right hand side,

$$\begin{aligned} \left(\frac{\partial}{\partial t} + u^b \frac{\partial}{\partial x} \right) \nabla^2 v' - \frac{d^2 u^b}{dy^2} \frac{\partial v'}{\partial x} - \frac{1}{Re} \nabla^4 v' &= -\frac{\partial}{\partial y} [C_{pm} \nabla \cdot (\mathbf{M} \cdot \nabla \mathbf{H}' + \mathbf{M}' \cdot \nabla \mathbf{H})] \\ &+ C_{pm} \nabla^2 \left(M_1 \frac{\partial H'_2}{\partial x} + M_2 \frac{\partial H'_2}{\partial y} + M'_1 \frac{\partial H_2}{\partial x} + M'_2 \frac{\partial H_2}{\partial y} \right). \end{aligned} \quad (11)$$

The left-hand side, by putting $C_{pm} = 0$ is the Orr-Sommerfeld classical equation. Now the expressions on right-hand side of the equation above are developed, using the sub-index that indicates the partial derivative with respect to the variable.

$$\begin{aligned} - \left(\left(\frac{\partial}{\partial t} + u^b \frac{\partial}{\partial x} \right) \nabla^2 v' - \frac{d^2 u^b}{dy^2} \frac{\partial v'}{\partial x} - \frac{1}{Re} \nabla^4 v' \right) &= \frac{\partial}{\partial y} [C_{pm} \nabla \cdot (\mathbf{M} \cdot \nabla \mathbf{H}' + \mathbf{M}' \cdot \nabla \mathbf{H})] \\ &- C_{pm} \nabla^2 \left(M_1 \frac{\partial H'_2}{\partial x} + M_2 \frac{\partial H'_2}{\partial y} + M'_1 \frac{\partial H_2}{\partial x} + M'_2 \frac{\partial H_2}{\partial y} \right). \end{aligned} \quad (12)$$

On the left side, we have the Orr-Sommerfeld Operator, which for C_{pm} takes us to the already known case. In this way, we can write the above expression as:

$$\begin{aligned}\mathcal{L}_{OS}\hat{v} &= C_{pm} \frac{\partial}{\partial y} [\nabla \cdot (\mathbf{M} \cdot \nabla \mathbf{H}' + \mathbf{M}' \cdot \nabla \mathbf{H})] \\ &\quad - C_{pm} \nabla^2 \left(M_1 \frac{\partial H'_2}{\partial x} + M_2 \frac{\partial H'_2}{\partial y} + M'_1 \frac{\partial H_2}{\partial x} + M'_2 \frac{\partial H_2}{\partial y} \right).\end{aligned}\quad (13)$$

In order to make algebraic manipulations on the RHS of Eq. (13), we consider a vector \mathbf{X} with components $\mathbf{X} = (X_1, X_2)$, that simulates RHS above, then we obtain,

$$\frac{\partial}{\partial y} (\nabla \cdot \mathbf{X}) - \nabla^2 X_2 = \frac{\partial}{\partial x} \left(\frac{\partial X_1}{\partial y} - \frac{\partial X_2}{\partial x} \right), \quad (14)$$

and applying this simplification to Eq. (13) with $\mathbf{X} = (\mathbf{M} \cdot \nabla \mathbf{H}' + \mathbf{M}' \cdot \nabla \mathbf{H})$, allows us to access the following expression,

$$\mathcal{L}_{OS}\hat{v} = C_{pm} \frac{\partial}{\partial x} \left(\frac{\partial ((\mathbf{M} \cdot \nabla) H'_1 + (\mathbf{M}' \cdot \nabla) H_1)}{\partial y} - \frac{\partial ((\mathbf{M} \cdot \nabla) H'_2 + (\mathbf{M}' \cdot \nabla) H_2)}{\partial x} \right). \quad (15)$$

The expression above is the stability analysis equation for the case of magnetic fluid, note that by taking $C_{pm} = 0$, we obtain the typical Orr-Sommerfeld equation. Using the magnetic field (6.31), we have H_1 being a constant and $H_2 = H_2(y)$ in order to satisfy the Maxwell's equations. On the other hand, we remark that M_1 and M_2 functions depend on the y variable, what incorporate additional simplifications to (15), as follows:

$$\mathcal{L}_{OS}\hat{v} = C_{pm} \frac{\partial}{\partial x} \left(\frac{\partial M_1^b}{\partial y} \frac{\partial H'_1}{\partial x} + \frac{\partial M_2^b}{\partial y} \frac{\partial H'_1}{\partial y} - \frac{\partial H_2^b}{\partial y} \frac{\partial M'_2}{\partial x} \right), \quad (16)$$

then additional simplifications come from Eqs (6.65) together with (6.46) and substituting the (6.63), allowing us to get Eq.(6.64).

I.2 Perturbation of the magnetization evolution equation

Let's consider the perturbed quantities of the magnetization evolution equation given by (6.58)-(6.59) which we rewrite here in vector form:

$$\frac{\partial \mathbf{M}'}{\partial t} + \mathbf{u}^b \cdot \nabla \mathbf{M}' + \mathbf{M}' \cdot \nabla \mathbf{u}^b = \frac{(\chi_0 \mathbf{H}' - \mathbf{M}')}{\tau^*} + \frac{1}{2} (\boldsymbol{\Omega}' \times \mathbf{M} + \boldsymbol{\Omega} \times \mathbf{M}'), \quad (17)$$

where the approximation (6.45) is taken for the equilibrium magnetization \mathbf{M}_0 .

The equation in the x -direction is given by:

$$\begin{aligned}\frac{\partial M'_1}{\partial t} + u^b \frac{\partial M'_1}{\partial x} + v' \frac{dM_1^b}{dy} &= \frac{(\chi_0 H'_1 - M'_1)}{\tau^*} \\ &\quad + \frac{1}{2} \left(-\frac{\partial v'}{\partial x} M_2^b + \frac{\partial u'}{\partial y} M_2^b + \frac{du^b}{dy} M'_2 \right).\end{aligned}\quad (18)$$

The equation in the y -direction is given by:

$$\begin{aligned} \frac{\partial M'_2}{\partial t} + u^b \frac{\partial M'_2}{\partial x} + v' \frac{dM_2^b}{dy} &= \frac{(\chi_0 H'_2 - M'_2)}{\tau^*} \\ &+ \frac{1}{2} \left(\frac{\partial v'}{\partial x} M_1^b - \frac{\partial u'}{\partial y} M_1^b - \frac{du^b}{dy} M_1' \right). \end{aligned} \quad (19)$$

Replacing the ansatz (6.63), provides for the x -direction,

$$\begin{aligned} -i\alpha c \tilde{M}_1 + i\alpha u^b \tilde{M}_1 + \tilde{v} \frac{dM_1^b}{dy} &= \frac{(\chi_0 \tilde{H}_1 - \tilde{M}_1)}{\tau^*} \\ &+ \frac{1}{2} \left(-i\alpha \tilde{v} M_2^b + D \tilde{u} M_2^b + \frac{du^b}{dy} \tilde{M}_2 \right), \end{aligned} \quad (20)$$

and in the y -direction,

$$\begin{aligned} -i\alpha c \tilde{M}_2 + i\alpha u^b \tilde{M}_2 + \tilde{v} \frac{dM_2^b}{dy} &= \frac{(\chi_0 \tilde{H}_2 - \tilde{M}_2)}{\tau^*} \\ &+ \frac{1}{2} \left(i\alpha \tilde{v} M_1^b - D \tilde{u} M_1^b - \frac{du^b}{dy} \tilde{M}_1 \right). \end{aligned} \quad (21)$$

By multiplying $i\alpha$ both expressions and introducing Eq. (6.60), we get:

$$\begin{aligned} -(i\alpha)^2 c \tilde{M}_1 + (i\alpha)^2 u^b \tilde{M}_1 + i\alpha \tilde{v} \frac{dM_1^b}{dy} &= \frac{i\alpha(\chi_0 \tilde{H}_1 - \tilde{M}_1)}{\tau^*} \\ &+ \frac{1}{2} \left(-(i\alpha)^2 \tilde{v} M_2^b - D^2 \tilde{v} M_2^b + i\alpha \frac{du^b}{dy} \tilde{M}_2 \right), \end{aligned} \quad (22)$$

whit the same procedure in y -direction,

$$\begin{aligned} -(i\alpha)^2 c \tilde{M}_2 + (i\alpha)^2 u^b \tilde{M}_2 + i\alpha \tilde{v} \frac{dM_2^b}{dy} &= \frac{i\alpha(\chi_0 \tilde{H}_2 - \tilde{M}_2)}{\tau^*} \\ &+ \frac{1}{2} \left((i\alpha)^2 \tilde{v} M_1^b + D^2 \tilde{v} M_1^b - i\alpha \frac{du^b}{dy} \tilde{M}_1 \right). \end{aligned} \quad (23)$$

Putting similar terms together:

$$\begin{aligned} -\alpha^2 (u^b - c) \tilde{M}_1 + i\alpha \tilde{v} \frac{dM_1^b}{dy} &= \frac{i\alpha(\chi_0 \tilde{H}_1 - \tilde{M}_1)}{\tau^*} \\ &+ \frac{1}{2} \left(\alpha^2 \tilde{v} M_2^b - D^2 \tilde{v} M_2^b + i\alpha \frac{du^b}{dy} \tilde{M}_2 \right). \end{aligned} \quad (24)$$

Doing the same with component y ,

$$\begin{aligned} -\alpha^2 (u^b - c) \tilde{M}_2 + i\alpha \tilde{u}_2 \frac{dM_2^b}{dy} &= \frac{i\alpha(\chi_0 \tilde{H}_2 - \tilde{M}_2)}{\tau^*} \\ &+ \frac{1}{2} \left(-\alpha^2 \tilde{u}_2 M_1^b + D^2 \tilde{u}_2 M_1^b - i\alpha \frac{du^b}{dy} \tilde{M}_1 \right). \end{aligned} \quad (25)$$

In order to close the system (17), we assume that Eqs (6.65) is satisfying (6.61) and leave the system (24)-(25) in terms of \tilde{M}_1 , \tilde{M}_2 and \tilde{v} which is possible to access through Eq. (15) and u^b and its derivative, which are known.

APPENDIX B

II.3 Young Laplace mean curvature

The expression for the mean curvature κ is given by:

$$\kappa = \nabla \cdot \mathbf{n},$$

where \mathbf{n} is the unitary normal vector to the free surface $r = R(z, t)$. In order to calculate the expression for mean curvature, we consider a function $F(r, z, t) = r - R(z, t)$ and note that the normal vector is given by $\mathbf{n} = \nabla F / |\nabla F|$. The nabla operator ∇ must be expressed in cylindrical coordinates, then ∇F is given by:

$$\nabla F = \left(\frac{\partial F}{\partial r}, \frac{1}{r} \frac{\partial F}{\partial \theta}, \frac{\partial F}{\partial z} \right),$$

then considering the function $F(r, z, t)$, last expression provides:

$$\nabla F = \left(1, 0, -\frac{\partial R}{\partial z} \right),$$

which allows us to express the normal vector as,

$$\mathbf{n} = \left(1, 0, -\frac{\partial R}{\partial z} \right) / \sqrt{1 + \left(\frac{\partial R}{\partial z} \right)^2}.$$

With the normal vector expression, we calculate the mean curvature by using $\nabla \cdot \mathbf{n}$ and again we remark that the nabla dot product is compute using cylindrical coordinates, that is,

$$\nabla \cdot \mathbf{n} = \frac{1}{r} \frac{\partial(rn_r)}{\partial r} + \frac{1}{r} \frac{\partial n_\theta}{\partial \theta} + \frac{\partial n_z}{\partial z}.$$

where $\mathbf{n} = (n_r, n_\theta, n_z)$. Finally, substituting the normal vector expression we get,

$$\nabla \cdot \mathbf{n} = \frac{1}{R} \left(1 + \left(\frac{\partial R}{\partial z} \right)^2 \right)^{-\frac{1}{2}} - \frac{\partial^2 R}{\partial z^2} \left(1 + \left(\frac{\partial R}{\partial z} \right)^2 \right)^{-\frac{3}{2}},$$

where the first term on the right hand side is radii of curvature R_1 and the second term is R_2 , which leads to write this last expression as $\nabla \cdot \mathbf{n} = R_1^{-1} + R_2^{-1}$.

II.4 Normal stress balance

In this section we verify the the following affirmation

$$\mathbf{n}^t \cdot \Sigma_{HM}^{\text{In}} \cdot \mathbf{n} = \mathcal{O}(\epsilon^2).$$

For this we must compute,

$$\mathbf{n}^t \cdot \Sigma_{HM}^{\text{In}} \cdot \mathbf{n} = \left(1, 0, -\epsilon \frac{\partial R}{\partial z} \right) \cdot \Sigma_{HM} \cdot \left(1, 0, -\epsilon \frac{\partial R}{\partial z} \right)^t$$

where $\mathbf{n} = \left(1, 0, -\epsilon \frac{\partial R}{\partial z} \right)$ is the scaled unitary normal vector and Σ_{HM}^{In} is the stress tensor considering the diadic product between \mathbf{H} and \mathbf{M}

$$\begin{aligned} \mathbf{n}^t \cdot \Sigma_{HM}^{\text{In}} \cdot \mathbf{n} &= \left(\epsilon^2 H_r M_r - \epsilon^2 \frac{\partial R}{\partial z} (1 + H_z) M_r, 0, \epsilon H_r M_z - \epsilon \frac{\partial R}{\partial z} (1 + H_z) M_z \right) \cdot \mathbf{n}, \\ &= \epsilon^2 H_r M_r - \epsilon^2 \frac{\partial R}{\partial z} (1 + H_z) M_r - \epsilon \frac{\partial R}{\partial z} \left(\epsilon H_r M_z - \epsilon \frac{\partial R}{\partial z} (1 + H_z) M_z \right), \\ &= \epsilon^2 \left(H_r M_r - (1 + H_z) M_r \frac{\partial R}{\partial z} - H_r M_z \frac{\partial R}{\partial z} - (1 + H_z) M_z \left(\frac{\partial R}{\partial z} \right)^2 \right), \end{aligned}$$

which confirms our statement.

II.5 Tangential stress balance

In this section we verify the the following affirmation

$$\mathbf{t}^t \cdot \Sigma_{HM}^{\text{In}} \cdot \mathbf{n} = \mathcal{O}(\epsilon).$$

For this we must compute,

$$\mathbf{t}^t \cdot \Sigma_{HM}^{\text{In}} \cdot \mathbf{n} = \left(\epsilon \frac{\partial R}{\partial z}, 0, 1 \right) \cdot \Sigma_{HM} \cdot \left(1, 0, -\epsilon \frac{\partial R}{\partial z} \right)^t$$

where $\mathbf{t} = \left(\epsilon \frac{\partial R}{\partial z}, 0, 1 \right)$ is the scaled unitary tangential vector, \mathbf{n} as above and Σ_{HM}^{In} is the stress tensor considering the diadic product between \mathbf{H} and \mathbf{M}

$$\begin{aligned}
\mathbf{t}^t \cdot \Sigma_{HM}^{\text{In}} \cdot \mathbf{n} &= \left(\epsilon^3 H_r M_r \frac{\partial R}{\partial z} + \epsilon(1 + H_z) M_r, 0, \epsilon^2 H_r M_z \frac{\partial R}{\partial z} + (1 + H_z) M_z \right) \cdot \mathbf{n}, \\
&= \epsilon^3 H_r M_r \frac{\partial R}{\partial z} + \epsilon(1 + H_z) M_r - \epsilon \frac{\partial R}{\partial z} \left(\epsilon^2 H_r M_z \frac{\partial R}{\partial z} + (1 + H_z) M_z \right), \\
&= \epsilon^3 H_r M_r \frac{\partial R}{\partial z} - \epsilon(1 + H_z) M_r - \epsilon^3 H_r M_z \left(\frac{\partial R}{\partial z} \right)^2 - \epsilon(1 + H_z) M_z \frac{\partial R}{\partial z}, \\
&= \epsilon \left(\epsilon^2 H_r M_r \frac{\partial R}{\partial z} - (1 + H_z) M_r - \epsilon^2 H_r M_z \left(\frac{\partial R}{\partial z} \right)^2 - (1 + H_z) M_z \frac{\partial R}{\partial z} \right).
\end{aligned}$$

which confirms our statement.